9. SITE 653: CORNAGLIA TERRACE[1]

Shipboard Scientific Party[2]

HOLE 653A

Date occupied: 29 January 1986

Date departed: 31 January 1986

Time on hole: 2 days, 13.7 hr

Position: 40°15.86′N; 11°26.99′E

Water depth (sea level, corrected m, echo-sounding): 2817

Water depth (rig floor, corrected m, echo-sounding): 2828

Bottom felt (m, drill pipe length from rig floor): 2831.8

Total depth (m): 3072.5

Penetration (m): 240.7

Number of cores: 26

Total length of cored section (m): 240.7

Total core recovered (m): 211.5

Core recovery (%): 87.8

Deepest sedimentary unit cored:
Depth sub-bottom (m): 220
Nature: evaporitic sequence
Age: Messinian
Measured vertical sound velocity (km/s): 1.7–4.9

Igneous or metamorphic basement: none

HOLE 653B

Date occupied: 31 January 1986

Date departed: 2 February 1986

Time on hole: 2 days, 10.5 hr

Position: 40°15.86′N; 11°26.95′E

Water depth (sea level, corrected m, echo-sounding): 2817

Water depth (rig floor, corrected m, echo-sounding): 2828

Bottom felt (m, drill pipe length from rig floor): 2831.4

Total depth (m): 3095.7

Penetration (m): 264.3

Number of cores: 28

Total length of cored section (m): 264.3

Total core recovered (m): 216.5

Core recovery (%): 81.9

Deepest sedimentary unit cored:
Depth sub-bottom (m): 216
Nature: evaporitic sequence
Age: Messinian
Measured vertical sound velocity (km/s): 1.7–4.9

Igneous or metamorphic basement: none

Principal results: Site 653 was located 1/2 mi northeast of DSDP Site 132, on the eastern rim of the Cornaglia Basin in the western Tyrrhenian Sea (Figs. 1 and 2).

Neither hole was logged. Five heat flow measurements on Hole 653A revealed a nonlinear thermal gradient that decreases steeply downsection from 12.9°C/100 m in the top of the hole to 5.04°C/100 m near the base of the hole.

Two major sedimentary units were recovered (Fig. 3):

Unit I: Cores 107-653A-1H to 107-653A-25X-1, 23 cm, 0–221.6 mbsf; Cores 107-653B-1H to 107-653B-24X-1, 50 cm; 0–216.6 mbsf; Age: Pliocene-Quaternary.

In general, Unit I represents an interval of open marine hemipelagic to pelagic sedimentation; the sediments are dominantly grey and brown nannofossil ooze and foraminiferal nannofossil ooze with minor mud. Carbonate content ranges from 12% to 90%, averaging 50%. The unit can be further divided into Unit Ia, characterized by lower carbonate content and the occurrence of sapropels (maximum organic carbon concentration = 4.2%), clastic layers and volcanic ash layers; Unit Ib, characterized by higher carbonate content and the absence of sapropels, clastic layers, and volcanic ash layers; and Unit Ic, characterized by a reddish and yellowish coloration attributed to iron oxides. Site 653 Unit I correlates with Units I plus II of DSDP Site 132.

The Messinian-Pliocene boundary (near the boundary between Units I and II) has been recognized by the base of foraminiferal zone MPl1 (*Sphaeroidinellopsis* acme zone) and as such occurs at approximately 230 mbsf in Hole 653A and 225 mbsf in Hole 653B. Zone MPl1 is underlain by a 10-m-thick "non-distinctive" biozone (Iaccarino and Salvatorini, 1982) which lacks age-diagnostic species of planktonic foraminifers. Nannoplankton of smaller size, indicating somewhat restricted marine conditions, are few to common down to the base of Hole 653A (240 mbsf; within lithologic Unit II) and down to 245 mbsf in Hole 653B.

---

[1] Kastens, K. A., Mascle, J, Auroux, C., et al., 1987. *Proc., Init. Repts. (Pt. A), ODP*, 107.

[2] Kim A. Kastens (Co-Chief Scientist), Lamont-Doherty Geological Observatory, Palisades, NY 10964; Jean Mascle (Co-Chief Scientist), Laboratoire de Géodynamique Sous-Marine, Université Pierre et Marie Curie, BP 48, 06230 Villefranche-sur-Mer, France; Christian Auroux, Staff Scientist, Ocean Drilling Program, Texas A&M University, College Station, TX 77843; Enrico Bonatti, Lamont-Doherty Geological Observatory, Palisades, NY 10964; Cristina Broglia, Lamont-Doherty Geological Observatory, Palisades, NY 10964; James Channell, Department of Geology, 1112 Turlington Hall, University of Florida, Gainesville, FL 32611; Pietro Curzi, Istituto di Geologia Marina, Via Zamboni, 65, 40127 Bologna, Italy; Kay-Christian Emeis, Ocean Drilling Program, Texas A&M University, College Station, TX 77843; Georgette Glaçon, Laboratoire de Stratigraphie et de Paleoécologie, Centre Saint-Charles, Université de Provence, 3, Place Victor Hugo, 13331 Marseille Cedex, France; Shiro Hasegawa, Institute of Geology, Faculty of Science, Tohoku University, Aobayama, Sendai, 980, Japan; Werner Hieke, Lehrstuhl für Allgemeine, Angewandte und Ingenieur-Geologie, Abt. Sedimentforschung und Meeresgeologie, Technische Universität München, Lichtenbergstrasse 4, D-8046 Garching, Federal Republic of Germany; Floyd McCoy, Lamont-Doherty Geological Observatory, Palisades, NY 10964; Judith McKenzie, Department of Geology, University of Florida, 1112 Turlington Hall, Gainesville, FL 32611; Georges Mascle, Institut Dolomieu, Université Scientifique et Médicale de Grenoble, 15 Rue Maurice Gignoux, 38031 Grenoble Cedex, France; James Mendelson, Earth Resources Laboratory E34-366, Department of Earth, Atmospheric and Planetary Sciences, Massachusetts Institute of Technology, 42 Carleton Street, Cambridge, MA 02142; Carla Müller, Geol.-Paläont. Institut, Universität Frankfurt/Main, 32–34 Senckenberg-Anlage, D-6000 Frankfurt/Main 1, Federal Republic of Germany (current address: 1 Rue Martignon, 92500 Rueil-Malmaison, France); Jean-Pierre Réhault, Laboratoire de Géodynamique Sous-Marine, Université Pierre et Marie Curie, BP 48, 06230 Villefranche-sur-Mer, France; Alastair Robertson, U.S. Geological Survey, 345 Middlefield Road, Menlo Park, CA 94025 (current address: Department of Geology, Grant Institute, University of Edinburgh, Edinburgh, EH9 3JW, United Kingdom); Renzo Sartori, Istituto di Geologia Marina, Via Zamboni, 65, 40127 Bologna, Italy; Rodolfo Sprovieri, Istituto di Geologia, Corso Tukory, 131, Palermo, Italy; Masayuki Torii, Department of Geology and Mineralogy, Faculty of Science, Kyoto University, Kyoto, 606, Japan.

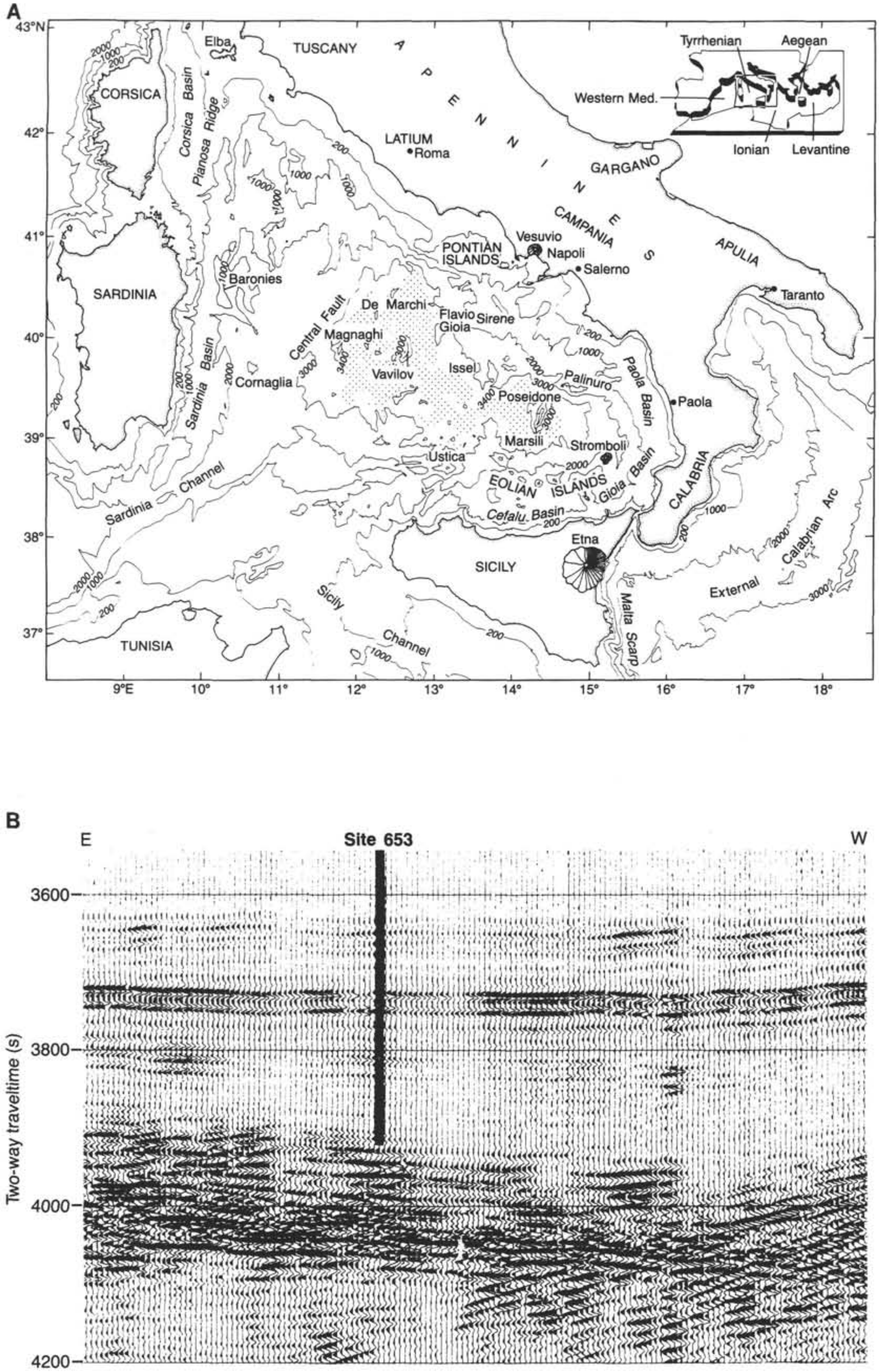

Figure 1. A. Location of Site 653 on bathymetric map of Tyrrhenian Sea. B. Location of Site 653 on single channel seismic line collected during approach to site.

Unit II: Cores 107-653A-25X-1, 23 cm, to 107-653A-26X, CC, 221.6–240.7 mbsf; Cores 107-653B-24X-1, 50 cm; to 653B-28X, CC, 216.6–264.3 mbsf; Age: Messinian.

Unit II represents sediments of restricted marine to evaporitic and subaerial environments. Carbonate content is low (0%–20%). Lithologies present in the two holes include: biotite- and gypsum-bearing sands, calcite-cemented siltstone, nannofossil mud, dolomitic nannofossil mud, calcareous mud, nannofossil- and foraminifer-bearing marly calcareous (dolomitic?) mud, and brilliant yellow and red muds and silts containing iron oxides, sulfur, and sulfates. Gypsum is present as very friable gypsum with wavy laminations, balatino-type laminated gypsum, powdery white gypsum interbedded within dull-red muds, and as centimetric layers of lenticular and nodular gypsum intercalated within calcareous dolomitic(?) nannofossil muds. The correlation among the Messinian sediments of Holes 132, 653A, and 653B is not straightforward, suggesting significant lateral facies variability.

BACKGROUND AND OBJECTIVES

Regional Setting and Previous Work

Of all of the holes drilled in the Mediterranean during DSDP Legs 13 and 42, only Site 132, in the western Tyrrhenian Sea, recovered a near-complete Pliocene-Quaternary pelagic section (Fig. 4). Every other site suffered from unconformities, most commonly of early Pliocene age. Because of this difficulty in finding a complete stratigraphic section in the deep Mediterranean, there was a groundswell of support among the various stratigraphic communities for a reoccupation of this thus-far unique site. By coring two adjacent holes with the advanced piston core (APC)/extended core barrel (XCB) combination, Site 653 might recover a more complete and less disturbed sedimentary section than had been achieved by rotary drilling on Leg 13.

Site 132/653 is located at the eastern rim of the Cornaglia Basin (Fig. 5), an area where relatively flat-lying seafloor is underlain by a thick evaporite-bearing sedimentary sequence. Based on interpretation of seismic reflection and refraction profiles (Figs. 4 and 6; Finetti et al., 1970; Fabbri and Curzi, 1979; Malinverno et al., 1981; Duschenes et al., 1986), the Cornaglia Basin appears to be one of the few parts of the Tyrrhenian where the complete Messinian evaporite sequence is well developed, including the halite-bearing, diapir-forming "lower evaporite unit."

Acoustic basement rises gradually toward a peak to the east, from 4.75 s below sea level at Site 132/653, to 3.9 s below sea level about 20 km east of the site (Figs. 4 and 6). This basement high seems to be the along strike continuation of Monte Secchi, a seamount from which calcareous phyllites and calc-schists have been dredged (Colantoni et al., 1981). These dredge results, as well as seismic refraction data (Recq et al., 1984; Steinmetz et al., 1983; Duschenes et al., 1986), suggest that Site 132/653 is located on thinned continental lithosphere. A detailed heat flow survey just west of the site determined a mean heat flow of 134 ± 8 mW/m^2 (Hutchison et al., 1985).

At Site 132, Pleistocene and Pliocene foraminferal marl oozes, volcanic ash, and sand were found between the seafloor and 188 mbsf (Ryan et al., 1973). Sands and ash layers are more common between the seafloor and 50 mbsf (Site 132 lithologic Unit I) and uncommon between 50 and 188 mbsf (Site 132 lithologic Unit II). The Pliocene/Pleistocene boundary occurred at 70 mbsf, and has no lithologic expression. From 188 to 223 mbsf, DSDP 132 recovered an evaporitic series of Messinian age. From top to bottom, the evaporitic series comprised (1) interbedded sands and marls containing micritic calcite and very fine-grained anhedral dolomite (182–191 mbsf), (2) laminated gypsum with traces of quartz and fragments of chert (191–198 mbsf), (3) dolomitic marl with thin intercalations of gypsum (207–214 mbsf), and (4) interbedded layers of consolidated and plastic gypsum (214–223 mbsf).

Objectives

The primary objective at Site 653 was to recover, as completely as possible, a near-continuous pelagic Pliocene-Pleistocene sedimentary sequence. A secondary objective was to recover the upper 50 m of the Messinian evaporitic sequence to document the evolution from the desiccated basin into marine conditions. This site was envisioned as a "deep-sea type section" at which various stratigraphies based on paleomagnetics, tephra, stable isotopes, and paleontology could be compared and calibrated. A high-resolution, focused study on one site has potential benefits in several disciplines. The coring summary is shown in Table 1.

Pliocene-Pleistocene Biostratigraphy

Detailed biostratigraphic investigations will be carried out on benthic and planktonic foraminifers, calcareous nannoplankton, and pollen. This coordinated approach should allow a definitive correlation between the different zonal schemes currently in use in the Mediterranean area for different microfossil groups.

All stratotypes of the chronostratigraphic units for the Pliocene and Pleistocene (Zanclean, Tabianian, Piacenzian, Calabrian, Sicilian, Selinuntian), as well as the Pliocene-Pleistocene boundary section (Vrica section), are located in Italy. Unfortunately, these type sections are less than ideal because of dilution by varying amounts of allochthonous detritus and because planktonic markers are sometimes sparse or of only local significance. By correlation of these stratotypes with the deep-sea sequence recovered in Site 653, it should be possible to test the reliability of the biostratigraphic events recognized in these classic type sections.

Absolute dates for the biostratigraphic events recorded in the Italian type sections have been difficult to establish. Unfortunately, efforts at correlations to the paleomagnetic time scale have been hindered by chemical overprinting and low intensities of magnetization in the type sections. The only magnetostratigraphy available directly from the Mediterranean Neogene is that from the Vrica section, where the section is so short that the correlation is ambiguous. Because of the lack of reliable dates in the type sections, the dates for Pliocene-Pleistocene chronostratigraphic units have depended on extrapolation from the Atlantic or elsewhere, where chronologic constraints are stronger. However, the assumption that these events were synchronous in the enclosed basin of the Mediterranean and in the open ocean is controversial (Cita, 1973, 1975; Ryan et al., 1974; Thunnell, 1979; Spaak, 1983; Rio et al., 1984). We were optimistic that it would be possible to obtain a useable paleomagnetic stratigraphy at Site 653; this would allow a relatively unambiguous demonstration of the synchroneity or diachroneity between biostratigraphic events in the type sections and in the rest of the world.

Finally, detailed stratigraphy and paleoenvironmental reconstruction provide the necessary framework to study the evolution of certain Pliocene species which are unknown from the Atlantic and appear to have evolved only in the Mediterranean, e.g., *Globoratalia bononicusis* (Colalongo and Sartoni, 1967; Conato and Follador, 1967; Gradstein, 1974; Zachariasse, 1979; Scott, 1980; Spaak, 1981).

Miocene-Pliocene Boundary and the Cause of the Messinian Salinity Crisis

The Miocene-Pliocene boundary signifies the end of the Messinian salinity crisis and the return of marine conditions. The boundary stratotype is in Sicily at Capo Rossello where the boundary coincides with the base of the Trubi marls and the base of the *Sphaeroidinellopsis* acme zone (Cita et al., 1973). The use of an acme (abundance rather than first appearance or extinction) zone is an inherently unsatisfactory means of identifying such an important boundary. Furthermore, because of the drastic en-

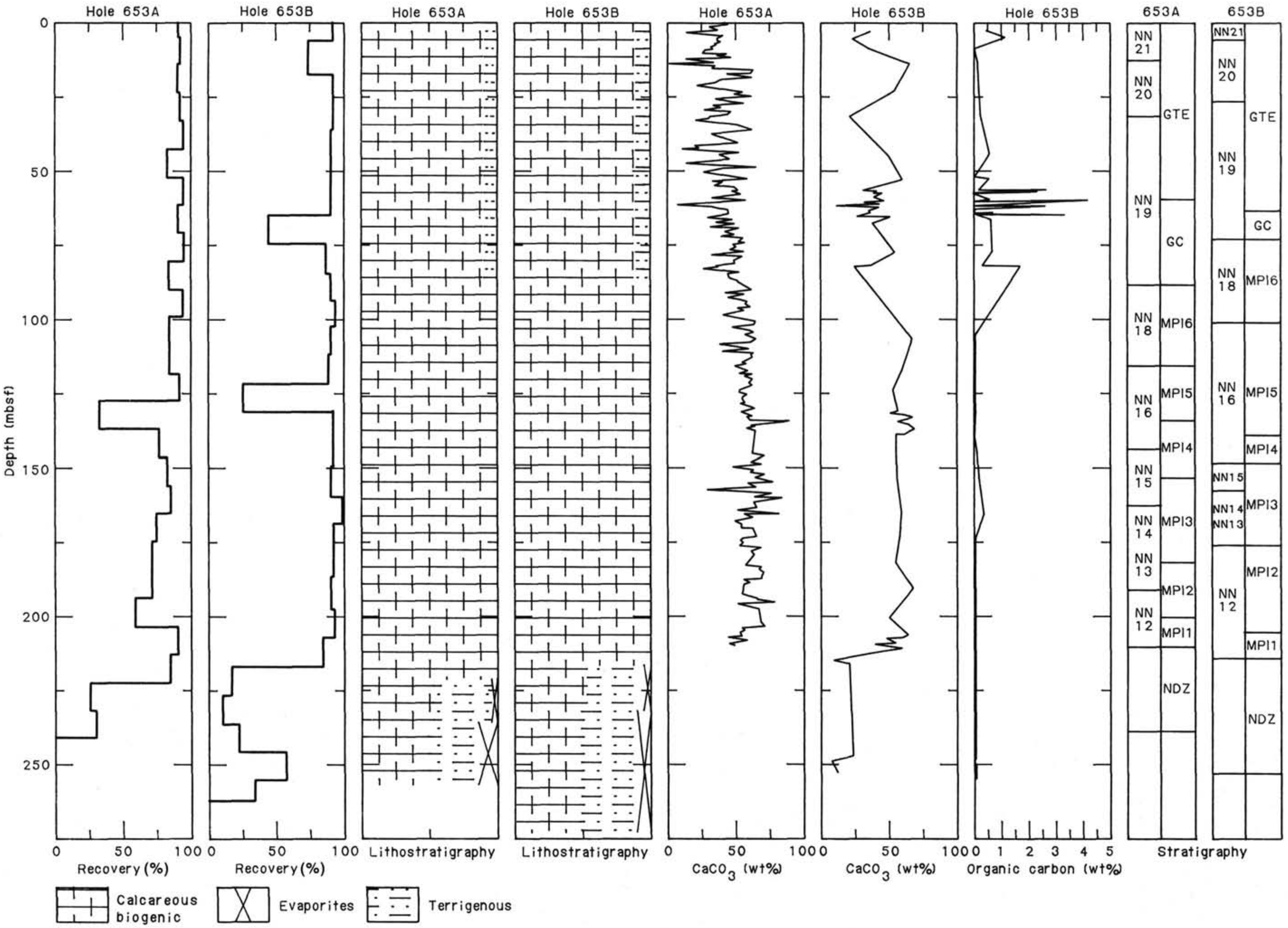
Hole 653A
Hole 653B
Hole 653A
Hole 653B
Hole 653A
Hole 653B
Hole 653B
653A
653B
Depth (mbsf)
0
50
100
150
200
250
Recovery (%)
0
50
100
Recovery (%)
Lithostratigraphy
Lithostratigraphy
CaCO3 (wt%)
CaCO3 (wt%)
Organic carbon (wt%)
0
1
2
3
4
5
Stratigraphy
NN 21
NN 20
NN 19
NN 18
NN 16
NN 15
NN 14
NN 13
NN 12
GTE
GC
MPl6
MPl5
MPl4
MPl3
MPl2
MPl1
NDZ
NN21
NN 20
NN 19
NN 18
NN 16
NN15
NN14
NN13
NN 12
GTE
GC
MPl6
MPl5
MPl4
MPl3
MPl2
MPl1
NDZ
Calcareous biogenic
Evaporites
Terrigenous

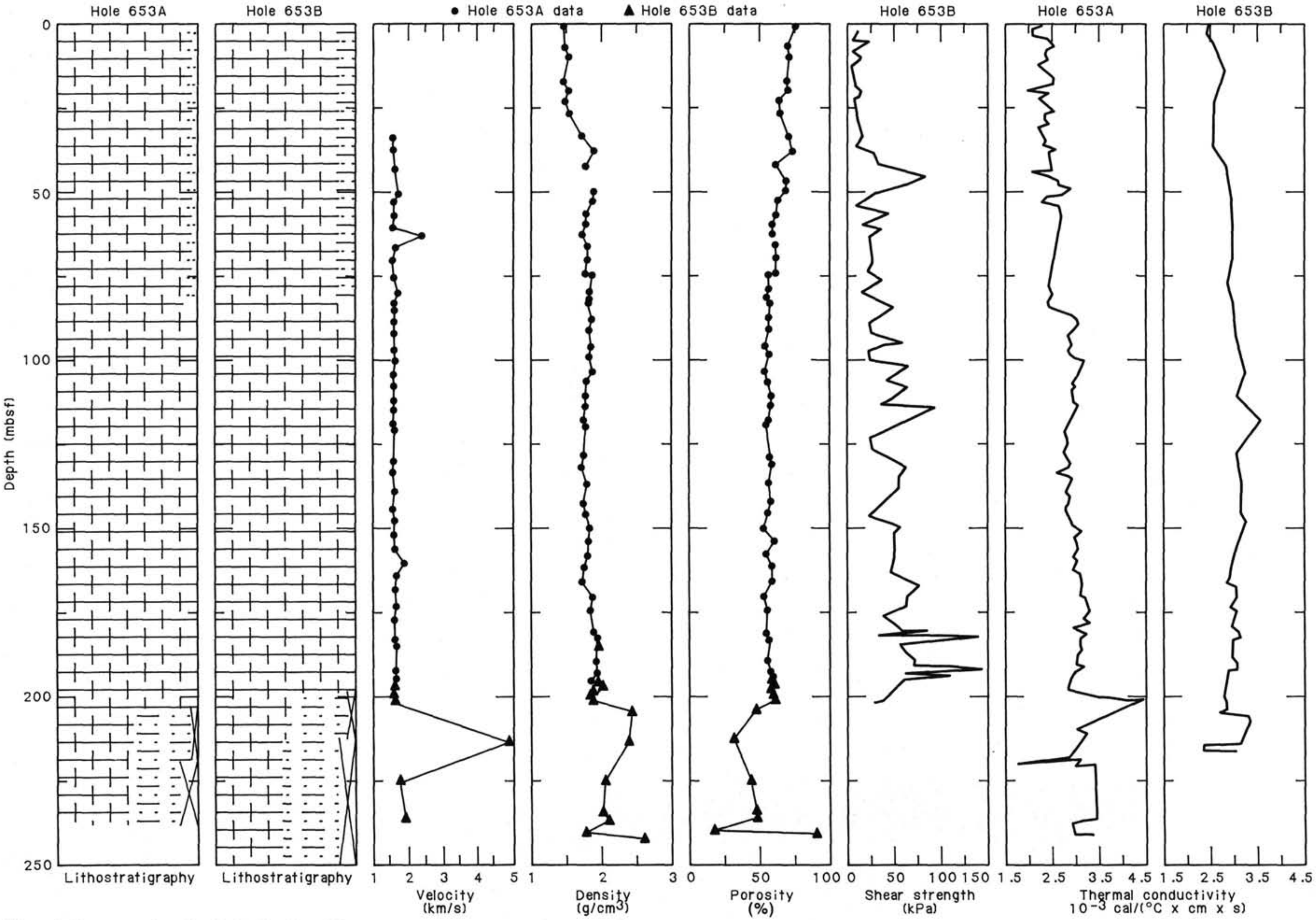

Figure 2. Summary of results obtained at Site 653.

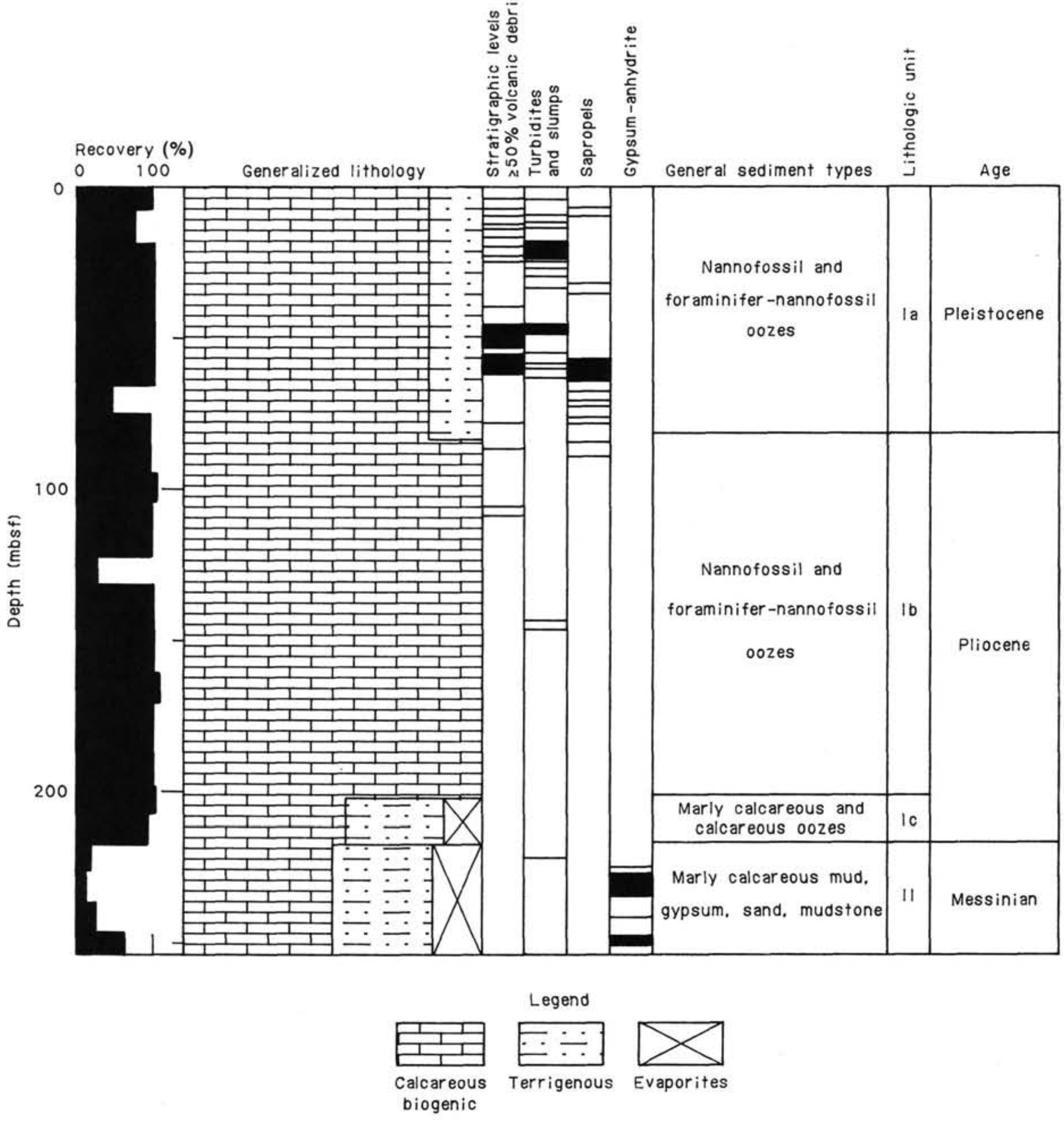

Figure 3. Composite log obtained for Site 653.

vironmental changes occurring at the end of the Messinian, it seems very likely that this biostratigraphic event was not synchronous in the Sicilian type section and the rest of the world. Magnetostratigraphy provides the most promising opportunity to tie the Miocene/Pliocene boundary of the Mediterranean into the open ocean.

The correlation between Mediterranean Messinian events and the open ocean provides a critical constraint for understanding the causal relationship (if any) between Messinian Mediterranean salinity crisis and glacio-eustatic cycles. It has been suggested that southern hemisphere late Miocene glaciation triggered desiccation by lowering sea level below the sill into the Mediterranean (Adams et al., 1977; McKenzie et al., 1979). Was eustatic sea level change also responsible for the end of the Mediterranean desiccation? A rigorous comparison of the timing of the terminal Messinian flooding with the timing of Atlantic glacial/interglacial cycles would test this hypothesis by determining whether global eustatic sea level was rising or falling at the time of the terminal flooding.

Paleoenvironment

Glacial-interglacial cycles became evident in the Mediterranean at about 2.5 Ma (Bizon and Müller, 1977; 1978; Thunnell and Williams, 1983) with an intensification at the beginning of the glacial Pleistocene (0.9 Ma). These world-wide climatic fluctuations are recognized by changes of foraminiferal and nannoplankton assemblages (Ciaranfi and Cita, 1973; Cita et al., 1973; Thunnell, 1979; Müller, 1978), as well as in the oxygen isotopic record (Thunnell and Williams, 1983). However, more subtle details of the stable isotope and faunal records are probably related to local climatic and hydrographic changes. For example, the ^{18}O record for Site 132 contains some very light isotope val-

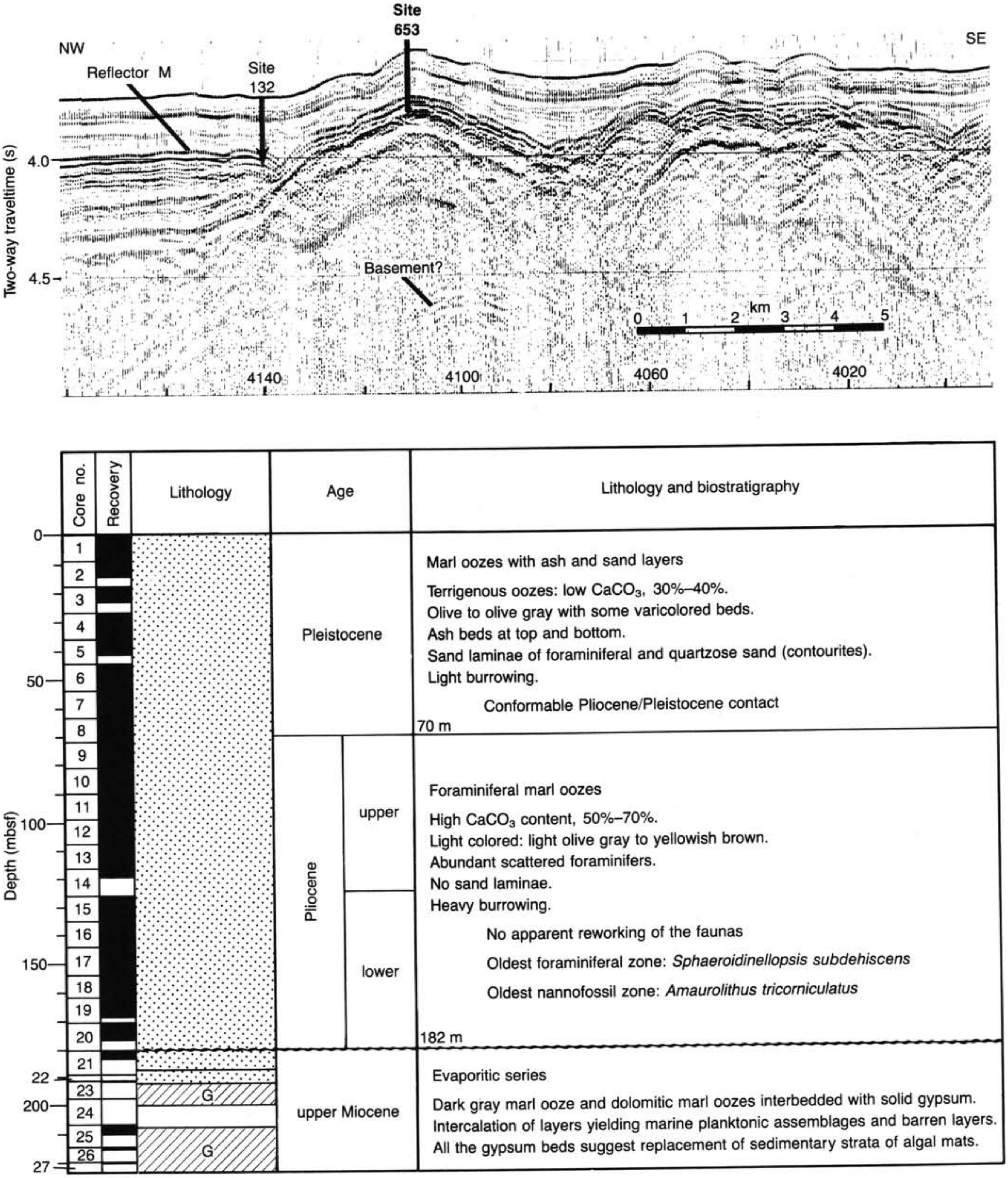

Marl oozes with ash and sand layers

Terrigenous oozes: low $CaCO_3$, 30%–40%.

Olive to olive gray with some varicolored beds.

Ash beds at top and bottom.

Sand laminae of foraminiferal and quartzose sand (contourites).

Light burrowing.

Conformable Pliocene/Pleistocene contact

Foraminiferal marl oozes

High $CaCO_3$ content, 50%–70%.

Light colored: light olive gray to yellowish brown.

Abundant scattered foraminifers.

No sand laminae.

Heavy burrowing.

No apparent reworking of the faunas

Oldest foraminiferal zone: *Sphaeroidinellopsis subdehiscens*

Oldest nannofossil zone: *Amaurolithus tricorniculatus*

Evaporitic series

Dark gray marl ooze and dolomitic marl oozes interbedded with solid gypsum.

Intercalation of layers yielding marine planktonic assemblages and barren layers.

All the gypsum beds suggest replacement of sedimentary strata of algal mats.

Figure 4. Seismic line, lithology, and biostratigraphy at DSDP Site 132 (from Ryan, Hsü, et al., 1973), located on the Tyrrhenian Rise. G = gypsum.

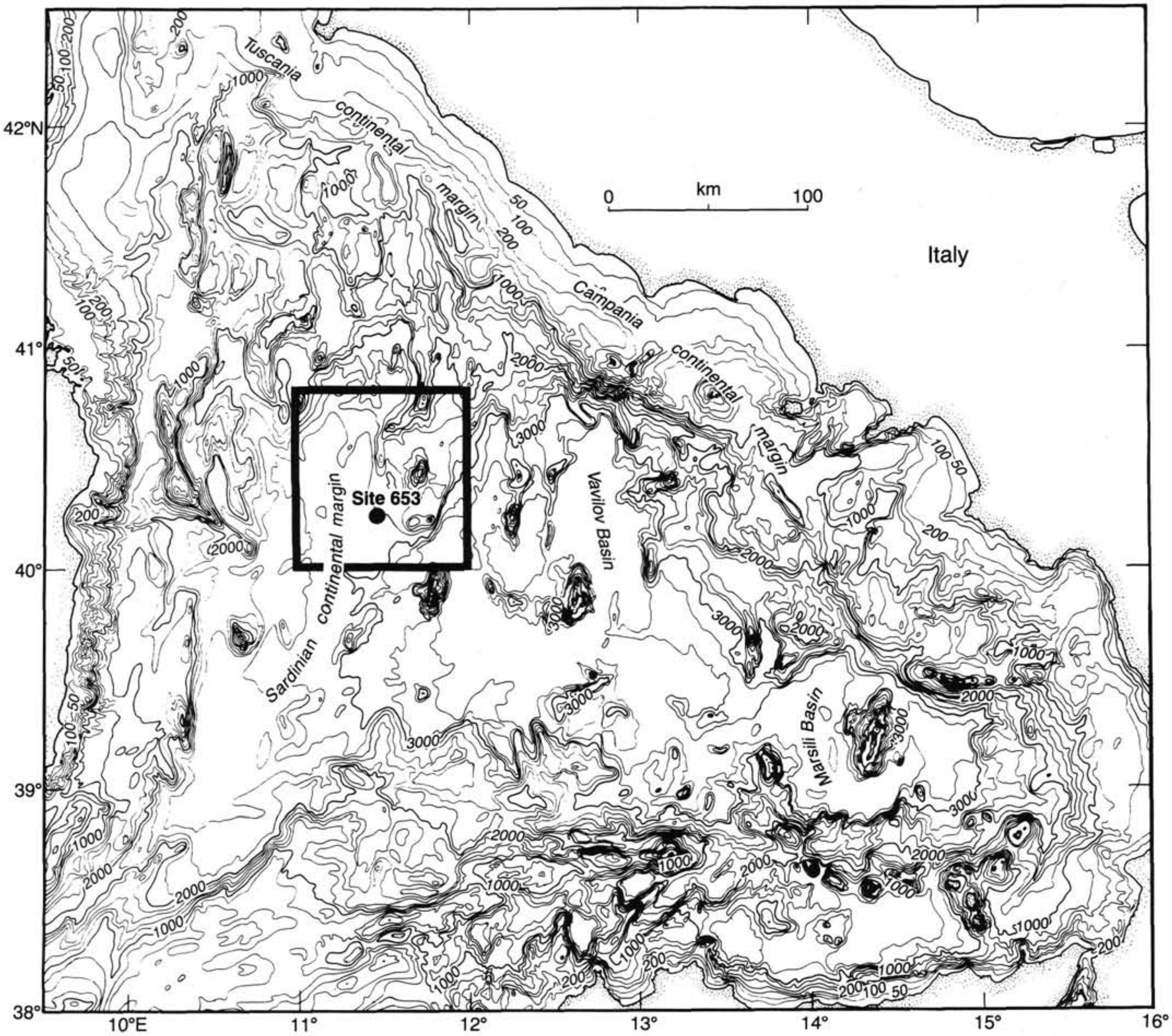

Figure 5. Location of Site 653 (Holes 653A and 653B) on the Sardinian margin (so-called Cornaglia Basin). Site 653 is 1/2 mi east of former DSDP Site 132 where an almost complete Pliocene-Pleistocene section was drilled.

ues which have been related to decreases in surface water salinities (Thunnell and Williams, 1983). Similarly, the accumulation of large specimens of *Braarudosphaera biglowi*, which is seen in the lowermost part of nannoplankton Zone NN19 in the eastern and western Mediterranean (Müller, 1978; 1985), may indicate locally decreased salinity. A more detailed isotope and faunal stratigraphy is needed to distinguish and date these subtle, local changes in paleoenvironment which are superimposed on top of the world-wide trends.

Paleoceanography

The physical oceanography of the modern Mediterranean is dominated by the excess of evaporation over precipitation. This single characteristic leads to downwelling in the basin, isohaline and isothermal conditions down to the seafloor, and an export of high density salty water out through the Straits of Gibraltar where it forms a distinct warm-water mass which profoundly influences the circulation of the North Atlantic. It is not clear when this condition developed; in the early Pliocene, the deep waters of the Mediterranean apparently originated in the Atlantic (Vergnaud-Grazzini, 1985). Site 653 provides an opportunity to make a detailed comparison of benthic and planktonic faunal and isotopic records in order to reconstruct bottom and surface water conditions in the Tyrrhenian Sea during the Pliocene-Pleistocene, and thus date the onset of the Mediterranean anti-estuarine (lagoonal) circulation pattern.

Site Selection

As originally proposed, Site TYR2 was 10 nmi south of DSDP 132, in an area where the seismic documentation was more complete. This position was rejected during the application for clearance to drill in Italian waters because of the proximity of a telephone cable. The site was therefore repositioned adjacent to DSDP Site 132.

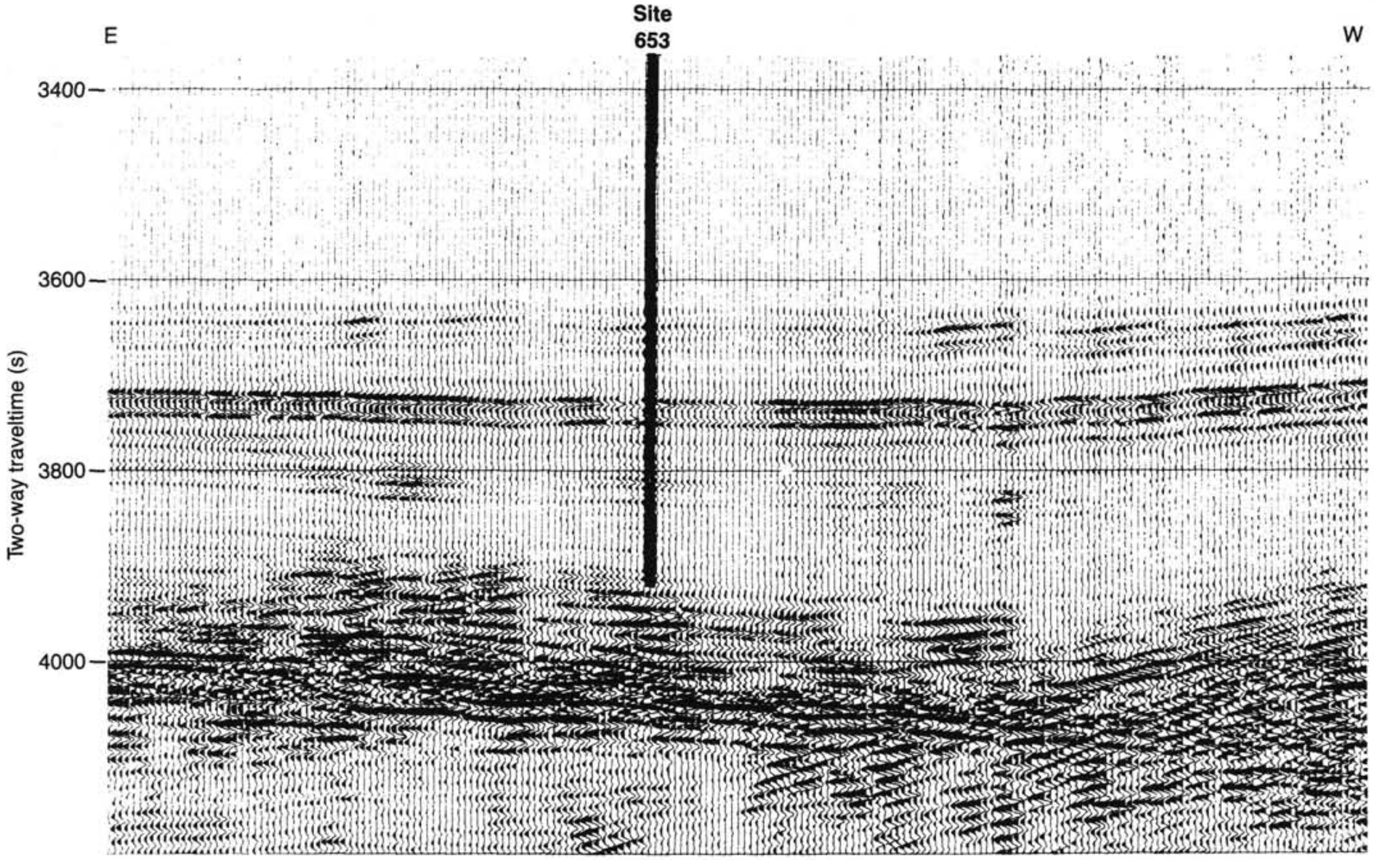

Figure 6. Survey seismic line during approach to Site 653 and location of Site 653. The top of the upper evaporite sequence and the top of the acoustic basement rise eastward toward a small seamount.

OPERATIONS

Strategy

Since the major goal at Site 653 was to obtain as complete as possible recovery of the Pliocene-Pleistocene sequence, the coring program was planned as two adjacent holes. The first hole was planned to reach to the Miocene-Pliocene boundary. If time allowed, the second hole could be extended as much as 50 m into the Messinian. Each hole was to be cored as deep as possible with the advanced piston corer (APC); after APC refusal, the extended core barrel system (XCB) would be used to core down to the target depth. Since magnetostratigraphy was important, all APC cores except for the shallowest two at each hole (before the bottom hole assembly was stabilized) would be oriented with the compass inside the multishot camera tool. Heat flow measurements were planned at 40-m intervals in the first hole, with a maximum of 5 measurements, using the Von Herzen instrument while APC coring and the Uyeda probe after the switch to XCB coring.

This site was planned as a reoccupation of DSDP Site 132. Thus, in contrast to our previous site approaches, the goal on the approach to site 653 was to drop the positioning beacon at an exact latitude and longitude, rather than a geologically defined position on a given seismic reflection profile. Therefore the plan was to steam directly from Site 652 to the new site, timing the arrival on site to fall within the operational window of the Global Positioning System (GPS), which was predicted between 1920 on 28 January and 0140 on 29 January. Since the existing seismic profiles across and near DSDP site 132 were of poor quality, new seismic data would be collected beginning about 10 nmi before the site (Fig. 6).

Approach to Site

During the latter part of the transit from Site 652, the vessel was navigated using GPS; Loran was monitored, but appeared to be unstable. At 2300 on 28 January 1986, the vessel slowed to 6 kt to stream seismic gear. The course remained unchanged at 265°. Seismic source, receiver, recording, and processing techniques are described in the "Explanatory Notes" chapter, this volume.

At 2313, almost 3 hr before the predicted end of the window, the GPS system stopped tracking, and began displaying the message "IAC," indicating initial acquisition of a GPS satellite. Although the system was apparently locked onto four satellites, each with good signal to noise ratio (41 to 46) and good elevation (27° to 57°), it produced no fixes for the next hour. Loran position continued to fluctuate erratically with frequent leaps of several miles, and Loran cycle skip and signal strength warning lights were displayed intermittently for both master/slave pairs. The ship was steered by dead reckoning, but since there had been no independent position fixes since the change of speed, and since the ship's pit log is often in error by a knot, the dead reckoning position had to be viewed with suspicion.

By 0000 on 29 January, it was apparent that a beacon drop could not be considered without additional navigation control. Bathymetric and geological features could not serve as reliable landmarks, because we had chosen not to follow a pre-existing seismic line on our approach. We therefore decided to reinitialize the GPS system and slow the ship from 65 to 40 rpm in hopes that GPS would be operational again and/or a transit satellite scheduled for 0105 would come in before we crossed the site. At 0053, GPS started again, giving a position nearly 2 mi

Table 1. Coring summary table for Holes 653A and 653B.

Core no.	Date (1986)	Time	Sub-bottom depths (m)	Length cored (m)	Length recovered (m)	Recovery (%)
Hole 653A:						
1H	Jan 29	1200	0.0-3.7	3.7	3.7	100.8
2H	29	1300	3.7-13.2	9.5	9.8	102.7
3H	29	1400	13.2-22.7	9.5	9.6	101.4
4H	29	1500	22.7-32.2	9.5	9.8	102.8
5H	29	1700	32.2-41.6	9.4	9.9	104.9
6H	29	1800	41.6-51.0	9.4	8.7	92.1
7H	29	1915	51.0-60.5	9.5	10.0	105.2
8H	28	2015	60.5-70.0	9.5	9.6	101.2
9H	29	2200	70.0-79.6	9.6	10.2	106.4
10H	29	2315	79.6-89.0	9.4	8.8	93.6
11H	30	0045	89.0-98.2	9.2	9.6	104.8
12H	30	0145	98.2-107.7	9.5	9.0	94.6
13H	30	0345	107.7-117.3	9.6	9.0	94.1
14X	30	0630	117.3-126.6	9.3	9.5	102.4
15X	30	0800	126.6-136.1	9.5	3.6	37.7
16X	30	1000	136.1-145.6	9.5	8.3	87.1
17X	30	1130	145.6-155.2	9.6	8.9	92.9
18X	30	1445	155.2-164.1	8.9	8.4	94.2
19X	30	1630	164.1-173.7	9.6	8.1	84.0
20X	30	1800	173.7-183.2	9.5	7.7	80.6
21X	30	1945	183.2-192.9	9.7	7.8	80.3
22X	30	2330	192.9-202.4	9.5	6.4	67.0
23X	31	0130	202.4-211.9	9.5	9.6	101.5
24X	31	0315	211.9-221.4	9.5	9.0	94.5
25X	31	0530	221.4-231.0	9.6	3.0	30.7
26X	31	0930	231.0-240.7	9.7	3.5	36.1
Hole 653B:						
1H	Jan 31	1930	0.0-6.1	6.1	6.1	100.3
2H	Feb 1	0130	6.1-17.6	11.5	9.2	79.9
3H	1	0215	17.6-27.1	9.5	9.7	101.9
4H	1	0330	27.1-36.6	9.5	9.7	101.9
5H	1	0430	36.6-46.0	9.4	9.5	100.5
6H	1	0515	46.0-55.4	9.4	9.5	100.7
7H	1	0600	55.4-64.9	9.5	9.6	101.0
8H	1	0700	64.9-74.4	9.5	4.7	49.0
9X	1	0845	74.4-84.0	9.6	9.3	97.1
10X	1	1015	84.0-93.4	9.4	9.3	99.0
11X	1	1130	93.4-102.6	9.2	9.6	104.6
12X	1	1315	102.6-112.1	9.5	9.5	100.2
13X	1	1445	112.1-121.6	9.5	9.5	99.5
14X	1	1615	121.6-131.0	9.4	2.6	27.8
15X	1	1800	131.0-140.5	9.5	9.7	102.1
16X	1	1945	140.5-150.0	9.5	9.7	102.2
17X	1	2130	150.0-159.6	9.6	9.7	100.7
18X	1	2330	159.6-168.5	8.9	9.6	108.2
19X	2	0115	168.5-178.0	9.5	9.7	102.0
20X	2	0300	178.0-187.0	9.0	9.7	107.4
21X	2	0445	187.0-197.2	10.2	9.8	95.6
22X	2	0700	197.2-206.7	9.5	9.7	102.3
23X	2	0845	206.7-216.1	9.4	8.8	93.4
24X	2	1100	216.1-225.7	9.6	1.7	18.0
25X	2	1345	225.7-235.3	9.6	1.6	16.9
26X	2	1545	235.3-244.9	9.6	2.4	24.5
27X	2	1830	244.9-254.6	9.7	6.6	68.4
28X	2	2245	254.6-264.3	9.7	2.8	29.1

to the northeast of the dead reckoned position; less than 5 min after this position was recorded, GPS reached the end of its night window. A transit satellite at 0110 confirmed the GPS position. At 0125, the ship changed course to 242°, to come down to the site from the GPS/transit satellite position. As soon as the ship changed course, the Loran warning lights spontaneously cleared up, and the Loran position more or less stabilized at a location 1/2 mi east of the position inferred from dead reckoning since the 0110 transit satellite position.

The ship continued at 40 rpm on course 242°. At 0158, when the dead reckoned position agreed with the position of DSDP Site 132 (40°15.70′N; 11°26.47′E) the beacon was dropped. The Loran position at the drop was 40°15.74′N; 11°27.09′E. In retrospect, the Loran was more accurate at the time of the drop than the dead reckoning, since the final position of Site 653 did lie east of Site 132. The seismic line was extended approximately 3 km past the drop point to collect a high-quality line to illustrate the geologic setting of the site. Seismic gear was brought on board at 0235.

The observation that the Loran quality had markedly and suddenly improved when the ship changed course from 265° to 242° raised the possibility that the derrick might be shadowing the Loran antenna from the Lampedusa (southern Italy) Loran station. To test this suspicion, the ship was turned slowly through 540° before proceeding back to the beacon. Throughout this pirouette, the Loran position remained steady and no Loran warning lights were observed.

The vessel returned toward the beacon to begin dynamic positioning. A transit satellite fix at 0345 suggested that the beacon was east of DSDP site 132, so the ship was positioned 400 m west of the beacon to begin drilling. An average of transit and GPS fixes while drilling gave a position of 40°15.86′N; 11° 26.99′E for Hole 653A and 40°15.86′N; 11°26.95′E for Hole 653B. The Loran C coordinates of Hole 653B were 40°15.72′N; 11°26.80′E, using the X and Z slaves. Loran time delays were: X, 12943; Z, 51805. The signal from the Y Loran slave was unusable.

Hole 653A

Hole 653A was spudded at 1120, January 29. The advanced piston corer (APC) was used for Cores 107-653A-1H through Core 653A-13H. Cores 107-653A-3H through 653A-13H were oriented with respect to north. The sticky nannofossil ooze of lithostratigraphic Unit I proved to be difficult material to core using piston coring techniques. Core 107-653A-6H was at least half flow-in; Cores 653A-7H, 653A-8H, and 653A-9H appeared to be in good condition; but then Cores 107-653A-10H, 653A-11H, 653A-12H, and 653A-13H had shattered or collapsed liners and considerable visible disturbance. Officially, APC recovery averaged 100%. However several percent of this may be due to the expansion of the sediment during recovery; expansion is inferred because several cores protruded as much as 5 cm beyond the end of the liner, and several liners arrived on deck split lengthwise.

Extended core barrel coring began at 117.3 mbsf with Core 107-653A-14X. A previously unused, prototype venturi vent sub was used with the XCB system. The venturi vent sub is credited for the very undisturbed, high recovery cores in the XCB part of the hole. Recovery while XCB coring in the Pliocene-Quaternary section was 88%, with the exception of Core 107-653A-15X (127–136 mbsf) which recovered only 37%. As the same interval in the 653B hole (Core 107-653B-14X, 122–131 mbsf) also had very poor (28%) recovery, it seems that there was a stratum with anomalous hard-to-recover physical properties at this level, but no trace of unusual lithology was noted in the cores. Evidence that the cores were expanding during recovery was seen down to at least 200 mbsf. From Core 107-653A-15X onward an "overtrimming" cutting shoe was used which cuts a core that is smaller in diameter than the inside diameter of the core liner. This technique avoided the coring disturbance that had been fairly pervasive in Cores 653A-1H through 653A-14X.

Heat flow measurements were made in the Pliocene-Quaternary section at 41.6, 79.6, and 117.3 mbsf using the Von Herzen instrument and then at 155.2 and 192.9 mbsf using the Uyeda probe.

The top of the Messinian evaporites was noted on the rig floor by a marked drop in rate of penetration at 224.5 mbsf. The hole was terminated according to plan at a depth of 240.7 mbsf.

The pipe was pulled to 70 mbsf and a down-looking, black and white remote video camera was lowered on a frame that encircles the pipe. The goals of this exercise were to observe the hole and mound of cuttings of the 653A hole, to attempt a reentry into Hole 653A without a reentry cone, and to observe the seafloor penetration of the first core of Hole 653B. The hole was seen as a barely perceptible circle too faint to relocate and reenter.

Hole 653B

The ship was offset 180 ft to the west before spudding Hole 653B. The drill string was positioned 4 m deeper to shoot the first piston core of Hole 653B than it had been for 107-653A-1H, so that the unrecovered gaps between cores would fall at different levels in the stratigraphic section. Whereas Core 653A-1H of Hole 653A had penetrated 3.6 mbsf, Core 653B-1H of Hole 653B penetrated 6.1 mbsf. The first piston core of Hole 653B released prematurely, probably due to severe heave of the vessel.

Hole 653B was APC cored through Core 107-653B-8H, where liner failures were once again observed. Since XCB cores had been nearly as full and not nearly as disturbed as APC cores in Hole 653A, the switch to XCB coring was made earlier in Hole 653B, at 74 mbsf. Cores in Hole 653B were not oriented, and no heat flow measurements were made.

The change in drilling characteristics associated with the top of the Messinian evaporitic sequence was noted at 223 mbsf. Within the Messinian, recovery dropped to 31%. The hole was terminated according to plan after 40 m of penetration into Messinian, at a total depth of 264.3 mbsf.

Recovery in the Pliocene-Quaternary sequence averaged 92% while piston coring and 100% while using the XCB (leaving out Core 653A-14X as noted above). These percentages include six APC cores and nine XCB cores which had apparent recovery over 100%, presumably the sediment expanded after the overburden pressure was removed.

LITHOSTRATIGRAPHY

Description of Lithologic Units

Two major lithologic units were identified between the seafloor and the base of the drilled holes at 241 mbsf (Hole 653A) and 264 mbsf (Hole 653B). Definition of these two units is based upon lithologic, textural, and carbonate content changes that occur at and below the Pliocene/Miocene boundary. Correlations between Holes 653A and 653B remain tentative, but observations based upon physical stratigraphic similarities suggest comparable sequences, particularly between lithologic units and their subunits (see next section).

Lithologic Units I and II at DSDP Site 132 correspond to Unit I at Site 653; DSDP Site 132 Unit III corresponds to Unit II at Site 653.

Unit I

Cores 107-653A-1H to 107-653A-25X-1, 23 cm; depth 0-221.6 mbsf; thickness 221.6 m.

Cores 107-653B-1H to 107-653B-24X-1, 50 cm; depth 0-216.6 mbsf; thickness 216.6 m. Age: Quaternary, Pliocene, plus several tens of centimeters of probable Messinian.

In general, Unit I represents an interval of hemipelagic to pelagic sedimentation. Carbonate content increases steadily downcore from an average of 40% (maximum 67%) in the upper part (Subunit Ia; see below) to an average of 60% (maximum 91%) (Subunits Ib and Ic). These are values measured from Hole 653A, where two samples were taken from each section for calcium carbonate determination; at Hole 653B, sampling was less frequent, about one sample per core (see "Geochemistry" section, this chapter). Volcanic ash layers and sapropels (black muds with measured or presumed organic carbon content greater than 2%) are present within Unit I. Sediment colors reflect these varied lithologies: light gray to brown in oozes and muds, black in sapropels, various gray shades in volcanic ash deposits, and brown-red-yellow in sediments at the base of the unit.

Unit I was deposited at an average sedimentation rate (not corrected for compaction) of about 3.9 cm/1000 yr. Slightly lower rates of 3.2 and 3.8 cm/1000 yr were calculated at neighboring Site 132 for approximately the equivalent time duration. This unit is equivalent to lithologic Units I and II at DSDP Site 132.

Subunit Ia: Cores 107-653A-1H to 107-653A-10X; depth 0-85.7 mbsf; thickness 85.7 m. Cores 107-653B-1H to 107-653B-10X; depth 0-86 mbsf; thickness 86 m; corresponds to lithologic Unit I, DSDP Site 132.

Subunit Ia is delineated by lower carbonate content values in oozes (large fluctuations in these values), the occurrence of calcareous muds, as well as by more varied lithology including thin deposits of tephra, sapropels, and foraminifer sands than elsewhere in lithologic Unit I.

Subunit Ia contains light gray and brown marly nannofossil ooze and marly foraminiferal-nannofossil ooze as the dominant lithologies; calcareous mud is a minor constituent. Carbonate content averages 40%, but fluctuates between 12% and 67% (lowest value 1.2% within a normally-graded volcaniclastic layer), and increases downsection. Large fluctuations in these values possibly reflect glacial-interglacial changes.

Sapropels are present as gray sediments with considerably varying carbonate content (observations mainly from nannoplankton study) with an organic carbon content of 2% or more. In the absence of organic carbon measurements on all layers, sapropels tentatively are identified by dark colored calcareous muds or oozes usually with a yellow-brown lamina of diagenetic (oxidation) origin a few centimeters above the mud/clay. Pteropod shell fragments often are scattered within these sapropels as well as within oozes.

About 30 clastic layers (different numbers in each hole, depending on the completeness of cored sequences) containing volcanic debris, usually glass or pumice fragments, were identified in smear slides or presumed present on the basis of similar appearance in split cores. Textural sorting characteristics or admixtures of biogenic material suggest an epiclastic origin by turbidity currents for at least half of these deposits. Volcanicity, nevertheless, was and continues to be a major factor in sedimentation. Thin siliciclastic layers with normal grading but with minor volcanic component detritus are rarely present.

A debris flow about 50 cm thick with deformed multicolored nannofossil ooze/mud clasts in a mud/clay matrix occurs in both holes at comparable intervals (Sections 107-653A-3H-5, 55-105 cm, 19.75-20.25 mbsf, and 107-653B-3H-1, 121 cm, to Core 653B-2H, 20 cm, 18.81-19.30 mbsf. In both holes it is overlain by a foraminifer sand (Fig. 7). The similarity in appearance and stratigraphic position of this deposit argues against its origin as a drilling disturbance, despite severe coring disturbances in surrounding cores at both holes. Interestingly, the occurrence of multiple overturned strata in Sections 107-653B-3H-3, 0-150 cm, 107-653A-4H-3, 0-150 cm, and Cores 107-653A-5H, 60 cm, to 107-653A-6H, 40 cm, controversially interpreted (drilling deformation?), may represent slumps which are not equivalents in both holes. Slumping probably occurred off the Secchi Seamount and the Monte della Rondine south of it, the only nearby high ground.

Subunit Ib: Cores 107-653A-10X to 107-653A-23X-6; depth: 85.7-210.1 mbsf; thickness: 124.4 m. Cores 107-653B-10X to 107-653B-23X-2; depth: 86.0-209.1 mbsf; thickness: 123.1 m. Presumably corresponds, together with Subunit Ic, to lithologic Unit II at DSDP Site 132.

Subunit Ib is defined, and distinguished from Subunit Ia, by a thick sequence of homogeneous foraminiferal-nannofossil oozes

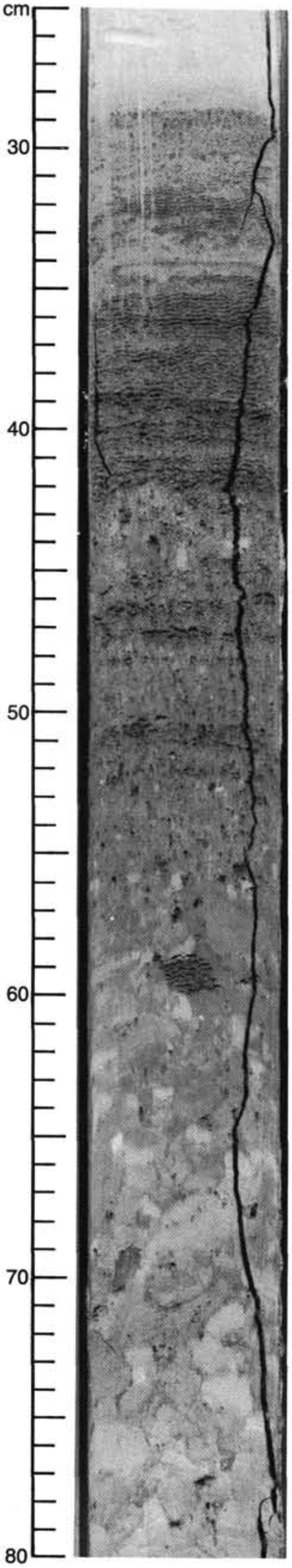

Figure 7. Contact between upper part of debris flow with deformed multicolored nannofossil ooze/mud clasts and overlying nannofossil sand (Sample 107-653A-3H-5, 25-80 cm).

and nannofossil oozes without interbedded sapropels and volcaniclastic deposits, and by higher carbonate contents (average 60% with a minimum value of 30% and a maximum of 91%). These oozes are light gray and light brown with gradational contacts; black specks of hydrotroilite are scattered throughout. Burrowing is noticeable and common. A few thin foraminifer-rich sands occur.

Subunit Ic: Cores 107-653A-23X-6 to 107-653A-25X-1, 23 cm; depth 210.1-221.6 mbsf; thickness: 11.5 m. Cores 107-653B-23X-2 to 107-653B-24X-1, 50 cm; depth 209.1-216.6 mbsf; thickness: 7.5 m.

Subunit Ic is characterized by reddish brown, yellowish brown, and red calcareous muds and marly nannofossil oozes. These colors define this subunit and are probably caused by a considerable mixture of iron oxides (limonite, hematite, and/or goethite) in the sediment. Carbonate content (measured in Hole 653B) varies between 42% and 60% (similar to three values measured in the lower portion of Subunit Ib), but decreases in the lowest meter of Subunit Ic.

The basal sedimentary sequence at the contact with Unit II consists of, in sequential order downsection:

(a) olive brown, dark brown, or red mud/marl
(b) gray calcareous mud/marl
(c) thin layer of gypsum- and biotite-bearing sand
(d) interval of calcareous(?) mud and intercalated sand (bearing gypsum), interpreted as a drilling breccia in the visual core description
(e) thick gypsum- and biotite-bearing sand.

This stratigraphic sequence was cored in Hole 653A; the sequence in Hole 653B is the same except for the absence of the thin sand layer (c). Since layer (d) occurs on the top of a core in both holes, this layer may be an artificial one caused by fill in the hole. Thus, layer (c) in Hole 653A may be considered as the top of layer (e).

We place the boundary between lithologic Units I and II at the top of the sand layer (Hole 653A, (c); Hole 653B, (e)) and presume this to be equivalent to the boundary between lithologic Units II and III in DSDP Site 132. Note that this position is slightly below the biostratigraphically-defined Messinian/Pliocene boundary (see "Biostratigraphy" section, this chapter).

Unit II

Cores 107-653A-25X-1, 23 cm, to 107-653A-26X, CC; depth 221.6-240.7 mbsf; thickness: 19.1 m. Cores 107-653B-24X-1, 50 cm, to 107-653B-28X, CC; depth 216.6-264.3 mbsf; thickness: 47.7 m. Age: Messinian.

Unit II represents sediments deposited in restricted marine to evaporitic and continental(?) environments.

At Hole 653A, drilling was terminated after penetration of the first gypsum-bearing sediments, thus little of Unit II was recovered. At Hole 653B, however, a considerably thicker sequence of Messinian sediments was cored. In both holes recovery was poor with concomitant drilling disturbances (observed and inferred).

The sequence (described from top to bottom) starts with a layer of dark gray biotite- and gypsum-bearing sand (noted above as (c) plus (e) in Hole 653A and as (e) in Hole 653B) about 70-110 cm thick (Cores 653A-24X, CC and 653A-25X, Sections 1 and 2; 107-653B-24X, Sections 1 and CC) (Fig. 8). This sand has faint parallel laminations. Cross-bedding as described at Site 132 was not obvious. This sand layer is followed in Hole 653A by 1.2 m of gray and red calcareous clay to nannofossil mud (Core 107-653A-25X, Sections 2 and CC) and by a very friable gypsum with wavy laminations (possibly stromatolitic), which was brecciated by drilling (107-653A-25X, CC) (Fig. 9). Then

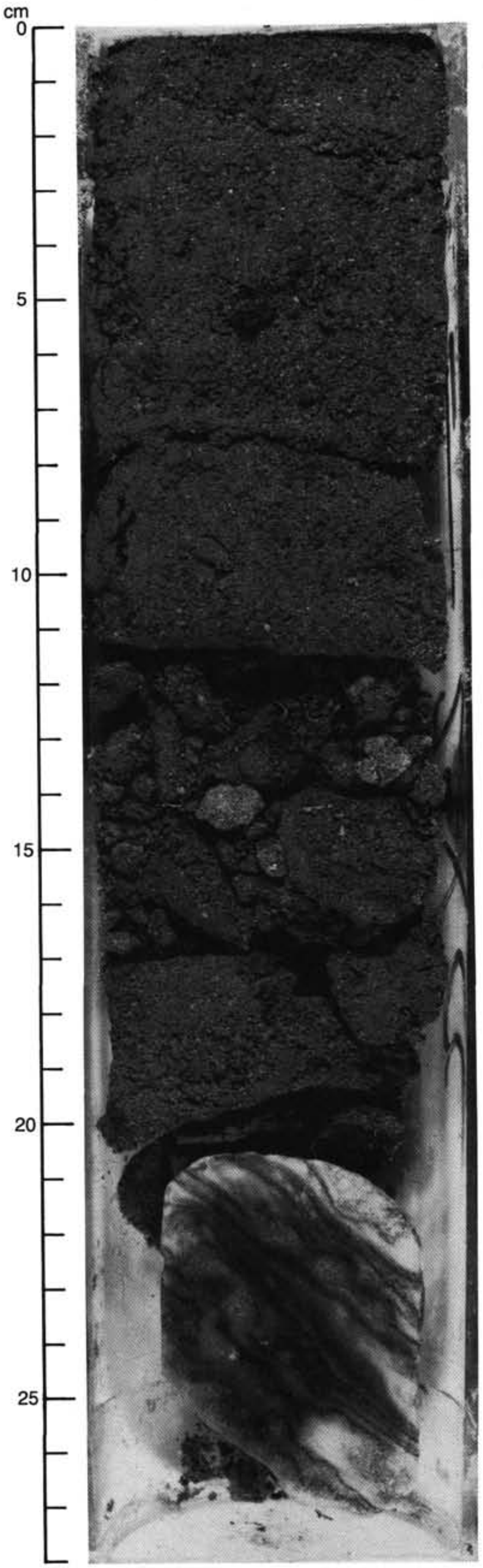

Figure 8. Base of the biotite- and gypsum-bearing sand in the uppermost part of Unit II and the first gypsum layer in Hole 653B (contact deformed by drilling) (Sample 107-653B-24X, CC, 0–28 cm).

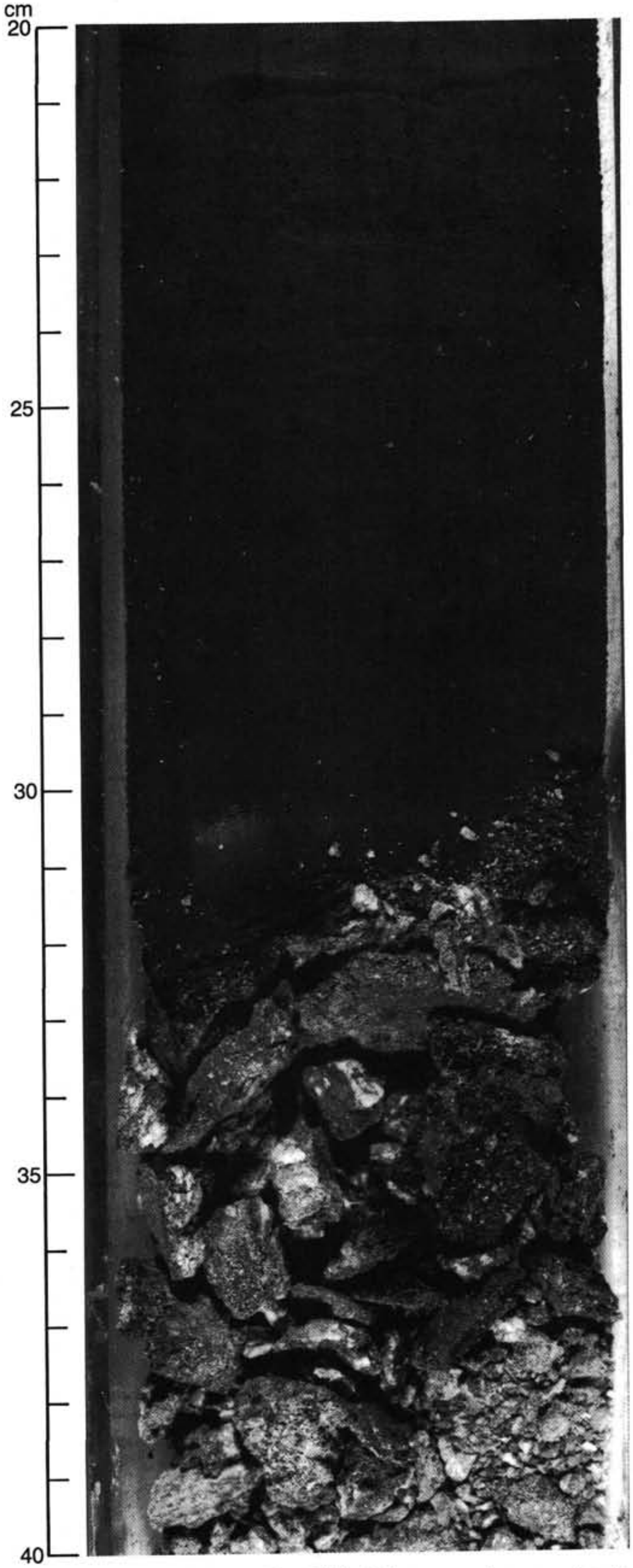

Figure 9. Contact (deformed by drilling?) between calcareous clay to nannofossil mud and the uppermost, very friable gypsum with wavy laminations in Unit II of Hole 653A (Sample 107-653A-25X, CC, 20–40 cm).

follows an olive gray nannofossil- and foraminifer-bearing marly calcareous (or dolomitic) mud about 3.5 m thick with fine laminations. Centimetric to decimetric intercalations of large (as much as a centimeter) lenticular gypsum crystals occur throughout this mud (Core 107-653A-26X-1 to CC) (Fig. 10). Their euhedral character suggests secondary displacive growth during early synsedimentary diagenesis; their concentration at specific intervals suggests nucleation along sedimentary horizons, whose original characteristics and paleoenvironmental significance now seem lost. At the base of Hole 653A there is a piece of calcareous (calcite-cemented?) siltstone and a basal 2-cm-thick layer of calcareous mud (Core 107-653A-26X, CC).

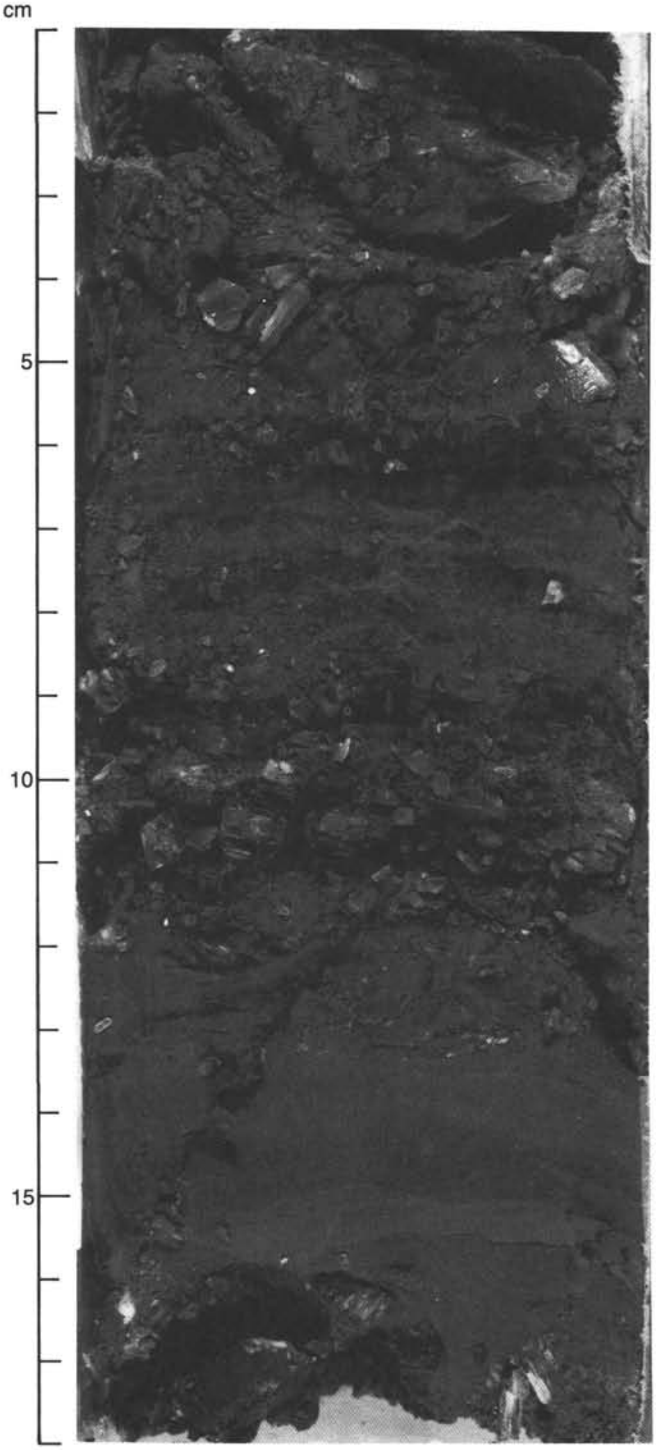

Figure 10. Intercalations of lenticular gypsum (secondary growth) within nannofossil- and foraminifer-bearing marly calcareous (or dolomitic) mud showing fine laminations, Unit II of Hole 653A (Sample 107-653A-26X-3, 1-18 cm).

In Hole 653B the biotite- and gypsum-bearing sand is underlain by about 90 cm of cloudy (see Fig. 8) to balatino-type laminated gypsum (Cores 107-653B-24X, CC to 653B-25X-1). Between 85 and 90 cm in Section 107-653B-25X-1 there occurs a siltstone. Underlying this is an additional 3 cm of balatino-type gypsum.

Below this laminated gypsum, dark gray to olive gray and, at the base, red dolomitic nannofossil muds are interbedded with nodular and lenticular gypsum (Cores 107-653B-25X-1 through 107-653B-27X, CC). The host mud becomes progressively enriched in dolomite and silt-sized gypsum downsection in Hole 653B, with fewer nannofossils. Interbedded throughout this sequence are centimeter-thick layers of black shales. They have a well-developed fissility and contain wavy, thin laminae of gypsum. Core 107-653B-27X, CC, contains putrid-smelling and brilliantly red and yellow colored muds and silts interbedded with white/gray/black wavy-laminated gypsum. The odor and red and yellow colors are tentatively attributed to the presence of sulfur and of iron oxides (hematite, limonite, and/or goethite). The oldest cored sediments are represented by calcareous clays/muds of grayish, brownish, and yellowish colors and three several decimeter-thick layers of powdery white gypsum. Carbonate content within the muds is low (8%-24%). This sequence is disturbed by drilling.

Sedimentation Rates (Hole 653A and Site 132)

Average sedimentation rate for the Pliocene-Quaternary sequence of Hole 653A is 3.9 cm/1000 yr (not corrected for compaction). For Site 132, an average rate of 3.4 cm/1000 yr can be calculated based on a thickness of 183 m and an age of 5.4 m.y. for the Messinian/Pliocene boundary.

In Hole 653A the Pliocene-Quaternary sequence can be divided into three intervals as has been done for Site 132:

	Sedimentation rate (cm/1000 yr)	
	653A	132
Pleistocene	4.8	4.4
D. brouweri ex. to *Globorotalia margaritae* ex.	4.4	3.2
G. margaritae ex. to Messinian/Pliocene boundary	2.7	2.8

The downsection decrease in sedimentation rate apparent in these intervals may be an artifact due to compaction deeper in the sediment column. The second column of the table shows sedimentation rates of Site 132 for intervals delimited by the same biostratigraphic events used for Site 653. These rates differ from those published by Ryan, Hsü, et al. (1973), because new absolute data have been used for the biostratigraphic events. Average sedimentation rate at Hole 653A is about 0.4 cm/1000 yr higher than it is in Site 132.

Correlations: Holes 653A and 635B — Hole 132

Tentative correlations can be attempted between DSDP Site 132 and Holes 653A and 653B. Correlations are based mainly upon lithologic criteria from smear-slide data and visual core descriptions for all cores but also upon the similarity in sedimentation rates.

It must be emphasized that these correlations are attempted between cores that represent: first, incomplete recovery of cored intervals, often as low as 17% in the Messinian stratigraphic section; second, sediments originally deposited in an environment where significant and rapid lateral changes in facies would be expected, particularly in the Messinian stratigraphic section; and third, different coring techniques. All of these place serious constraints on the quality of correlations attempted.

Pliocene-Quaternary

Correlation has been made for Subunit Ia in Holes 107-653A and 107-653B using clearly corresponding sapropels and ash layers as well as foraminifer sands, debris flow deposits, and color boundaries (Fig. 11A in back pocket). This correlation shows that:

1. Unrecovered gaps of varying thicknesses can be inferred between the base of one core and the top of the subsequent core in most cases. In contrast, between Cores 107-653A-9H and 653A-10H), the base and top seem to overlap.
2. At the top of a core there is often soft, highly disturbed sediment. Sometimes it seems to represent the autochthonous but disturbed interval. Sometimes, however, the top of a core seems to represent sediments which have filled the bottom of the hole between recovery of the two cores.
3. Differences in thickness of corresponding intervals in the two holes can be caused by drilling disturbance, but can also be due to different sedimentation rates or slumping processes.

Detailed correlations between the physical stratigraphy of Core 107-653A-1H and the upper 3 m of Core 107-653B-1H are sketched in Figure 11B. The differing thicknesses, or recovery, of equivalent sediment sequences between the two cores is interesting, especially considering the small (55 m) distance separating the holes. Indeed, a half-meter sequence of light-grey soupy muds recovered in Sections 2 and 3 of 107-653B-1H was not recovered in Hole 653A. Yet a gray-brown mud layer in Core 107-653A-1H was shortened considerably in Hole 653B. The first piston core of Hole 653B was shot from a position closer to the seafloor than the first core of Hole 653A. As each subsequent core was advanced by one pipe joint, a vertical offset was maintained between the cores for Holes 653A and 653B. Thus initial seafloor penetration at Hole 653A was 3.6 m, while at Hole 653B penetration was 6.1 m; however, any offset resulting from these efforts is not apparent in the first core but does become noticeable farther downsection where cores recovered slightly stiffer sediment.

On the basis of gross lithologic similarities represented by lithologic units, Site 132 and Holes 653A and 653B can be compared as follows:

Site 132	Holes 653A and 653B
Unit I	Ia
Unit II	Ib
	Ic
Unit III	II

The differing thickness of the entire section, of individual lithologic units, and position of correlative layers (discussed below) can in part be attributed to differing drilling and coring techniques between rotary (Leg 13) and advanced piston coring/extended core-barrel coring (Leg 107).

Some sedimentary layers seem applicable for attempting finer-scale correlations between these holes. A prominent quartz-rich (smear slide = 50% quartz) sand layer, about 20 cm thick, is described in Core 132-1R-2, 60–80 cm, at about 2.6–2.8 mbsf, the only such layer described in the Pliocene-Pleistocene sequence at this site. This would seem to correlate to a quartz-rich sand layer in Cores 107-653A-2H-6, 65–80 cm, at 11.85 mbsf (smear slide = 20% quartz; 15 cm thick) and 107-653B-1H-4, 110–118 cm, at 5.7 mbsf (smear-slide = 43% quartz; 8 cm thick), both the only quartz-rich sands in the upper 12 m at either Leg 107 holes.

Some volcanic ash layers also are correlative. Two occur near the boundary between Units Ia and Ib (Site 653), and one occurs near the boundary between lithologic Units I and II (132). In Holes 653A and 653B, the lower ash layer contains a distinctive zeolite, the other is distinctive by its induration. In Hole 653A, the zeolitic ash lies at 85.6 mbsf; the indurated ash lies above this at 82 mbsf. In Hole 653B, the zeolite-bearing ash lies at 85.88 mbsf; the indurated ash lies above this at 81 mbsf. All are 2 cm, or less, in thickness. The indurated ash at Hole 653B occurs in lithologic Subunit Ia. All others occur within Subunit Ib, just below (1.6–6 m) the contact with Subunit Ia. In Hole 132, the tephra is described as "thin" (site chapter description) and occurs at about 49.3 mbsf, 0.7 m above the lithologic Unit I and II contact (or the Unit Ia-Ib contact at Site 653). It is described as indurated and containing zeolites, but further mineralogical criteria are not available. Thus, it may be correlative with either of the ash layers described in Holes 653A and 653B. At all holes, these are the only ash deposits described within 15 or more meters of section.

Unfortunately, the sapropel layers in Holes 653A and 653B cannot be correlated to Site 132 because core descriptions for the hole drilled earlier do not identify sapropels.

Intervals of poor recovery are obvious in Cores 107-653A-15X (37.7%) and 107-653B-14X (27.8%). These intervals correspond due to the vertical offset mentioned above. Similar poor recovery is reported from Site 132, Core 14 (29%) at a comparable depth below seafloor. This points to a distinct layer which has been washed out in all three holes.

Messinian

The lithologic similarities of Messinian sediments recovered in Site 132 and both holes of Site 653 are obvious. Nevertheless, an exact correlation between the three holes cannot be made because (1) the recovery varied considerably (17%–68% in Holes 653A and 653B, 0%–80% in Site 132), (2) the sub-bottom penetration was different, and (3) one has to expect rapid changes of lithology within short lateral distances caused by little rises or drops of water level or small changes of relief due to tectonic activity.

At all three sites, muds of brownish (and in Site 653, grayish) colors are underlain by a sand layer (biotite- and gypsum-bearing sand in Site 653 holes and sand layer with "oblique laminations at the top [and] horizontal laminations below" (Ryan, Hsü, et al., 1973, p. 444)). Below this layer, the occurring lithologies are very similar but the stratigraphic sequence cannot be exactly correlated. For Holes 653A and 653B, the downhole stratigraphic order below the sand layer (a) comprises:

1. For Hole 653A: (b) gray and red calcareous clay to nannofossil mud, (c) very friable gypsum with wavy laminations (possibly stromatolitic), (d) olive gray nannofossil- and foraminifer-bearing marly calcareous (dolomitic?) mud with intercalations of centrimetric lenticular gypsum layers, (e) calcite-cemented siltstone and calcareous mud.
2. For Hole 653B: (b) cloudy and balatino-like laminated gypsum with a 5-cm-thick calcite-cemented siltstone intercalated near the base, (c) dark gray to olive gray dolomitic nannofossil muds interbedded with nodular and lenticular gypsum plus centimetric black shale layers, (d) brilliant yellow and red muds and silts containing iron oxides, sulfur, and sulfates, and (e) grayish, brownish, and yellowish calcareous clays/muds with layers of powdery white gypsum.

Two alternative schemes have been proposed for correlating the Messinian lithologies recovered in Holes 653A and 653B.

1. *Correlation scheme A*: Lithology (a) occurs in both holes. Lithologies (b) and (c) of Hole 653A and lithology (b) of Hole 653B are considered to be lateral facies equivalents. This correlation would then make lithology (d) of Hole 653A equivalent to lithology (c) of Hole 653B. Lithology (e) of Hole 653B may have limited lateral continuity and not reach Hole 653A. Lithologies (d) and (e) of Hole 653B would then be considered stratigraphically deeper than the bottom of Hole 653A.
2. *Correlation scheme B*: Lithology (a) occurs in both holes. The calcite-cemented siltstone of lithology (e) of Hole 653A is correlative with the calcite-cemented siltstone interbedded within lithology (b) of Hole 653B. In that case, lithology (d) of Hole 653A and lithology (b) of Hole 653B must be considered as lateral facies equivalents. Lithologies (c), (d), and (e) of Hole 653B would then be stratigraphically deeper than the bottom of Hole 653A. Lithologies (b) and (c) of Hole 653A have no equivalent in Hole 653B; this may be a drilling artifact because the contact between (a) and (c) seems to be a drilling contact.

BIOSTRATIGRAPHY

Summary

Holes 653A and 653B were drilled in the western Tyrrhenian Sea approximately 1/2 mi northeast of DSDP Site 132. A complete Pliocene-Pleistocene sequence was recovered in both holes, overlying Messinian evaporitic sediments deposited in a somewhat restricted environment.

Site 653 was drilled as reference section for the Mediterranean Pliocene-Pleistocene. The recovery was good. Disturbance due to sedimentary processes and/or to drilling effects were found in the upper part of the Quaternary.

The zonations given by Cita (1973) and Martini (1971) were used for age determinations in the Pliocene (Fig. 12). The sediments are rich in well-preserved micro- and nannofossils which should allow establishment of a precise biostratigraphy. Unfortunately only limited paleomagnetic data were obtained on board.

Benthic foraminifers are rare in the intervals from top to 74 mbsf in Hole 653A and to 75 mbsf in Hole 653B. An increasing number of benthic foraminifers can be observed in the Pliocene with a maximum at 117-146 mbsf in Hole 653A and 120-150 mbsf in Hole 653B corresponding to the lowermost part of the upper Pliocene (at about 3.0-3.2 Ma). This interval is characterized by an increase in primary productivity and an increase of the sediment-accumulation rate.

Based on changes of planktonic foraminiferal assemblages throughout the Quaternary it was possible to identify several isotopic stages and to correlate tephra and sapropel layers.

The earliest Pliocene *Sphaeroidinellopsis* zone (MPl1) is underlain in Hole 653A by 28 m, and in Hole 653B by 39 m, of sand, clay, and evaporitic sediments deposited in a somewhat restricted environment. This interval corresponds to the "non-distinctive" zone of Iaccarino and Salvatorini (1982). The poor planktonic foraminiferal assemblages are represented by *Globigerinita quinqueloba* and *G. glutinata* of small size. Nannofossils are few to common with the same assemblages as above. They are diluted by detrital material and reworked Cretaceous and Paleogene species. Benthic foraminifers are considered as reworked and/or displaced. The mixed assemblages consist of inner shelf to upper slope species of normal marine environment.

These observations indicate that the Mediterranean was not entirely desiccated during latest Miocene time.

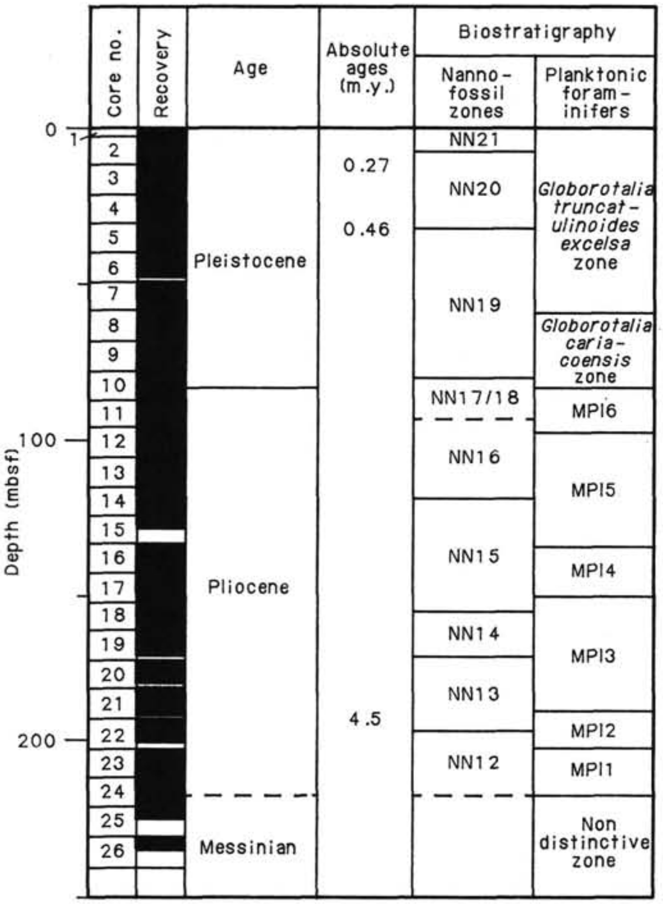

Figure 12. Biostratigraphic determinations made at Hole 653A.

Sedimentation averages 3.9 cm/1000 yr. The rate is higher (about 6.5 cm/1000 yr) within the upper Quaternary, and within the nannoplankton Zone NN16 of late Pliocene age.

Planktonic Foraminifers

Holes 653A and 653B are located 1/2 mi from Site 132 (DSDP Leg 13) where an almost complete Pliocene-Pleistocene section was recovered and extensively studied (Cita, 1973; Ryan et al., 1974; Watkins et al., 1974; Raffi and Rio, 1979; Rio et al., 1984; Thunell and Williams, 1983).

The base of the Quaternary, coincident with the base of *Globigerina cariacoensis* Zone, has been recorded in Sample 107-653A-10X-4, 15-19 cm (84.4 mbsf) at the first peak of sinistral *Neogloboquadrina pachyderma*. *Globigerinoides obliquus* occurs up till Sample 107-653A-10X-1, 129-130 cm (80.7 mbsf). The base of the *Globorotalia truncatulinoides excelsa* Zone was recognized in Sample 107-653A-7H, CC (60.5 mbsf) in which only one specimen is present. This marker is common from Sample 107-653A-6H-2, 30-32 cm (52.6 mbsf) upward.

Holocene was observed at the top of Core 107-653A-1H with the characteristic planktonic assemblage described by Cifelli (1975) from plankton tows and by Parker (1955), Todd (1958), and Thunell (1979) from surface sediments. Sinistral *Globorotalia truncatulinoides excelsa* occur with large *Orbulina universa* (diameter more than 400 μm) and *Hastigerina siphonifera*. *Globigerinita quinqueloba* is relatively more abundant than in the recent sediments. Poorly preserved pteropods are frequent. The presence of *Hyalocylix striata* and *Styliola subula* characterizes the sediments younger than 4000 years. No living benthic foraminifers were found.

The Pleistocene-Holocene boundary should be within Core 107-653A-1H at Hole 653A. The top of Hole 653B has not been studied.

Age determinations for the Pliocene are based on the zonation given by Cita (1973, 1975) and Rio et al. (1984). The base of MPl6 was recognized in Sample 107-653A-12H-1, 19–21 cm (98.4 mbsf). *Globorotalia tosaensis* and its descendant *G. truncatulinoides* s.s. together with *Sphaeroidinella dehiscens* can be observed in Samples 107-653A-11X-4, 30–32 cm (93.7 mbsf) till 107-653A-11X-3, 30–32 cm (92.3 mbsf). They are also present in Sample 653A-10X-6, 75 cm (87.8 mbsf). The lower part of MPl5 was observed in Sample 107-653A-16X-1, 15–17 cm, (136.2 mbsf) where the last *Sphaeroidinellopsis* sp. are present. *Globorotalia margaritae* together with *G. puncticulata* occur for the last time in Sample 107-653A-17X-6, 15–17 cm, (153.3 mbsf) where the base of MPl4 was recognized.

G. puncticulata's first appearance is in Sample 107-653A-21X-3, 15–17 cm (186.3 mbsf) indicating the base of MPl3. MPl2 is recognized between 186.3 and 208.8 mbsf (Sample 653A-23X-5, 75–77 cm) where the first *Globorotalia margaritae* has been recognized.

The *Sphaeroidinellopsis* acme zone (Cita, 1973) has been identified between 208.8 mbsf and 653A-23X, CC (216.1 mbsf). It is underlain by the "non-distinctive" zone of Iaccarino and Salvatorini (1982) characterized by an assemblage of small *Globigerinita quinqueloba* and *G. glutinata*.

In Hole 653A the first occurrence of *Globorotalia margaritae* is in Sample 653A-23X-5, 75–77 cm. In Hole 653B this event occurs in Sample 653A-23X-2, 30–32 cm, and therefore those two levels can be correlated. The last abundant occurrence of *Sphaeroidinellopsis* spp. in Hole 653A is in 653A-23X, CC. In Hole 653B this event is recognized in Sample 653A-23X-4, 75–77 cm. Therefore, those two levels can be correlated. From these correlations it appears that in Hole 653A the MPl2 biozone has a thickness of about 11 m whereas in Hole 653B its thickness in only about 7 m. Bottom topography at the top of the Messinian might explain this difference in thickness in the MPl2 biozone of the two holes.

Benthic Foraminifers

Benthic foraminifers in Site 653 occurred in all the samples from the top, down to 212 mbsf of Hole 653A and from 6 to 216 mbsf of Hole 653B. In the top sample of Core 107-653A-1H, several agglutinated forms and a few calcareous ones can be found. *Placopsilinella* sp., *Ammolagena clavata*, and *Glomospira charoides* are frequent in the assemblage. Among the calcareous species, *Articulina tubulosa* is relatively frequent.

In the interval between 2 mbsf (Core 107-653A-1H-2, 45–47 cm) and 74 mbsf (Core 107-653A-9H-3, 105–107 cm) of Hole 653A, and between 6 mbsf (Core 107-653B-1H, CC) and 65 mbsf (Core 107-653B-7H, CC) of Hole 653B, the species diversity is generally low. *A. tubulosa, Parafissurina* spp., and *Gyroidina neosoldanii* are consistently found in the interval. This assemblage resembles that between 17 and 58 mbsf of the Hole 652A, but displaced specimens included are less frequent than in the latter.

Between 75 mbsf (Core 107-653A-9H-4, 45–47 cm) and 212 mbsf (Core 107-653A-23X, CC) of Hole 653A, and between 74 mbsf (Core 107-653B-8H, CC) and 216 mbsf (Core 107-653B-24X-1, 11–13 cm) of 653B, many species were found, and displaced specimens are very rare. Through the interval of both Holes 653A and 653B, the remarkable trend in the species diversity can be recognized as found in Hole 652A. In Hole 653A, diversity increases from 212 mbsf upsection, and attains a maximum around Cores 107-653A-16X and 107-653A-14X (145–126 mbsf). Between the top of this interval and 70 mbsf (Core 107-653A-8H, CC), many species disappear. In Hole 653B, a maximum abundance is recognized in the interval between Cores 107-653B-16X and 653B-14X (150–131 mbsf). These maximum abundance intervals of both holes correspond to MPl4 zone through the lower part of MPl5 zone of planktonic foraminifers.

In the sequences of both holes the following characteristic occurrences of some species can be found upwards. The first occurrence of *A. tubulosa* is found at 83.9 mbsf (Core 107-653A-10H, 130–131 cm) and at 78 mbsf (Core 107-653B-9H, CC) both in the lower part of *G. cariacoensis* Zone. This level has been found just below the Pliocene-Pleistocene boundary in the Vrica section in Italy (D'Onofrio, 1981), and Leg 13, Site 125 (Raffi and Sprovieri, 1985), as well as in the other sites of this leg. The top level of *C. italicus* is currently understood as just above the base of MPl5 zone (AGIP, 1982; Sprovieri and Barone, 1984), and is also found at the same level in Sites 652A and 654A. *Cibicidoides italicus* disappears above 125.9 mbsf (Core 107-653A-14X, 105–107 cm) and above 131 mbsf (Core 107-653B-14X, CC) both in the lower part of MPl5 zone.

Below the maximum abundance in both holes, *Cibicidoides italicus, C. robertsomianus, Oridorsalis stellatus, Pullenia bulloide*, and *Siphonina reticulata* consistently occur in the interval belonging to MPl4–MPl2 biozones. *Uvigerina pygmaea* consistently occurs in MPl1 and lower part of MPl2 biozones.

Below the base of Pliocene, some specimens can be found in the very fine- to coarse-grained sand layers. The assemblage consists of *Ammonia* spp., *Bolivina* spp., *Bulimina* spp., *Cibicides* spp., *Elphidium* spp., *Gyroidina* spp., *Pullenia* spp., and *Uvigerina* spp., and are frequently associated with echinoid spines and sponge spicules. All the specimens are, however, broken or recrystallized, and seem to be displaced from shallower environment (inner neritic to upper epibathyal zones) and/or reworked from the pre-Pliocene sequences.

Nannofossils

Disturbance was significant within the upper part of the Quaternary due to gravity sliding (sedimentary breccias, slumps) and/or drilling disturbance. Recovery was good in both holes except for Core 107-653A-15R and Core 107-653B-14X belonging to the same biostratigraphic interval (lower Pliocene, NN15). Recovery was also poor within the lowermost part of the series (Messinian). Results given in this report are restricted to Hole 653A, since only core-catcher samples were studied from Hole 653B.

Nannoplankton Zone NN21 (*Emiliania huxleyi* Zone) was determined from Core 107-653A-1H to Sample 107-653A-2H-2, 18 cm, by the presence of *Emiliania huxleyi*. Nannofossils are generally abundant and they are well preserved. They are somewhat diluted within the turbiditic layers by volcaniclastic components, detrital carbonates, and reworked nannoplankton species of Cretaceous to early Pliocene age.

Coccolithus pelagicus, a cold water species, is absent from the surface sediments; it becomes common within Zone NN21 only in a few layers. The *Gephyrocapsa oceanica* Zone (NN20) is present from Samples 107-653A-2H-2, 83 cm, to 107-653A-4H, CC, (6.0–32.3 mbsf). This zone is characterized by the abundance of different species of the genus *Gephyrocapsa*. Very small *Gephyrocapsa* sp. are common in certain levels of Core 107-653A-2H (Zone NN20) where several sapropel layers also occur. The occurrence of this species in the Pacific is linked to rapid changes of the ice volume as inferred from the oxygen isotope record.

Helicosphaera sp. (with two large pores) was observed in Sample 107-653A-3H-1, 40 cm, and becomes common from Samples 107-653A-3H, CC to 107-653A-4H-6, 40 cm, i.e., within the lowermost part of Zone NN20. This species is typical for this stratigraphic interval and was found in all other sites drilled in the Tyrrhenian Sea.

The interval from Samples 107-653A-5H-1, 38 cm, to 107-653A-10H-1, 60 cm (32.5–80.0 mbsf) belongs to the *Pseudoemiliania lacunosa* Zone (Zone NN19). Several sapropel layers are present in Cores 107-653A-5H and 107-653A-7H through 107-653A-9H. This part of the sequence is characterized by the dominance of the small *Gephyrocapsa* sp. between Core 107-653A-6H and the top of Core 107-653A-9H. Only a few large nannofossils occur within this interval.

The last occurrence of *Helicosphaera sellii* was observed in Samples 107-653A-7H-6, 40 cm, within the zone of small *Gephyrocapsa. Discolithina japonica* and *Pontosphaera pacifica* are common within Zone NN19. Large specimens of *Braarudosphaera bigelowi* are common around the Pliocene/Pleistocene boundary as observed at all other sites. This increase is explained by a decrease of surface water salinity due to heavy rainfalls and/or influx of freshwater from the rivers (Müller, 1978; 1985).

In some cases the abundance of *Braarudosphaera bigelowi* corresponds to the formation of sapropel layers (Samples 107-653A-9H-3, 88–90 cm, and 107-653A-10H-2, 96 cm).

The Pliocene/Pleistocene boundary is determined between Sample 107-653A-10H-1, 60 cm, and 107-653A-10H-1, 70 cm (80.0 mbsf) by the extinction of *Cyclococcolithus macintyrei* and the first occurrence of *Gephyrocapsa oceanica*. Discoasters are rare or absent within the uppermost Pliocene. This interval is characterized by small coccoliths and tiny fragments of calcite in certain horizons. Discoasters are common from Sample 107-653A-13H-3, 130 cm. The boundary between nannoplankton Zones NN17/NN18 and Zone NN16 lies between Samples 107-653A-11H-3, 130 cm, and 107-653A-11H-4, 20 cm (93.5 mbsf). Discoasters are still rare within the upper part of Zone NN16; they are common downsection from Sample 107-653A-13H-3, 130 cm. The same observation is described from the other sites and is typical for the western Mediterranean (Müller, 1978; 1985) indicating the initiation of the northern hemisphere glaciation. *Discoaster tamalis* disappears within Zone NN16 (Sample 107-653A-12H-3, 120 cm). Fluctuations in the abundance of the different species of the genus *Discoaster* can be observed throughout the Pliocene. The upper part of Zone NN16 is characterized by the scarcity of *Discoaster surculus*, and the absence of *Discoaster pentaradiatus*, whereas *Discoaster brouweri* is rare. *Discoaster surculus* becomes abundant within the lower part of this zone together with *Discoaster brouweri*.

The *Reticulofenestra pseudoumbilica* Zone (NN15) is recognized from Samples 107-653A-14X-2, 130 cm, to 107-653A-17X, CC (120.3–155.2 mbsf).

The last occurrence of *Reticulofenestra pseudoumbilica* was observed in Sample 107-653A-14X-2, 130 cm, and of *Sphenolithus abies* in Sample 107-653A-14X-5, 130 cm. *Reticulofenestra pseudoumbilica* is smaller within the upper part of Zone NN15 and disappears in several layers. The large specimens of this species are present from Sample 107-653A-15X, CC downsection. Also *Sphenolithus abies* is rare in the upper part of Zone NN15. This part is characterized by the abundance of discoasters (*Discoaster brouweri, Discoaster tamalis, Discoaster asymmetricus*). The discoasters are of large size indicating a change in water masses (3.0–3.4 m.y.). This change seems to be confirmed also by benthic foraminifers which show more diversified assemblages.

The *Discoaster asymmetricus* Zone (NN14) was encountered from Samples 107-653A-18X-1, 60 cm, to 107-653A-19X-5, 80 cm (156.0–171.0 mbsf). Samples 107-653A-19X-5, 140 cm, to 107-653A-22X-2, 130 cm (171.5–196.0 mbsf) belong to the *Ceratolithus rugosus* Zone (NN13). *Discoaster variabilis* is present within the lowermost part of Zone NN14 (Sample 107-653A-19X-4, 100 cm) and upper part of Zone NN13 where this species becomes more frequent (Core 107-653A-20X). Below this level it occurs only sporadically. The same observation was made in the other sites and it seems that in the Tyrrhenian Sea its presence can be used as a stratigraphic marker. This peak of *Discoaster variabilis* in the Mediterranean does not correspond with that described by Backman and Schackleton (1983) at 3.4–3.6 m.y. from the world oceans. The discoasters are generally few in Zone NN14 dominated by *Discoaster brouweri* and in several horizons by *Discoaster asymmetricus; Discoaster surculus* and *Discoaster pentaradiatus* are few to rare. *Discoaster tamalis* has its occurrence within the lowermost part of Zone NN14. *Discoaster pentaradiatus* becomes common within certain levels of Zone NN13.

The *Amaurolithus tricorniculatus* Zone (NN12) was encountered from Samples 107-653A-22X-3, 110 cm, to 107-653A-24X-5, 100 cm (197.5–219.0 mbsf). The sediments are rich in nannofossils; within the lowermost part of this zone, corresponding to foraminifer zone MPl1, the nannofossils are of smaller size. At the same time discoasters become less frequent and the color of the sediments changes from beige above to reddish brown below.

The definition of the Miocene/Pliocene boundary in the Mediterranean is determined by the re-establishment of permanent open ocean conditions. Within the uppermost part of the Miocene sediments, nannofossils are less common and are diluted by detrital material, secondary dolomite, and reworked Cretaceous to middle Miocene nannofossils. Diagenesis is also an important factor controlling the abundance of nannoplankton. The assemblages are less diversified consisting predominantly of *Reticulofenestra pseudoumbilica, Discolithina multipora, Coccolithus pelagicus, Helicosphaera carteri, Cyclococcolithus leptoporus*, and *Sphenolithus abies* of often smaller size. Discoasters are few to rare as well as *Amaurolithus delicatus*.

The red clays in Core 107-653A-25X are barren of nannofossils. Below this level nannofossils are few and of smaller size reflecting somewhat restricted marine conditions.

PALEOMAGNETICS

This site was to be the prime site for magnetostratigraphic, biostratigraphic, and isotopic correlation in the Pliocene-Pleistocene. Double APC/XBC coring gave us the the potential for complete undisturbed recovery. Unfortunately, the magnetic properties of the cores were much more complex than at the three previous sites. Rather than a straightforward drill-string viscous overprint, which was easily removed by alternating field (AF) demagnetization, here we had a higher coercivity secondary magnetization not easily removed by alternating fields. The origin of this secondary overprint is presently unclear. We hypothesize that the overprint is due to diagenetic growth of iron mono-sulfides (namely mackinawite, troilite) some of which are ferromagnetic (s.l.). These meta-stable sulfides can revert to more stable sulfides such as pyrite or pyrrhotite, of which pyrrhotite can be ferrimagnetic. In more oxidizing conditions, goethite and/or hematite may grow as the stable iron phase, although it is unclear at present to what extent this has occurred at this site. Iron mono-sulfides are ubiquitous in smear slides and pyrite/pyrrhotite becomes common in the Pliocene.

Three hundred forty-eight discrete 7-cm^3 samples were collected from Hole 653A, and twenty-one from Hole 653B. We intend to study the downhole variations in magnetic phases in order to determine the sequence of diagenetic changes that accounts for the secondary magnetic overprint. This site provides the opportunity for a detailed study of the magnetic properties of iron sulfides and the variations in magnetic properties which accompany the downhole phase changes. From Core 107-653A-17X downward, we observe a sequence of reversals where the characteristic component appears to be carried by magnetite.

We are confident that after thermal demagnetization on shore, we will be able to isolate a primary magnetic stratigraphy from this lower Pliocene part of the section. Above this level, it is unclear whether the primary detrital or biogenic magnetite has survived the rigors of diagenesis, and here the iron mono-sulfides may be derived in part from primary magnetite.

Volume susceptibility was measured on all cores from Holes 653A and 653B prior to splitting using the Bartington Core Scanning Loop Sensor (Fig. 13). These susceptibility data provide a means of correlation between holes, although there is a general lack of distinctive features in the curves to facilitate this correlation. Very variable susceptibility values are recorded in the top 45 mbsf. The values range up to 1.65×10^{-4} c.g.s. in this interval (the plots are cut off at values of 6×10^{-5} to more clearly illustrate variations farther downcore). We interpret this pattern as indicating variations in concentration of magnetite which in turn reflects variations in the amount of volcanogenic detritus. Individual volcanic-rich layers should be correlative in this interval.

The decrease in the variability and mean of susceptibility values from 40 to 75 mbsf may indicate that the primary detrital magnetite is being reduced to iron mono-sulfide in this interval (iron sulfides have much lower susceptibilities than magnetite). However, this decrease also coincides with the lithologic change between lithologic subunits 1a and 1b; the former being characterized by thin tephras, the latter by their absence. The mean susceptibility decreases down to 150 mbsf where values begin to climb to the Miocene/Pliocene boundary at approximately 221.4 and 216.1 mbsf in Holes 653A and 653B, respectively. The rapid climb in mean susceptibility from about 205 mbsf to the boundary coincides with the reddening of the sediment (denoting the presence of iron oxides) which first appears in Core 23X-2 in both holes. Negative susceptibility values at 225.7 and 226.7 mbsf characterize the gypsum in Core 107-653B-25X-1.

PHYSICAL PROPERTIES

Introduction

At Site 653, Cores 107-653A-1H to 653A-23X and 107-653B-21X to 653B-28X were used for shipboard analysis of bulk density, porosity, grain density, and velocity. Thermal conductivity was measured on all cores of Hole 653A and on all sections of Hole 653B. Shear strength measurements were done on each core of Hole 653B. Results for Site 653 are discussed below.

Physical properties measured at Site 653 include GRAPE density and thermal conductivity from full-round core sections, and vane shear strength, compressional wave velocity, and index properties (porosity, bulk density, and grain density) from split sections. Methods of analysis are described in the "Explanatory Notes" chapter, this volume.

Results

Index Properties and Compressional Velocity

Porosity, bulk density, grain density, and compressional velocity from Holes 653A and 653B are plotted relative to subbottom depth in Figures 14–16 and are listed in Tables 2–5.

In Hole 653A, grain density is near constant (2.7–2.9 g/cm^3) from the mud line to 196 mbsf. Below that depth, higher grain densities were measured. The data from Hole 653B (195–256 mbsf) also remain constant. One high value (3.96 g/cm^3) can be noted at 251 mbsf and is related to hematitic clays. The bulk density values are in good agreement with the porosity values and reflect the same trend along the cores.

Three main physical property units can be distinguished in Site 653:

Physical Property Unit 1: This unit appears as an increase in bulk density from 1.5 g/cm^3 at the seafloor to 1.80 g/cm^3 at 40 mbsf, and a decrease in porosity from 75% at the mud line to 61% around 40 mbsf (Fig. 14).

Physical Property Unit 2: This unit was recognized from 40 mbsf to the bottom of Hole 653A and was also observed in Hole 653B down to 213 mbsf. Unit 2 shows a constant decrease of porosity (61% to 54%) and quite constant bulk density values from 1.80 g/cm^3 to 1.90 g/cm^3 at the base of the unit.

Physical Property Unit 3: Observed between 216 mbsf and the bottom of Hole 653B, this unit is bounded at its top by an increase of bulk density and a decrease of porosity corresponding to the gypsum layers. Deeper (230 mbsf), the bulk density and porosity values reflect the lithology. The calcareous claystones, the gypsum, and the selenite samples have high density (2.03 g/cm^3 to 2.62 g/cm^3) and low porosity (down to 20%); the noncalcareous samples have low density (1.8 g/cm^3). The last sample was taken from a sand layer and shows both high porosity and high bulk density.

The compressional wave velocity plot (Fig. 16) also shows two main trends:

1. Unit 1: Recognized in Hole 653A from the mud line to about 213 mbsf, this unit was sampled in Hole 653B between 196 and 214 mbsf. The velocities measured on samples remain constant with an average value of 1.636 km/s.
2. Unit 2: This unit was sampled only in Hole 653B, between 225 mbsf and the bottom of the hole. This trend is characterized by high values measured on gypsum samples.

Shear Strength

Measurements were done in Hole 653B (Tables 6 and 7) between the sea floor and 217 mbsf (Fig. 17). The data show an increase vs. depth from the seafloor to 125 mbsf (50–60 kPa) with high values at 50 mbsf (60–80 kPa) and at 123 mbsf (95 kPa), related respectively to indurated volcanic ash layers and probably to diagenetic laminations. The shear strength remains constant in the interval 126–190 mbsf. Below, an increase was measured in the reddish layers (200–216 mbsf). These high values can also be explained by diagenetic processes.

Thermal Conductivity

Due to an abnormal decrease of the geothermal gradient, particular attention was given to thermal conductivity at Site 653. Thermal conductivity was routinely measured on each core of Hole 653A and was measured on each section (sometimes more frequently) at Hole 653B. The results are plotted in Figure 18 and are listed in Tables 7 and 8.

Results from Holes 653A and 653B correlate relatively well. Both holes have a downhole increasing thermal conductivity from 2.5×10^{-3} cal $\times$ °C^{-1} $\times$ cm^{-1} $\times$ s^{-1} at the sea floor to 3.6×10^{-3} cal $\times$ °C^{-1} $\times$ cm^{-1} $\times$ s^{-1} in Hole 653A and 3.1×10^{-3} cal $\times$ °C^{-1} $\times$ cm^{-1} $\times$ s^{-1} in Hole 653B at about 120 mbsf in both holes. Below that depth a slight discrepancy appears: Hole 653A shows a gentle decrease of thermal conductivity from 3.0×10^{-3} cal $\times$ °C^{-1} $\times$ cm^{-1} $\times$ s^{-1} to about 2.9×10^{-3} cal $\times$ °C^{-1} $\times$ cm^{-1} $\times$ s^{-1} at 220 mbsf. Hole 653B shows constant values of about 2.9×10^{-3} cal $\times$ °C^{-1} $\times$ cm^{-1} $\times$ s^{-1} from 120 to 157 mbsf. Then the thermal conductivity increases up to 3.23×10^{-3} cal $\times$ °C^{-1} $\times$ cm^{-1} $\times$ s^{-1} at 181 mbsf. Below that depth it decreases to 2.92×10^{-3} cal $\times$ °C^{-1} $\times$ cm^{-1} $\times$ s^{-1} at 213 mbsf.

The top of the evaporitic series is marked in both holes by an important increase of thermal conductivity, which reaches 4.5

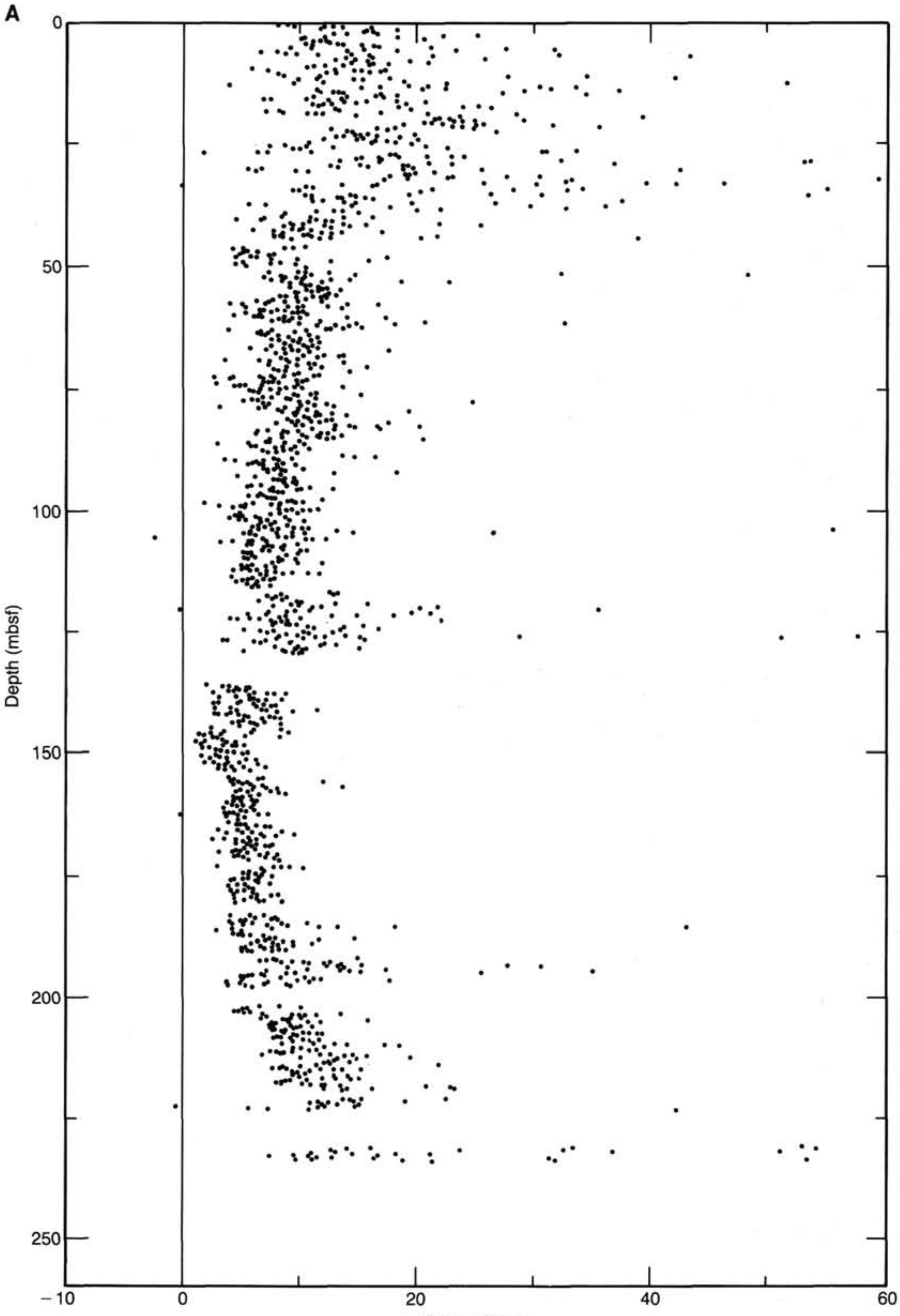

Figure 13. Magnetic-susceptibility values (× 10^{-6} G/Oe) plotted vs. depth for: A. Hole 653A. B. Hole 653B. See text for discussion of variations.

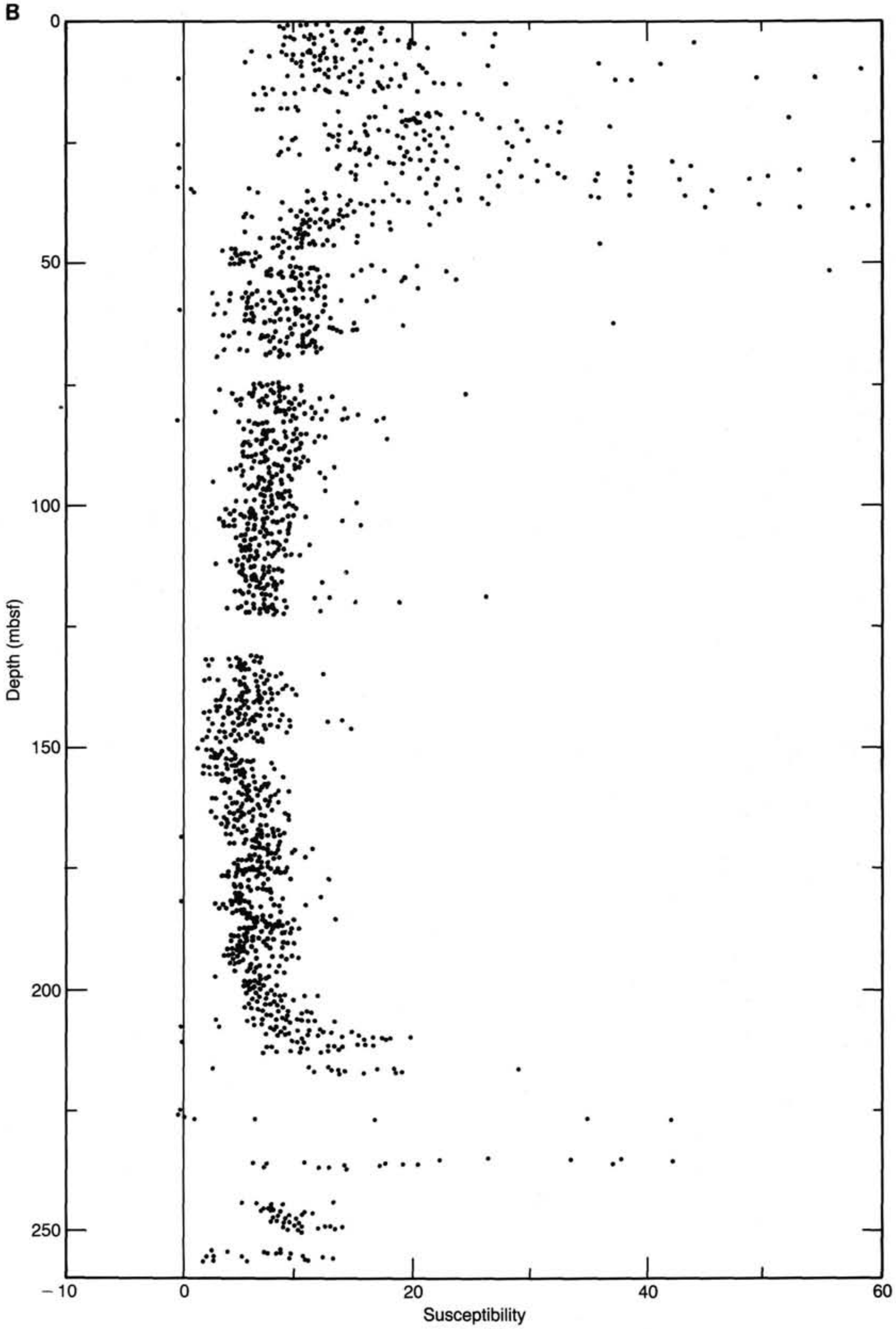

Figure 13 (continued).

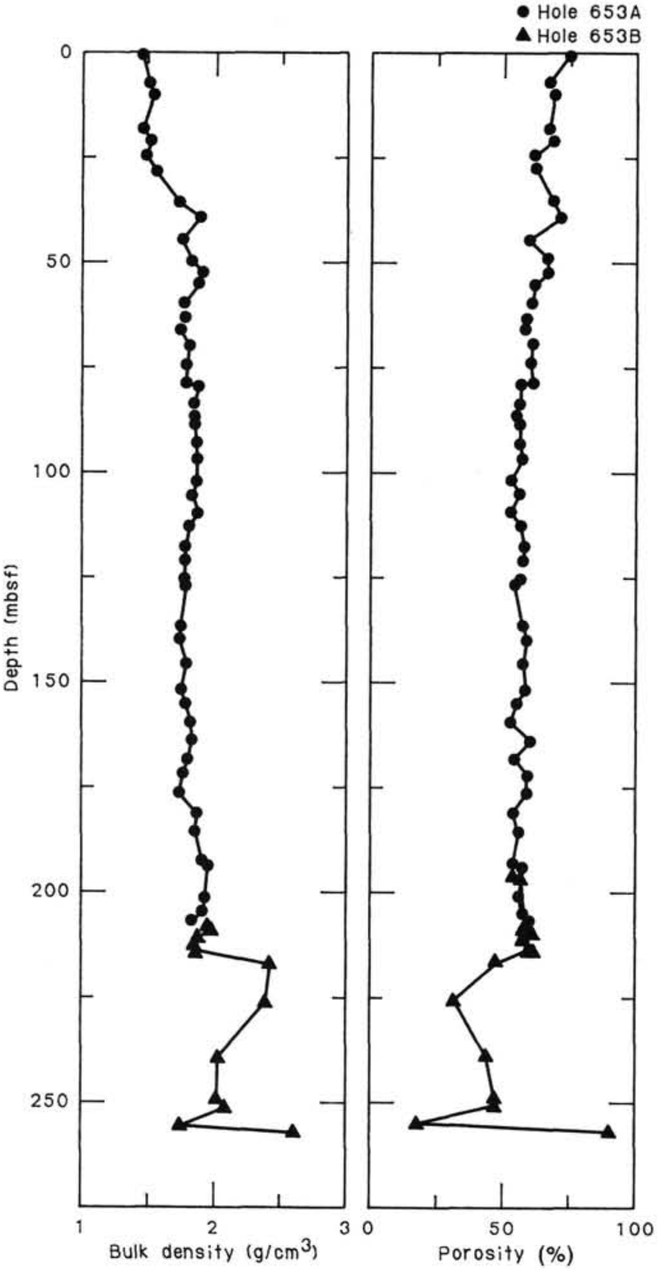

Figure 14. Bulk density and porosity vs. depth at Site 653.

× 10^{-3} cal × °C^{-1} × cm^{-1} × s^{-1} in Hole 653B and 3.35 × 10^{-3} cal × °C^{-1} × cm^{-1} × s^{-1} in Hole 653A. Below, Hole 653A shows values ranging between 2.3 and 3.1 × 10^{-3} cal × °C^{-1} × cm^{-1} × s^{-1}. Hole 653B, which penetrated deeper, indicates that the thermal conductivity of the nonevaporitic Messinian is comparable to the values of the Pliocene-Quaternary series. In summary the Miocene-Pliocene boundary at Site 653 appears to be an important thermal conductor.

INORGANIC GEOCHEMISTRY

Carbonate Analyses

Holes 653A and 653B, intended to provide a high resolution profile of the Pliocene-Quaternary sedimentation of the Tyrrhenian Sea, are treated together in this section. Because of the similarities in lithologies recovered and in the different sampling and analytical strategies employed for these holes, results for one hole may be applicable for the other. In addition to the dense sampling strategy for shore-based high-resolution biostratigraphic, isotopic, and magnetostratigraphic work, we decided to sample and analyze a large number of carbonate samples of sediments from Hole 653A. Taken in two distinct intervals of each section, these analyses may provide a basis for a high resolution carbonate stratigraphy, when compared to results of the above mentioned stratigraphic methods. Results of these analyses are listed in Table 9 and depicted as depth plots in Figure 19. Much less densely sampled, the corresponding plot of calcium carbonate concentrations vs. depth for Hole 653B (Fig. 19) appears to lack the pronounced fine-scale variability of Hole 653A. That this is an artifact of sampling becomes apparent in three more-densely-sampled cores from Hole 653B (Cores 653B-7H, 653B-15X, and 653B-23X), where fluctuations are as intense as in sediments of Hole 653A.

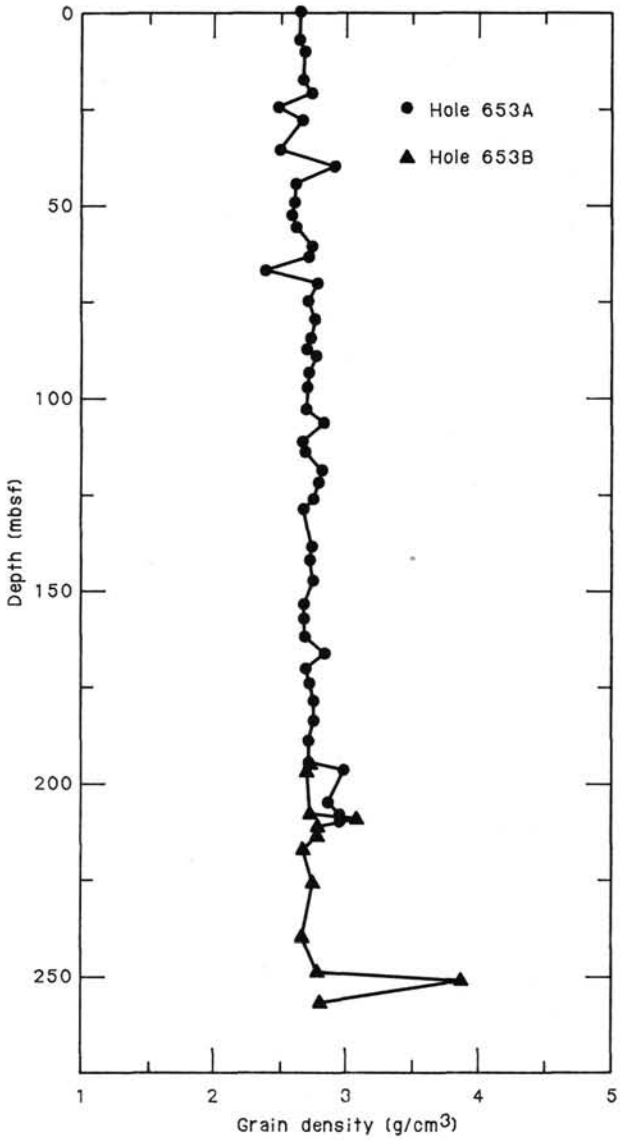

Figure 15. Grain density vs. depth at Site 653.

Variability of $CaCO_3$ concentrations in the Quaternary of Hole 653A (Core 653A-1H to Section 653A-9H-7, 54–55 cm; 0–79.5 mbsf) indeed is very high with values ranging from 1 to 67

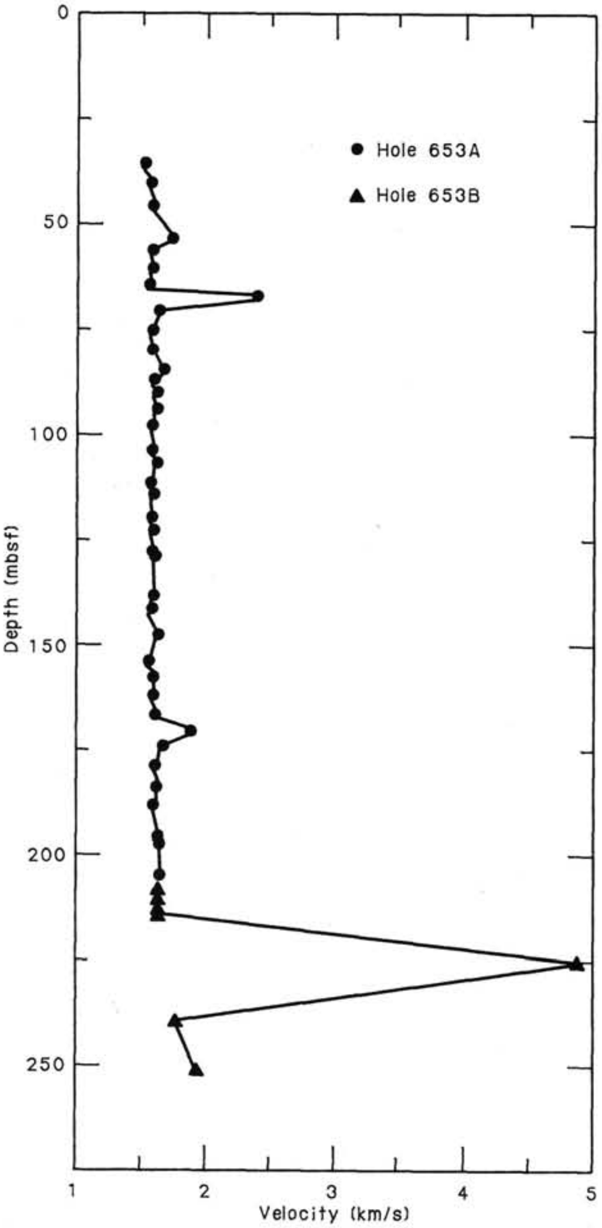

Figure 16. Velocity vs. depth at Site 653.

weight %. A distinct climatic signal is not readily discernible. As a follow-up, correlation studies on smoothed carbonate data sets, faunal, and isotopic curves have to be performed to verify the hypothesis of a climatic impact on $CaCO_3$ sedimentation in this area.

A gradual downsection increase of $CaCO_3$ in the less variable Pliocene sediments leads to a peak between 140 and 160 mbsf, corresponding to Cores -17X and -18X. This interval, according to paleontological investigation, marks the transition from lower to middle Pliocene. For further discussion of carbonate data, the reader is referred to "Lithostratigraphy" section, this chapter.

Interstitial Waters

Results of chemical analyses of interstitial waters sampled in Holes 653A and 653B are presented in Table 10 and Figures 20A and -B. As observed in previous holes of this leg, gradients of

Table 2. Physical properties index, Hole 653A.

Core section	Interval (cm)	Depth sub-bottom (m)	Bulk density (g/cm^3)	Porosity (%)	Grain density (g/cm^3)
1H-1	69–71	0.70	1.48	76.4	2.70
2H-3	69–71	7.39	1.52	69.8	2.70
2H-5	69–71	10.20	1.55	71.5	2.72
3H-4	69–71	18.40	1.47	69.9	2.72
3H-6	69–71	21.40	1.53	71.1	2.78
4H-2	68–70	24.88	1.50	64.0	2.54
4H-5	68–70	28.38	1.56	64.4	2.71
5H-3	69–71	35.89	1.75	71.3	2.55
5H-6	69–71	40.09	1.91	74.4	2.97
6H-3	69–71	45.29	1.77	61.8	2.67
6H-6	80–83	49.80	1.48	69.0	1.90
7H-2	80–83	53.31	1.92	68.9	2.65
7H-4	69–72	56.20	1.90	63.8	2.68
7H-7	68–71	60.70	1.79	62.6	2.80
8H-3	68–71	64.20	1.79	60.2	2.78
8H-5	68–71	67.20	1.75	59.7	2.46
9H-1	69–72	70.70	1.82	62.5	2.84
9H-4	68–71	75.20	1.80	62.6	2.76
9H-7	67–70	79.70	1.79	62.8	2.83
10H-1	69–71	80.30	1.90	58.0	2.81
10H-4	93–96	85.05	1.85	57.8	2.78
10H-6	69–72	87.80	1.87	56.7	2.75
11H-1	68–71	89.70	1.86	57.8	2.83
11H-4	69–72	94.20	1.88	57.6	2.78
11H-C	7–10	98.10	1.86	58.9	2.76
12H-4	69–71	103.40	1.87	55.3	2.76
12H-6	69–71	106.40	1.85	58.3	2.90
13H-3	69–71	111.40	1.90	54.7	2.73
13H-5	69–71	114.40	1.82	58.1	2.76
14X-2	69–71	119.50	1.80	60.5	2.88
14X-4	69–71	122.50	1.79	59.7	2.86
15X-1	69–71	127.30	1.78	58.5	2.82
15X-2	69–71	128.80	1.80	56.7	2.76
16X-1	69–71	138.80	1.77	58.9	2.80
16X-3	68–70	141.80	1.75	60.6	2.78
17X-2	69–71	147.80	1.81	58.9	2.80
17X-6	69–71	153.80	1.77	60.2	2.75
18X-2	69–71	157.40	1.81	56.9	2.74
18X-5	69–71	161.90	1.85	54.6	2.76
19X-2	69–71	166.30	1.84	62.5	2.91
19X-5	69–71	170.50	1.82	55.7	2.76
20X-1	69–71	174.40	1.76	61.1	2.78
20X-4	69–71	178.90	1.74	60.9	2.83
21X-1	69–71	183.90	1.89	55.0	2.83
21X-4	65–68	188.35	1.86	57.5	2.79
22X-2	96–99	195.37	1.93	55.7	2.81
22X-3	65–68	196.55	1.98	60.0	3.07
23X-2	69–71	204.60	1.94	57.1	2.93
23X-4	69–71	207.60	1.94	59.3	3.02
23X-6	69–71	210.30	1.85	61.6	3.03

Table 3. Physical properties index, Hole 653B.

Core section	Interval (cm)	Depth sub-bottom (m)	Bulk density (g/cm^3)	Porosity (%)	Grain density (g/cm^3)
21X-6	55–58	195.05	1.90	56.7	2.80
21X-6	94–97	195.45	1.91	53.9	2.82
21X-7	1–4	196.05	1.89	56.0	2.73
21X-7	43–46	196.45	1.95	58.4	2.76
23X-1	84–87	207.55	1.96	59.3	2.80
23X-2	68–71	208.90	2.02	62.0	3.16
23X-3	70–73	210.40	1.89	59.0	2.87
23X-4	80–83	212.02	1.86	60.6	2.86
23X-5	83–86	213.55	1.89	62.5	2.84
24X-1	69–70	216.80	2.45	49.0	2.75
25X-1	23–26	225.95	2.40	33.4	2.83
26X-2	44–46	239.15	2.05	45.6	2.74
27X-3	84–87	248.75	2.03	48.5	2.86
27X-5	12–15	251.04	2.11	48.9	3.96
28X-1	56–59	255.19	1.78	19.3	2.89
28X-2	61–64	256.72	2.62	91.4	2.89

Table 4. Compressional velocity, Hole 653A.

Core section	Interval (cm)	Depth sub-bottom (m)	Compressional velocity (km/s)
5H-3	69–71	35.89	1.567
5H-6	69–71	40.09	1.605
6H-3	69–71	45.29	1.641
7H-2	80–83	53.31	1.756
7H-4	69–72	56.20	1.605
7H-7	68–71	60.70	1.615
8H-3	68–71	64.20	1.586
8H-5	68–71	67.20	2.390
9H-1	69–72	70.70	1.663
9H-4	68–71	75.20	1.593
9H-7	67–70	79.70	1.605
10H-1	69–71	80.30	1.622
10H-4	93–96	85.05	1.712
10H-6	69–72	87.80	1.634
11H-1	68–71	89.70	1.637
11H-4	69–72	94.20	1.636
11H-C	07–10	98.10	1.622
12H-4	69–71	103.40	1.626
12H-6	69–71	106.40	1.650
13H-3	69–71	111.40	1.606
13H-5	69–71	114.40	1.620
14X-2	69–71	119.50	1.603
14X-4	69–71	122.50	1.616
15X-1	69–71	127.30	1.609
15X-2	69–71	128.80	1.638
16X-1	69–71	138.80	1.624
16X-3	68–70	141.80	1.601
17X-2	69–71	147.80	1.648
17X-6	69–71	153.80	1.585
18X-2	69–71	157.40	1.652
18X-5	69–71	161.90	1.632
19X-2	69–71	166.30	1.638
19X-5	69–71	170.50	1.915
20X-1	69–71	174.40	1.686
20X-4	69–71	178.90	1.636
21X-1	69–71	183.90	1.673
21X-4	65–68	188.35	1.632
22X-2	96–99	195.37	1.651
22X-3	65–68	196.55	1.691
23X-2	69–71	204.60	1.673
23X-4	69–71	207.60	1.673
23X-6	69–71	210.30	1.656

Table 5. Compressional velocity, Hole 653B.

Core section	Interval (cm)	Depth sub-bottom (m)	Compressional velocity (km/s)
21X-6	55–58	196.05	1.664
21X-6	94–97	195.45	1.706
21X-7	1–4	196.05	1.665
21X-7	43–46	196.45	1.733
23X-1	84–87	207.55	1.668
23X-2	68–71	208.90	1.636
23X-3	70–73	210.40	1.639
23X-4	80–83	212.02	1.625
23X-5	83–86	213.55	1.649
25X-1	23–26	225.95	4.920
26X-2	44–46	239.15	1.770
27X-3	84–87	248.75	1.780
27X-5	12–15	251.04	1.950

major ions in interstitial waters of Tyrrhenian sediments differ considerably from those of other marine sediments. The reason is the continuing input of ions from underlying Messinian evaporites. Diffusion and compaction export ions to the lower water column, establishing a gradient from the source (the halite, gypsum, or anhydrite) to the sediment/water interface. Differences in gradients are due to different diffusion coefficients of individual ions and physical properties of the sediments through

Table 6. Shear strength measurements, Hole 653B.

Core section	Interval (cm)	Depth sub-bottom (m)	Shear strength (kPa)
1H-2	84	2.34	10.761
1H-4	39	4.89	8.121
1H-4	75	5.25	4.873
1H-4	123	5.73	23.146
2H-2	85	8.45	6.091
2H-3	129	10.39	15.634
2H-4	77	11.37	12.588
2H-5	81	12.91	5.076
3H-2	81	19.91	9.746
3H-3	80	21.40	15.227
3H-4	101	23.11	12.791
3H-5	65	24.25	7.309
3H-7	26	26.86	10.152
4H-3	25	30.35	10.819
4H-7	18	36.28	17.258
5H-2	101	39.11	10.558
5H-4	55	41.65	28.425
5H-6	63	44.73	33.511
6H-2	134	48.84	83.049
6H-4	109	51.59	61.922
6H-6	93	54.43	29.869
7H-2	108	57.98	10.199
7H-4	116	61.06	45.167
7H-6	100	63.90	18.213
8H-1	77	65.67	37.153
8H-3	77	68.67	24.041
9X-2	107	76.97	27.683
9X-4	67	79.57	24.769
9X-6	30	82.20	36.425
10X-2	64	86.14	16.027
10X-5	76	90.76	50.995
11X-2	87	95.77	25.498
11X-4	74	98.64	26.955
11X-6	126	102.16	58.280
11X-7	20	102.60	40.067
12X-2	57	104.67	24.041
12X-4	59	107.69	26.226
12X-6	35	110.45	65.965
13X-2	96	114.56	42.981
13X-4	62	117.15	64.836
13X-6	85	120.45	49.538
14X-1	51	122.11	36.425
14X-2	60	123.70	94.705
15X-2	81	133.31	25.498
15X-4	101	136.51	29.140
15X-6	102	139.52	45.895
16X-2	58	142.58	64.108
16X-4	58	145.58	58.280
16X-6	35	148.35	56.823
17X-5	51	158.01	25.498
17X-6	89	160.39	51.723
18X-2	55	161.65	58.280
18X-4	29	163.39	52.452
18X-6	102	168.12	52.452
19X-2	66	170.66	52.452
19X-5	85	175.35	47.352
20X-2	112	180.62	78.678
20X-4	95	183.45	65.565
20X-6	65	186.15	65.565
21X-2	92	189.42	40.067
21X-4	56	192.06	52.452
21X-6	29	194.79	60.465
21X-6	34	194.84	85.963
21X-6	87	195.37	33.511
21X-7	12	196.12	98.347
21X-7	39	196.39	140.600
22X-2	62	199.32	56.823
22X-4	60	202.30	63.379
23X-1	91	204.67	72.827
23X-1	120	204.90	69.414
23X-2	75	205.95	71.393
23X-2	86	206.06	110.379
23X-3	67	207.37	142.241
23X-4	29	208.49	63.379
23X-4	66	208.86	110.379
23X-5	19	209.89	62.586
24X-1	44	216.54	39.827
24X-1	87	216.97	30.724

Table 7. Thermal conductivity, Hole 653A.

Core section	Interval (cm)	Depth sub-bottom (m)	Thermal conductivity (10^{-3} cal/cm^2/s)
1H-1	96	0.96	2.46089
1H-3	30	3.20	2.47163
2H-2	66	5.86	2.57260
3H-2	78	15.48	2.83020
4H-2	75	24.75	2.58765
5H-6	70	40.10	2.58765
6H-3	75	45.35	2.84489
7H-4	75	56.25	2.96730
8H-3	80	64.30	2.98474
9H-4	75	75.25	2.99034
10H-3	75	83.35	2.87902
11H-1	75	89.75	3.01800
12H-2	75	100.45	3.07272
13H-4	75	112.96	3.28256
14X-2	75	119.55	3.08360
15X-2	72	128.10	3.60570
16X-2	94	138.32	3.08735
17X-2	90	148.00	3.21793
18X-2	83	157.53	3.15479
18X-4	75	160.45	3.28560
19X-3	80	167.90	3.07400
20X-1	76	174.46	2.94500
20X-2	76	177.45	2.92700
20X-4	75	178.94	2.86700
20X-5	79	180.49	3.08100
21X-1	75	183.95	3.06647
21X-2	75	185.45	3.05209
21X-3	75	186.95	2.97945
21X-4	75	188.45	3.07255
21X-5	75	189.20	3.09605
22X-1	75	193.65	2.97717
22X-2	75	195.15	3.10944
22X-3	75	196.65	3.17045
22X-4	75	198.05	3.00883
23X-1	75	203.15	2.99649
23X-2	75	204.65	3.09472
23X-3	75	206.15	3.10689
23X-4	75	207.65	2.92155
23X-6	75	210.55	2.87124
24X-2	75	213.40	2.83380
24X-3	75	215.65	2.79247
24X-4	75	217.15	2.86633
24X-5	75	218.65	2.85606
24X-6	75	220.15	2.72193
25X-1	75	222.15	3.32946
25X-2	50	223.40	3.34830
25X-C	5	230.65	3.16050
25X-C	17	230.77	3.19705
25X-C	27	230.87	3.11650
26X-1	12	231.12	2.36900
26X-1	30	231.30	2.96229
26X-1	48	231.48	2.52056
26X-1	80	231.80	2.97357
26X-1	125	231.95	2.87760
26X-2	10	232.60	2.39120
26X-2	25	232.75	2.88254
26X-2	54	233.04	2.96976
26X-2	82	233.32	2.34780
26X-2	126	233.76	3.05203

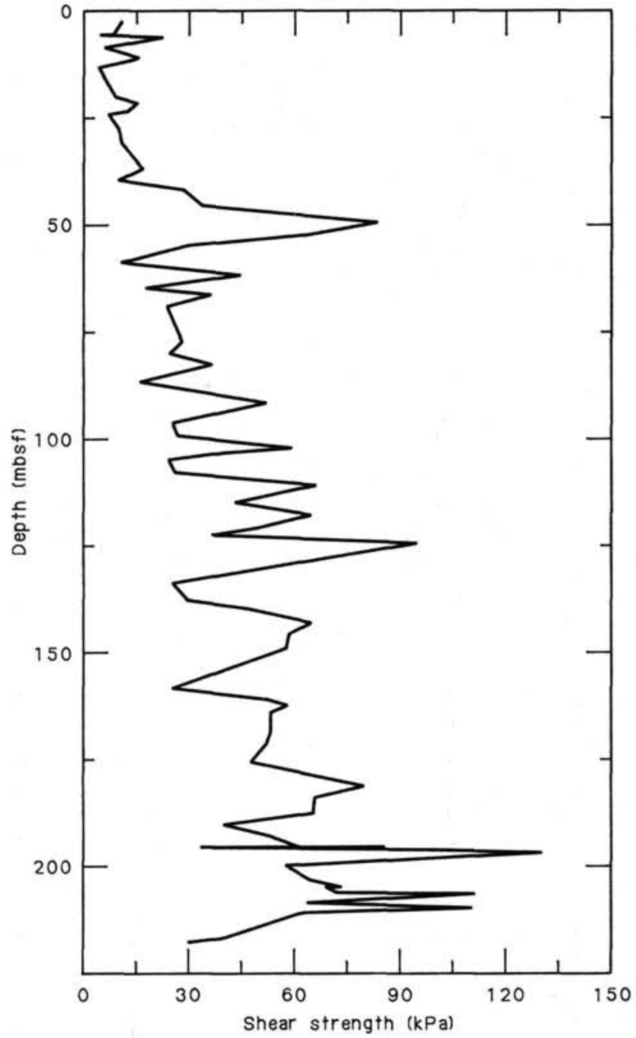

Figure 17. Shear strength vs. depth at Hole 653B.

which they diffuse. Close sampling of small quantities of interstitial waters in Hole 653B shows that concentrations of both anions (Cl^-, SO_4^{2-}) and cations (Ca^{2+}, Mg^{2+}) are subject to quite pronounced changes within a few meters. These changes must be related to bulk sediment properties, such as chemistry or porosity of a particular layer. Typical features of other marine sediments, such as sulfate depletion by bacterial degradation of organic matter at the expense of oxidized sulfur with concordant rise in alkalinity concentration, or downhole depletion of magnesium and concordant stoichiometric increase in calcium, are almost or totally absent. Comparison of chlorinity and salinity gradients and concentrations in this hole with those of Sites 650 and 652 is difficult because Site 653 is relatively shallow. Even over this shallow interval of 210 m, however, we found a downsection increase both in salinity and chlorinity, as well as an increase in Mg^{2+}. This is interpreted as an indication of evaporite dissolution in the subsurface of Site 653.

Organic Geochemistry

Few analyses of organic carbon content were performed on sediments of Holes 653A and 653B. Interesting coarse-grained, thin layers of organic carbon-rich sapropels encountered in the Quaternary succession of Hole 653B were analyzed. A high value of 4.2% was detected in Sample 653B-7H-4, 36–38 cm, a dark green sapropel sandwiched between organic-carbon-lean (0.00% and 0.19%, respectively) background sediments. Results of C_{org} analyses of sediments from Hole 653B are given in Table 11 and depicted in Figure 21.

HEAT FLOW

Introduction

Site 653 is located 0.8 km east of DSDP Site 132 in the Cornaglia Basin, near a pinch-out of Messinian sequences against the eroded basement of the Della Rondine Seamount, a horst-type structure of high relief along the main Central Fault (Fig. 22).

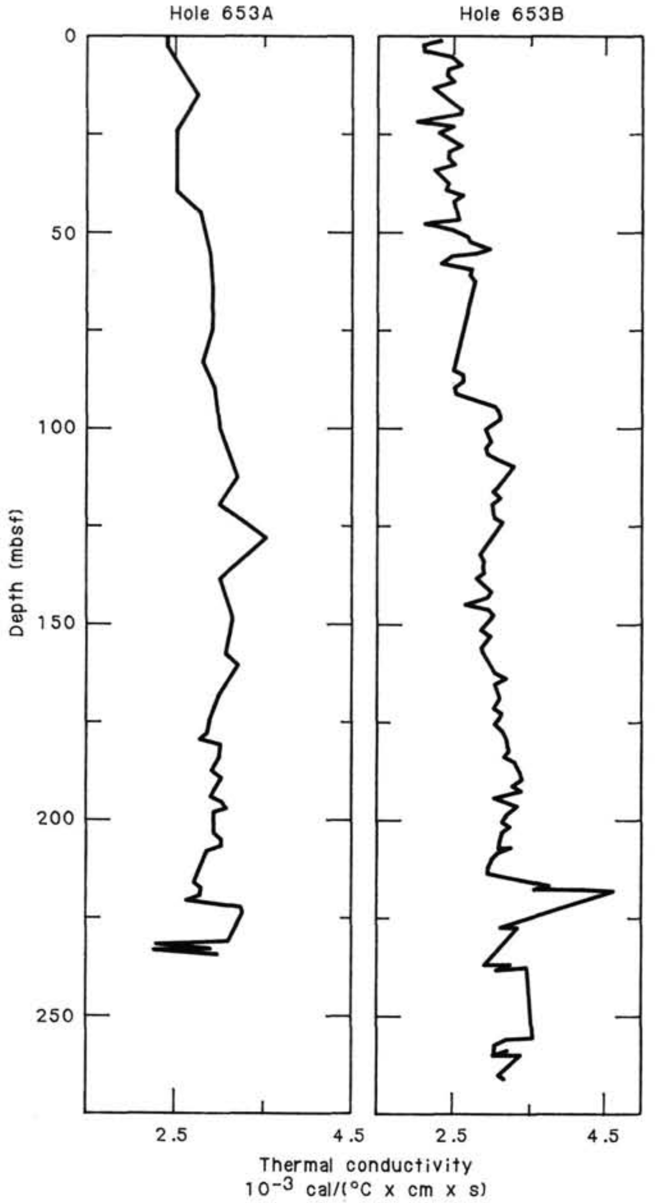

Figure 18. Thermal conductivity vs. depth at Site 653.

Data

Five temperature measurements were recorded in Hole 653A, three using the Von Herzen temperature probe during Advanced Piston Coring (APC) operations, and two using the Uyeda temperature probe during Extended Core Barrel (XCB) coring operations.

Temperature records 1 to 4 are of good quality at 41.6, 79.6, 117.3, 155.2 sub-bottom depth, respectively (Figs. 23 and 24). Measurement 5 at 192.90 mbsf, shows no apparent frictional heating at the beginning of the run, then a temperature plateau for about 10 min followed by a slow increase to a maximum temperature of 29.78°C (Fig. 24).

Examination of the temperature profile (Fig. 25) shows a decrease in the geothermal gradient with depth. Considering thermal gradients and conductivity harmonic means in order to obtain interval heat flow values indicates that the conductive heat flux is not constant with depth (Table 12). Such a significant decrease vs. depth in thermal gradient would indicate a loss of heat beneath the level of the last measurement.

Table 8. Thermal conductivity, Hole 653B.

Core section	Interval (cm)	Depth sub-bottom (m)	Thermal conductivity $(10^{-3}$ cal/cm^2/s)	(W/H/C)
1H-1	75	0.75	2.3269	0.974
1H-2	75	2.25	2.1079	0.882
1H-3	75	3.75	2.1148	0.885
1H-4	75	5.25	2.4702	1.034
2H-1	75	7.05	2.5966	1.087
2H-2	75	8.55	2.4270	1.016
2H-3	75	10.05	2.4103	1.009
2H-4	75	11.55	2.5093	1.050
2H-5	75	13.05	2.2383	0.937
3H-1	75	18.35	2.6004	1.090
3H-2	75	19.85	2.5985	1.088
3H-3	75	21.35	2.0121	0.842
3H-4	75	22.85	2.4879	1.042
3H-5	75	24.35	2.2928	0.960
4H-1	75	27.85	2.5966	1.087
4H-2	75	29.35	2.4270	1.016
4H-3	29	30.85	2.4103	1.009
4H-4	75	32.35	2.5093	1.051
4H-5	36	33.85	2.2383	0.937
5H-1	75	37.35	2.4245	1.015
5H-2	75	38.85	2.3860	0.999
5H-3	75	40.35	2.6243	1.099
5H-4	75	41.85	2.4864	1.041
6H-1	75	46.75	2.5601	1.072
6H-2	75	47.50	2.0954	0.877
6H-3	75	49.00	2.4862	1.041
6H-4	75	50.75	2.6680	1.117
6H-5	75	52.00	2.7211	1.139
6H-6	75	53.75	2.9731	1.245
6H-7	75	55.00	2.7989	1.172
7H-1	75	56.15	2.4599	1.030
7H-2	75	57.65	2.3403	0.980
7H-3	75	59.15	2.7437	1.148
7H-4	75	60.65	2.7097	1.134
7H-5	75	62.15	2.7726	1.161
10X-1	75	84.75	2.4886	1.042
10X-2	75	86.25	2.6296	1.013
10X-3	75	87.75	2.6317	1.102
10X-4	75	89.25	2.4993	1.046
10X-5	75	90.75	2.5227	1.056
11X-1	75	94.15	3.0472	1.275
11X-2	71	95.61	3.1137	1.303
11X-3	72	97.12	3.1234	1.307
11X-4	72	98.62	3.0081	1.259
11X-5	73	100.13	2.9143	1.220
12X-1	75	103.35	2.9944	1.253
12X-2	75	104.85	2.9033	1.215
12X-3	75	106.35	2.9533	1.236
12X-4	75	107.85	3.0813	1.290
12X-5	75	109.35	3.2869	1.376
13X-2	76	114.36	3.0867	1.292
13X-3	76	115.86	3.0123	1.261
13X-4	76	117.36	3.1149	1.261
13X-6	76	118.86	3.0055	1.258
14X-1	124	122.84	3.0354	1.271
14X-2	53	123.63	3.1532	1.320
15X-2	75	131.75	2.8503	1.193
15X-3	75	133.75	2.8975	1.213
15X-4	75	134.75	2.8674	1.200
15X-5	75	136.25	2.9106	1.218
15X-6	75	137.75	2.8225	1.181
16X-1	75	141.25	3.0014	1.256
16X-2	75	142.75	2.9604	1.239
16X-3	75	144.25	2.6563	1.112
16X-4	75	145.75	2.9562	1.237
16X-5	75	147.25	3.0389	1.272
17X-1	91	150.91	2.8614	1.198
17X-2	99	152.49	2.9835	1.249
17X-3	100	154.00	2.9298	1.226
17X-4	92	155.48	2.8593	1.197
17X-5	92	156.98	2.8873	1.209
18X-2	75	161.85	3.0543	1.278
18X-3	75	163.35	3.2103	1.344
18X-4	75	164.85	3.0488	1.276
18X-5	75	166.35	3.0980	1.297
18X-6	75	167.85	3.1119	1.303
19X-2	75	170.75	3.0362	1.271

Table 8 (continued).

Core section	Interval (cm)	Depth sub-bottom (m)	Thermal conductivity $(10^{-3}$ cal/cm^2/s)	(W/H/C)
19X-3	75	172.25	3.1520	1.319
19X-4	75	173.75	3.1185	1.305
19X-5	75	175.25	3.0381	1.272
19X-6	75	176.75	3.1404	1.315
20X-1	75	178.75	3.1970	1.338
20X-2	75	180.25	3.2181	1.347
20X-3	75	181.75	3.2382	1.355
20X-4	75	183.25	3.1708	1.327
20X-5	75	184.75	3.3051	1.383
21X-1	75	187.75	3.3692	1.410
21X-2	75	189.25	3.4042	1.425
21X-3	75	190.75	3.2798	1.373
21X-4	75	192.25	3.4102	1.427
21X-5	75	193.75	3.0385	1.272
21X-6	75	195.25	3.2128	1.358
21X-7	20	196.20	3.3447	1.400
22X-1	75	197.95	3.2032	1.341
22X-2	75	199.95	3.1405	1.315
22X-3	75	200.95	3.2419	1.357
22X-4	75	202.45	3.1373	1.313
22X-5	75	203.95	3.1137	1.303
22X-6	75	205.95	3.0838	1.291
22X-7	20	206.40	3.2515	1.361
23X-1	75	207.45	3.0903	1.294
23X-2	75	208.95	3.0078	1.259
23X-3	75	210.45	2.9626	1.240
23X-4	75	211.95	2.9446	1.233
23X-5	75	213.45	2.9233	1.224
24X-1	20	216.30	3.7610	1.574
24X-1	50	216.60	3.5753	1.497
24X-1	100	217.10	4.2051	1.760
24X-1	125	217.35	4.4391	1.858
24X-C	5	217.65	4.5974	1.924
25X-1	100	226.70	3.1352	1.312
25X-1	125	226.95	3.3115	1.386
25X-C	10	227.30	3.3357	1.396
26X-1	50	235.80	2.9030	1.215
26X-1	75	236.05	3.2507	1.361
26X-1	100	236.30	2.9870	1.250
26X-1	125	236.55	2.8950	1.212
26X-2	15	236.95	1.8085	0.757
26X-2	40	237.20	3.0845	1.291
26X-C	18	237.40	3.4866	1.459
27X-1	50	255.10	3.5430	1.278
27X-1	100	255.60	3.2103	1.344
27X-2	50	256.60	3.0488	1.276
27X-2	100	257.10	3.0980	1.297
27X-3	50	257.60	3.1119	1.303
27X-3	100	258.10	3.0543	1.278
27X-3	140	258.50	3.2103	1.344
27X-4	15	258.75	3.0488	1.276
27X-4	50	259.10	3.1119	1.303
27X-4	75	259.35	3.4217	1.432
27X-4	100	259.60	3.0339	1.270
27X-4	125	259.85	3.1054	1.300
27X-4	150	260.00	3.1953	1.337
27X-5	10	260.10	3.3501	1.402
27X-C	18	260.40	3.2884	1.376
28X-1	100	264.70	3.0969	1.296
28X-1	130	265.00	3.1104	1.302
28X-2	30	265.50	3.1746	1.329

Thermal conductivities have been measured in the shipboard lab on sampled cores, using the needle probe method. Twenty-nine measurements were performed on Hole 653A cores, both above and below measurement 5 (see Fig. 18 and Table 13). Thermal conductivities tend to increase with depth from 1.03 W/mK (2.5 × 10^{-3} cal/(°C × cm × s) to 1.35 W/mK (3.2 × 10^{-3} cal/°C × cm × s), with higher values up to 1.5 W/mK (3.6 × 10^{-3} cal/°C × cm × s) measured between 215 and 225 mbsf; below this level, high and low values alternate from 1.35 (3.2 × 10^{-3} cal/°C × cm × s) to 1.15 W/mK (2.75 × 10^{-3} cal/°C × cm × s) (Fig. 18). The 59 closely spaced measure-

Table 9. Calcium carbonate concentrations in Hole 653A.

Sample	Depth	% $CaCO_3$
1-1, 54–55	0.54	45.79
1-1, 69–71	0.69	44.78
1-1, 116–117	1.16	30.40
1-2, 54–55	2.04	36.85
1-2, 116–117	2.66	36.65
1-3, 54–55	3.54	13.81
2-1, 55–56	4.25	41.06
2-1, 115–116	4.85	37.11
2-2, 55–56	5.75	37.81
2-2, 115–116	6.35	39.77
2-3, 55–56	7.25	35.00
2-3, 69–71	7.39	35.96
2-3, 115–116	7.85	32.12
2-4, 55–56	8.75	34.45
2-4, 115–116	9.35	27.42
2-5, 55–56	10.25	25.52
2-5, 69–71	10.39	44.34
2-5, 115–116	10.85	36.16
2-6, 55–56	11.75	48.05
2-6, 115–116	12.35	13.22
2-7, 55–56	13.25	35.26
3-1, 55–56	13.75	1.24
3-1, 115–116	14.35	36.01
3-2, 55–56	15.25	31.94
3-2, 115–116	15.85	64.64
3-3, 55–56	16.75	60.79
3-3, 115–116	17.35	43.68
3-4, 55–56	18.25	62.89
3-4, 115–116	18.85	39.38
3-5, 115–116	20.35	35.44
3-6, 55–56	21.25	21.27
3-6, 115–116	21.85	30.73
4-1, 56–57	23.26	56.41
4-1, 115–116	23.85	48.75
4-2, 56–57	24.76	62.12
4-2, 115–116	25.35	34.29
4-3, 56–57	26.26	44.46
4-3, 115–116	26.85	57.29
4-4, 56–57	27.76	33.63
4-4, 115–116	28.35	39.77
4-5, 56–57	29.26	27.23
4-5, 115–116	29.85	47.08
4-6, 56–57	30.76	44.83
4-6, 115–116	31.35	31.73
4-7, 56–57	32.26	30.34
5-1, 54–55	32.76	20.74
5-2, 54–55	34.24	51.00
5-3, 54–55	35.74	63.16
5-4, 54–55	37.24	32.13
5-5, 54–55	38.74	36.98
5-6, 54–55	40.24	53.41
5-7, 54–55	41.74	11.31
6-1, 54–55	42.14	25.02
6-1, 115–116	42.75	10.92
6-2, 54–55	43.64	54.38
6-2, 116–117	44.25	35.73
6-3, 54–55	45.14	47.47
6-3, 115–116	45.75	46.22
6-4, 54–55	46.64	13.49
6-4, 115–116	47.25	14.39
6-5, 52–53	48.12	67.03
6-5, 115–116	48.75	40.37
6-6, 54–55	49.64	34.95
6-6, 111–112	50.21	25.16
7-1, 54–55	51.54	47.30
7-1, 115–116	52.15	60.03
7-2, 54–55	53.04	34.30
7-2, 116–117	53.63	41.56
7-3, 54–55	54.54	35.37
7-3, 115–116	55.15	49.69
7-4, 54–55	56.04	53.16
7-4, 115–116	56.65	48.35
7-5, 54–55	57.54	55.76
7-5, 115–116	58.15	43.92
7-6, 54–55	59.04	32.30
7-6, 115–116	59.65	58.84
7-7, 54–55	60.54	42.39

Table 9 (continued).

Sample	Depth	% $CaCO_3$
8-1, 52–53	61.02	7.65
8-1, 115–116	61.65	33.31
8-2, 52–53	62.52	39.04
8-2, 117–118	63.15	45.10
8-3, 52–53	64.02	45.50
8-3, 116–117	64.65	46.23
8-4, 52–53	65.52	29.44
8-4, 116–117	66.15	49.36
8-5, 52–53	67.02	35.42
8-5, 116–117	67.65	50.52
8-6, 52–53	68.52	31.76
8-6, 115–116	69.15	53.71
9-1, 54–55	70.54	43.50
9-1, 115–116	71.15	50.40
9-2, 54–55	72.04	39.02
9-2, 115–116	72.65	57.20
9-3, 54–55	73.54	51.55
9-3, 115–116	74.15	58.22
9-4, 54–55	75.04	49.26
9-4, 115–116	75.65	51.23
9-5, 54–55	76.54	45.47
9-5, 115–116	77.15	56.81
9-6, 54–55	78.04	34.16
9-6, 115–116	78.65	56.73
9-7, 54–55	79.54	52.82
10-1, 54–55	80.14	45.72
10-1, 115–116	80.75	50.75
10-2, 54–55	81.64	35.87
10-2, 115–116	82.25	38.61
10-3, 54–55	83.14	26.18
10-3, 115–116	83.75	53.31
10-4, 54–55	84.64	44.32
10-4, 115–116	85.25	46.67
10-5, 54–55	86.14	46.73
10-5, 115–116	86.75	52.76
10-6, 54–55	87.64	52.75
11-1, 54–55	89.54	63.34
11-1, 115–116	90.15	59.28
11-2, 54–55	91.04	42.71
11-2, 115–116	91.65	57.34
11-3, 54–55	92.54	44.77
11-3, 115–116	93.15	54.08
11-4, 54–55	94.04	59.43
11-4, 115–116	94.65	57.64
11-5, 54–55	95.54	62.37
11-5, 115–116	96.15	51.66
11-6, 54–55	97.04	57.18
11-6, 115–116	97.65	48.43
12-1, 54–55	98.74	42.98
12-1, 115–116	99.35	41.74
12-2, 54–55	100.24	58.47
12-2, 115–116	100.85	66.51
12-3, 54–55	101.74	64.83
12-3, 115–116	102.35	57.00
12-4, 54–55	103.24	47.79
12-4, 115–116	103.85	60.50
12-5, 54–55	104.74	65.34
12-5, 115–116	105.35	56.60
12-6, 54–55	106.24	64.02
12-6, 115–116	106.85	66.67
13-1, 54–55	108.24	61.96
13-1, 115–116	108.85	37.53
13-2, 54–55	109.74	53.45
13-2, 115–116	110.35	60.63
13-3, 54–55	111.24	41.66
13-3, 115–116	111.85	64.83
13-4, 54–55	112.74	61.98
13-4, 115–116	113.35	63.52
13-5, 54–55	114.24	59.28
13-5, 115–116	114.85	55.80
13-6, 54–55	115.74	58.82
13-6, 115–116	116.35	49.41
14-1, 54–55	117.84	60.57
14-1, 115–116	118.45	54.15
14-2, 54–55	119.34	64.15
14-2, 115–116	119.95	56.52
14-3, 54–55	120.84	63.86
14-3, 115–116	121.45	61.98
14-4, 54–55	122.34	60.31
14-4, 115–116	122.95	63.35
14-5, 54–55	123.84	59.78
14-5, 115–116	124.45	53.95
14-6, 54–55	125.34	53.39
14-6, 115–116	124.95	60.46
15-1, 54–55	127.14	55.95
15-1, 115–116	127.75	55.15
15-2, 55–56	128.64	58.57
15-2, 115–116	129.25	54.54
16-1, 54–55	130.14	62.90
16-1, 115–116	130.75	65.23
16-2, 54–55	131.64	58.87
16-2, 115–116	132.25	54.61
16-3, 54–55	133.14	63.05
16-3, 115–116	133.75	58.22
16-4, 54–55	134.64	62.00
16-4, 115–116	135.25	90.63
16-5, 54–55	136.14	62.21
16-5, 115–116	136.75	65.93
16-6, 54–55	137.64	58.87
16-6, 115–116	138.25	65.93
17-1, 54–55	146.14	62.38
17-1, 115–116	146.75	73.65
17-2, 54–55	147.64	70.65
17-2, 115–116	148.25	66.64
17-3, 54–55	149.14	61.09
17-3, 115–116	149.75	71.10
17-4, 115–116	150.64	48.67
17-5, 54–55	151.25	64.46
17-5, 115–116	152.14	61.79
17-6, 54–55	152.75	72.11
17-6, 115–116	153.64	64.74
18-1, 54–55	155.74	78.06
18-1, 115–116	156.35	59.81
18-2, 54–55	157.24	65.52
18-2, 115–116	157.85	65.63
18-3, 54–55	158.24	29.95
18-3, 115–116	159.35	64.18
18-4, 54–55	159.74	77.68
18-4, 115–116	160.85	65.15
18-5, 54–55	161.24	84.65
18-5, 115–116	162.35	65.07
18-6, 54–55	162.74	64.44
19-1, 54–55	164.64	66.54
19-1, 115–116	165.25	52.19
19-2, 54–55	166.14	82.41
19-2, 115–116	166.75	57.27
19-3, 54–55	167.64	63.49
19-3, 115–116	168.25	61.41
19-4, 54–55	169.14	49.22
19-4, 115–116	169.75	55.47
19-5, 54–55	170.64	54.12
19-5, 115–116	171.25	63.18
20-1, 54–55	174.24	66.22
20-1, 115–116	174.65	55.82
20-2, 54–55	175.74	54.18
20-2, 115–116	176.15	55.99
20-3, 54–55	177.24	52.64
20-3, 115–116	177.65	69.80
20-4, 54–55	178.74	64.79
20-4, 115–116	179.15	61.69
20-5, 54–55	180.24	64.31
20-5, 115–116	181.65	60.70
21-1, 54–55	183.74	57.55
21-1, 115–116	184.35	69.75
21-2, 54–55	185.24	67.82
21-2, 115–116	185.85	70.56
21-3, 54–55	186.74	71.84
21-3, 115–116	187.35	69.86
21-4, 54–55	188.24	69.78
21-4, 115–116	188.85	56.42
21-5, 54–55	189.74	61.26
21-5, 115–116	190.24	56.25
22-1, 56–57	193.44	54.77
22-2, 56–57	194.94	65.62
22-2, 117–118	195.55	67.18
22-3, 56–57	196.44	78.72

Table 9 (continued).

Sample	Depth	% $CaCO_3$
22-3, 115-116	197.05	50.67
22-4, 117-118	198.56	67.18
23-1, 54-55	202.94	68.76
23-1, 115-116	203.55	70.66
23-2, 54-55	204.44	72.77
23-2, 115-116	205.05	55.94
23-3, 54-55	205.94	56.03
23-3, 115-116	206.55	53.48
23-4, 54-55	207.44	55.01
23-4, 115-116	208.05	45.07
23-5, 54-55	208.94	59.35
23-5, 115-116	209.55	52.23
23-6, 54-55	210.44	43.52
23-6, 115-116	211.05	49.97

ments on Hole 653B cores confirm the steady increase of the conductivity with depth in the Pliocene-Pleistocene sediments. Higher values up to 1.9 W/mK (4.5×10^{-3} cal/°C × cm × s), were measured around 220 mbsf in the Messinian sediments (see Table 13).

Heat Flow Determination and Conclusions

Heat flow is highly variable with depth (see Table 12), decreasing from 141.7 mW/m^2 between surface and 41.6 mbsf to 66 mW/m^2 between 155.2 and 192.9 mbsf.

The most probable explanation for such a variability in geothermal gradient and heat flow with depth is the proximity of the upper Messinian evaporitic sequence, the conductivity of which is commonly about twice that of the overlying sediments. The presence of such a highly conductive layer may have trig-

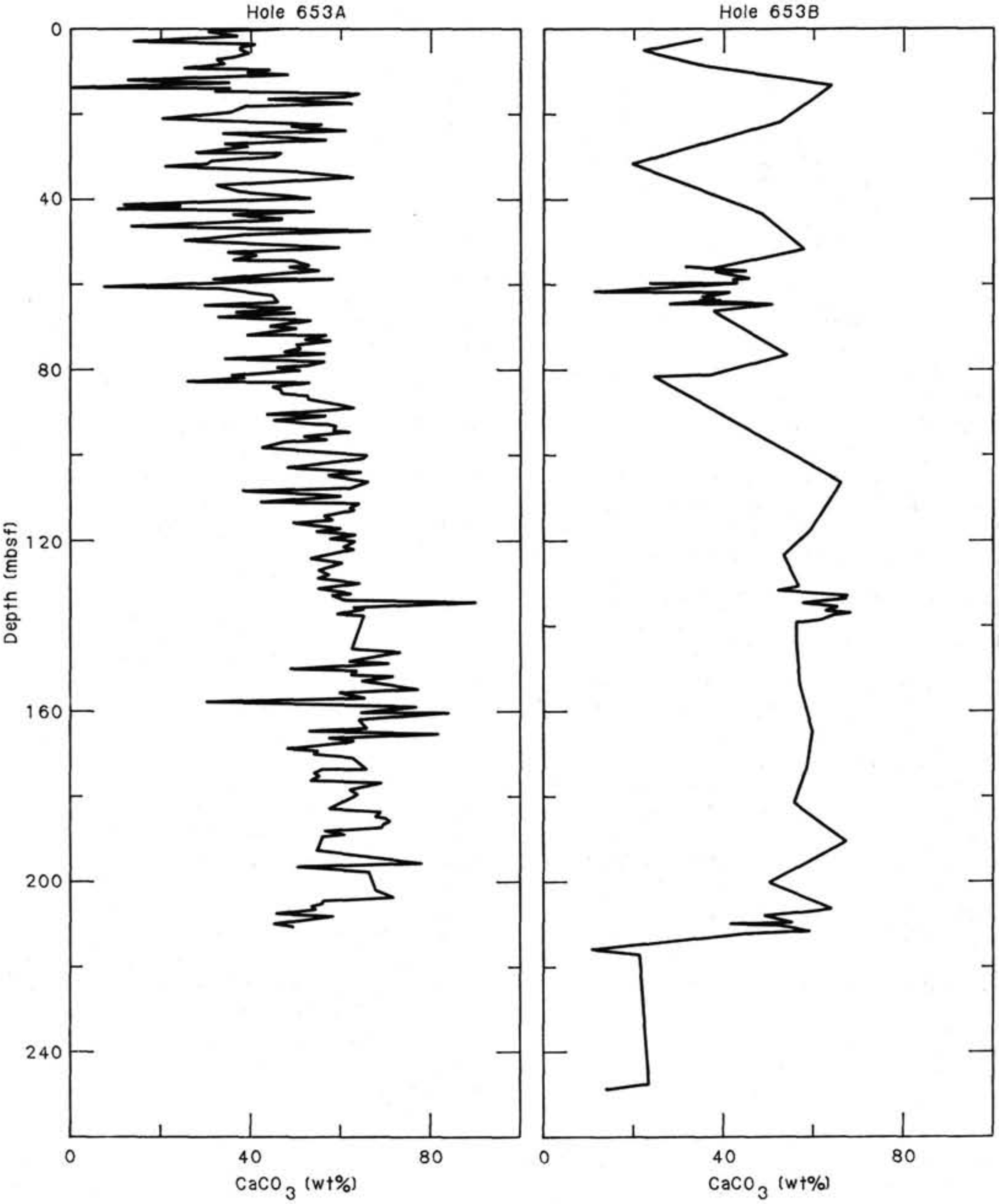

Figure 19. Weight % $CaCO_3$ vs. depth, Hole 653A and Hole 653B. Sedimentation rates were calculated using the paleontological data.

Table 10. Analyses of interstitial waters, Holes 653A and 653B.

Sample No.	Depth	Sal.	Alk.	pH	Cl^-	SO_4^{2-}	Ca^{2+}	Mg^{2+}	Ca/Mg
Surface	0.0	37.0	2.36	8.16	580	27.2	9.0	57.2	0.16
Hole 653A:									
1H-2, 140–150	2.9	37.5	2.99	7.68	606	24.6	6.9	51.1	0.13
6H-5, 140–150	49.0	38.0	2.80	7.49	550	30.5	18.4	66.5	0.28
11H-5, 140–150	96.4	40.0	2.66	7.11	634	24.0	18.9	53.3	0.36
17X-5, 140–150	153.0	42.5	2.20	7.29	653	26.1	17.9	50.3	0.35
22X-3, 140–150	197.3	44.5	1.07	7.16	543	33.2	22.3	71.4	0.31
Hole 653B:									
1H-4, 39–46	4.9	39.5	n.d.	n.d.	614	22.6	8.3	47.5	0.17
2H-5, 140–150	13.5	36.0	3.73	7.51	524	26.3	9.3	50.7	0.18
3H-4, 143–149	22.0	39.0	n.d.	n.d.	581	24.6	8.5	54.0	0.16
4H-3, 142–149	31.5	38.0	n.d.	n.d.	600	21.5	7.0	47.2	0.15
5H-5, 142–148	44.0	39.5	n.d.	n.d.	608	25.3	15.6	60.5	0.26
6H-4, 140–148	51.9	38.5	n.d.	n.d.	613	26.8	7.7	35.7	0.21
6H-5, 58–66	52.6	40.0	n.d.	n.d.	611	26.1	17.9	58.4	0.31
7H-5, 140–150	62.8	40.0	3.25	7.38	623	17.6	15.3	59.7	0.26
8H-2, 50–56	66.9	40.0	n.d.	n.d.	589	28.0	12.2	57.8	0.21
9X-2, 120–126	77.1	41.5	n.d.	n.d.	636	31.7	15.1	63.0	0.24
12X-3, 142–148	107.0	42.0	n.d.	n.d.	665	34.2	21.1	63.6	0.33
13X-4, 142–149	118.0	42.5	n.d.	n.d.	654	33.5	22.3	61.9	0.36
14X-2, 104–110	124.1	44.5	n.d.	n.d.	630	34.1	21.8	59.7	0.37
16X-3, 140–148	144.9	45.0	n.d.	n.d.	621	34.5	26.9	61.9	0.43
17X-3, 140–148	154.4	42.0	n.d.	n.d.	636	37.3	25.4	64.5	0.39
18X-4, 142–150	165.5	44.0	n.d.	n.d.	683	40.5	28.6	67.5	0.42
19X-4, 115–121	174.2	45.0	n.d.	n.d.	700	44.0	33.4	70.7	0.47
21X-3, 141–148	191.4	44.0	n.d.	n.d.	690	43.3	36.3	67.7	0.54
22X-3, 80–86	201.0	46.0	n.d	n.d.	681	36.8	29.8	72.2	0.41
23X-3, 80–86	210.5	45.0	n.d.	n.d.	695	31.7	28.2	75.1	0.38

Sample No.: Hole 653A/B, Core-Section, Interval. Depth is given in meters below seafloor. Sal.: Salinity in parts per thousand; Alk.: Alkalinity in mmol/L; Cl^-, SO_4^{2-}, Ca^{2+}, Mg^{2+} are given in mmol/L; n.d. = not measured.

gered lateral heat transfer, especially in the area where the salt pinches out.

Depending on the two-dimensional geometry of the evaporitic layer, lateral heat transfer could generate a temperature distribution capable of accounting for the observed heat flow variability. These effects can be investigated through model studies.

DISCUSSION AND CONCLUSIONS

Pliocene-Quaternary Section

The Pliocene-Quaternary section recovered at Site 653 is very similar to that from DSDP 132; however, 15 years of progress in drilling and coring technology are apparent in increased recovery and decreased coring disturbance. Over 3500 samples were taken at this site. The quality and quantity of core recovered seem to be suitable for the shore-based, high-resolution, Pliocene-Quaternary stratigraphic studies which were the main objective of the site. An exception may be in magnetostratigraphy; the natural remanent magnetism in the upper 165 m of both holes was severely overprinted and it was not possible to identify geomagnetic reversals with shipboard techniques.

The Messinian and the Miocene/Pliocene Boundary

Biostratigraphic Evidence

The Miocene/Pliocene boundary has been recognized as the first occurrence of open marine foraminifer community, i.e., the base of foraminiferal zone MPl1 (*Sphaeroidinellopsis* acme zone) (Cita, 1973, 1975). By this criterion, the Messinian/Pliocene boundary is not necessarily time-equivalent throughout the Mediterranean. The Messinian/Pliocene boundary falls between 107-653A-24X, CC and 653A-25X, CC (between 221.4 and 231.0 mbsf) and between 107-653B-23X, CC and 653B-24R, CC (between 216.1 and 225.7 mbsf). The most likely position in Hole 653A is at the contact between overlying dark grayish brown clay and underlying gray marl at 107-653A-24X, CC, 8 cm; the corresponding position in Hole 653B is probably at the contact between overlying reddish mud and underlying gray marl at 107-653B-23X, CC, 27 cm. Note that these positions do not coincide exactly with the boundary between lithostratigraphic Units I and II, which falls slightly deeper in both cores (107-653A-25X-1, 23 cm, and 107-653B-24X-1, 50 cm).

The sequence underlying Zone MPl1, lacking age-diagnostic foraminifers, is attributed to the "non-distinctive" zone described by Iaccarino and Salvatorini (1982). As described, this non-distinctive zone is an upper Messinian unit characterized by brackish-water facies ("lago mare" facies). Although this "lago mare" facies is well known from the eastern Mediterranean, in the western Mediterranean it seems to be replaced by less-restricted environments (Hsü et al., 1978). At Site 653, the non-distinctive zone contains small planktonic and benthic foraminiferal assemblages with *Globigerinita quinqueloba, Globigerinita glutinata,* and several species of the *Globigerina* group. Benthic foraminifers of the genera *Bolivina, Gyroidina, Pullenia, Elphidium, Cibicides, Uvigerina, Ammonia,* and *Gyroidinoides* were observed. Nannoplankton are few to common. The nannoplankton assemblage is more diversified than the foraminiferal assemblages and includes predominantly species which are more tolerant of changes in water depth, salinity, and temperature. However, there are also discoasters and amauroliths which are generally known from normal marine environments. They are generally of smaller than usual size.

In addition to these micro- and nannofossil assemblages which can be considered to be autochthonous, reworked species from the Cretacous, Paleogene, and Neogene (Burdigalian-Tortonian) have been found. Similar observations have been described by Hsü, Montadert, et al. (1978) from Site 372 in the Balearic Basin.

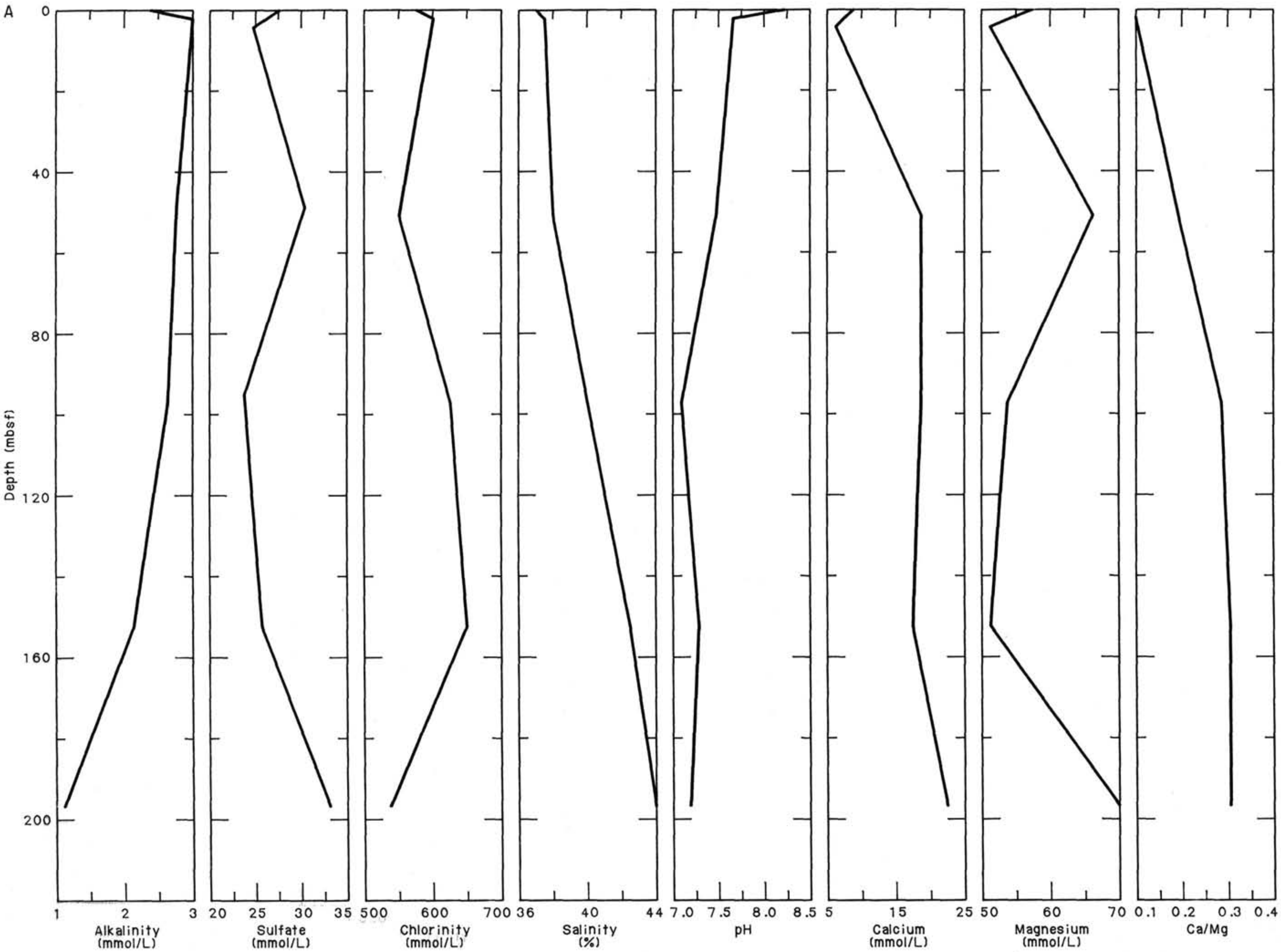

Figure 20. Plot of interstitial water data vs. depth. A. Hole 653A. B. Hole 653B.

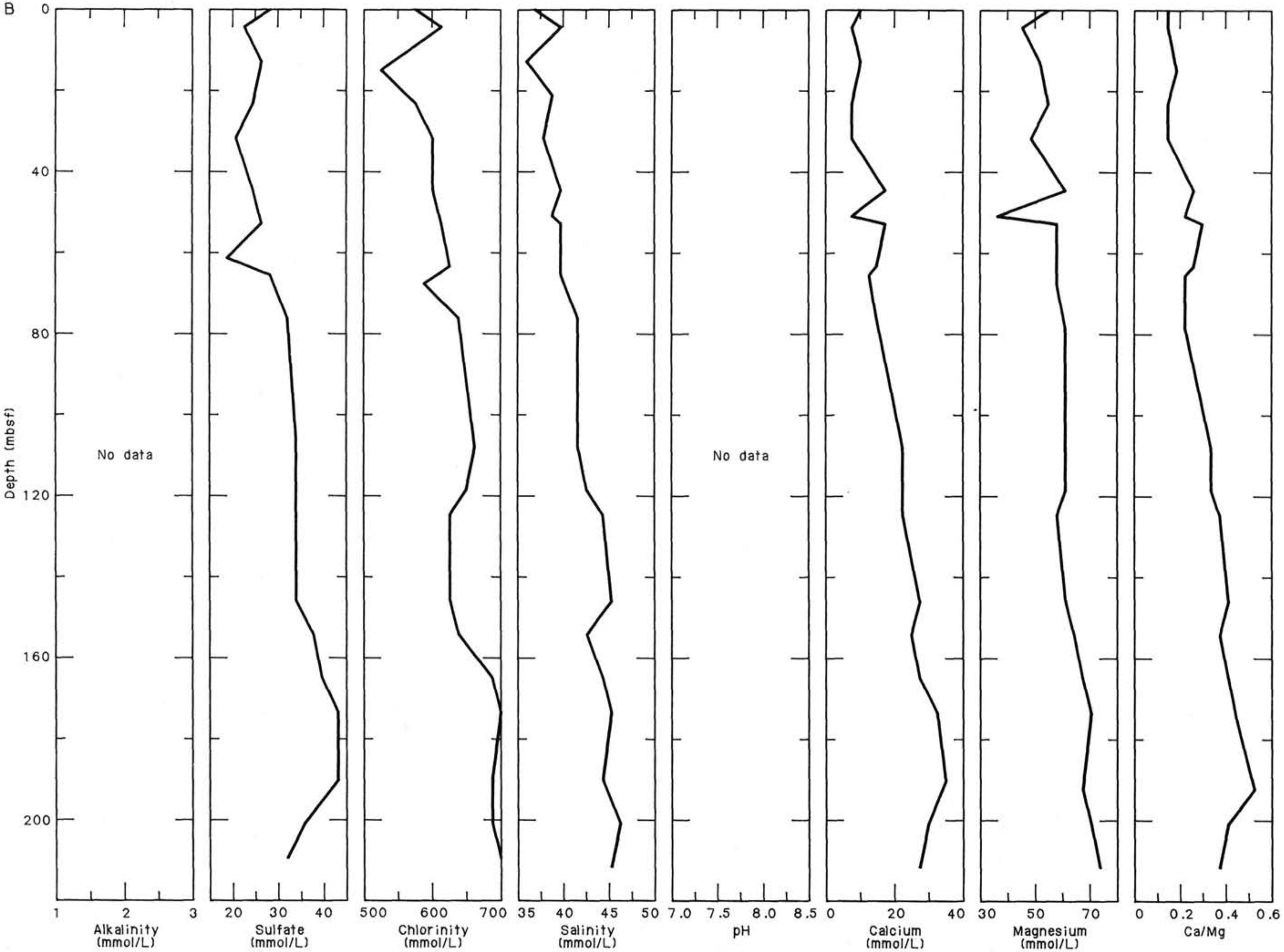

Figure 20 (continued).

Table 11. Calcium carbonate and organic carbon in Hole 653B.

Sample	Depth	$CaCO_3$ %	C_{org} %
1-2, 119–120	2.69	35.87	0.48
1-4, 39–46	4.9	23.48	1.12
2-2, 119–120	8.79	35.87	
2-5, 140–150	13.50	65.20	0.13
3-4, 143–149	22.03	53.81	0.17
4-3, 142–149	31.52	20.97	0.26
5-5, 142–148	44.02	49.34	0.61
6-4, 140–148	51.90	59.01	0.00
6-5, 58–66	52.58	58.73	0.57
7-1, 70–71	56.10	38.92	0.21
7-1, 71–72	56.11	41.48	0.34
7-1, 72–73	56.12	39.18	1.57
7-1, 73–74	56.13	33.89	0.70
7-1, 75–76	56.15	32.01	2.67
7-1, 76–77	56.16	37.20	0.55
7-1, 78–79	56.18	40.18	1.26
7-2, 62–64	57.12	45.49	0.06
7-2, 71–73	57.21	42.84	2.30
7-2, 81–83	57.31	38.46	0.02
7-3, 143–149	59.43	46.77	0.57
7-4, 22–24	60.12	33.13	0.00
7-4, 29–31	60.19	24.05	4.20
7-4, 36–38	60.26	43.97	0.19
7-5, 54–56	61.94	12.41	0.10
7-5, 63–65	62.03	38.52	2.62
7-5, 67–69	62.07	42.16	0.19
7-5, 140–150	62.80	36.28	0.25
7-6, 112–113	64.02	40.31	0.15
7-6, 113–114	64.03	40.32	0.74
7-6, 115–116	64.05	35.12	
7-6, 117–118	64.07	39.84	0.01
7-6, 118–119	64.08	38.81	
7-7, 32–34	64.72	48.66	0.07
7-7, 36–38	64.76	44.77	
7-7, 40–42	64.80	44.06	0.42
8-1, 1–3	64.91	29.24	0.53
8-1, 4–6	64.94	44.26	2.70
8-1, 8–10	64.98	37.28	3.39
8-1, 13–15	65.03	51.68	0.25
8-2, 50–56	66.90	38.40	0.65
9-2, 120–126	77.10	55.14	0.69
9-5, 119–121	81.59	37.81	0.28
9-5, 138–141	81.78	28.30	0.02
9-6, 4–7	81.94	25.58	1.73
12-3, 142–148	107.02	67.27	0.00
13-4, 142–149	118.02	60.12	
14-2, 104–110	124.12	54.30	
15-1, 54–55	131.54	57.94	
15-1, 115–116	132.15	53.23	
15-2, 54–55	133.04	63.09	
15-2, 115–116	133.64	68.61	
15-3, 54–55	134.54	66.62	
15-3, 115–116	135.15	58.44	
15-4, 54–55	136.04	65.71	
15-4, 115–116	136.65	64.60	
15-5, 54–55	137.54	69.46	
15-5, 115–116	138.15	65.54	
15-6, 54–55	139.04	62.79	
15-6, 115–116	139.65	57.12	
16-3, 140–148	144.90	57.06	0.03
17-3, 140–148	154.40	57.74	0.15
18-4, 142–150	165.52	60.99	0.29
19-4, 115–121	174.15	59.20	
20-3, 141–148	182.41	56.24	
21-3, 141–148	191.41	68.43	
22-3, 80–86	201.00	56.05	
23-1, 54–55	207.24	50.30	
23-1, 115–116	207.85	65.26	
23-2, 54–55	208.74	61.57	
23-2, 115–116	209.35	48.86	
23-3, 54–55	210.24	50.08	
23-3, 80–86	210.50	46.76	
23-3, 115–116	210.85	41.93	
23-4, 54–55	211.74	54.66	
23-4, 115–116	212.35	59.07	
23-5, 54–55	213.24	60.38	
24-1, 69–71	216.79	10.74	
26-2, 44–46	218.04	22.31	
27-3, 84–87	248.74	24.13	
27-5, 12–15	251.02	8.08	
28-1, 56–59	255.16	13.17	

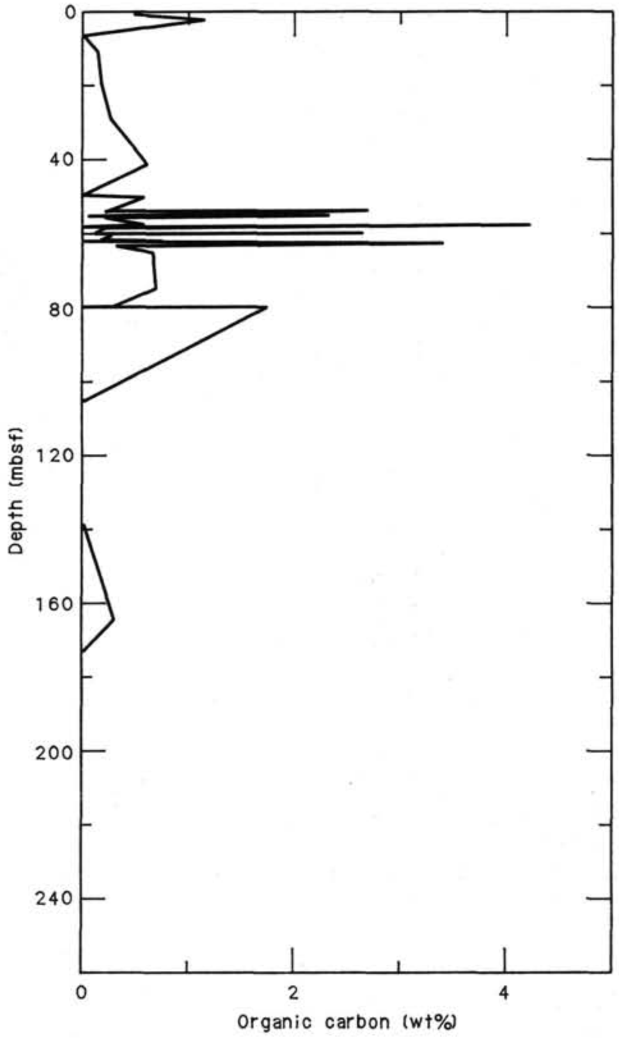

Figure 21. Weight % organic carbon vs. depth, Hole 653B.

Two interpretations may be offered for the observation of foraminiferal assemblages characterized by small species of uniform size: first, the assemblage may be a dwarfed fauna, indicative of restricted marine conditions. Alternatively, these individuals may be reworked from marine lower Messinian sediments and size-sorted during transport into a nonmarine environment.

Lithologic Evidence

The lithologic section which coincides with the paleontologically identified Miocene/Pliocene boundary consists, from top to bottom, of reddish and yellowish brown marls and oozes, in abrupt contact with approximately 70 cm of gray clays. The clays in turn lie in abrupt contact with a 70–90-m thick layer of dark gray biotite- and gypsum-bearing sand. The reddish and yellowish brown color of the marls and oozes over the contact is attributed to input of fine sediment which had been weathered subaerially during the Messinian and then eroded and transported to the site during the post-Messinian transgression.

The Messinian sediments recovered at Site 653 record restricted marine to evaporitic and subaerial environments. The lithologies are very similar in the two holes, but an exact correlation cannot be made. Two alternative schemes have been proposed for correlating these lithologies (see "Lithostratigraphy" section, this chapter). Shore-based studies, particularly paleontological, may distinguish between these options or provide yet a third op-

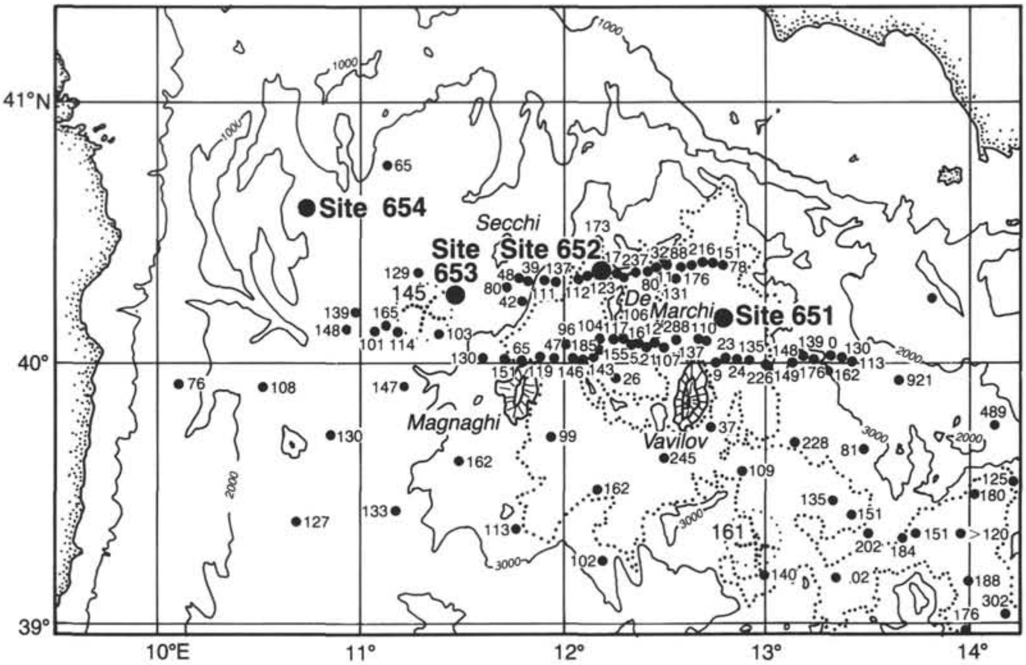

Figure 22. Location of Site 653 with previously measured heat flow values in mW/m^2.

tion. In any case, the variation in lithologies between two holes so close together suggests that the uppermost Messinian had rapid lateral facies changes in this area. This is not at all surprising, given the position of the site on the edge of a basement ridge, and the small-scale lateral environmental variability in some modern evaporitic settings.

Hypothetical Sequence of Events

The sequence of lithologies recovered in the upper Miocene through the Miocene/Pliocene boundary can be explained by a gradual stepwise increase in water depth through time. We emphasize that this scenario is to be considered a tentative working hypothesis. In particular, paleontological environmental indicators have not yet been fully exploited. Furthermore, this scenario is based predominantly on the lithostratigraphy of Hole 653B; the lateral variability among Holes 653A, 653B, and DSDP 132 has not been fully accounted for.

1. The brilliant red-yellow muds and silts, in which iron oxides (hematite, goethite, and/or limonite), and sulfur have been tentatively identified, are presumed to be a by-product of chemical weathering. Iron in the reduced state could have been transported by acidic ground water which subsequently emerged and deposited iron oxides *in situ* at Site 653. Modern analogies for this facies can be found in Australia in the supratidal to continental range of restricted hypersaline embayments along the semiarid northeast shore of Spencer Gulf (Ferguson et al., 1983), as well as in continental saline lacustrine environments, e.g., Lake Tyrrell, Victoria (Teller et al., 1982). In these semiarid to arid climatic regions, acidic ground water, passing through red-bed aquifer systems, leaches and transports high concentrations of reduced iron. This iron is deposited as red, yellow, and purple iron oxides (goethite, hematite) and black unstable iron sulfides when the ground waters emerge as springs along the shoreline. These Australian spring deposits occur at the boundary between contrasting salinity layers (more saline seawater or lake water and less saline ground water); thus their presence at Hole 653B suggests, by analogy, subaerial discharge of springs with subsequent precipitation of iron-rich lenses adjacent to a saline body of water.

2. The postulated presence of stromatolites interbedded with red muds is the first indication for transgressive conditions. Blue-green algae (or cyanobacteria) producing the stromatolitic laminations require both light and moisture to maintain growth. Although algal mats can flourish on the marginal edges of hypersaline environments, they can also grow at depths within the photic zone down to 50 m (Schreiber, 1982). The base of the photic zone is of course dependent upon local conditions.

3. The dark gray dolomitic muds with interbedded layers of small, lenticular gypsum crystals and black shales are an association characteristic of an intertidal facies (Shearman, 1982). The black shales could be remnants of algal mats. In modern intertidal zones, small lenticular gypsum crystals are found scattered within the algal mats and the underlying sediments. They are observed to be growing within the near-surface sediment, rather than precipitating directly from a standing body of water. Frequently, the gypsum crystals are abundant enough to form a gypsum mush (Shearman, 1982; McKenzie et al., 1980). Again by analogy to modern environments, the dolomitic mud could represent an early diagenetic alteration product of a former aragonitic marine mud; such aragonitic mud is observed forming today in semi-restricted lagoonal environments where salinities reach aragonite saturation (McKenzie et al., 1980). Early dolomitization of these prograding carbonate sequences in an evaporitic environment begins soon after burial when hypersaline brines circulate through the sediments. The presence of a marine nannofossil assemblage in these sediments suggests that at the time of deposition there was restricted communication with an open marine environment. An impoverished planktonic foraminifer assemblage, likewise, indicates improving marine conditions upsection. The site of this flourishing, albeit stressed, planktonic community may have been the middle of the Cornaglia Basin (west of Site 653/132), or it could have been farther west, perhaps in the Balearic Basin.

4. The laminar (balatino-type) gypsum occurs in Hole 653B but not in Hole 653A. This might result from limited recovery at Hole 653A; however, the distinctive drilling characteristics of

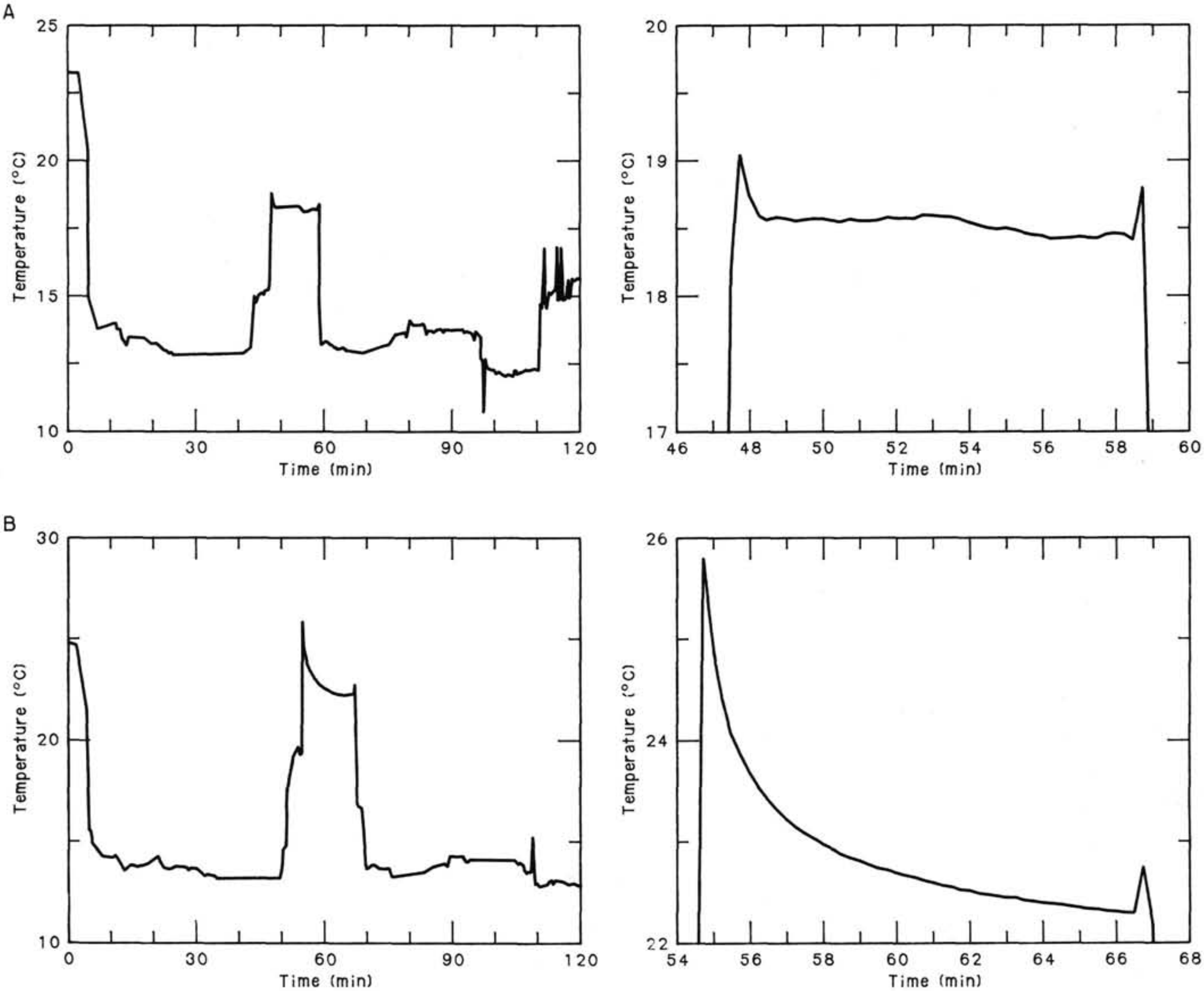

Figure 23. Temperature records at Stations (A) HF1 (41.6 mbsf) and (B) HF2 (79.6 mbsf).

the balatino-type gypsum (slow penetration, vibrating drill string) were not noticed either. The limited lateral extent of the laminar gypsum suggests that the body of water in which it was deposited was small and thus possibly shallow. The lack of sedimentary structures indicative of current reworking suggests a quiet, restricted depositional environment.

The facies association described in 2, 3, and 4 above are all indicative of a shallow, semi-restricted to restricted, marginal-marine environment.

5. The 70–90-cm-thick sand interval suggests a higher energy environment. The upsection change from a carbonate/gypsum depositional environment (chemical sedimentation) to a clastic depositional environment suggests that a new source of sediment has been activated. The appearance of clastic sediments can be explained by a transgression onto the western flank of the 250-m-high basement ridge whose crest is 20 km east of the site. As water level rose, the inferred physiographic barrier which had isolated Site 653 from the open ocean was submerged. Without a restricted environment, chemical sedimentation ceased. As the sea transgressed the basement ridge, erosion was active at the new shoreline. Sand eroded nearshore was transported downslope and deposited at the locations of Holes 653A, 653B, and at Site 132. The presence of biotite in the sand is compatible with a basement source and a short distance of transport. The gypsum in this sand is also tentatively interpreted as detrital. Since the source of sand lay to the east, the sand unit at Site 132 is only 25 cm thick as opposed to the 70–90 cm of sand observed at Site 653.

6. When the water level had risen significantly above the level of the crest of the basement ridge, input of sand to Site 653 ceased and marine deposition began. During this interval the sea continued to transgress across the continental slope. Of the material eroded at the now-distant shoreline, only the fine-grained particles (including the distinctively-colored iron oxide particles) could reach the site by transport in suspension. By this time the water depth at Site 653 was sufficiently deep that a normal marine foraminifer community was established. The development of this classic transgressive sequence in its entirety probably occurred in a relatively short period of geologic time, on the order of thousands of years, similar to Holocene transgressive events.

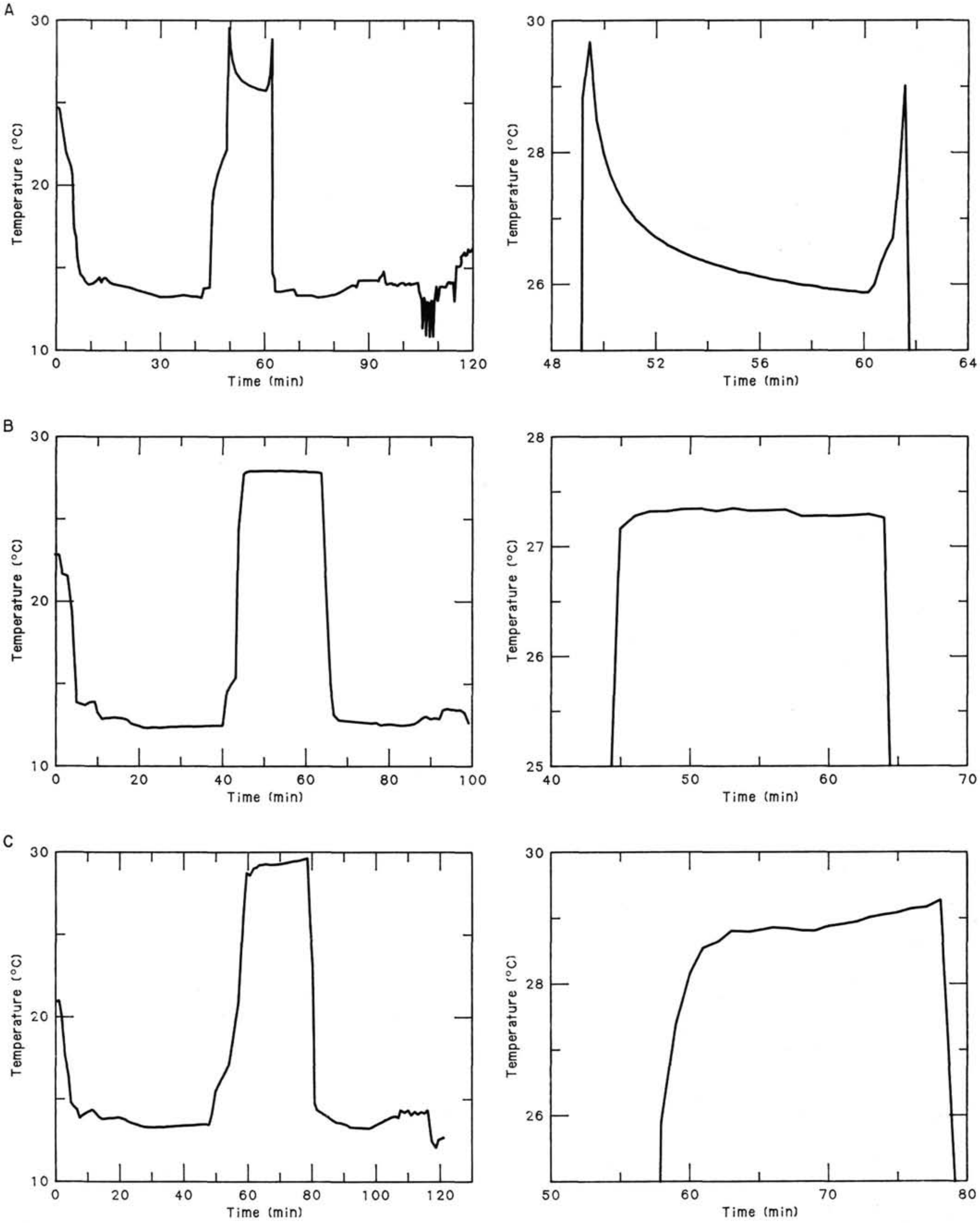

Figure 24. Temperature records at Stations (A) HF3 (117.3 mbsf), (B) HF4 (155.2 mbsf), and (C) HF5 (192.9 mbsf).

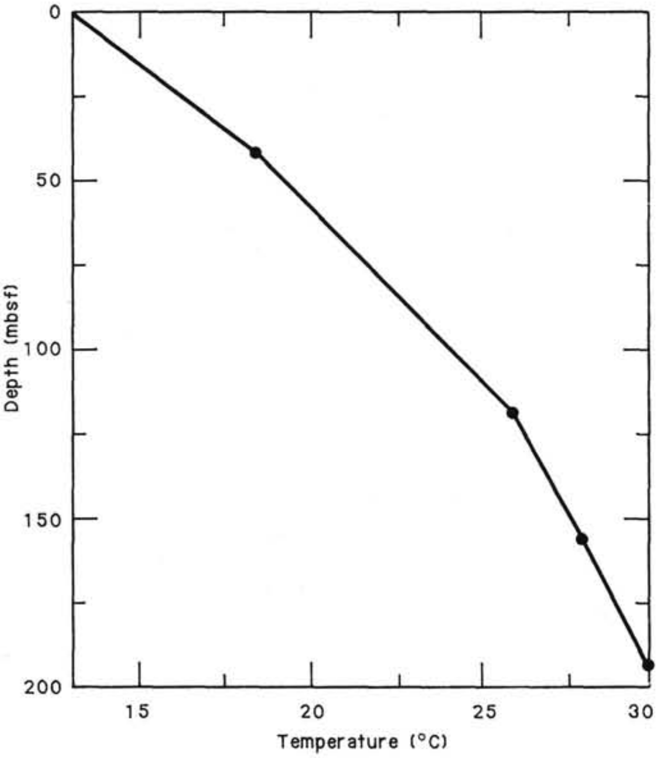

Figure 25. Sediment temperature vs. sub-bottom depth plot in Hole 653A (equivalent to geothermal gradient).

REFERENCES

Adams, C. G., Benson, R. H., Kidd, R. B., Ryan, W.B.F., and Wright, R. C., 1977. The Messinian salinity crisis and evidence of late Miocene eustatic changes in the world ocean. *Nature*, 269:383-386.

AGIP, 1982. *Foraminiferi padami (Terziario e Quatermario)*, (2nd ed.) Milano (AGIP).

Backman, J., and Shackleton, N. J., 1983. Quantitative biochronology of Pliocene and early Pleistocene calcareous nannofossils from the Atlantic, Indian and Pacific Oceans. *Mar. Micropaleontol.*, 8:141-170.

Bizon, G., 1985. Mediterranean foraminiferal changes as related to paleoceanography and paleoclimatology. *In* Stanley, D. J., and Wezel, F. G. (Eds.), *Geological Evolution of the Mediterranean Basin*: New York (Springer), 453-470.

Bizon, G., and Müller, C., 1977. Remarks on some biostratigraphic problems in the Mediterranean Neogene. *In* Biju-Duval, B., and Montadert, L. (Eds.), *Structural History of the Mediterranean Basin*: Paris (Technip), 381-390.

________, 1978. Remarks on the determination of the Pliocene/Pleistocene boundary in the Mediterranean. *In* Hsü, K. J., Montadert, L., et al., *Init. Repts. DSDP*, 42A: Washington (U.S. Govt. Printing Office), 847-853.

Blanc-Vernet, L., Froget, C., and Sgarella, F., 1983. Paleoclimatologie d'une carotte de la Mer Tyrrhenienne. *Geol. Mediter.* 10,2:93-104.

Ciaranfi, N., and Cita, M. B., 1973. Paleontological evidence of changes in the Pliocene Climates. *In* Ryan, W.B.F., Hsü, K. J., et al., *Init. Repts. DSDP*, 13: Washington (U.S. Govt. Printing Office), 1387-1399.

Cifelli, R., 1974. Planktonic foraminifera from the Mediterranean and adjacent Atlantic waters (Cruise 49 of the Atlantis II, 1969). *J. Foraminiferal Res.*, 4,4:171-183.

Cita, M. B., 1973. Pliocene biostratigraphy and chronostratigraphy. *In* Ryan, W.B.F., Hsü, K. J., et al., *Init. Repts. DSDP*, 13: Washington (U.S. Govt. Printing Office), 1343-1379.

________, 1975. Studi sul Pliocene e gli strati di passagio del Miocene al Pliocene, VIII. Planktonic foraminiferal biozonation of the Mediterranean deep sea record. A revision. *Riv. Ital. Paleontol. Stratigr.*, 81:527-544.

________, 1976. Planktonic foraminiferal biostratigraphy of the Mediterranean Neogene. *In* Takayanagi, Y., and Saito, T. (Eds.), *Progress in Micropaleontology*: New York (Micropaleontology Press), 47-68.

Cita, M. B., Chierici, M. A., Ciampo, G., Moncharmont Zei, M., D'Onofrio, S., Ryan, W.B.F., and Scorziello, R., 1973. The Quaternary record in the Tyrrhenian and Ionian Basins of the Mediterranean Sea. *In* Ryan, W.B.F., Hsü, K. J., et al., *Init. Repts. DSDP*, 13: Washington (U.S. Govt. Printing Office), 1263-1379.

Colalongo, M. L., and Sartoni, S., 1967. *Globorotalia hirsuta aemiliana* nuova sottospecie cronologica del Pliocene in Italia. *G. Geol.*, 34:1-15.

Colantoni, P., Fabbri, A., Gallignani, P., Sartori, R., and Rehault, J.-P., 1981. Carta lithologica e stratigraphica del Mari Italiano. *Consiglio Naz. Ricerchi Publ.* 4.

Conato, V., and Follador, U., 1967. *Globorotalia crotonensis* e *Globorotalia crassacrotonensis* nuove specie del Pliocene italiani. *Boll. Soc. Geol. Ital.*, 86:555-563.

Duschenes, J., Sinha, M. C., and Louden, K. E., 1986. A seismic refraction experiment in the Tyrrhenian Sea. *Geophys. J. R. Astron. Soc.*, 85:139-160.

Fabbri, A., and Curzi, P., 1979. The Messinian of the Tyrrhenian Sea: Seismic evidences and dynamic implications. *G. Geol.*, 2,43:215-248.

Ferguson, J., Burne, R. V., and Chambers, L. A., 1983. Iron mineralization of peritidal carbonate sediments by continental groundwater, Fisherman Bay, South Australia. *Sediment. Geol.*, 34:41-57.

Finetti, I., Morelli, C., and Zarudski, E., 1970. Reflection seismic study of the Tyrrhenian Sea. *Boll. Geofis. Teor. Appl.*, 12,41:311-346.

Gradstein, F. M., 1974. Mediterranean Pliocene Globorotalia. A biometrical approach. *Utrecht Micropaleontol. Bull.*, 7:1-128.

Hsü, K. J., Montadert, L., et al., 1978. Site 372: Menorca Rise. *In* Hsü, K. J., Montadert, L., et al., *Init. Repts. DSDP*, 42: Washington (U.S. Govt. Printing Office), 59-150.

Hsü, K. J., Montadert, L., Bernoulli, D., Cita, M. B., Erickson, A., Garrison, R. E., Kidd, R. B., Melieres, F., Müller, C., and Wright, R., 1978. History of the Mediterranean salinity crisis. *In* Hsü, K. J., Montadert, L., et al., *Init. Repts. DSDP*, 42, Pt. 1: Washington (U.S. Govt. Printing Office), 1053-1078.

Hutchison, I., Von Herzen, R., Louden, K., Sclater, J., and Jemsek, J., 1985. Heat flow in the Balearic and Tyrrhenian basins, Western Mediterranean. *J. Geophys. Res.*, 90(B1):685-701.

Iaccarino, S., 1985. Mediterranean Miocene and Pliocene planktonic foraminifera. *In* Bolli, H. M., Saunders, J. B., and Perch-Nielson, K. (Eds)., *Plankton Stratigraphy*: Cambridge (Cambridge Univ. Press), 282-314.

Iaccarino, S., and Salvatorini, G., 1982. A framework of planktonic foraminiferal biostratigraphy for early Miocene to late Pliocene Mediterranean area. *Paleontol. Stratigr. Evol.*, 2:115-125.

Malinverno, A., Cafiero, M., Ryan, W.B.F., and Cita, M. B., 1981. Distribution of Messinian sediments and erosional surfaces beneath the Tyrrhenian Sea: geodynamic implications. *Oceanol. Acta*, 4: 489-496.

McKenzie, J. A., Jenkins, H. C., and Bennet, G. G., 1979. Stable isotopic study of the cyclic diatomite-claystone from the Tripoli Formation, Sicily: A prelude to the Messinian salinity crisis. *Paleogeogr. Paleoclimatol. Paleoecol.*, 29:125-142.

McKenzie, J. A., Hsü, K. J., and Schneider, J. F., 1980. Movement of subsurface waters under the sabkha, Abu Dhabi, UAE, and its relation to evaporative dolomite genesis. *In* Zenger, D. H., Dunham, J. B., and Ethington, R. L. (Eds.), *Concepts and Models of Dolomitization:* Soc. Econ. Paleontol. Mineral. Spec. Publ., 28:11-30.

Martini, E., 1971. Standard Tertiary and Quaternary calcareous nannoplankton zonation. *Proc. II Planktonic Conf.*, Roma 1970:Rome (Ed. Technoscienza), 739-785.

Müller, C., 1978. Neogene calcareous nannofossils from the Mediterranean Leg 47A of the Deep-Sea Drilling Project. *In* Hsü, K. J., Montadert, L., et al., *Init. Rept. DSDP*, 42A: Washington (U.S. Govt. Printing Office), 727-751.

________, 1985. Late Miocene to Recent Mediterranean biostratigraphy and paleoenvironment based on calcareous nannoplankton. *In* Stanley, D. J., and Wezel, F. (Eds.), *Geological Evolution of the Mediterranean Basin*: New York (Springer), 471-485.

Parker, F. L., 1955. Distribution of planktonic Foraminifera in some Mediterranean sediments. *Papers in Marine Biology and Oceanography*: London (Pergamon Press), 204-211.

Phleger, F. B., 1947. Foraminifera of three submarine cores from the Tyrrhenian Sea. Goeteborgs Kungl. Vetensh. Och. Vitterhets—Samhaellews, Handl., *Sjaette Foeljdes*, 13, 5:1-19.

Raffi, I., and Rio, D., 1979. Calcareous nannofossil biostratigraphy of DSDP Site 132—Leg 13 (Tyrrhenian Sea-Western Mediterranean). *Riv. Ital. Paleontol. Stratigr.*, 85:127-172.

Rio, D., Sprovieri, R., and Raffi, I., 1984. Calcareous plankton biostratigraphy and biochronology of the Pliocene-Lower Pleistocene succession of the Capo Rossello area Sicily. *Mar. Micropaleontol.*, 9: 135-180.

Ryan, W.B.F., Cita, M. B., Dreyfus Rawson, M., Burckle, L. H., and Saito, T., 1974. A paleomagnetic assignment of Neogene stage boundaries and the development of isochronous datum planes between the Mediterranean, the Pacific and Indian Oceans in order to investigate the response of the world ocean to the Mediterranean "Salinity Crisis." *Riv. Ital. Paleontol. Stratigr.*, 80:631-688.

Ryan, W.B.F., Hsü, K. J., et al., 1973. Tyrrhenian Rise: Site 132. *In* Ryan, W.B.F., Hsü, K. J., et al., *Init. Repts. DSDP*, 13: Washington (U.S. Govt. Printing Office), 404-464.

Schreiber, B. C., 1982. Environments of subaqueous gypsum deposition. *In* Dean, W. E., and Schreiber, B. C. (Eds.), *Marine Evaporites:* Soc. Econ. Paleontol. Mineral. Short Course Notes, 4:43-73.

Scott, G. H., 1980. Upper Miocene biostratigraphy: Does *Globorotalia conomiozea* occur in the Messinian? *Rev. Esp. Micropaleontol.*, 12: 489-506.

Shearman, D. J., 1982. Evaporites of coastal sabkhas. *In* Dean, W. E., and Schreiber, B. C. (Eds.), *Marine Evaporites:* Soc. Econ. Paleontol. Mineral. Short Course Notes, 4:6-42.

Spaak, P., 1981. The distribution of the *Globorotalia inflata* group in the Mediterranean Pliocene. *Proc. K. Ned. Akad. Wet.*, B,84,2:201-215.

———, 1983. Accuracy in correlation and ecological aspects of the planktonic foraminiferal zonation of the Mediterranean Pliocene. *Utrecht Micropaleontol. Bull.*, 28:1-160.

Sprovieri, R., and Barone, G., 1984. I foraminiferi benthonici della sezione pliocenica di Punta Piccola (Agrigento, Sicilia). *Geol. Rom.*

Steinmetz, L., Ferrucci, F., Hirn, A., Morelli, C., and Nicolich, R., 1983. A 550 km long Moho traverse in the Tyrrhenian Sea from O.B.S. recorded Pn waves. *Geophys. Res. Lett.*, 10:428-431.

Teller, T. T., Bowler, J. M., and Macumber, P. G., 1982. Modern sedimentation and hydrology in Lake Tyrrell, Victoria. *J. Geol. Soc. Aust.*, 29:159-175.

Thunell, R. C., 1979. Pliocene-Pleistocene paleotemperature and paleosalinity history of the Mediterranean Sea: Results from DSDP Sites 125 and 132. *Mar. Micropaleontol.*, 4:173-187.

Thunnell, R. C., and Williams, D. F., 1983. The stepwise development of Pliocene-Pleistocene paleoclimatic and paleoceanographic conditions in the Mediterranean: Oxygen isotopic studies of DSDP Sites 125 and 132. *Utrecht Micropaleontol. Bull.*, 30:111-127.

Todd, R., 1958. Foraminifera from Western Mediterranean deep-sea cores. *Rep. Swed. Deep-Sea Exped.*, 8,3:169-215.

Vergnaud Grazzini, C., 1985. Mediterranean Late Cenozoic stable isotope record: Stratigraphic and paleoclimatic implications. *In* Stanley, D. J., and Wezel, F. C. (Eds.), *Geological Evolution of the Mediterranean Basin*: New York (Springer), 413-451.

Watkins, N. D., Kester, D. R., and Kennett, J. P., 1974. Paleomagnetism of the type Pliocene/Pleistocene boundary section at Santa Maria di Catanzaro, Italy, and the problem of post-depositional precipitation of magnetic minerals. *Earth Planet. Sci. Lett.*, 24:113-119.

Wright, R., 1978. Neogene paleobathymetry of the Mediterranean based on benthic foraminifers from DSDP Leg 42A. *In* Hsü, K. J., Montadert, L., et al., *Init. Repts. DSDP*, 42, Pt. 2: Washington (U.S. Govt. Printing Office), 837-846.

Zachariasse, W. J., 1979. The origin of *Globorotalia conomiozea* in the Mediterranean and the value of its entry level in biostratigraphic correlations. *Ann. Geol. Pays Hell.*, 3:1281-1292.

Zachariasse, W. J., and Spaak, P., 1979. The frequency distribution of *Globigerina nepenthes* in the Mediterranean lowermost Pliocene. *Ann. Geol. Pays Hell.*, 3:1293-1303.

Table 12. Interval temperatures, gradient, thermal conductivity, and heat flow at Site 653.

Sub-bottom interval (m)	Interval temperature difference °C	Thermal gradient °C/km	Thermal conductivity W/mk	n	Heat flow mW $m^{-2}s^{-1}$	HFU
41.6	5.4	129.8	A 1.092 ± 0.05	7	141.7	3.38
			B 1.007 ± 0.04	23	130.7	3.12
38	3.8	100.0	A 1.234 ± 0.02	4	123.4	2.94
			B 1.093 ± 0.005	12	109.3	2.61
37.7	3.55	94.2	A 1.283 ± 0.08	4	121.0	2.89
			B 1.272 ± 0.01	19	119.8	2.86
37.9	2.00	52.8	A 1.360 ± 0.1	4	71.8	1.71
			B 1.234	17	65.15	1.56
37.7	1.95	51.7	A 1.289 ± 0.05	13	66.6	1.59
			B 1.328	25	68.65	1.64
75.7	7.35	97.0	A 1.258		122.0	2.91
75.6	3.95	52.3	A 1.325		69.3	1.66

Note: A = from 653A; B = from 653B

Table 13. Thermal conductivity harmonic means for each core and for temperature measurement intervals, performed at Site 653.

	Hole 653B				Hole 653A		
Core	Measurement number	Thermal conductivity (W/mK)	Interval mean	Core	Measurement number	Thermal conductivity (W/mK)	Interval mean
1	4	0.943		1	2	1.033	
2	5	1.018		2	1	1.077	
3	5	1.005	n=23	3	1	1.185	
4	5	1.020	1.007	4	1	1.079	n=7
5	4	1.041	1	5	1	1.083	1.092
6	7	1.095		6	1	1.191	
7	5	1.091		7	1	1.243	
8	0	—	n=12	8	1	1.250	n=4
9	0	—	1.093 2	9	1	1.252	1.234
10	5	1.052		10	1	1.252	
11	5	1.273	n=14	11	1	1.264	n=4
12	5	1.274	1.272	12	1	1.287	1.283
13	4	1.268	3	13	1	1.374	
14	2	1.295		14	1	1.292	
15	5	1.201	n=17	15	1	1.510	n=4
16	5	1.273	1.234	16	1	1.293	
17	5	1.216	4	17	1	1.347	
18	5	1.300		18	1	1.321	
19	5	1.296	n=25	19	2	1.331	n=13
20	5	1.350	1.328	20	5	1.226	1.289
21	10	1.366	5	21	5	1.278	
22	10	1.326		22	4	1.284	
23	15	1.260		23	5	1.256	
24	5	1.722		24	5	1.178	n=29
25	3	1.365	n=59	25	5	1.353	1.245
26	6	1.298	1.372	26	10	1.153	
27	17	1.321					
28	3	1.309					

SITE 653 HOLE A CORE 1 H CORED INTERVAL 2817.0-2820.7 mbsl; 0-3.7 mbsf

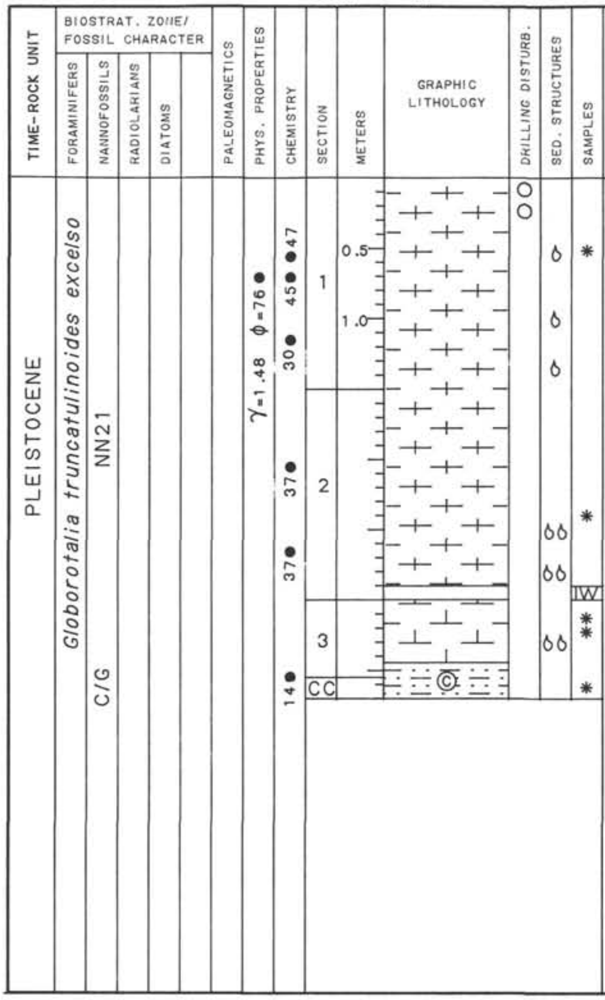

LITHOLOGIC DESCRIPTION

MARLY NANNOFOSSIL OOZE and CALCAREOUS MUD

Marly nannofossil ooze, yellowish brown (10YR 5/4) to yellow (10YR 7/8), and *calcareous mud, light olive-brown* (2.5Y 5/4) to light gray (2.5Y 7/2), and olive (5Y 5/3) to light olive. Principal colors: light olive-brown (2.5Y 5/4), light brownish gray (2.5Y 6/2), light yellowish brown (2.5Y 6/4), light gray (2.5Y 7/2), olive (5Y 5/3), light olive-gray (5Y 6/2), pale olive (5Y 6/3), and yellowish brown (10Y 5/2, 10YR 5/4, 10YR 6/4). Some very dark to black diffuse specks; burrowing rarely observed. Pteropod shells common and enriched in discrete levels, especially in Section 3, 29–36 cm.

Minor lithology: Mn(?)-rich layer at Section 3, 20 cm, mm-thin and dark bluish gray (5B 4/1).

SMEAR SLIDE SUMMARY (%):

	1, 50 D	2, 90 D	3, 3 D	3, 13 M	3, 26 M	CC, 3 M
TEXTURE:						
Sand	4	8	12	8	10	12
Silt	10	15	20	15	20	20
Clay	86	77	68	77	70	68
COMPOSITION:						
Quartz	5	6	10	10	10	8
Feldspar	—	1	—	—	—	—
Mica	—	1	Tr	—	—	Tr
Clay	31	26	32	42	28	70
Volcanic glass	1	2	1	5	3	5
Calcite/dolomite	3	5	15	15	5	5
Accessory minerals	—	1	1	2	2	3
Opaques	1	3	2	1	2	—
Pollen	2	2	2	1	1	3
Micrite	—	3	15	10	5	—
Gypsum?	—	—	—	—	—	2
Foraminifers	5	3	1	Tr	2	Tr
Nannofossils	50	45	20	15	40	4
Radiolarians	—	—	—	—	1	—
Sponge spicules	2	1	1	1	1	—
Fish remains	Tr	1	—	Tr	—	—

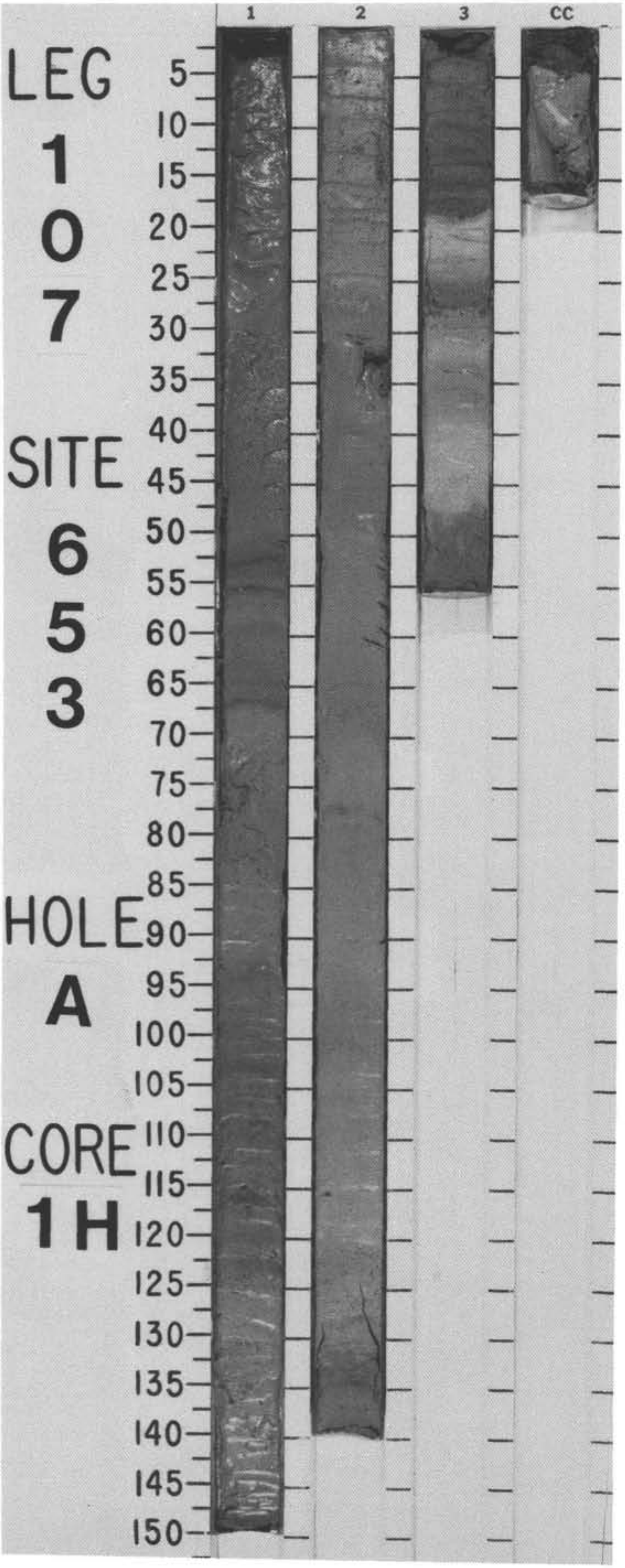
1
2
3
CC
LEG
1
0
7
SITE
6
5
3
HOLE
A
CORE
1H
5
10
15
20
25
30
35
40
45
50
55
60
65
70
75
80
85
90
95
100
105
110
115
120
125
130
135
140
145
150

SITE 653 HOLE A CORE 2 H CORED INTERVAL 2820.7-2830.2 mbsl; 3.7-13.2 mbsf

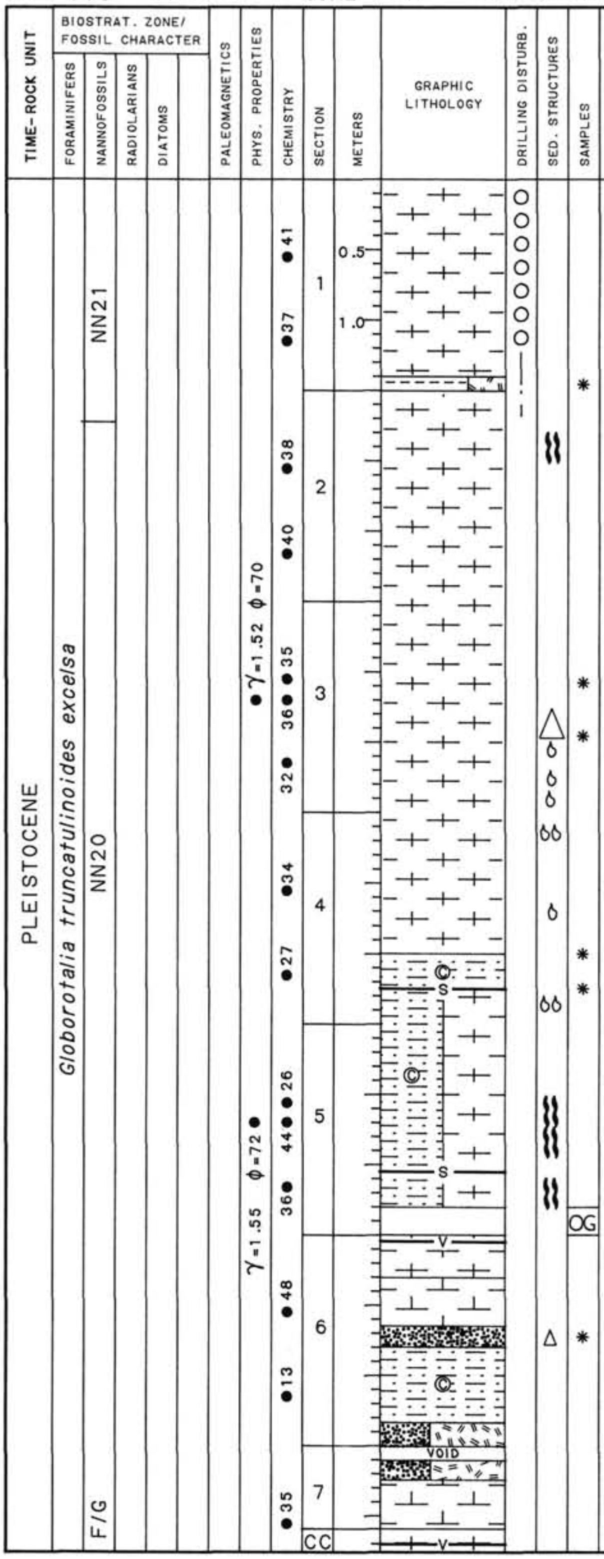

LITHOLOGIC DESCRIPTION

MARLY FORAMINIFERAL NANNOFOSSIL OOZE, intercalations of SANDS and VOLCANIC ASH, and SAPROPELS

Marly foraminiferal nannofossil ooze, light brownish gray (2.5Y 5/2, 6/2, 6/4), light gray (2.5Y 7/1, 7/2), gray (5Y 5/1, 6/1), olive-gray (5Y 5/2), light olive-gray (5Y 6/2), greenish gray (5BG 6/1), and gray (10Y 5/1). Some dark specks. Intensive burrowing in Sections 2 and 5. Pteropod shells common, enriched in discrete levels, especially in Section 3, 98–150 cm, Section 4, 60 cm, and base of Section 4.

Minor lithologies:

a) Volcanic-ash-bearing clay in Section 1, 140–150 cm, brown (10YR 5/3); Section 6, 6 cm, black (5Y 2.5/1); Section 6, 136–150 cm, and Section 7, 11–24 cm, dark gray (5Y 4/1).
b) Mn-rich nannofossil marl in Section 4, 101 cm, gray (5Y 4/1), and Section 5, 99 cm.
c) Dolomite-bearing clay (sapropel?) in Section 4, 124–130 cm, olive-gray (5Y 5/2) and dark olive-gray (5Y 3/1).
d) Sandy silt, 3-mm thick, Section 5, 20 cm.
e) Sapropelic layers in Section 5, 104–108 cm, dark olive-gray (5Y 3/2).
f) Sand, Section 6, 65–80 cm, gray (10Y 5/1).

SMEAR SLIDE SUMMARY (%):

	1, 147 M	3, 54 D	3, – M	4, 101 M	4, 129 M	6, 77 M
TEXTURE:						
Sand	20	5	20	10	1	50
Silt	20	15	30	30	15	20
Clay	60	80	50	60	84	30
COMPOSITION:						
Quartz	10	3	10	1	4	20
Feldspar	—	—	—	—	—	2
Mica	—	—	—	—	Tr	Tr
Clay	53	14	50	30	57	35
Volcanic glass	30	5	4	1	3	2
Calcite/dolomite	2	13	15	5	17	Tr
Accessory minerals	—	2	2	2	2	2
Opaques	1	—	2	—	—	—
Zeolites	1	—	—	—	—	—
Micrite	Tr	—	15	—	10	20
Authigenic gypsum	—	—	1	—	—	—
Gypsum(?)	—	2	—	—	—	10
Pyrite spherules	—	—	1	—	2	—
Opaques (amorph.)	—	—	—	25	—	—
Glauconite, Mg(?)	—	—	—	—	—	4
Foraminifers	2	1	—	1	—	8
Nannofossils	1	60	—	35	3	—
Diatoms	—	—	—	—	—	Tr
Radiolarians	—	—	—	—	Tr	1
Sponge spicules	—	—	—	—	Tr	—
Fish remains	—	—	—	—	—	Tr
Pollen	Tr	—	—	—	1	—
Organic matter	—	—	—	—	1	—

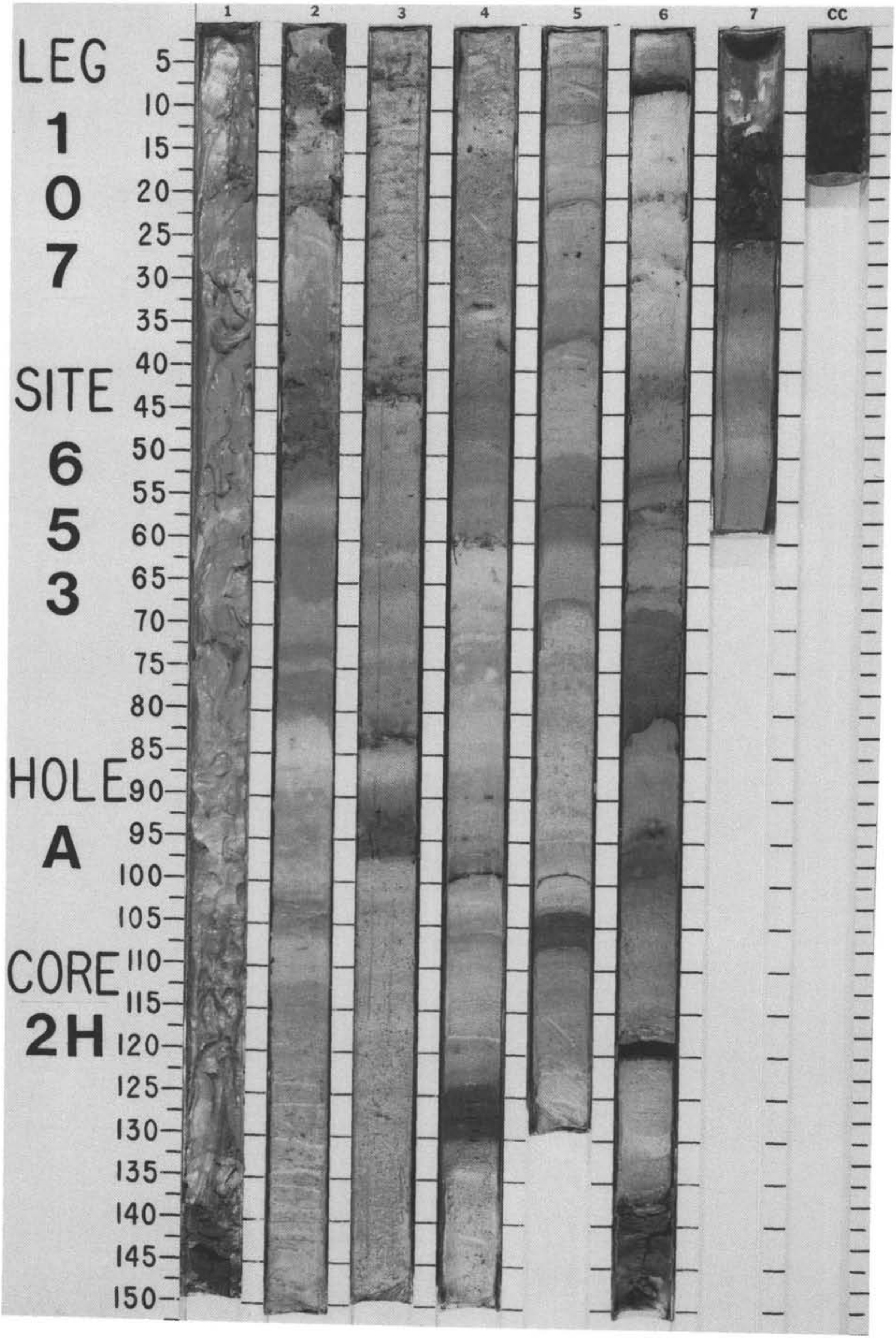
LEG
107
SITE
653
HOLE
A
CORE
2H
1
2
3
4
5
6
7
CC
5
10
15
20
25
30
35
40
45
50
55
60
65
70
75
80
85
90
95
100
105
110
115
120
125
130
135
140
145
150

SITE 653 HOLE A CORE 3 H CORED INTERVAL 2830.2-2839.7 mbsl; 13.2-22.7 mbsf

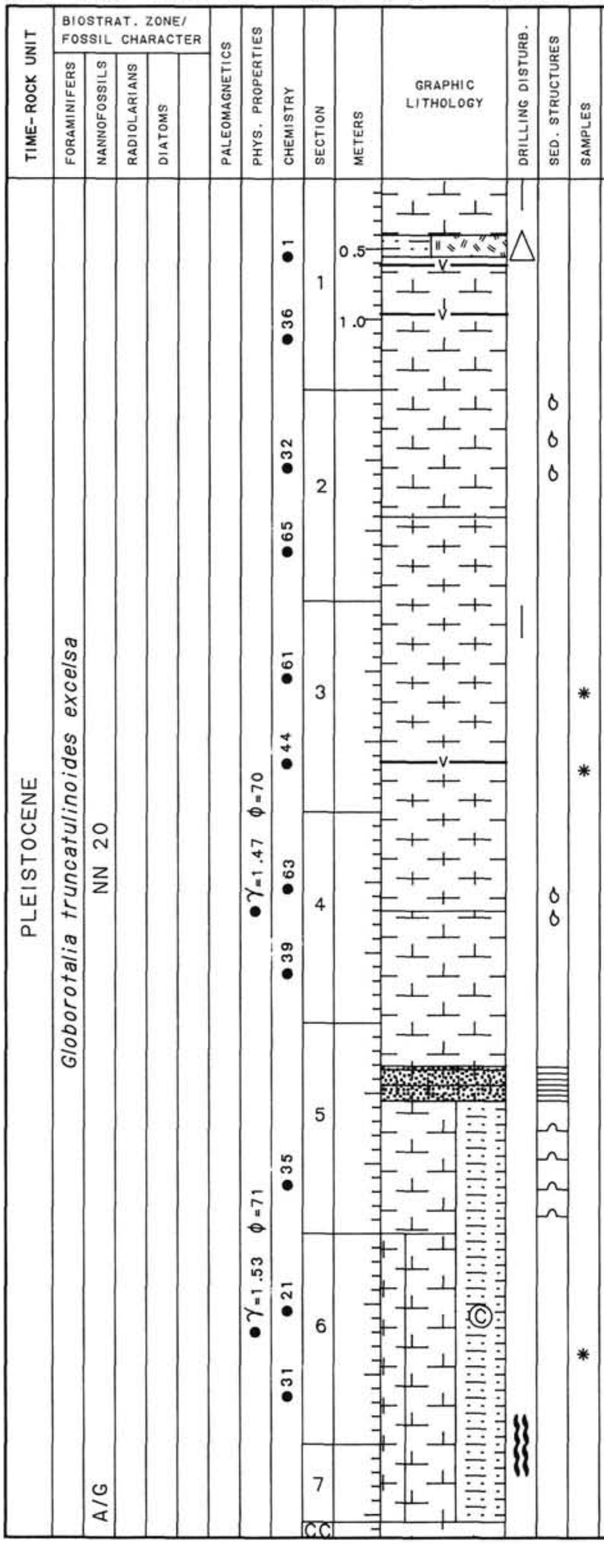

LITHOLOGIC DESCRIPTION

MARLY NANNOFOSSIL OOZE and MARLY FORAMINIFER-NANNOFOSSIL OOZE and intercalated SILTY/SANDY LAYERS

Marly nannofossil ooze and marly foraminifer-nannofossil ooze, dark grayish brown (2.5Y 4/2), gray (2.5Y 5/0; 5Y 5/1, 6/1), grayish brown (2.5Y 5/2), light brownish gray (2.5Y 6/2), yellowish brown (2.5Y 6/4, 10YR 5/4), light gray (2.5Y 7/2, 5Y 7/2), black (5Y 2.5/1), olive (5Y 5/3), light olive-gray (5Y 6/2), pale olive (5Y 6/3, 6/4), pale yellow (5Y 7/3, 7/4), white (5Y 8/1), dark grayish brown (10YR 4/2), brown (10YR 6/3), and very pale brown (10YR 7/3). At Section 5, 55–150 cm, there is a mud debris flow or slump containing mud balls of nannofossil ooze showing different colors as well as black sandy patches. Pteropod shells are enriched in discrete intervals.

Minor lithologies:
a) Ash layers in Section 1, 44–56 cm: very dark grayish brown (2.5Y 3/2) and dark grayish brown (2.5Y 4/2), normally graded; Section 1, 95–100 cm: dark grayish brown (2.5Y 4/2); and Section 3, 115–120 cm: black (5Y 2.5/1), rich in carbonate (44%).
b) Mn(?)-rich layer in Section 2, 132 cm.
c) Foraminifer sand in Section 5, 30–55 cm.

SMEAR SLIDE SUMMARY (%):

	3, 66 D	3, 119 M	6, 83 D
TEXTURE:			
Sand	5	25	5
Silt	2	30	10
Clay	93	45	85
COMPOSITION:			
Quartz	2	8	5
Feldspar	—	1	—
Mica	Tr	Tr	Tr
Clay	41	30	22
Volcanic glass	—	5	2
Calcite/dolomite	2	5	3
Accessory minerals	1	3	2
Opaques	1	6	2
Zeolites	—	—	Tr
Micrite	—	15	12
Foraminifers	3	—	2
Nannofossils	50	25	50
Radiolarians	—	—	Tr
Fish remains	—	—	Tr
Pollen	—	2	—

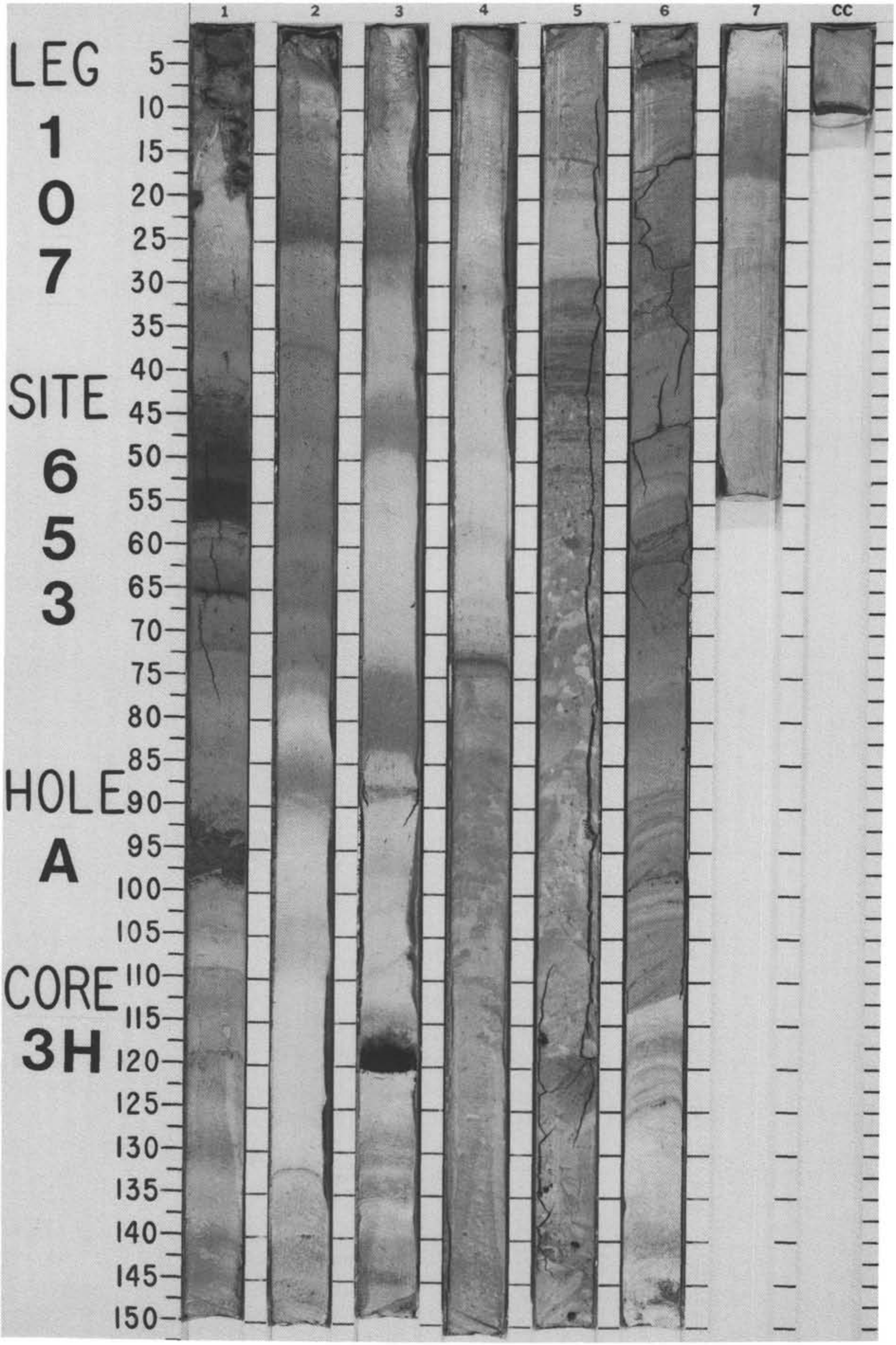
LEG
107
SITE
653
HOLE
A
CORE
3H
1
2
3
4
5
6
7
CC
5
10
15
20
25
30
35
40
45
50
55
60
65
70
75
80
85
90
95
100
105
110
115
120
125
130
135
140
145
150

SITE 653 HOLE A CORE 4 H CORED INTERVAL 2839.7-2849.2 mbsl; 22.7-32.2 mbsf

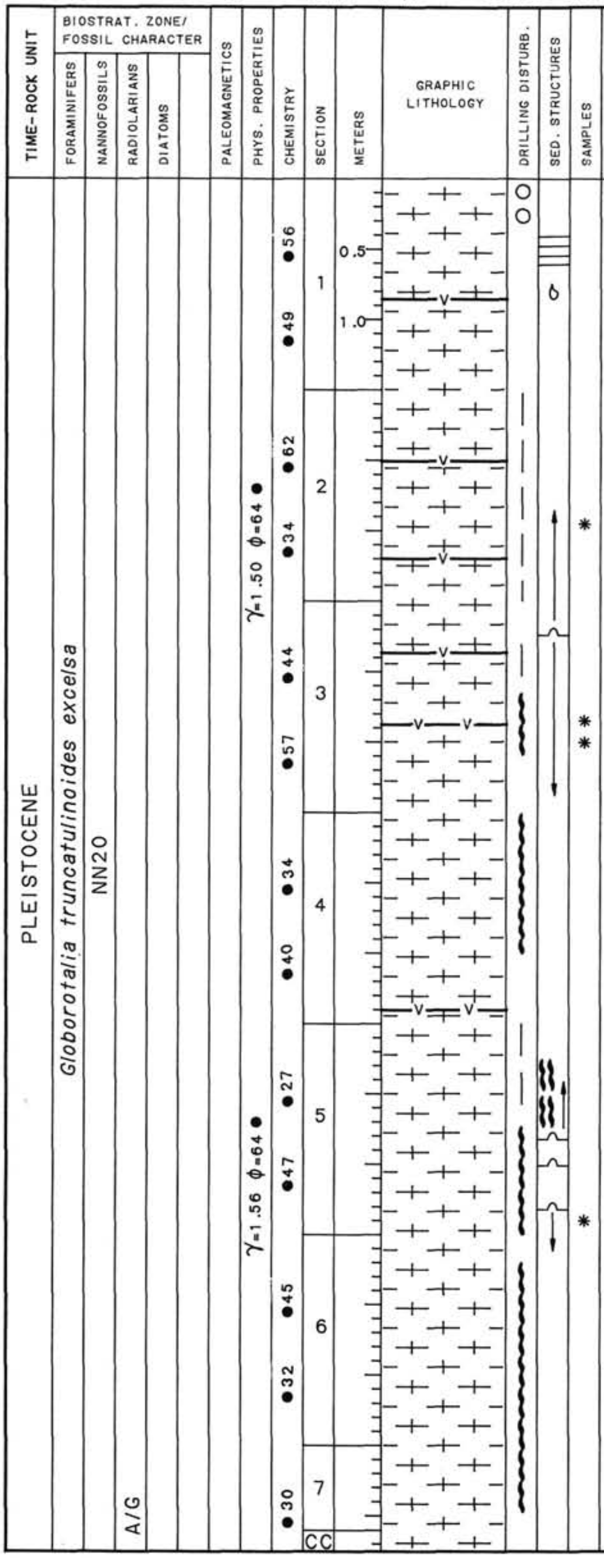

LITHOLOGIC DESCRIPTION

MARLY FORAMINIFER-NANNOFOSSIL OOZE, and intercalated SILTY/SANDY INTERVALS

Marly foraminifer-nannofossil ooze, gray (2.5Y 5/0; 5Y 5/1, 6/1; 10YR 5/1), grayish brown (2.5Y 5/2), light brownish gray (2.5Y 6/2), light yellowish brown (2.5Y 6/4), light gray (2.5Y 7/2; 5Y 7/2; 10YR 7/2), very dark gray (5Y 3/1), olive (5Y 4/3), olive-gray (5Y 5/2), light olive-gray (5Y 6/2), grayish green (5G 5/2), dusky yellow-green (5GY 5/2), (10YR 5/3) brown, (10YR 6/3) pale brown, (10YR 7/3) very pale brown, and white (10YR 8/2). Some colored laminae of centimeter thickness. Burrowing in Section 5. Sections 3 through 7: there are many disturbed intervals (not determined if caused by drilling or slumping).

Minor lithology:
Silty/sandy intervals in Section 1, 85 cm, Section 2, 50 and 120 cm, Section 3, 38 and 75–105 cm, and Section 4, 130–146 cm; ash layers, gray (10YR 5/1) to dark gray (10YR 4/1), generally 1 cm thick and overlain and underlain by indurated nannofossil ooze (also approximately 1 cm thick).

SMEAR SLIDE SUMMARY (%):

	2, 98 D	3, 89 M	3, 102 M	5, 139 D
TEXTURE:				
Sand	3	20	5	8
Silt	10	20	15	20
Clay	87	60	80	72
COMPOSITION:				
Quartz	2	15	5	5
Mica	—	2	Tr	3
Clay	31	31	34	14
Volcanic glass	2	6	5	5
Calcite/dolomite	1	—	3	3
Accessory minerals	1	3	1	2
Opaques	—	2	—	2
Micrite	—	10	—	5
Foraminifers	1	1	1	—
Nannofossils	60	30	50	60
Fish remains	Tr	—	—	—
Pollen	2	—	1	1

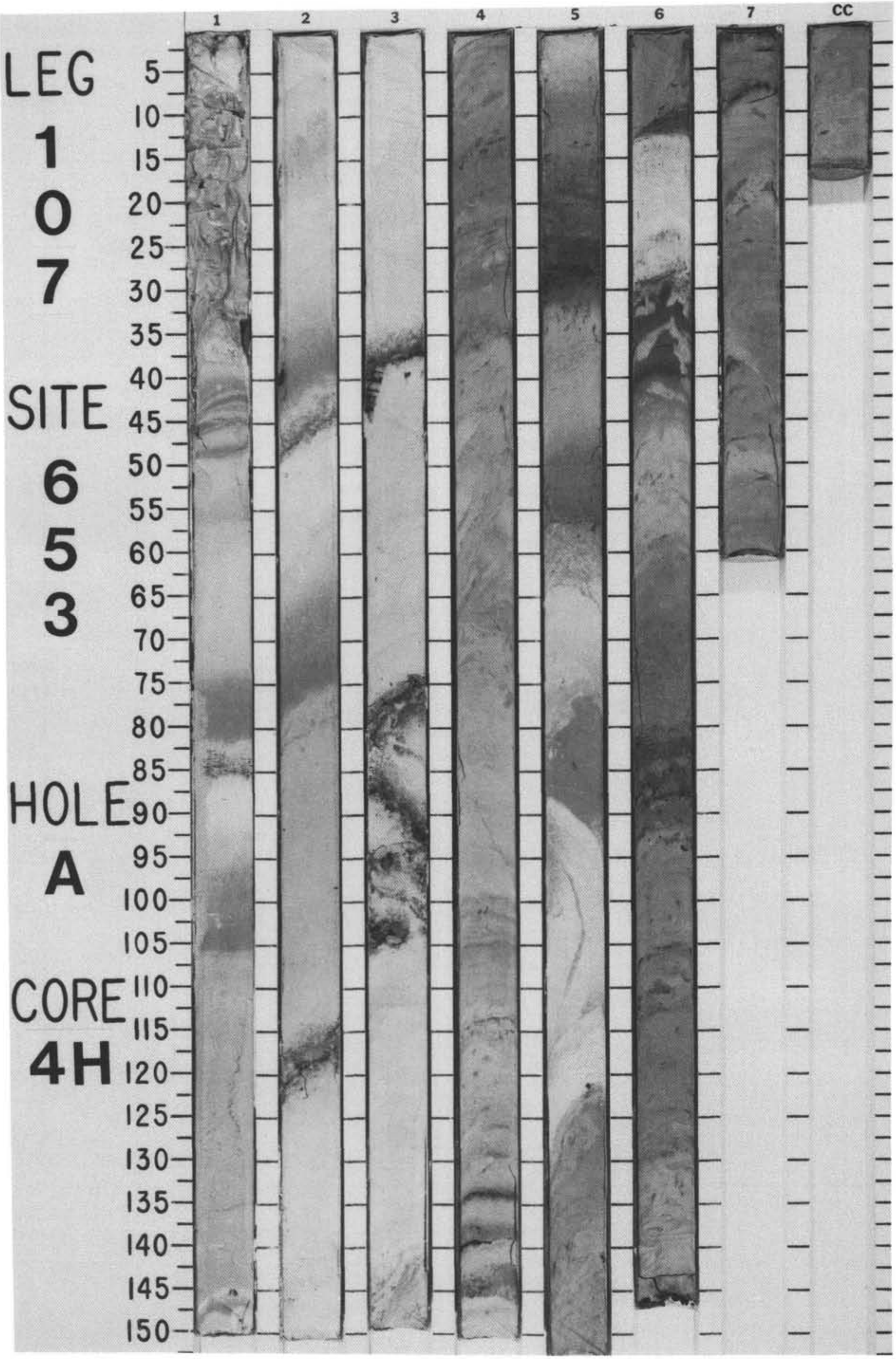
LEG
107
SITE
653
HOLE
A
CORE
4H
1
2
3
4
5
6
7
CC
5
10
15
20
25
30
35
40
45
50
55
60
65
70
75
80
85
90
95
100
105
110
115
120
125
130
135
140
145
150

SITE 653 HOLE A CORE 5 H CORED INTERVAL 2849.2-2858.6 mbsl; 32.2-41.6 mbsf

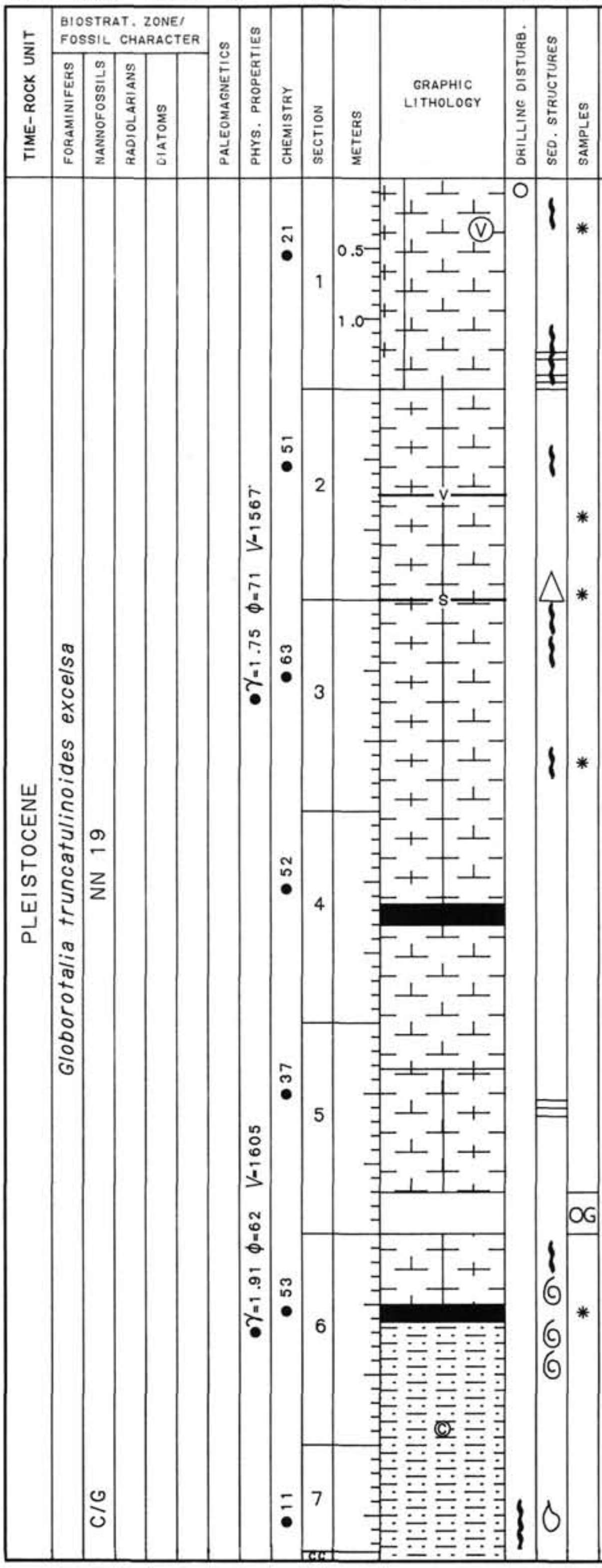

LITHOLOGIC DESCRIPTION

MARLY NANNOFOSSIL OOZE and MARLY FORAMINIFER-NANNOFOSSIL OOZE

Marly nannofossil ooze and marly foraminifer-nannofossil ooze, pale yellow (5Y 7/3), light gray (5Y 7/2), olive (5Y 5/3), light gray (5Y 7/1), pale olive (5Y 6/3), light yellowish brown (2.5Y 6/4), very dark gray (5Y 3/1) laminae, gray (5Y 5/1), light olive-gray (5Y 6/2), olive-gray (5Y 5/2), light gray (2.5Y 7/2), gray (2.5Y 5/0, 5Y 6/1), black (5Y 2.5/1) laminae, pale brown (10YR 6/3), light brownish gray (10YR 6/2), olive-yellow (5Y 6/6), gray (2.5Y 6/0, 10YR 6/1), dark gray (5Y 4/1), and olive (5Y 5/4). Within Section 1 there are three color cycles passing upward from pale olive (5Y 6/3) to light gray (5Y 7/1), possibly indicating an upward decrease of noncarbonatic material. Interbedded with very fine silty layers (ash-rich?). Section 1: burrows are filled with foraminiferal tests and large mica flakes. Otoliths in Section 6. Laminae as indicated.

Minor lithologies:
a) Pumice fragment (1 × 2 cm) in Section 1, 42 cm.
b) Silty layers (ash?), gray (2.5Y 5/0) and olive-gray (5Y 5/2) to pale olive (5Y 6/3), 1 to 15 cm thick.
c) Sapropelic layers (sapropels) in Section 3, 0–8 cm, and Section 4, 68–80 cm, olive (5Y 4/3), and Section 6, 52–62 cm, dark gray (5Y 4/1).
d) Mn-rich(?) layers in Section 5, 9 and 33 cm.
e) Calcareous mud in Section 6, 62 cm, to base of CC.

SMEAR SLIDE SUMMARY (%):

	1, 35 M	2, 90 M	2, 145 M	3, 115 D	6, 59 M
TEXTURE:					
Sand	15	20	10	15	12
Silt	20	20	20	10	20
Clay	65	60	70	75	68
COMPOSITION:					
Quartz	7	12	7	3	8
Feldspar	Tr	—	Tr	—	—
Mica	2	3	3	2	1
Clay	37	35	46	14	40
Volcanic glass	4	—	1	—	1
Calcite/dolomite	1	1	2	2	8
Accessory minerals	3	3	2	1	1
Pyrite	—	Tr	1	—	—
Opaques	—	—	Tr	1	2
Micrite	10	—	5	—	—
Foraminifers	2	18	2	15	10
Nannofossils	30	25	30	60	25
Diatoms	—	—	—	Tr	1
Radiolarians	Tr	2	Tr	1	2
Sponge spicules	1	1	Tr	2	1
Silicoflagellates	—	—	—	—	Tr
Fish remains	Tr	Tr	1	—	Tr
Pollens	2	—	—	1	—

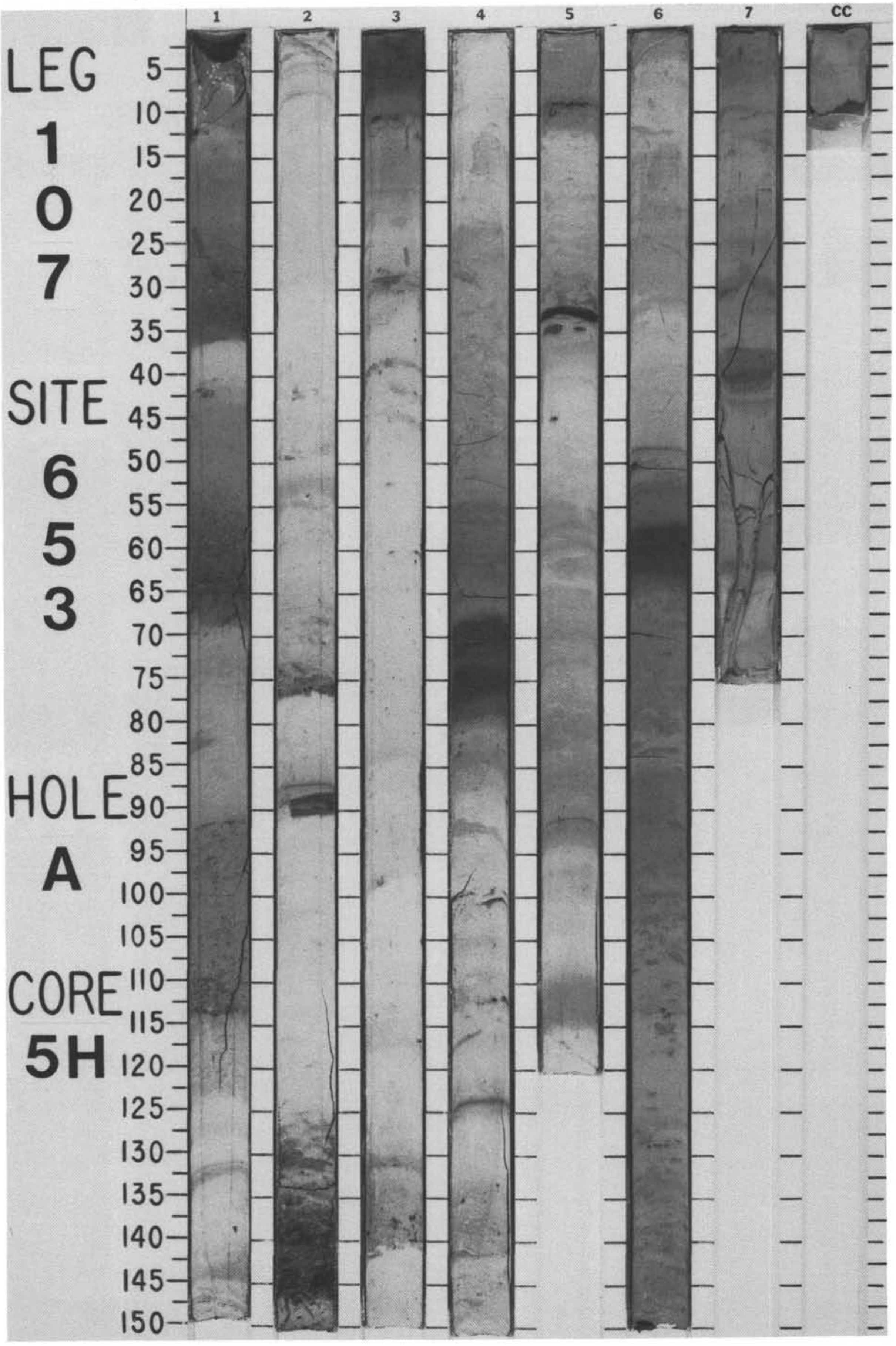
LEG
1
0
7
SITE
6
5
3
HOLE
A
CORE
5H
1
2
3
4
5
6
7
CC
5
10
15
20
25
30
35
40
45
50
55
60
65
70
75
80
85
90
95
100
105
110
115
120
125
130
135
140
145
150

SITE 653 HOLE A CORE 6 H CORED INTERVAL 2858.6-2868.0 mbsl; 41.6-51.0 mbsf

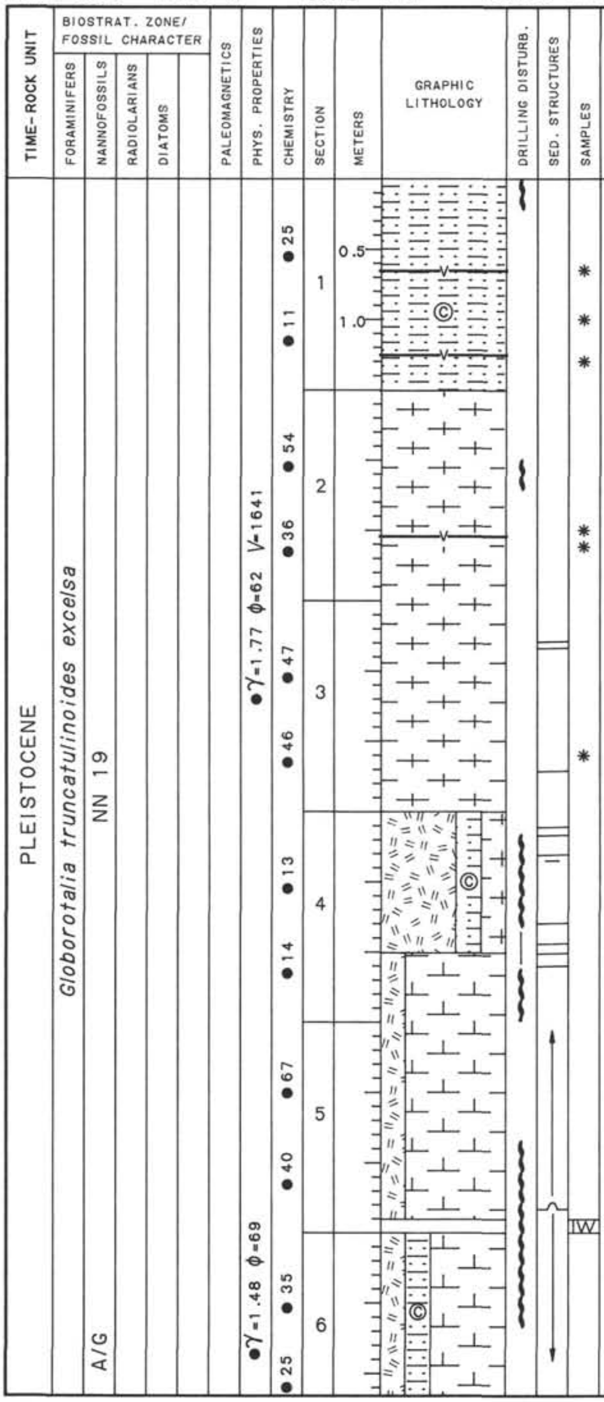

LITHOLOGIC DESCRIPTION

MARLY NANNOFOSSIL OOZE and MARLY FORAMINIFER-NANNOFOSSIL OOZE

Marly nannofossil ooze and marly foraminifer-nannofossil ooze, light olive-gray (5Y 6/2), light gray (5Y 7/2), olive-gray (5Y 4/2, 5/2), pale olive (5Y 6/3), olive-gray (5Y 7/1), gray (5Y 5/1), and white (5Y 8/1, 10GY 5/2). There are small burrows throughout. Scattered biotite crystals at Section 3, 105 and 112 cm. Coring disturbances particularly pronounced in Sections 5 and 6, probably caused by slumping (see corresponding stratigraphic interval in 107-653B-6H, Sections 2 and 3).

Minor lithologies:
a) Calcareous mud in Section 1, 0–150 cm.
b) volcanic ash-bearing nannofossil ooze or calcareous mud in Section 1, 68 and 126 cm, and Section 2, 109 cm, generally broken, 1 cm-thick lithified layers.

SMEAR SLIDE SUMMARY (%):

	1, 68 M	1, 90 D	1, 126 M	2, 108 M	2, 109 M	3, 107 M
TEXTURE:						
Sand	20	2	10		10	5
Silt	5	2	—	5	—	5
Clay	75	96	90	95	90	90
COMPOSITION:						
Quartz	1	1	5	1	3	1
Feldspar	5	1	—	1	—	1
Mica	—	—	—	—	2	5
Volcanic glass	22	2	20	79	20	5
Calcite/dolomite	2	2	1	—	2	3
Accessory minerals	—	2	—	—	—	—
	5	—	2	—	3	—
	1	—	—	—	—	—
Micrite	23	25	23	10	10	35
Spheroids	—	—	—	—	—	5
Foraminifers	10	5	10	5	10	10
Nannofossils	30	60	40	2	50	30
Sponge spicules	—	2	1	2	—	1
Silicoflagellates	1	Tr	—	—	—	2

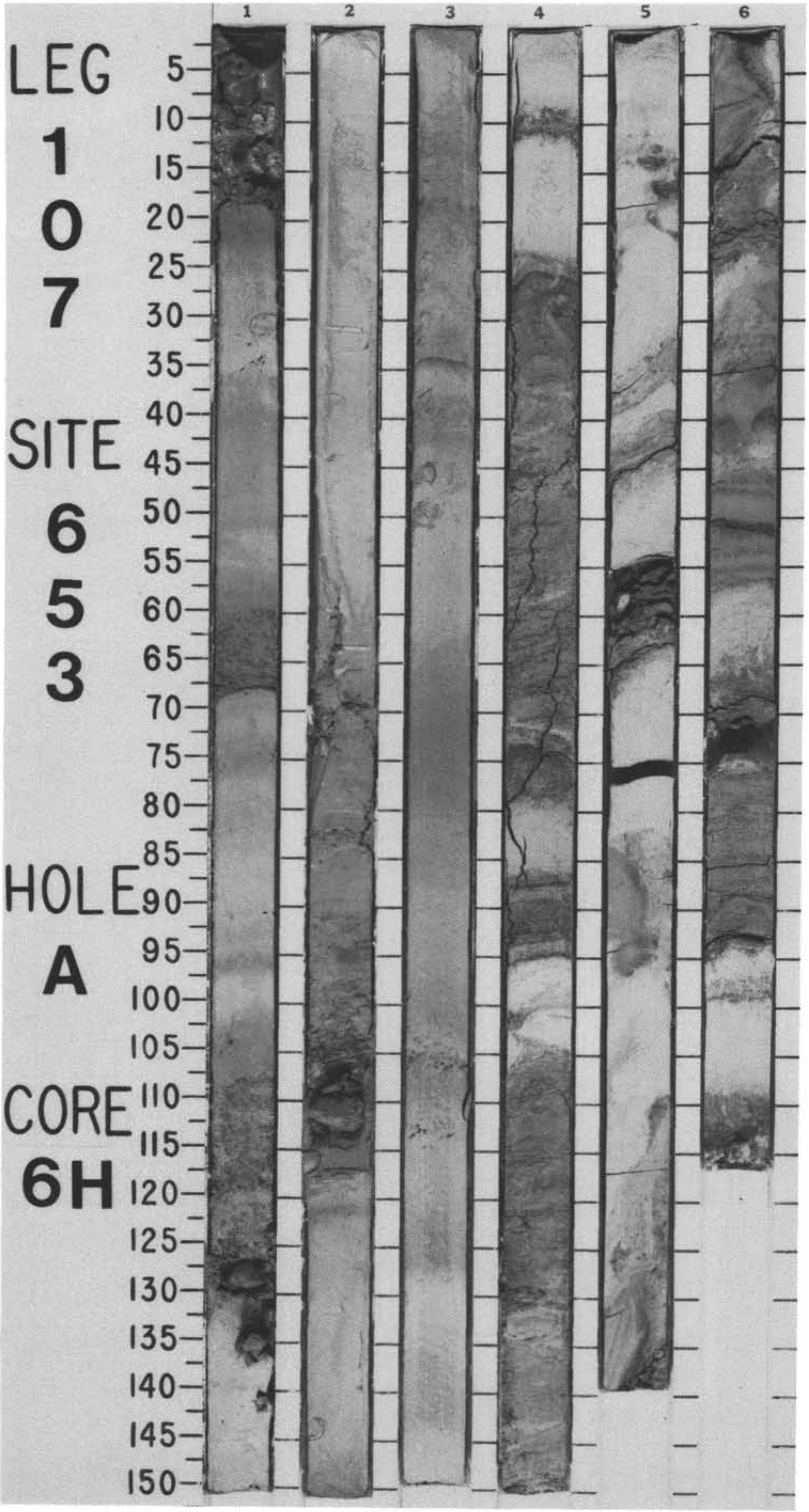
LEG
107
SITE
653
HOLE
A
CORE
6H
1
2
3
4
5
6
5
10
15
20
25
30
35
40
45
50
55
60
65
70
75
80
85
90
95
100
105
110
115
120
125
130
135
140
145
150

SITE 653 HOLE A CORE 7 H CORED INTERVAL 2868.0-2877.5 mbsl; 51.0-60.5 mbsf

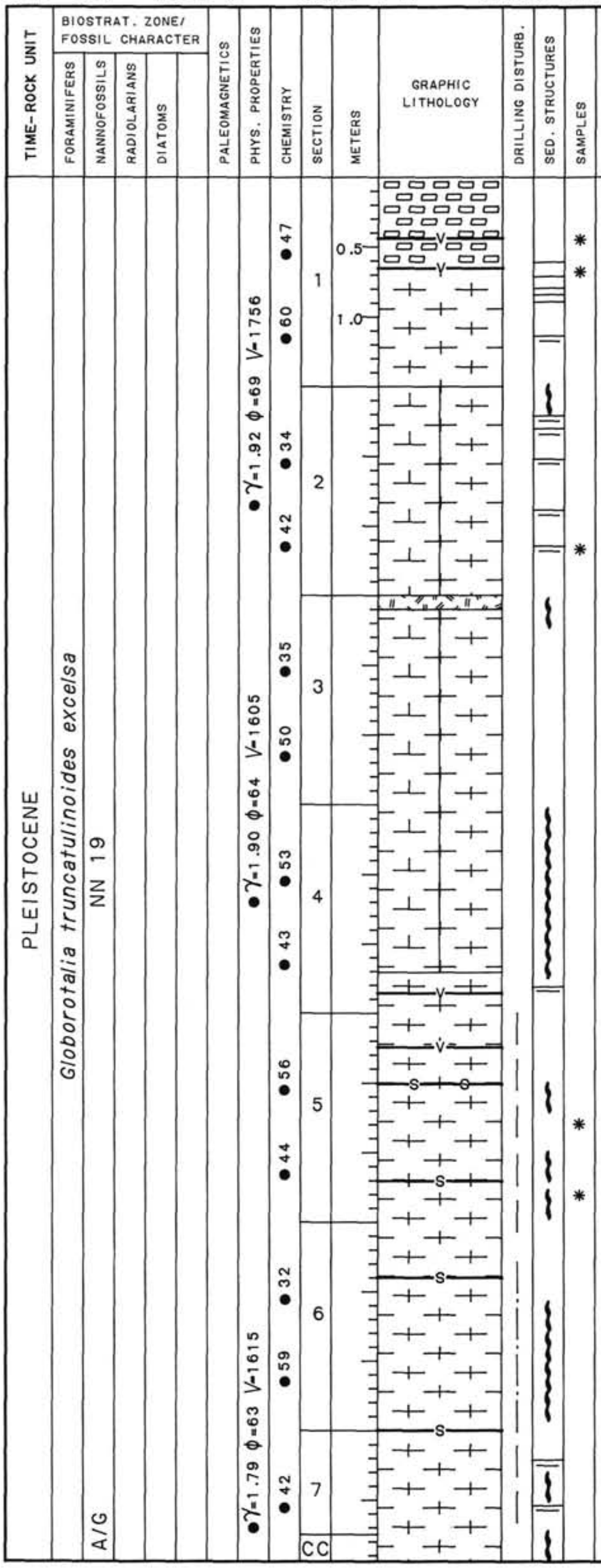

LITHOLOGIC DESCRIPTION

MARLY NANNOFOSSIL OOZE and MARLY FORAMINIFER-NANNOFOSSIL OOZE

Marly nannofossil ooze and marly foraminifer-nannofossil ooze, light gray (5Y 7/2), pale yellow (10YR 6/4, 5Y 7/3), pale yellow (10YR 6/6, 5Y 7/4), pale olive (5Y 6/3, 8/1; 2.5YR 6/3), dark gray (2.5YR 8/2, 5Y 4/1), olive (5Y 5/3), olive-gray (2.5Y 7/2, 5Y 5/2), dark olive-gray (2.5Y 6/1, 8/2; 5Y 3/2, 7/1); minor burrowing; scattered black specks (hydrotroilite?) *in Sections* 1, 3, 6, *and* 7.

Minor lithologies:
a) Volcanic ash in Section 1, 42 and 59–68 cm, Section 2, 70 cm, Section 3, 1–10 cm, Section 4, 137-140 cm, and Section 6, 44-47 cm, olive gray (5Y 5/2). Interval in Section 1, 59–68 cm, normally graded; upper portion disturbed by burrowing or coring disturbances.
b) Volcanic glass-bearing sandy silt in Section 2, 112–112.5 cm, dark gray (5Y 4/1), contacts are sharp.
c) Sapropelic layers in Section 5, 46–62 cm (sequence of layers of different thicknesses) and 121–126 cm, and Section 6, 38–44 and 142–146 cm.

SMEAR SLIDE SUMMARY (%):

	1, 42 M	1, 62 M	2, 112 M	5, 80 D	5, 118 M
TEXTURE:					
Sand	15	15	25	5	2
Silt	60	60	65	15	10
Clay	25	25	10	80	88
COMPOSITION:					
Quartz	25	12	20	3	2
Feldspar	6	4	5	1	5
Mica	9	2	6	1	1
Clay	7	34	37	48	34
Volcanic glass	29	31	9	2	1
Calcite	2	2	—	—	—
Dolomite	—	3	2	—	3
Accessory minerals	4	4	4	1	—
Zeolites	10	—	—	—	—
Micrite	—	—	—	—	2
Foraminifers	1	1	10	6	1
Nannofossils	5	4	3	34	34
Sponge spicules	—	—	—	—	2
Silicoflagellates	—	Tr	—	—	—
Amorphous organics	—	—	—	—	15
Bioclasts	2	3	4		

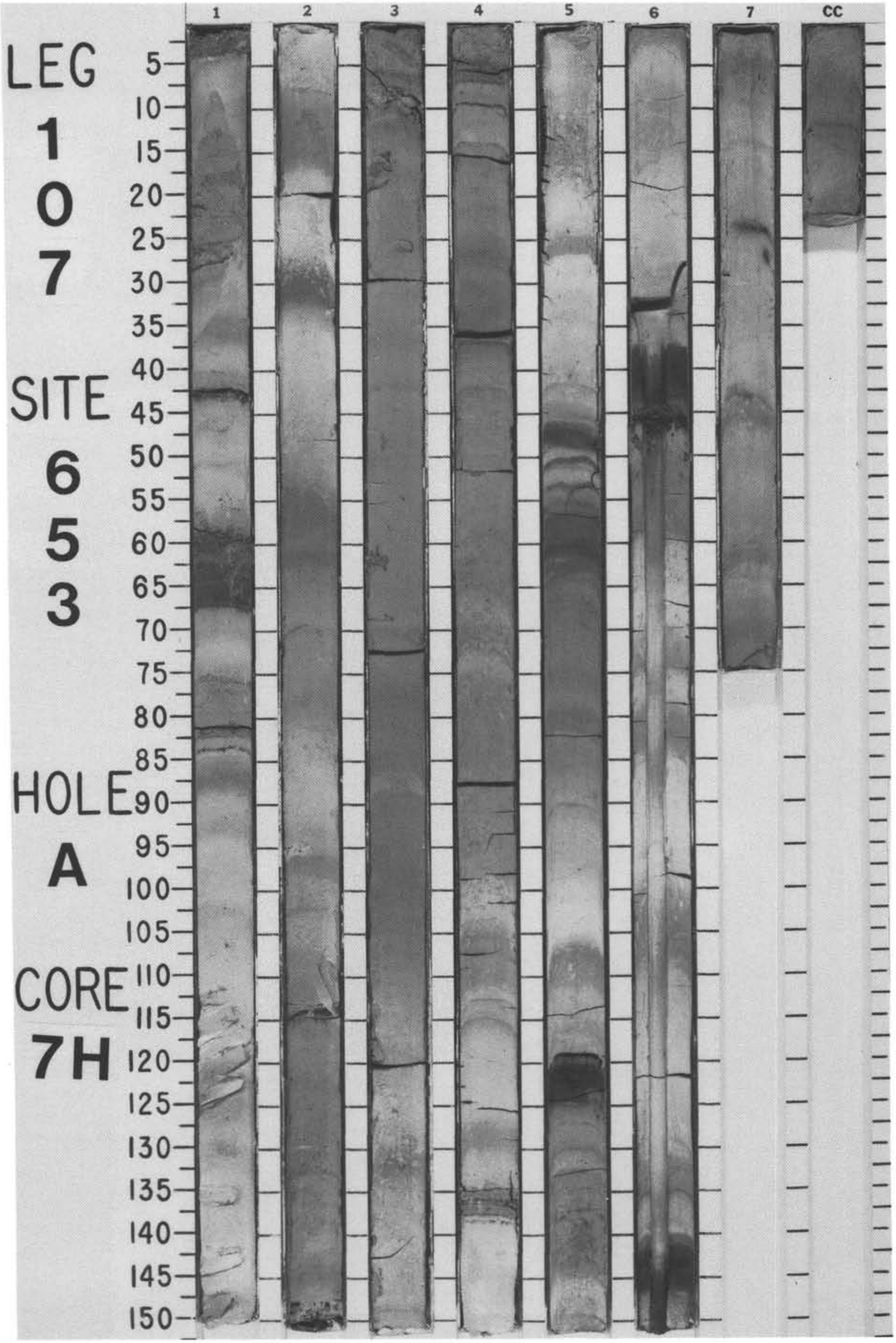

LEG
1
0
7
SITE
6
5
3
HOLE
A
CORE
7H
1
2
3
4
5
6
7
CC
5
10
15
20
25
30
35
40
45
50
55
60
65
70
75
80
85
90
95
100
105
110
115
120
125
130
135
140
145
150

SITE 653 HOLE A CORE 8 H CORED INTERVAL 2877.5-2887.0 mbsl; 60.5-70.0 mbsf

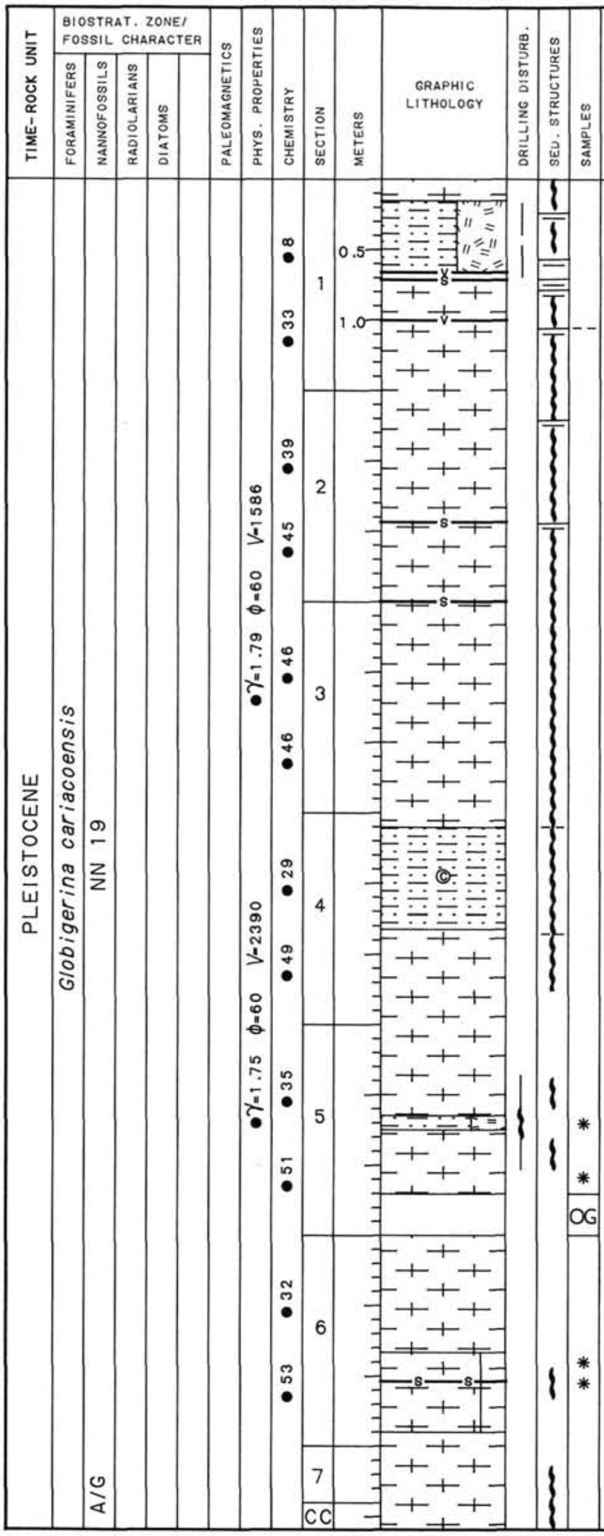

LITHOLOGIC DESCRIPTION

MARLY FORAMINIFER-NANNOFOSSIL OOZE, with intercalations of VOLCANIC ASH and SAPROPEL LAYERS

Marly foraminifer-nannofossil ooze, light gray (5Y 7/1, 5Y 7/2), gray (5Y 6/1), light olive-gray (5Y 6/2), olive-gray (5Y 8/1, 5Y 4/2), pale olive (5Y 4/4, 5Y 6/3), yellow (10YR 8/6), and olive (2.5Y 5/6, 6/2, 7/2, 7/3). Texturally homogeneous, except for moderate burrowing throughout, and as noted below.

Minor lithologies:
a) Volcanic ash-bearing layers in Section 1, 15–68 and 98–104 cm.
b) Indurated volcanic ash in Section 1, 68–71 cm, colors same as overlying sediment. Contacts unclear and broken.
c) Volcaniclastic ash-bearing mudstone, (5Y 5/1); occurs in core as several lithified pieces; contacts and continuity of layer not clear, Section 5, 68–74cm.
d) Sapropelic layers in Section 1, 71–75 cm, Section 2, 94–96 and 149 cm, Section 3, 2 cm, and Section 6, 96 cm (sharp upper and lower contacts) and 101–110 cm (gradational contacts, burrowed in upper portion).

SMEAR SLIDE SUMMARY (%):

	5, 68 M	5, 103 D	6, 82 M	6, 96 M
TEXTURE:				
Sand	20	15	60	—
Silt	50	20	20	10
Clay	30	65	20	90
COMPOSITION:				
Quartz	23	2	5	1
Feldspar	6	1	2	—
Mica	8	—	3	—
Clay	32	38	18	15
Volcanic glass	25	—	5	2
Dolomite	—	2	—	—
Accessory minerals	2	—	2	2
Foraminifers	1	5	50	2
Nannofossils	2	50	10	43
Organic matter	—	—	—	30
Intraclasts	1	—	5	—
Bioclasts	—	2	—	5

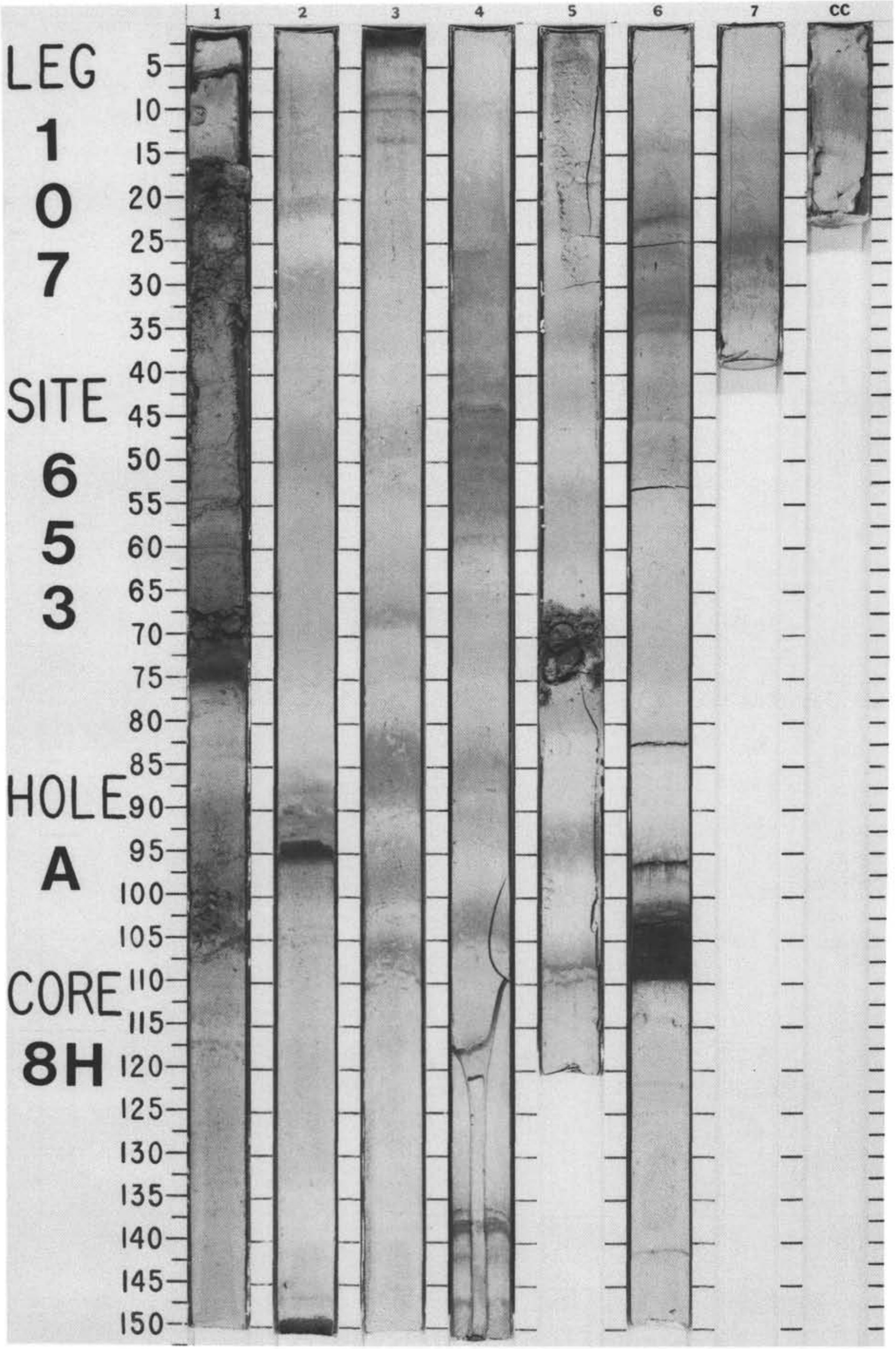
LEG
107
SITE
653
HOLE
A
CORE
8H
1
2
3
4
5
6
7
CC
5
10
15
20
25
30
35
40
45
50
55
60
65
70
75
80
85
90
95
100
105
110
115
120
125
130
135
140
145
150

SITE 653 HOLE A CORE 9 H CORED INTERVAL 2887.0-2896.6 mbsl; 70.0-79.6 mbsf

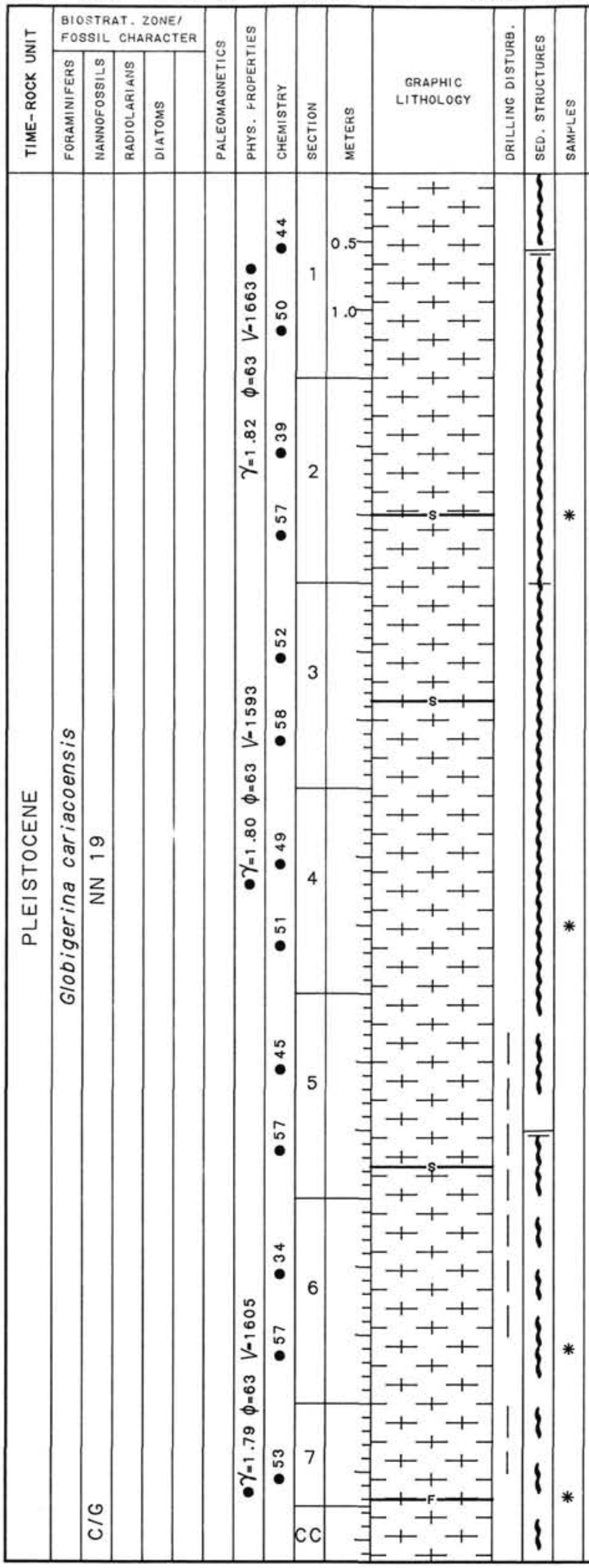

LITHOLOGIC DESCRIPTION

MARLY FORAMINIFER-NANNOFOSSIL OOZE

Marly foraminifer-nannofossil ooze, gray, light gray, and light olive-gray (5Y 3/1, 4/2, 5/2, 6/1, 6/2, 6/3, 7/2, 7/3, 8/1, 8/2); light gray (2.5Y 5/2, 6/1, 6/3, 7/2, 7/3), and gray (10YR 6/5, 7/1, 7/3, 7/6). Moderately burrowed throughout. Texturally and compositionally homogeneous, but with some diffuse dark gray and brownish layers

Minor lithologies:
a) Sapropelic layers in Section 2, 7–99 cm, Section 3, 83–89 cm, and *Section 5, 124–127 cm.*
b) Foraminifer sand in Section 7, 75 cm.

SMEAR SLIDE SUMMARY (%):

	2, 100 M	4, 100 D	6, 102 D	7, 63 M
TEXTURE:				
Sand	15	10	—	20
Silt	20	5	15	20
Clay	65	85	85	60
COMPOSITION:				
Quartz	2	2	1	2
Feldspar	—	3	—	1
Mica	1	2	—	—
Clay	25	34	31	33
Volcanic glass	3	1	1	2
Dolomite	—	—	1	—
Accessory minerals	2	1	1	—
Zeolites	5	—	—	—
Foraminifers	15	10	12	15
Nannofossils	45	45	48	45
Intraclasts	2	2	—	—
Bioclasts	—	—	5	2

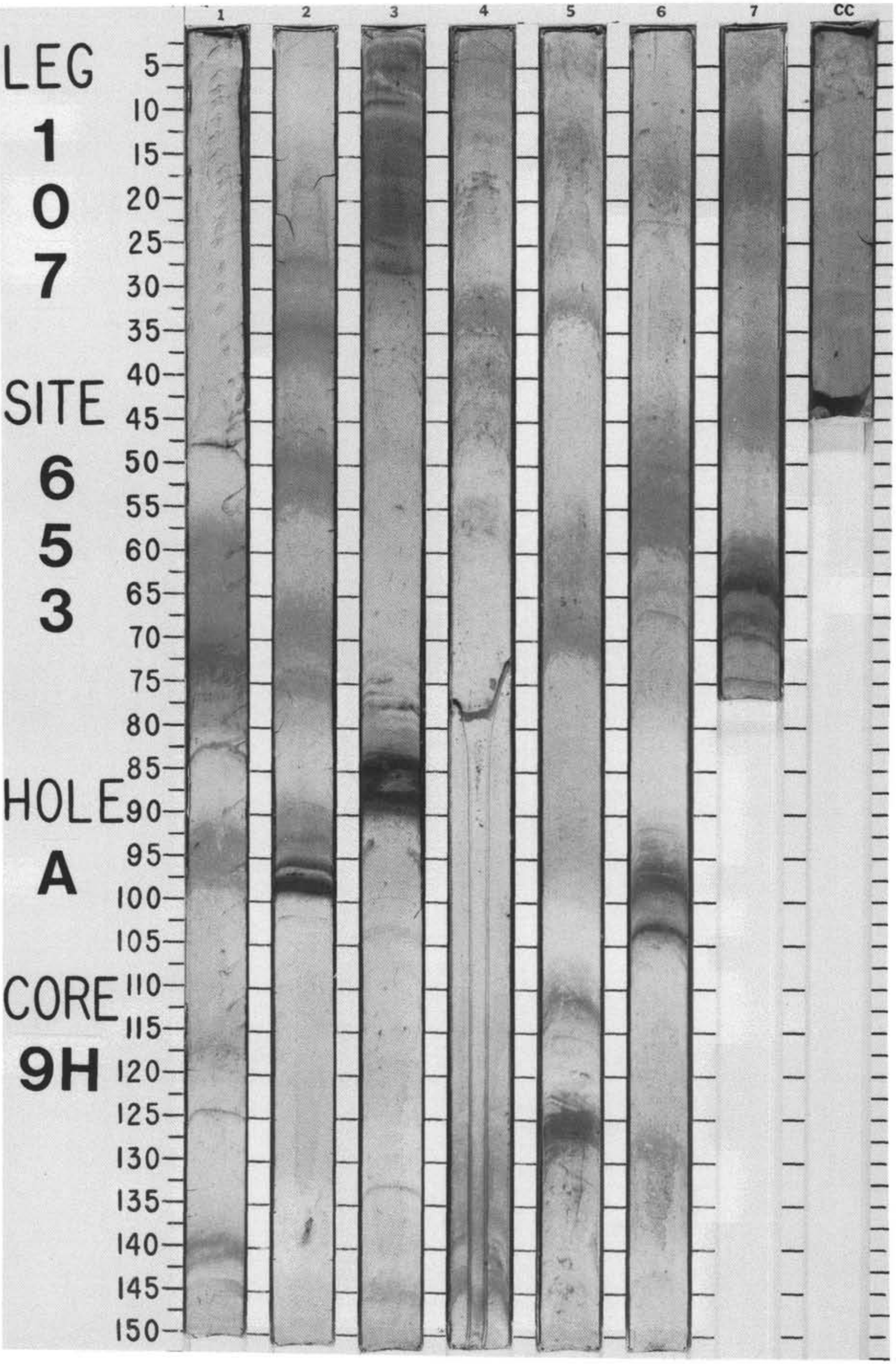
LEG
107
SITE
653
HOLE
A
CORE
9H
1
2
3
4
5
6
7
CC
5
10
15
20
25
30
35
40
45
50
55
60
65
70
75
80
85
90
95
100
105
110
115
120
125
130
135
140
145
150

SITE 653 HOLE A CORE 10 H CORED INTERVAL 2896.6-2906.0 mbsl; 79.6-89.0 mbsf

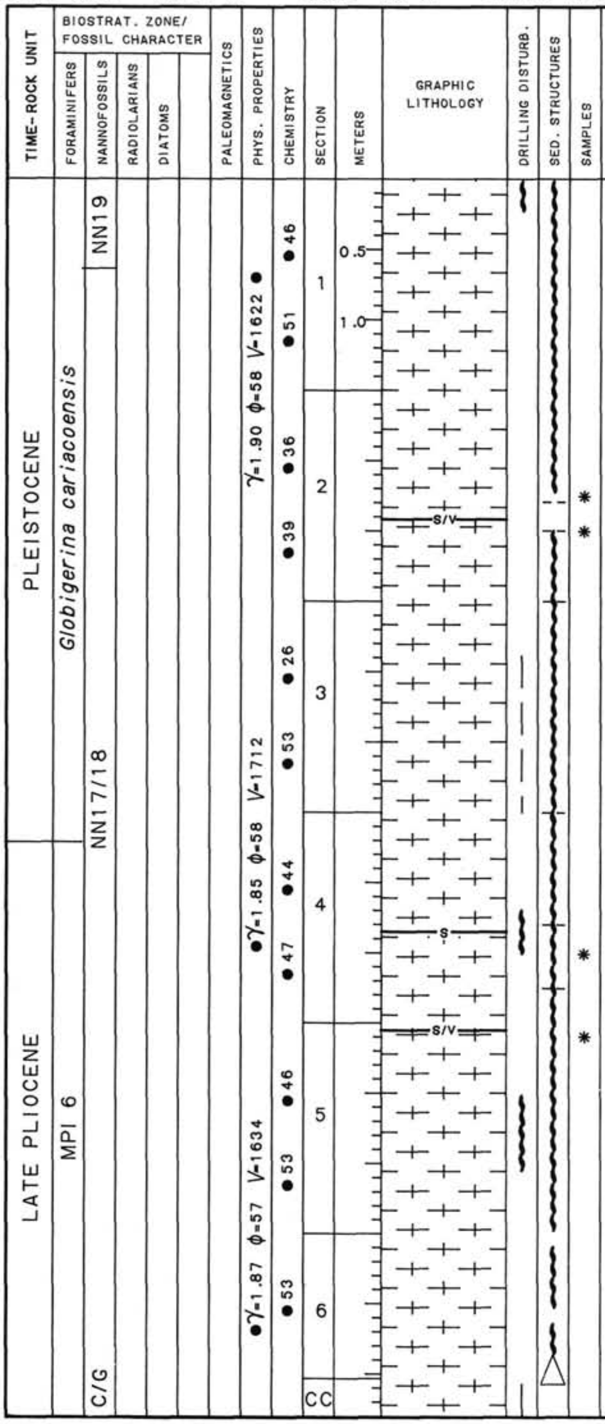

LITHOLOGIC DESCRIPTION

MARLY FORAMINIFER-NANNOFOSSIL OOZE

Marly foraminifer-nannofossil ooze, light gray (2.5Y 7/2, 5Y 7/2), light olive-gray (2.5Y 5/2, 6/2, 6/3, 8/2; 5Y 6/2), white (5Y 8/2), (5Y 6/2) light olive-gray, and yellow (10YR 6/8, 7/6). Moderate burrowing throughout. Texturally and compositionally homogeneous except as noted below; color changes do not reflect major changes in either category. Lower portion of Section 6, 65–100 cm, is normally graded with respect to distribution of foraminiferal tests; basal portion contains framboids.

Minor lithologies:
a) Volcanic ash in Section 2, 93–95 cm (indurated pieces interbedded in a sapropel layer), and Section 5, 6 cm, with sharp upper and lower contacts.
b) Sapropels in Section 2, 87–97 cm (intercalation of an ash layer at 93–95 cm), Section 4, 84–86 cm, and Section 5, 9–10 cm.

SMEAR SLIDE SUMMARY (%):

	2, 72 D	2, 95 D	4, 100	5, 6 M
TEXTURE:				
Sand	—	15	—	10
Silt	20	50	15	60
Clay	80	35	85	30
COMPOSITION:				
Quartz	2	18	2	4
Feldspar	1	5	1	3
Mica	1	5	1	1
Clay	24	6	44	20
Volcanic glass	1	31	1	45
Calcite	—	1	—	3
Accessory minerals	1	3	1	—
Zeolites	—	7	—	20
Foraminifers	15	2	10	1
Nannofossils	55	20	40	3
Bioclasts	—	2	—	—

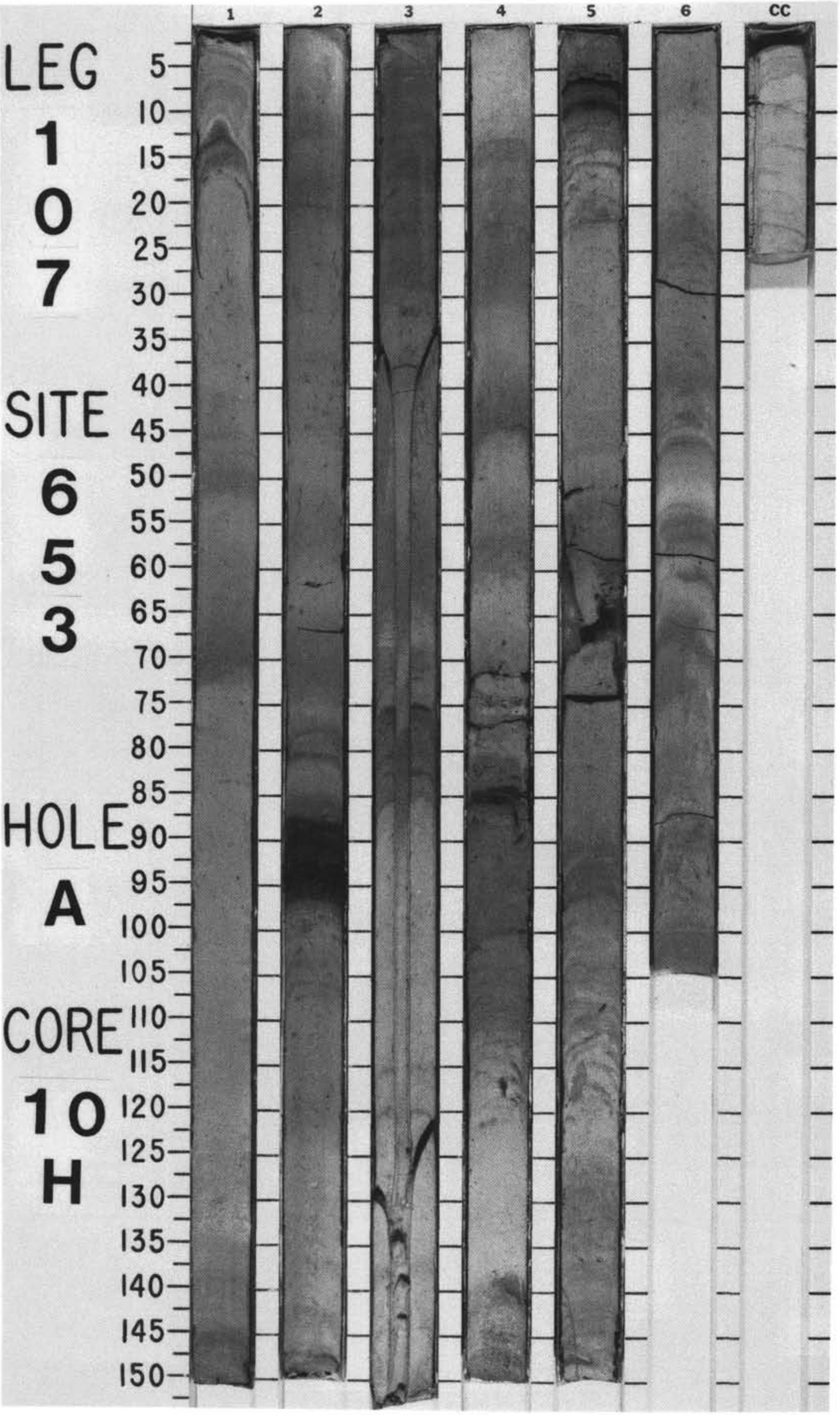
LEG
107
SITE
653
HOLE
A
CORE
10H
1
2
3
4
5
6
CC
5
10
15
20
25
30
35
40
45
50
55
60
65
70
75
80
85
90
95
100
105
110
115
120
125
130
135
140
145
150

SITE 653 HOLE A CORE 11 H CORED INTERVAL 2906.0-2915.2 mbsl; 89.0-98.2 mbsf

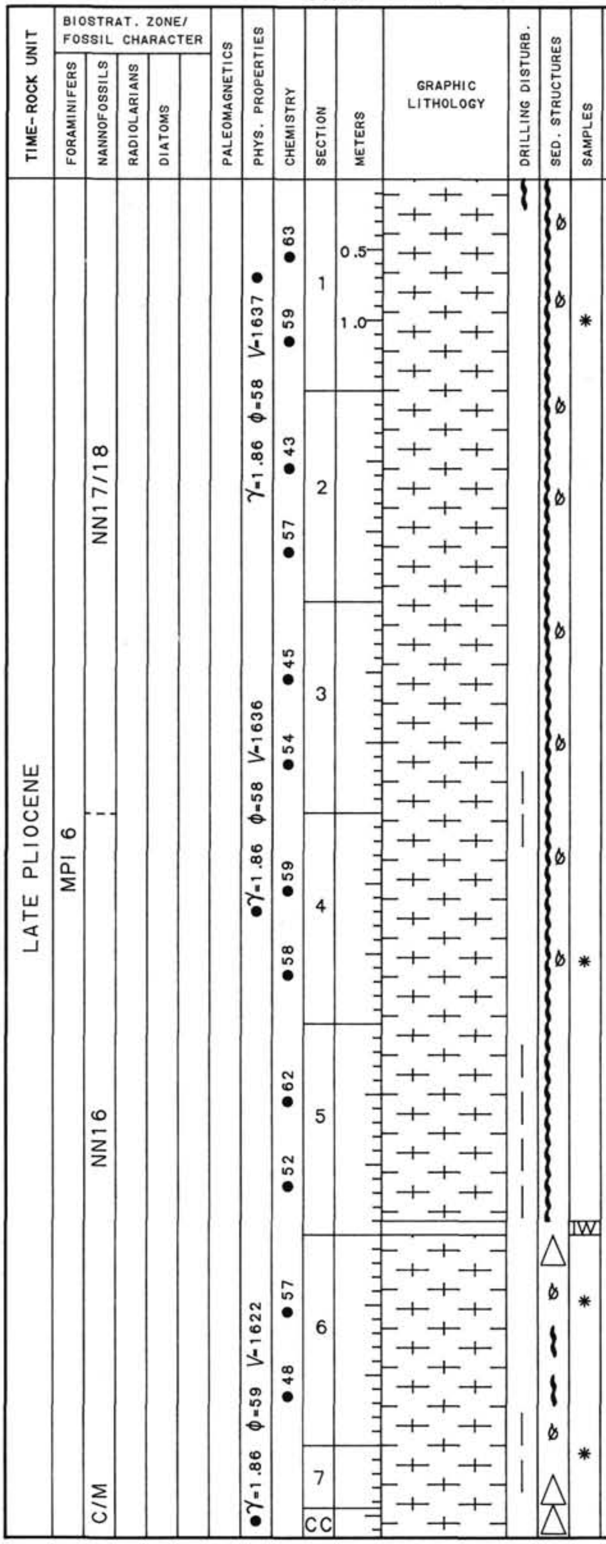

LITHOLOGIC DESCRIPTION

MARLY FORAMINIFER-NANNOFOSSIL OOZE

Marly foraminifer-nannofossil ooze, light gray (2.5Y 7/2, 5Y 7/1), pale yellow (2.5Y 7/3), white (2.5Y 8/2), light brownish gray (2.5Y 6/2), pale olive (5Y 6/3), light olive-gray (5Y 6/2), olive (5Y 5/3), and (2.5Y 6/3, 7/1, 7/4, 7/6, 8/1). Moderate burrowing throughout. Pteropod and black specks (hydrotroilite?) scattered throughout. Variable clay content causes two major lithologies; otherwise core is texturally and mineralogically homogeneous. Some normal-grading of foraminiferal tests over short intervals is suggested.

SMEAR SLIDE SUMMARY (%):

	1, 100 D	4, 100 D	6, 40 D	7, 8 M
TEXTURE:				
Sand	—	5	5	—
Silt	10	15	10	10
Clay	90	80	85	90
COMPOSITION:				
Quartz	2	3	4	2
Mica	1	—	—	1
Clay	46	—	—	46
Volcanic glass	—	3	—	—
Calcite	2	1	2	2
Dolomite	—	1	2	—
Accessory minerals	1	—	—	—
Foraminifers	2	10	15	2
Nannofossils	45	80	75	45
Diatoms	—	1	1	—
Sponge spicules	—	1	1	—
Bioclasts	1	—	—	2

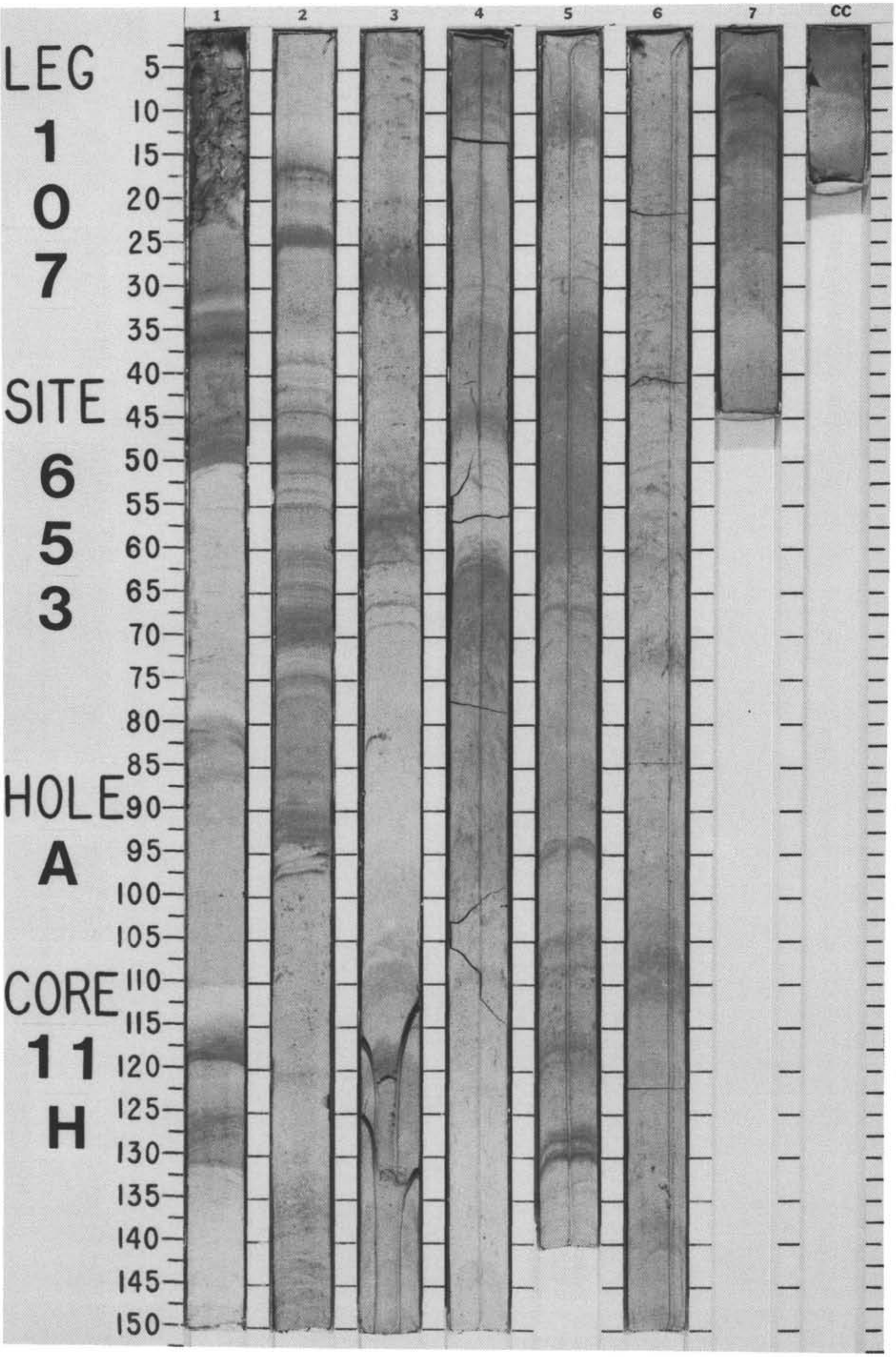
LEG
107
SITE
653
HOLE
A
CORE
11H
1
2
3
4
5
6
7
CC
5
10
15
20
25
30
35
40
45
50
55
60
65
70
75
80
85
90
95
100
105
110
115
120
125
130
135
140
145
150

SITE 653 HOLE A CORE 12 H CORED INTERVAL 2915.2-2924.7 mbsl; 98.2-107.7 mbsf

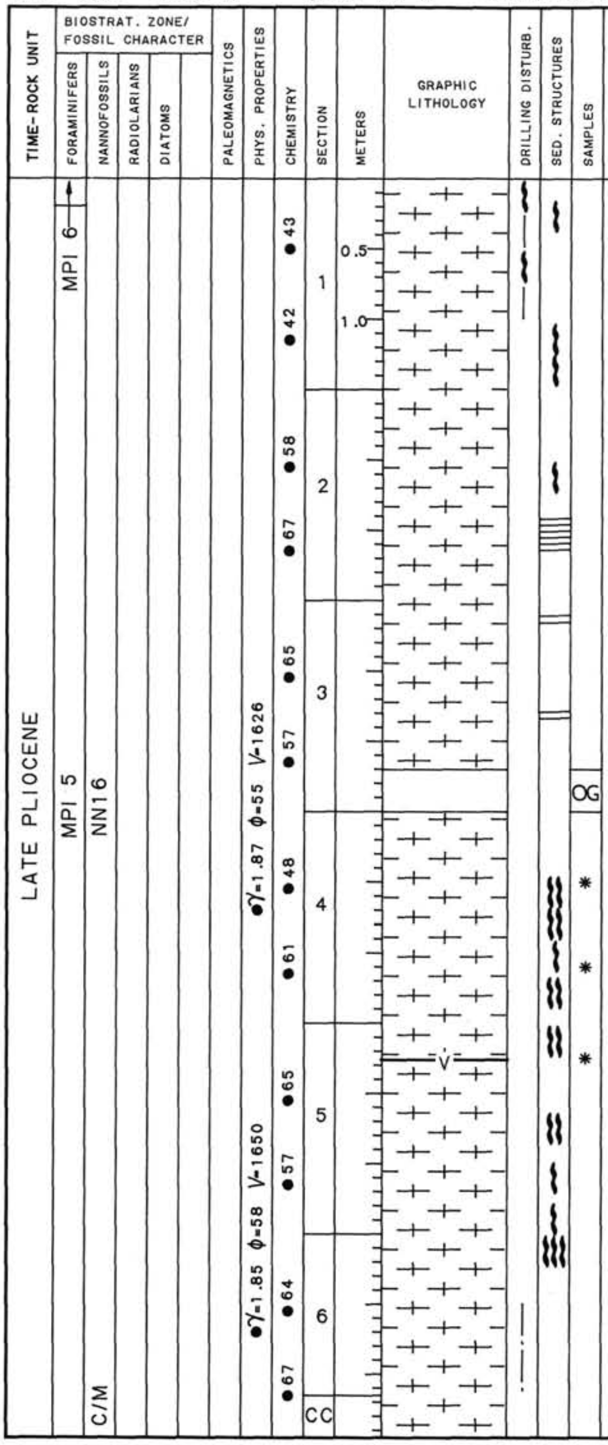

LITHOLOGIC DESCRIPTION

FORAMINIFER-NANNOFOSSIL OOZE

Foraminifer-nannofossil ooze, grayish brown (2.5Y 5/2), light olive-brown (2.5Y 5/4), light brownish gray (2.5Y 6/2), light yellowish brown (2.5Y 6/4), light gray (2.5Y 7/2, 5Y 7/2, 10YR 7/2), yellow (2.5Y 7/6), dark gray (5Y 4/1), olive (5Y 5/3), gray (5Y 6/1, 10YR 5/1), light olive-gray (5Y 6/2), pale olive (5Y 6/3), pale olive (5Y 6/4), pale yellow (5Y 7/1), dark yellowish brown (10YR 4/4), light brownish gray (10YR 6/2), light yellowish gray (10YR 6/4), brownish yellow (10YR 6/6), and white (5Y 8/2, 10YR 8/1). Colors are homogeneous as well as with patches and specks. Few laminated intervals. Burrowing in deeper parts. Scattered foraminifers (*Orbulina universa*).

Minor lithology: foraminifer-rich crystal vitric ash, gray (5Y 5/1), with mica flakes and pyrite, Section 5, 26–30 cm.

SMEAR SLIDE SUMMARY (%):

	4, 54 M	4, 115 D	5, 29 M
TEXTURE:			
Sand	10	8	60
Silt	5	7	30
Clay	85	85	10
COMPOSITION:			
Quartz	4	1	3
Feldspar	Tr	2	2
Rock fragments	—	—	Tr
Mica	1	1	3
Clay	15	5	4
Volcanic glass	Tr	3	55
Calcite/dolomite	2	—	2
Accessory minerals			
Pyroxene(?)	—	—	4
Opaques	2	—	—
Gypsum	—	—	2
Foraminifers	6	8	25
Nannofossils	70	79	2
Diatoms	Tr	1	—
Radiolarians	—	Tr	—

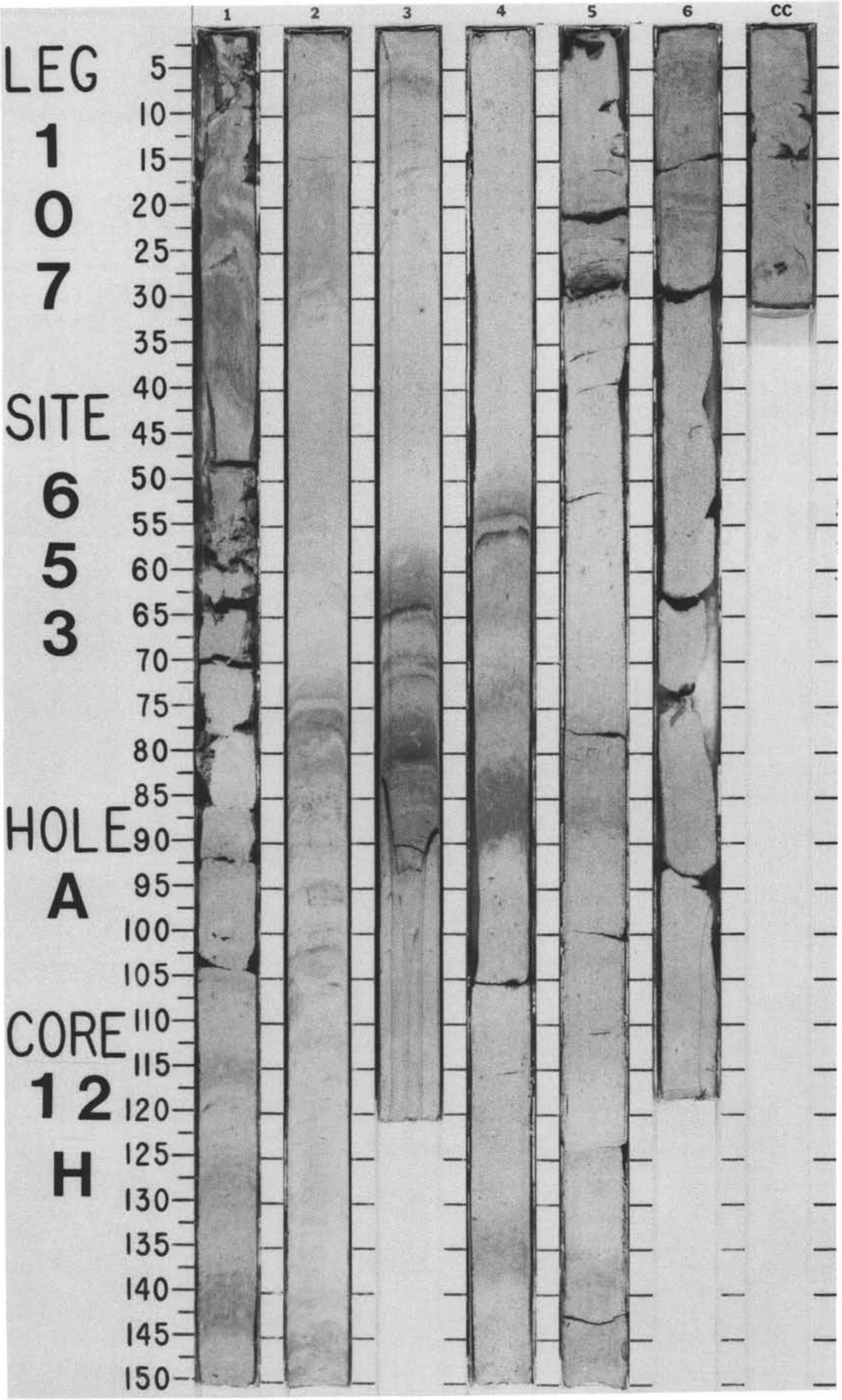
LEG
107
SITE
653
HOLE
A
CORE
12
H
1
2
3
4
5
6
CC
5
10
15
20
25
30
35
40
45
50
55
60
65
70
75
80
85
90
95
100
105
110
115
120
125
130
135
140
145
150

SITE 653 HOLE A CORE 13 H CORED INTERVAL 2924.7-2934.3 mbsl; 107.7-117.3 mbsf

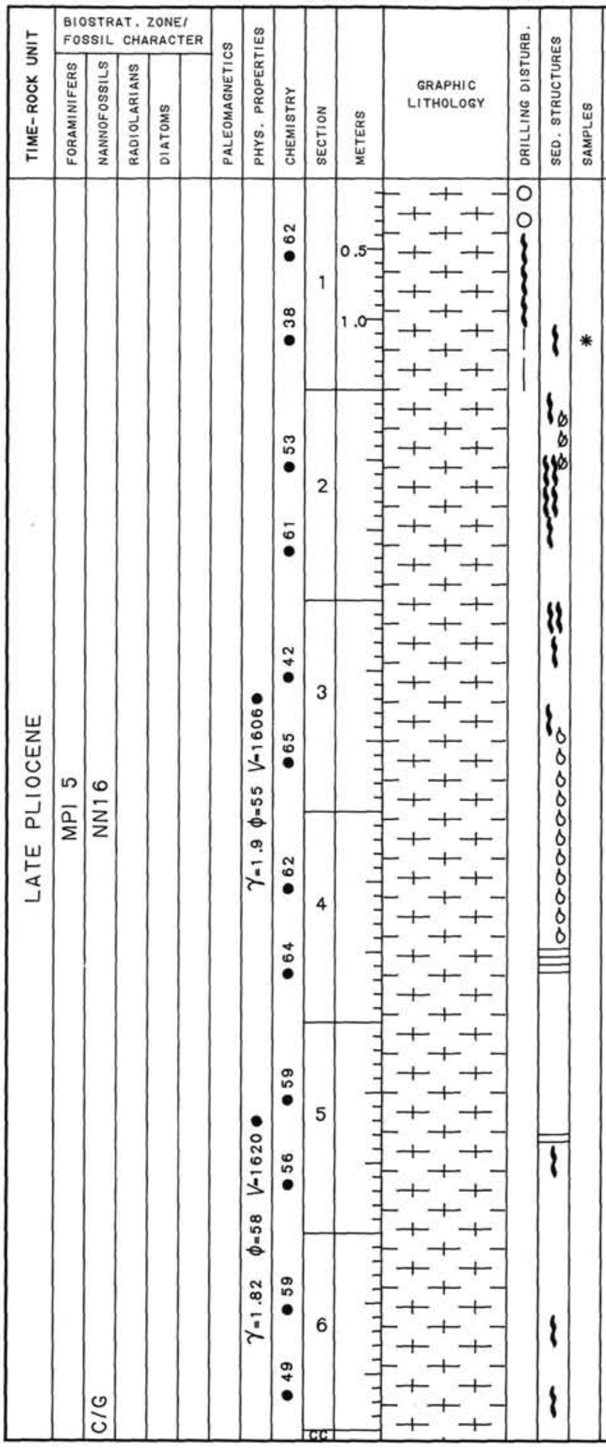

LITHOLOGIC DESCRIPTION

FORAMINIFER-NANNOFOSSIL OOZE

Foraminifer-nannofossil ooze, light brownish gray (2.5Y 6/2), light yellowish brown (2.5Y 6/4, 10YR 6/4), light gray (2.5Y 7/2; 5Y 7/1, 7/2), dark gray (5Y 4/1), gray (5Y 5/1, 6/1), olive-gray (5Y 5/2), light olive-gray (5Y 6/2), pale olive (5Y 6/3, 6/4), pale yellow (5Y 7/3, 7/4), pale brown (10YR 6/3), and brownish yellow (10YR 6/6); few laminations, scattered foraminifer shells.

Minor lithology: ash and foraminifer-rich layers, cm-thin, gray (5Y 5/1).

SMEAR SLIDE SUMMARY (%):

	1, 115 D	3, 115 D
TEXTURE:		
Sand	3	15
Silt	10	10
Clay	87	75
COMPOSITION:		
Quartz	3	3
Feldspar	Tr	—
Mica	Tr	1
Clay	19	5
Volcanic glass	1	—
Calcite/dolomite	4	4
Accessory minerals	1	1
Gypsum	—	1
Micrite	—	10
Foraminifers	2	15
Nannofossils	70	55
Diatoms	—	1
Radiolarians	Tr	2
Sponge spicules	Tr	1
Silicoflagellates	Tr	1
Fish remains	—	Tr
Plant debris	—	Tr

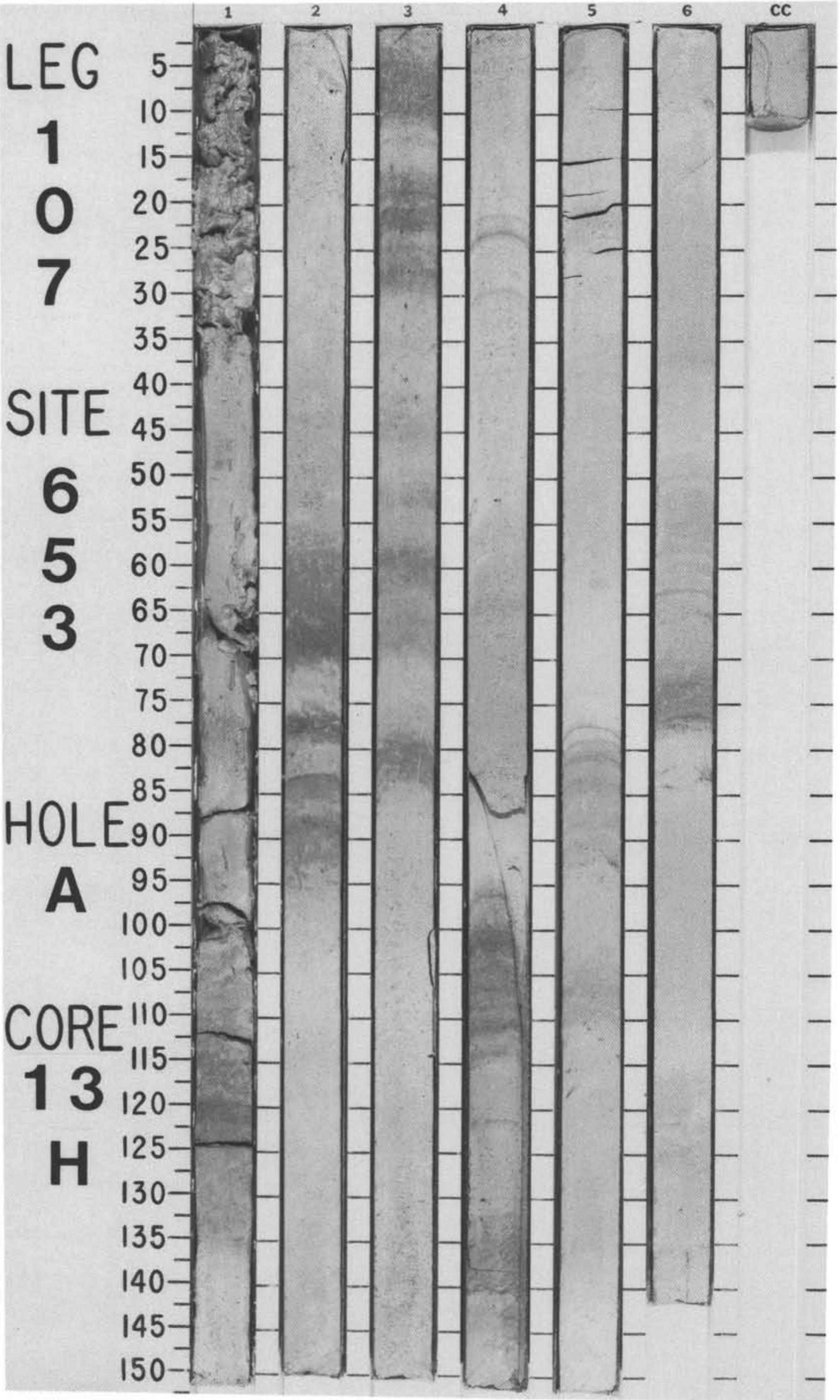
LEG
107
SITE
653
HOLE
A
CORE
13
H
1
2
3
4
5
6
CC
5
10
15
20
25
30
35
40
45
50
55
60
65
70
75
80
85
90
95
100
105
110
115
120
125
130
135
140
145
150

SITE 653 HOLE A CORE 14 X CORED INTERVAL 2934.3-2943.6 mbsl; 117.3-126.6 mbsf

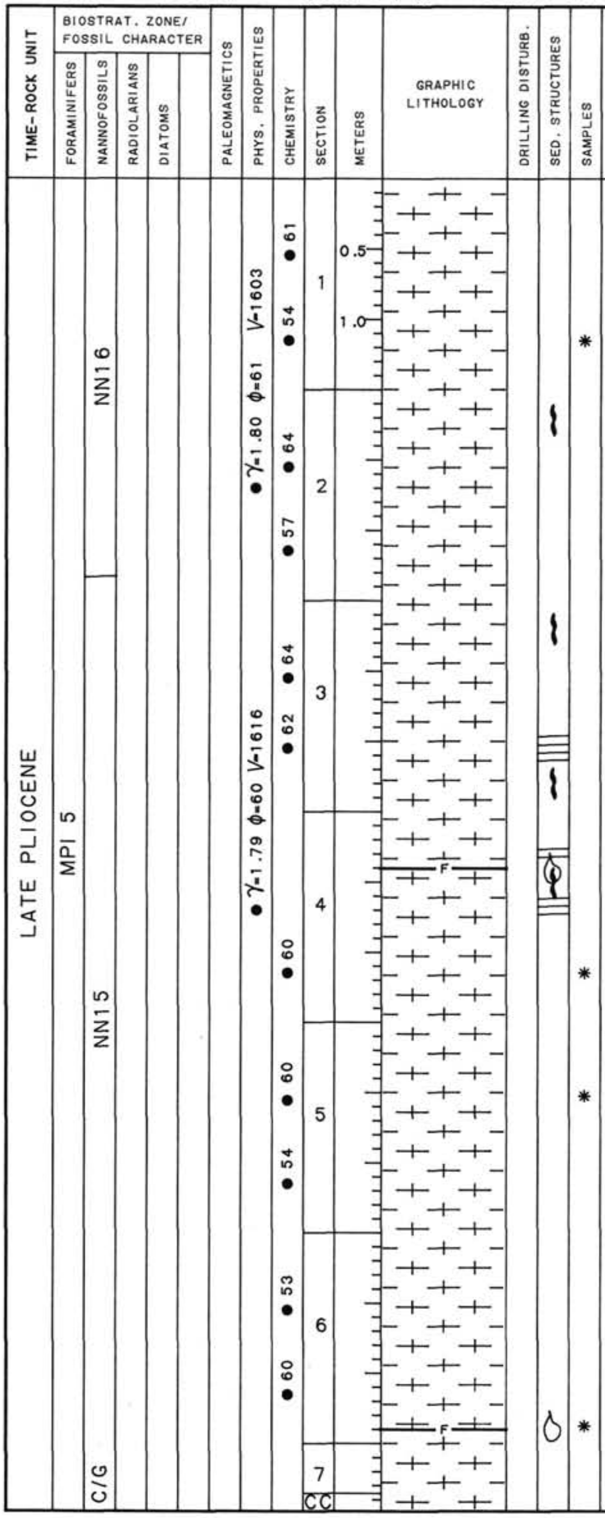

LITHOLOGIC DESCRIPTION

FORAMINIFER-NANNOFOSSIL OOZE

Foraminifer-nannofossil ooze, light olive-brown (2.5Y 5/4)(in diffuse bands), light brownish gray (2.5Y 6/2), light gray (2.5Y 7/2; 5Y 7/1, 7/2), gray (5Y 5/1, 6/1; 10YR 5/1, 6/1), light olive-gray (5Y 6/2), pale olive (5Y 6/4), pale yellow (5Y 7/3), greenish gray (10Y 7/2, 5GY 6/1), light yellowish brown (10YR 6/4), brownish yellow (10YR 6/6), and very pale brown (10YR 7/3). In Section 6 many color cycles, ranging from light gray (5Y 7/2) at the base to gray (5Y 5/1) on the top.

Minor lithology: few mm-thin layers rich in foraminifers (foraminifer-nannofossil sand); gray (10YR 6/1).

SMEAR SLIDE SUMMARY (%):

	1, 115 D	4, 115 M	5, 54 D	6, 138 M
TEXTURE:				
Sand	15	25	15	20
Silt	10	20	10	20
Clay	75	55	75	60
COMPOSITION:				
Quartz	5	2	2	3
Feldspar	—	—	Tr	—
Mica	1	Tr	1	Tr
Clay	10	20	19	16
Volcanic glass	1	2	2	—
Calcite/dolomite	2	4	5	3
Accessory minerals	2	2	2	2
Opaques	1	2	1	—
Gypsum(?)	—	—	1	—
Micrite	10	2	5	5
Foraminifers	3	15	5	15
Nannofossils	60	40	50	50
Diatoms	1	2	2	1
Radiolarians	2	3	2	3
Sponge spicules	1	Tr	1	1
Silicoflagellates	1	Tr	1	1
Fish remains	Tr	Tr	—	—

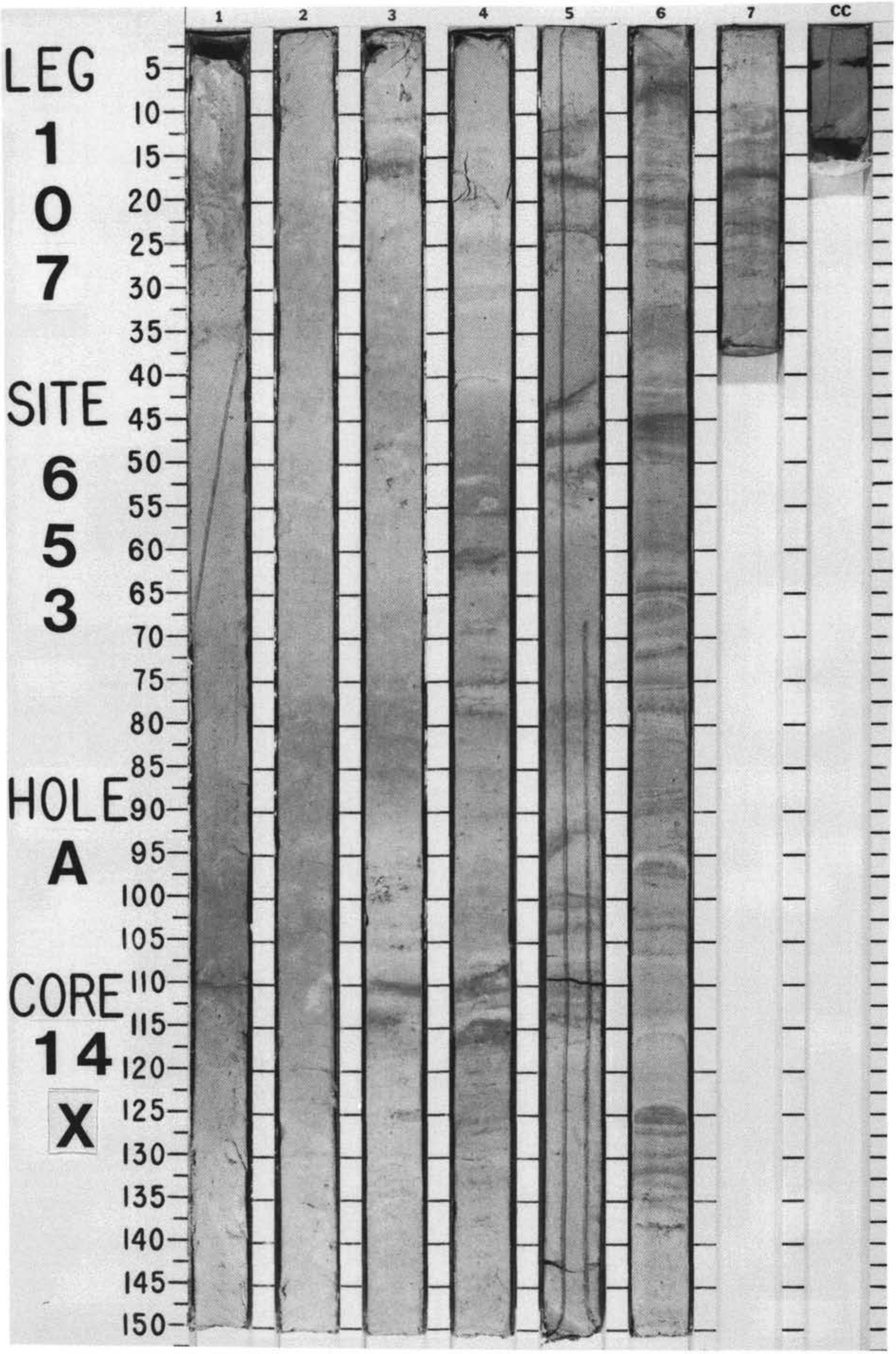
LEG
107
SITE
653
HOLE
A
CORE
14
X
1
2
3
4
5
6
7
CC
5
10
15
20
25
30
35
40
45
50
55
60
65
70
75
80
85
90
95
100
105
110
115
120
125
130
135
140
145
150

SITE 653 HOLE A CORE 15X CORED INTERVAL 2943.6-2953.1 mbsl; 126.6-136.1 mbsf

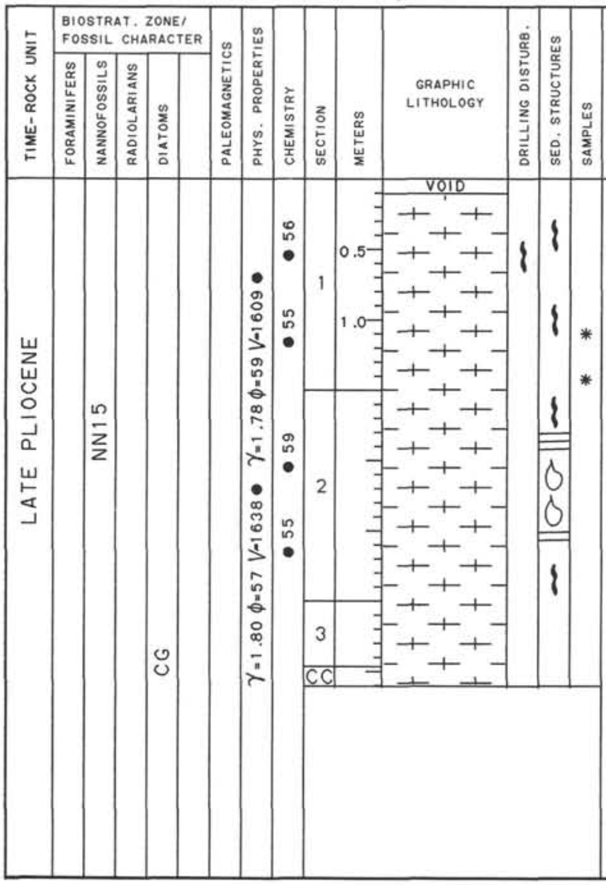

LITHOLOGIC DESCRIPTION

FORAMINIFER-NANNOFOSSIL OOZE

Foraminifer-nannofossil ooze, gray (5Y 5/1) (laminae), gray (5Y 6/1), pale olive (5Y 6/3), light gray (5Y 7/1, 7/2), pale yellow (5Y 7/3), light yellowish brown (10YR 6/4) (laminae), and brownish yellow (10YR 6/6). There are some lighter or darker streaks and laminae.

SMEAR SLIDE SUMMARY (%):

	1, 115 D	1, 142 M
TEXTURE:		
Sand	15	15
Silt	15	10
Clay	70	75
COMPOSITION:		
Quartz	5	3
Feldspar	Tr	—
Mica	1	Tr
Clay	14	18
Volcanic glass	2	2
Calcite/dolomite	5	1
Accessory minerals	1	Tr
Gypsum	1	—
Micrite	5	—
Foraminifers	12	10
Nannofossils	50	60
Diatoms	Tr	1
Radiolarians	3	3
Sponge spicules	1	1
Silicoflagellates	Tr	1
Fish remains	—	Tr

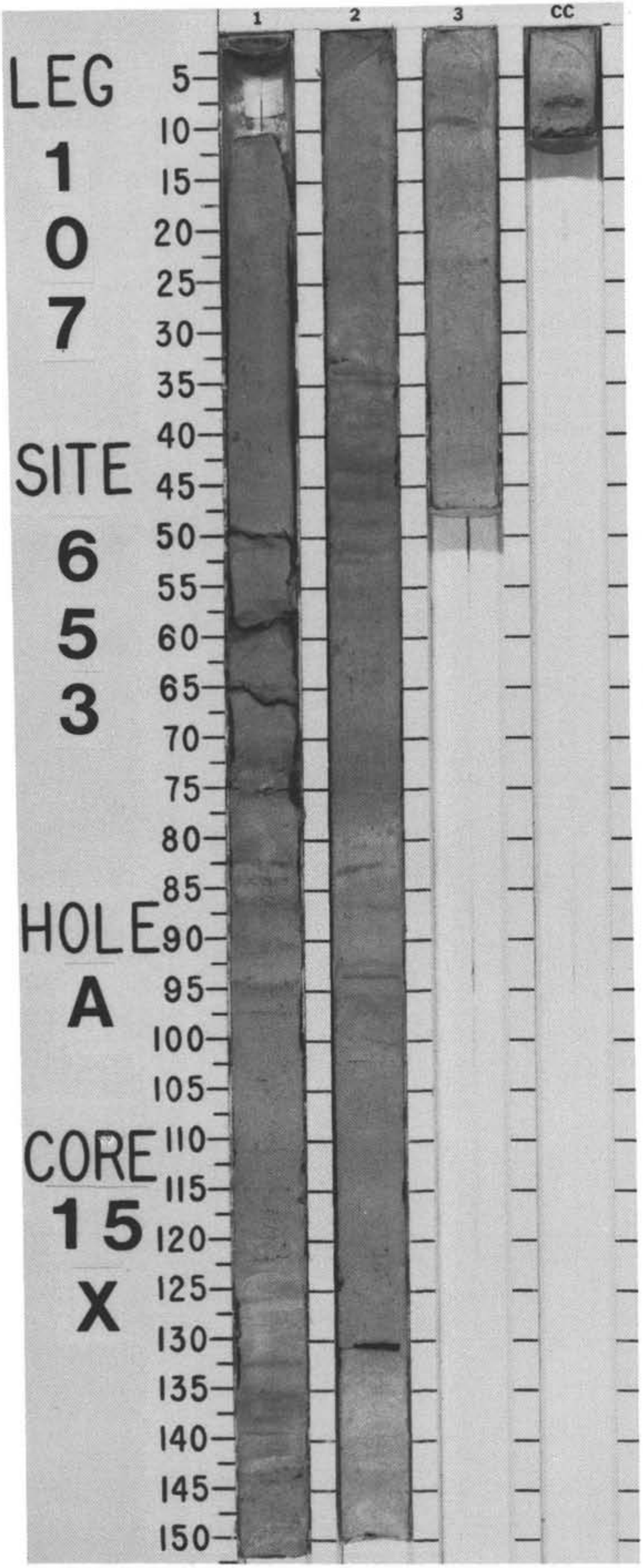
LEG
1
0
7
SITE
6
5
3
HOLE
A
CORE
1 5
X
1
2
3
CC
5
10
15
20
25
30
35
40
45
50
55
60
65
70
75
80
85
90
95
100
105
110
115
120
125
130
135
140
145
150

SITE 653 HOLE A CORE 16 X CORED INTERVAL 2953.1-2962.6 mbsl; 136.1-145.6 mbsf

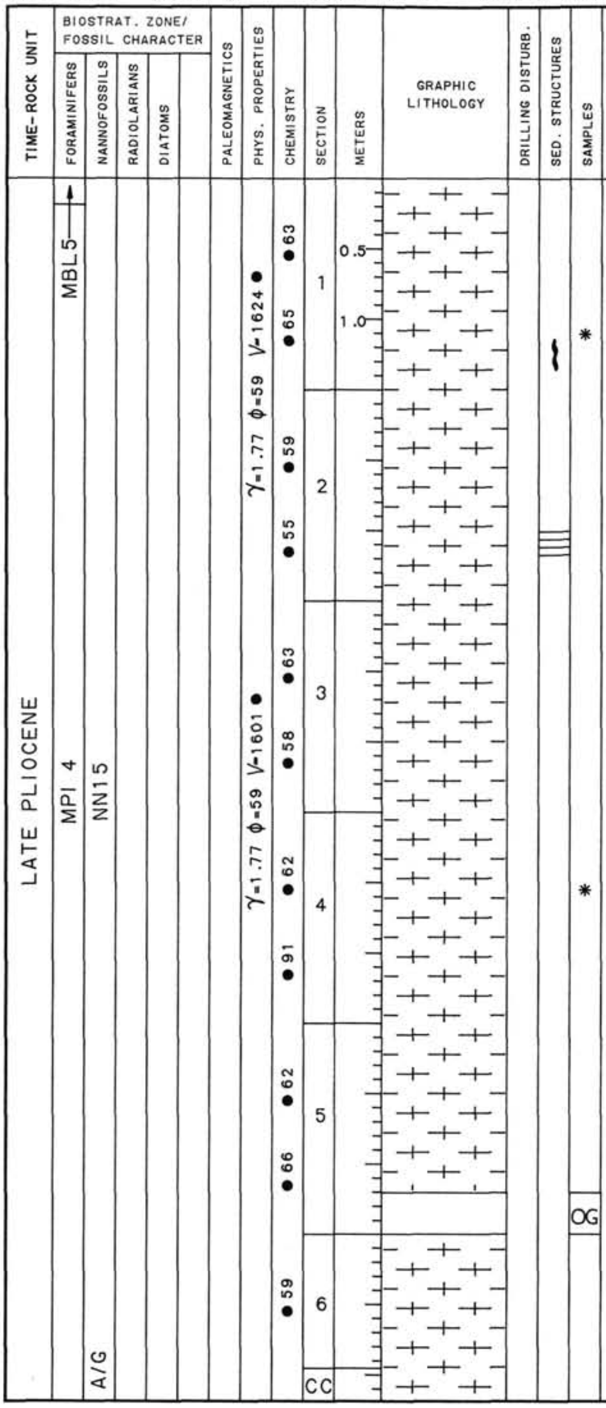

LITHOLOGIC DESCRIPTION

FORAMINIFER-NANNOFOSSIL OOZE

Foraminifer-nannofossil ooze, light gray (5Y 7/1, 7/2; 10YR 7/2), gray (5Y 5/1, 6/1), light olive-gray (5Y 6/2), gray (2.5Y 5/0) (laminae), light yellowish brown (10YR 6/4), and dark gray (5Y 4/1). Section 4, 10, 40, and 123–130 cm, and Section 5, 83–84, 96–104, and 114 cm: diffuse bands of olive-yellow (5Y 6/6). Enrichments of foraminifers in discrete intervals.

SMEAR SLIDE SUMMARY (%):

	1, 115 D	4, 53 M
TEXTURE:		
Sand	3	15
Silt	2	8
Clay	95	77
COMPOSITION:		
Quartz	2	2
Mica	Tr	—
Clay	13	26
Volcanic glass	2	—
Calcite/dolomite	3	5
Accessory minerals	Tr	Tr
Micrite	5	10
Foraminifers	3	12
Nannofossils	70	40
Diatoms	Tr	2
Radiolarians	2	2
Sponge spicules	Tr	1
Silicoflagellates	—	Tr
Fish remains	—	Tr

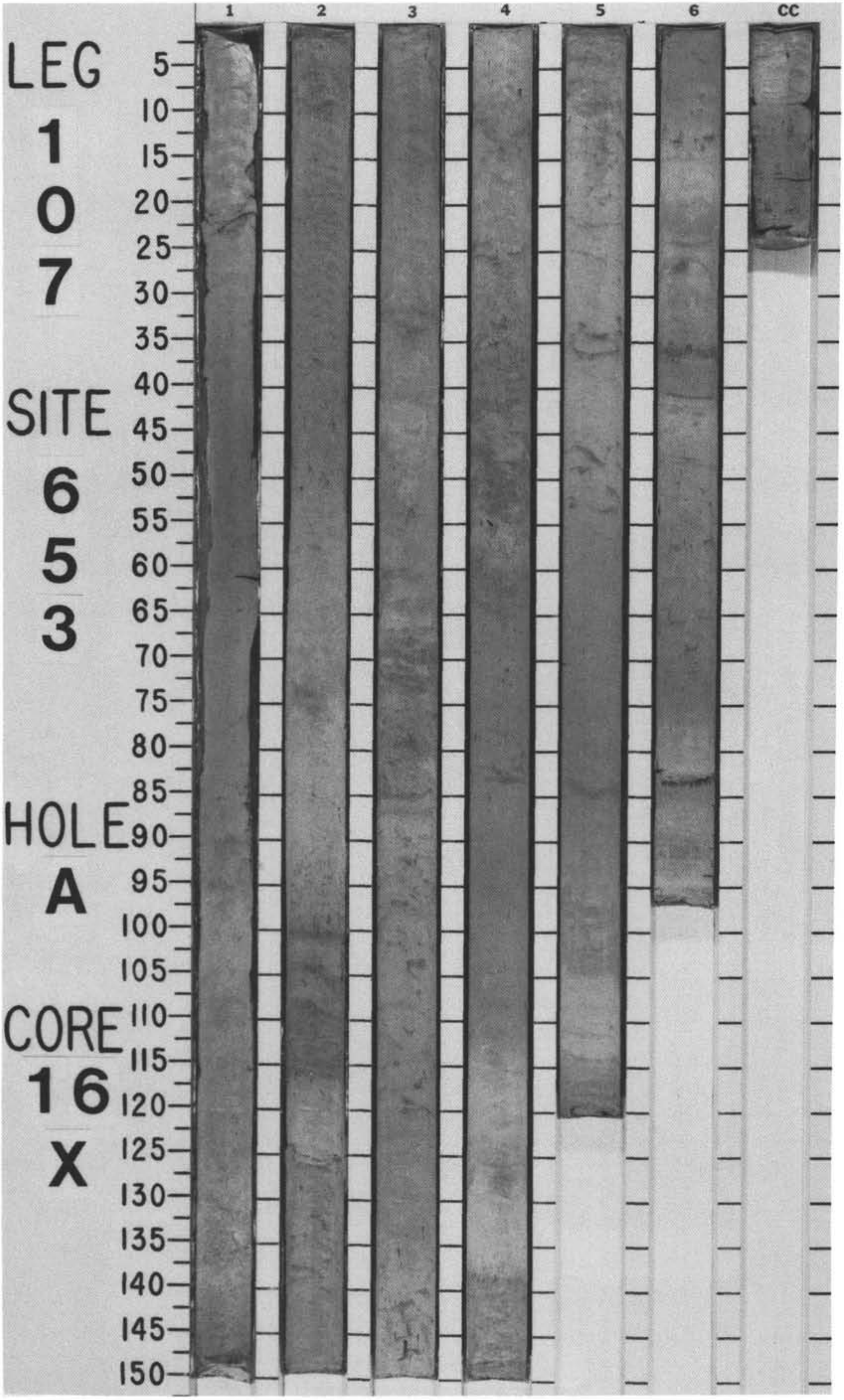
LEG
107
SITE
653
HOLE
A
CORE
16
X
1
2
3
4
5
6
CC
5
10
15
20
25
30
35
40
45
50
55
60
65
70
75
80
85
90
95
100
105
110
115
120
125
130
135
140
145
150

SITE 653 HOLE A CORE 17 X CORED INTERVAL 2962.6-2972.2 mbsl; 145.6-155.2 mbsf

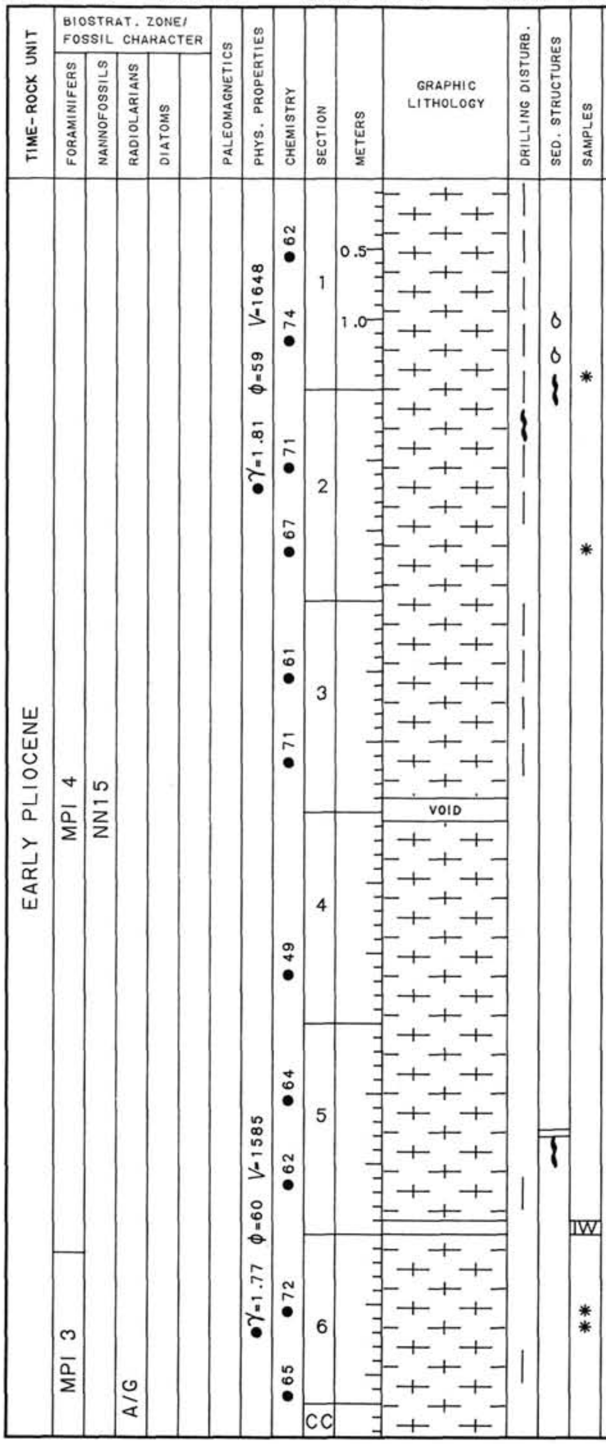

LITHOLOGIC DESCRIPTION

FORAMINIFER-NANNOFOSSIL OOZE

Foraminifer-nannofossil ooze, gray (5Y 5/1, 6/1), light gray (5Y 7/1, 7/2), pale yellow (5Y 7/3, 7/4), white (5Y 8/1), and light yellowish brown (10YR 6/4); irregular gray (5Y 5/1) streaks and blebs.

SMEAR SLIDE SUMMARY (%):

	1, 141 M	2, 114 D	6, 54 D	6, 65 M
TEXTURE:				
Sand	30	3	12	20
Silt	20	15	13	20
Clay	50	82	75	60
COMPOSITION:				
Quartz	4	1	5	3
Mica	Tr	Tr	—	Tr
Clay	5	17	14	14
Volcanic glass	4	—	2	Tr
Calcite/dolomite	2	3	1	2
Accessory minerals	1	1	—	1
Gypsum(?)	—	1	1	—
Micrite	14	—	10	10
Foraminifers	25	2	5	15
Nannofossils	40	75	60	50
Diatoms	—	—	—	Tr
Radiolarians	5	—	1	2
Sponge spicules	—	—	1	1
Silicoflagellates	—	—	—	Tr
Bryozoan detritus(?)	Tr	—	—	—
Foraminifer debris	—	—	—	2

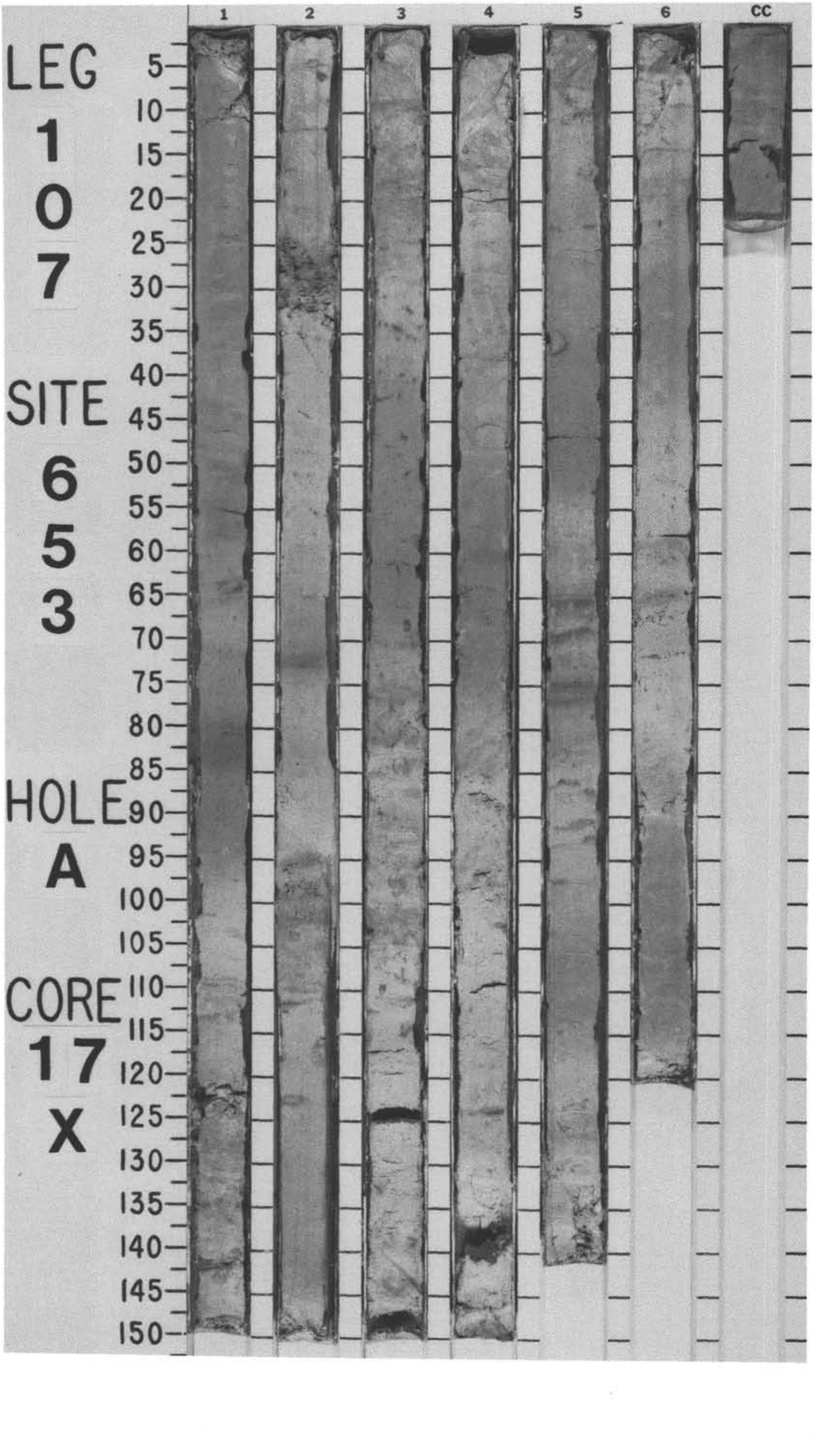
LEG
107
SITE
653
HOLE
A
CORE
17
X
1
2
3
4
5
6
CC
5
10
15
20
25
30
35
40
45
50
55
60
65
70
75
80
85
90
95
100
105
110
115
120
125
130
135
140
145
150

SITE 653 HOLE A CORE 18 X CORED INTERVAL 2972.2-2981.1 mbsl; 155.2-164.1 mbsf

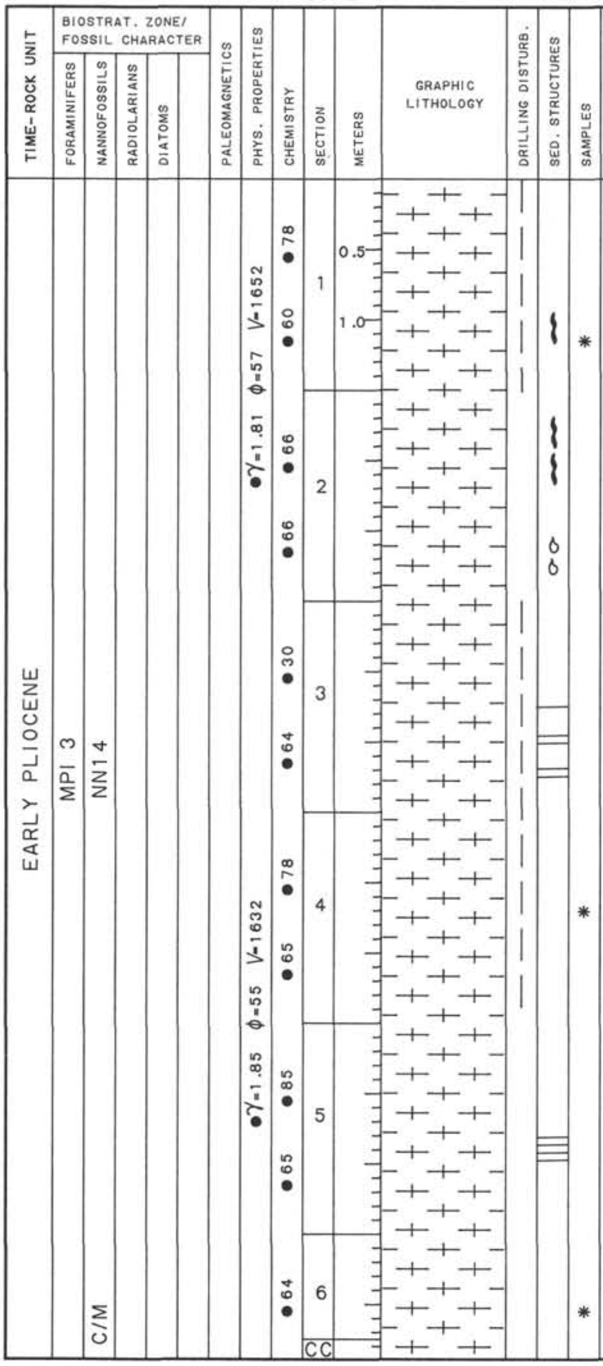

LITHOLOGIC DESCRIPTION

FORAMINIFER-NANNOFOSSIL OOZE

Foraminifer-nannofossil ooze, gray (5Y 5/1), light gray (5Y 7/1, 7/2), pale yellow (5Y 7/3), white (5Y 8/1), and light yellowish brown (10YR 6/4); specks of lighter and darker colors. Foraminifer-enriched in few thin layers and lenses. Very sharp contact in Section 3, 72 cm, testifies to possible erosion of part of the sequence.

SMEAR SLIDE SUMMARY (%):

	1, 115 D	4, 72 M	6, 54 D
TEXTURE:			
Sand	15	10	8
Silt	15	15	12
Clay	70	75	80
COMPOSITION:			
Quartz	5	6	5
Mica	Tr	Tr	Tr
Clay	19	17	18
Volcanic glass	2	1	2
Calcite/dolomite	2	3	3
Accessory minerals	1	1	1
Opaques	1	—	—
Gypsum	—	Tr	1
Foraminifers	15	8	7
Nannofossils	50	60	60
Diatoms	1	Tr	1
Radiolarians	2	3	2
Sponge spicules	1	1	Tr
Silicoflagellates	1	Tr	Tr
Fish remains	Tr	—	Tr

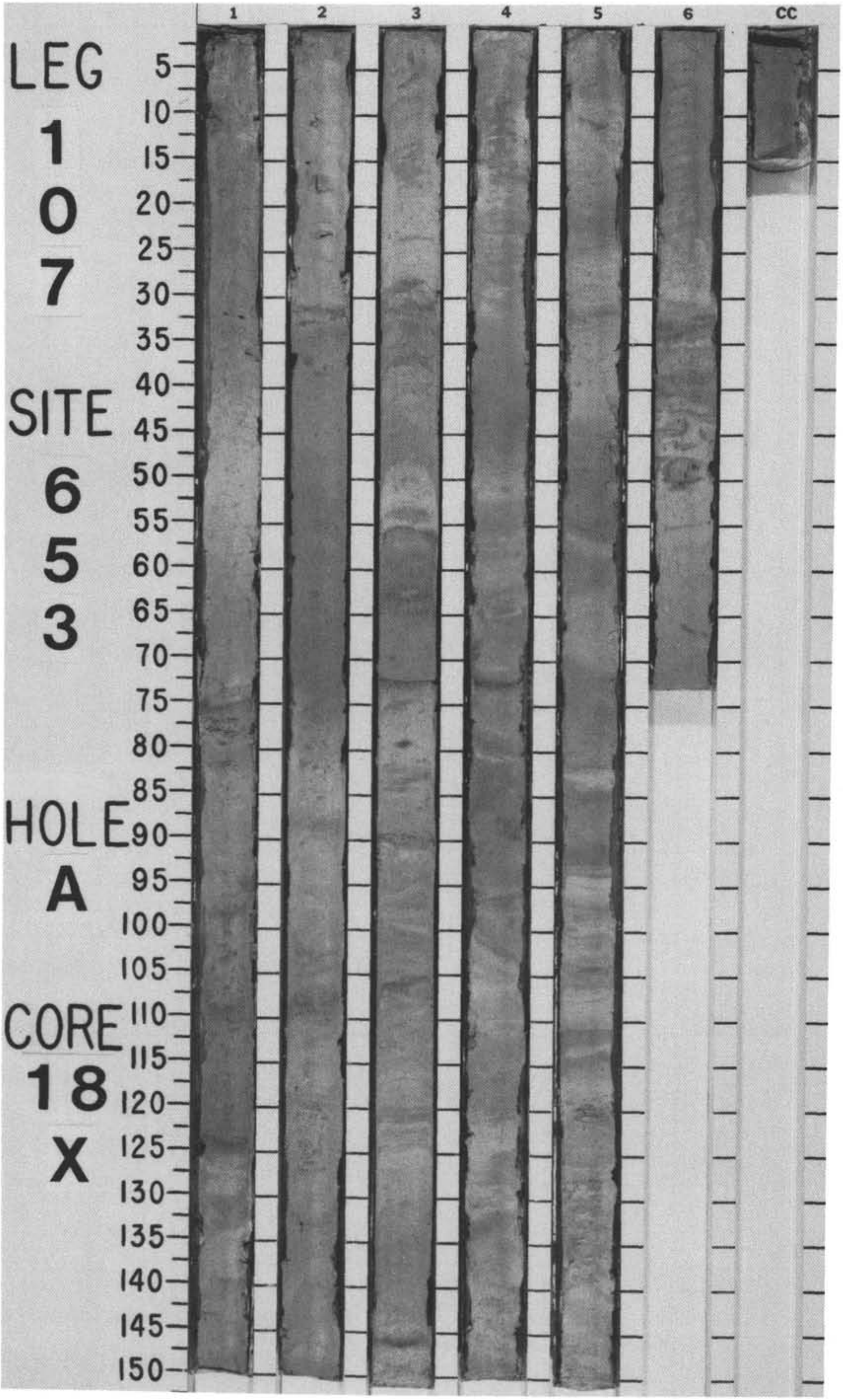
LEG
1
0
7
SITE
6
5
3
HOLE
A
CORE
18
X
1
2
3
4
5
6
CC
5
10
15
20
25
30
35
40
45
50
55
60
65
70
75
80
85
90
95
100
105
110
115
120
125
130
135
140
145
150

SITE 653 HOLE A CORE 19X CORED INTERVAL 2981.1-2990.7 mbsl; 164.1-173.7 mbsf

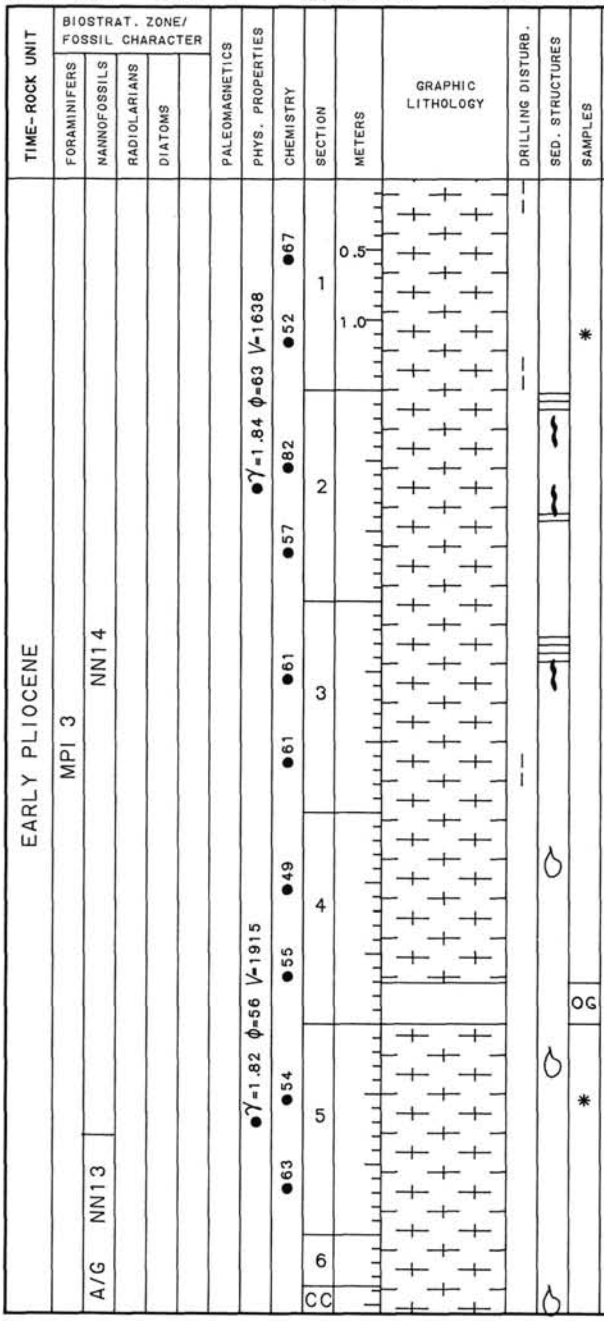

LITHOLOGIC DESCRIPTION

FORAMINIFER-NANNOFOSSIL OOZE

Foraminifer-nannofossil ooze, olive-yellow (2.5Y 6/6), gray (5Y 5/1, 6/1), light gray (5Y 7/1, 7/2), pale yellow (5Y 7/3), white (5Y 8/1), and light yellowish brown (10YR 6/4); some irregular streaks are darker or lighter than the background color. Few foraminifer-rich layers.

SMEAR SLIDE SUMMARY (%):

	1, 114 D	5, 54 D
TEXTURE:		
Sand	5	5
Silt	15	15
Clay	80	80
COMPOSITION:		
Quartz	5	4
Feldspar	112	—
Mica	1	—
Clay	13	24
Volcanic glass	1	1
Calcite/dolomite	3	4
Accessory minerals		
Pyrite	4	5
Foraminifers	10	5
Nannofossils	60	55
Sponge spicules	1	1
Bioclasts	1	1

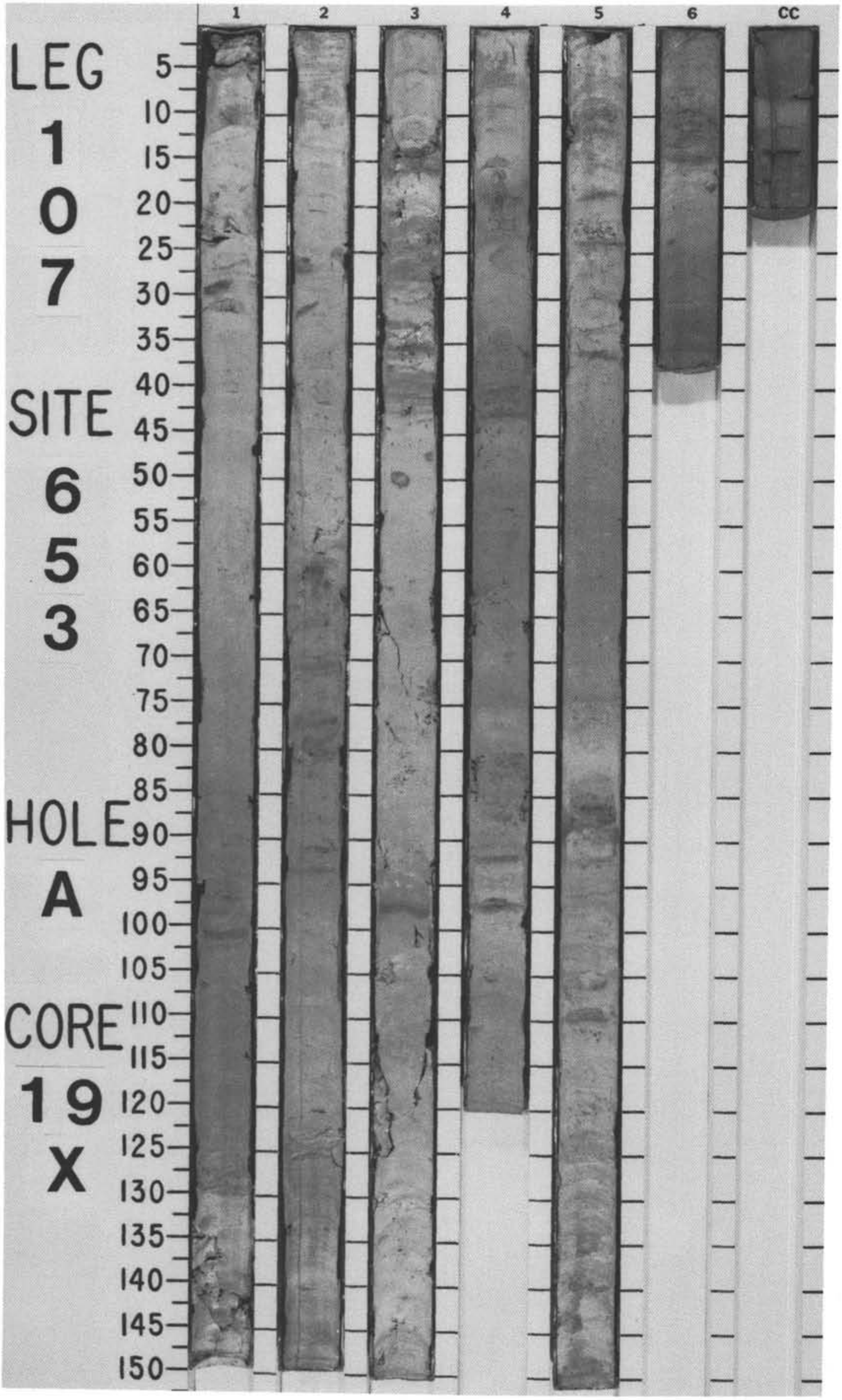
LEG
107
SITE
653
HOLE
A
CORE
19
X
1
2
3
4
5
6
CC
5
10
15
20
25
30
35
40
45
50
55
60
65
70
75
80
85
90
95
100
105
110
115
120
125
130
135
140
145
150

SITE 653 HOLE A CORE 20X CORED INTERVAL 2990.7-3000.2 mbsl; 173.7-183.2 mbsf

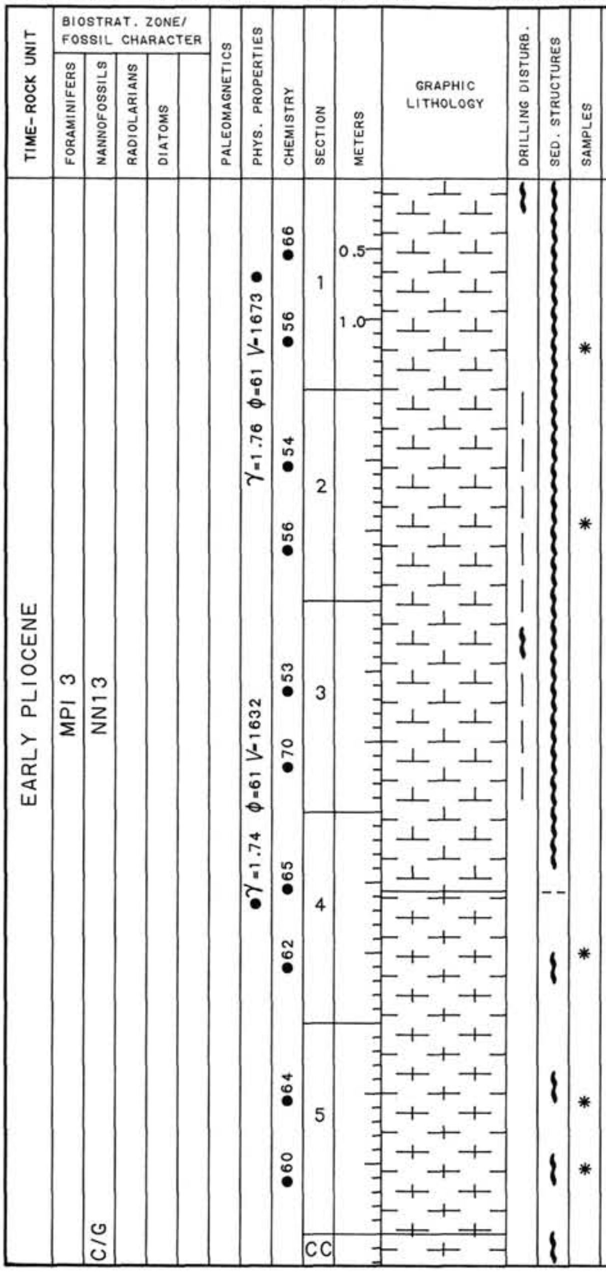

LITHOLOGIC DESCRIPTION

NANNOFOSSIL OOZE and FORAMINIFER-NANNOFOSSIL OOZE

Nannofossil ooze and foraminifer-nannofossil ooze, light gray (5Y 7/1, 7/2; 2.5Y 7/2), pale yellow (5Y 7/3), light olive-gray (5Y 6/2), and (2.5Y 6/2, 6/3, 6/6, 7/1, 7/3); diffuse and gradational contacts between colors. Foraminiferal tests and black specks (hyrotroilite?) throughout core in minor amounts, concentrated in intervals of foraminifers noted below. Texturally homogeneous.

Minor lithology: foraminifer-bearing nannofossil ooze, (5Y 6/1, 6/4, 7/1, 7/3), Section 4, 56–74 and 105–150 cm, Section 5, 23–65 and 105–144 cm, and CC.

SMEAR SLIDE SUMMARY (%):

	1, 114 D	2, 90 D	4, 100 D	5, 54 D	5, 100 M
TEXTURE:					
Sand	5	5	5	5	20
Silt	15	15	15	15	15
Clay	80	80	80	80	65
COMPOSITION:					
Quartz	5	2	1	4	2
Feldspar	1	—	—	—	—
Mica	1	—	—	—	—
Clay	13	16	21	20	20
Volcanic glass	1	—	—	1	—
Dolomite	3	—	—	4	—
Accessory minerals	—	—	—	—	3
Pyrite	4	1	1	5	—
Foraminifers	10	15	10	10	20
Nannofossils	60	65	60	54	55
Sponge spicules	1	1	—	1	—
Bioclasts	1	—	—	1	—

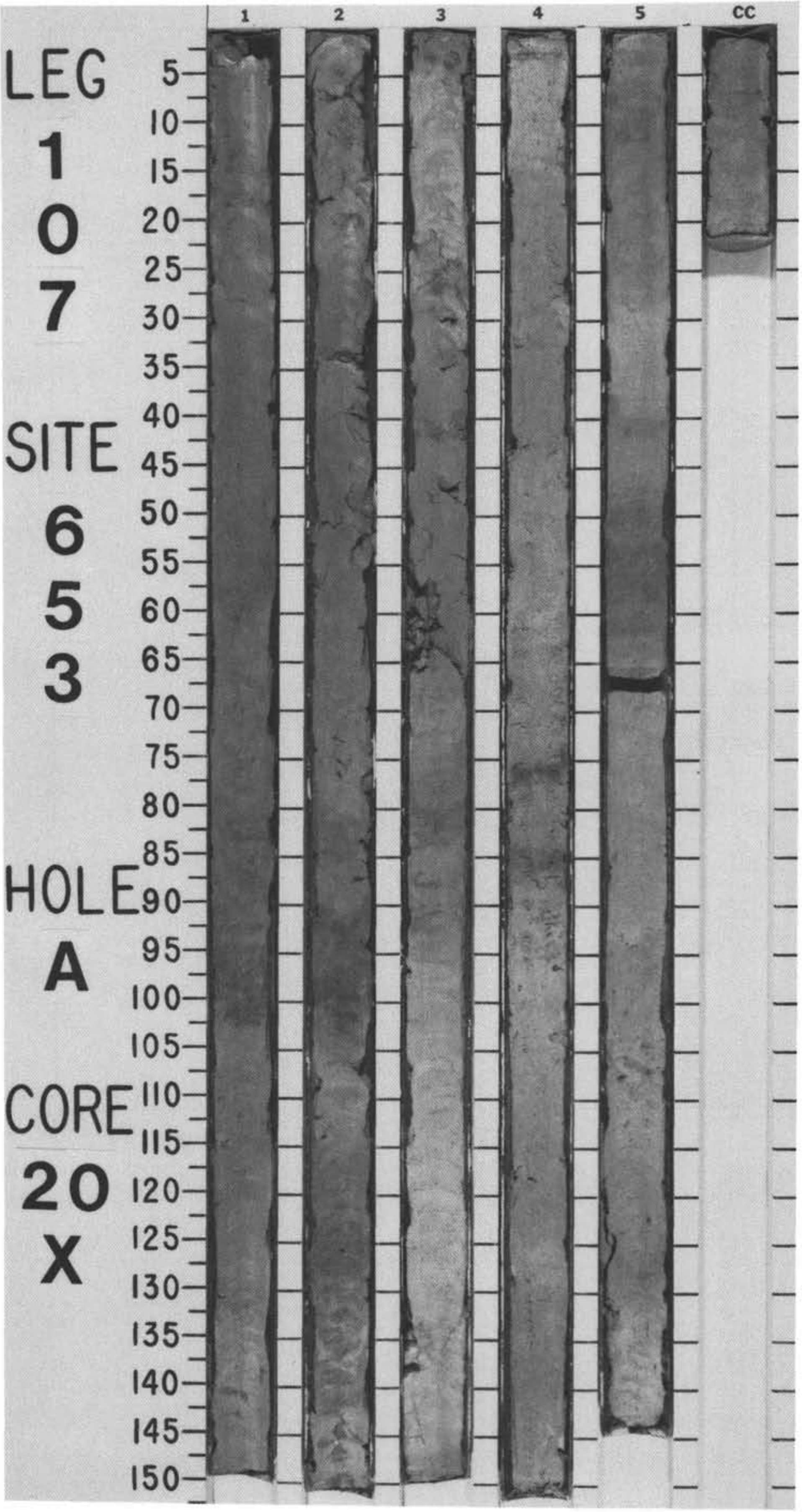
LEG
107
SITE
653
HOLE
A
CORE
20
X
1
2
3
4
5
CC
5
10
15
20
25
30
35
40
45
50
55
60
65
70
75
80
85
90
95
100
105
110
115
120
125
130
135
140
145
150

SITE 653 HOLE A CORE 21X CORED INTERVAL 3000.2-3009.9 mbsl; 183.2-192.9 mbsf

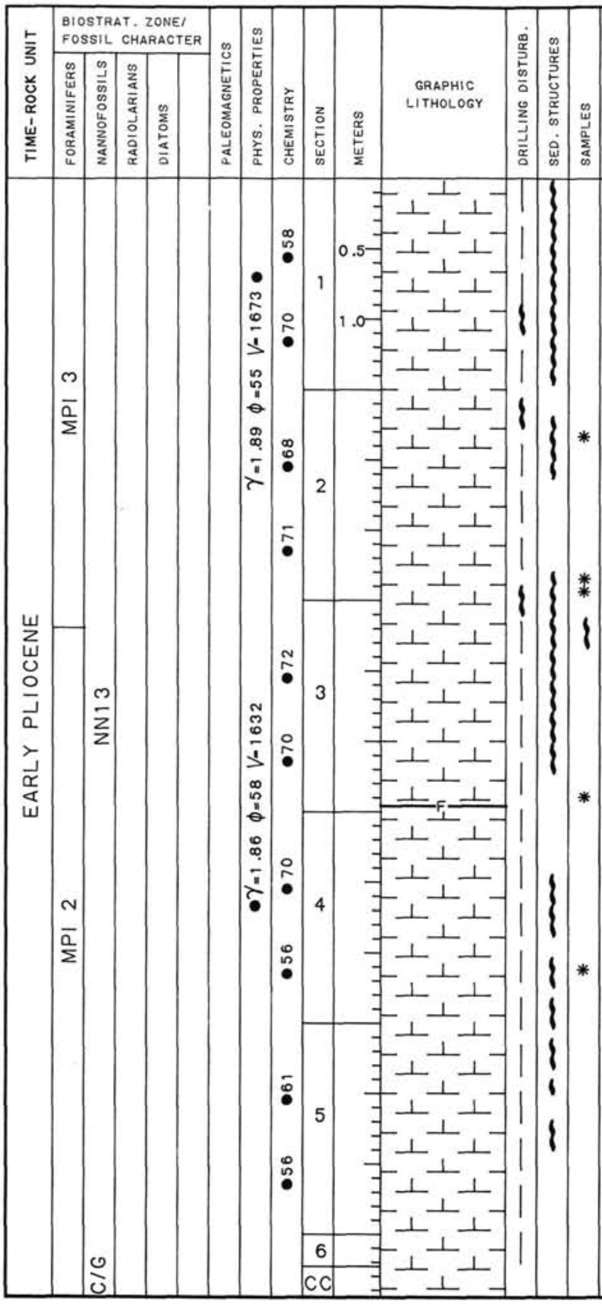

LITHOLOGIC DESCRIPTION

NANNOFOSSIL OOZE

Nannofossil ooze, light gray (2.5Y 5/6, 7/0, 7/1, 7/2, 7/3), pale yellow (5Y 7/3), pale olive (5Y 6/3), gray (5Y 6/1), light olive-gray (5Y 6/2), and (10GY 6/4); diffuse and gradational contacts between colors; slightly indurated zones in Section 2, 31, 37–38, 44–46, and 133–136 cm. Diagenetic laminae in Section 4 and Section 5. Mostly homogeneous in texture and color. Metal piece (from coring equipment?) in Section 6, 7 cm.

Minor lithology: foraminifers-bearing sandstone indurated and broken into small pieces, Section 3, 141–143 cm. It is thus difficult to distinguish layer contacts or original continuity in the core.

SMEAR SLIDE SUMMARY (%):

	2, 37 M	2, 137 M	2, 140 M	3, 141 M	4, 100 D
TEXTURE:					
Sand	—	5	15	60	10
Silt	—	5	—	5	—
Clay	100	90	85	35	90
COMPOSITION:					
Quartz	—	1	2	3	—
Feldspar	—	—	—	1	Tr
Clay	—	—	—	15	—
Volcanic glass	—	2	5	—	—
Calcite	—	—	2	—	—
Dolomite	1	2	1	—	1
Accessory minerals	—	—	—	1	—
Opaques	—	1	—	—	—
Foraminifers	5	10	15	60	10
Nannofossils	94	84	75	20	89
Sponge spicules	Tr	—	Tr	—	Tr

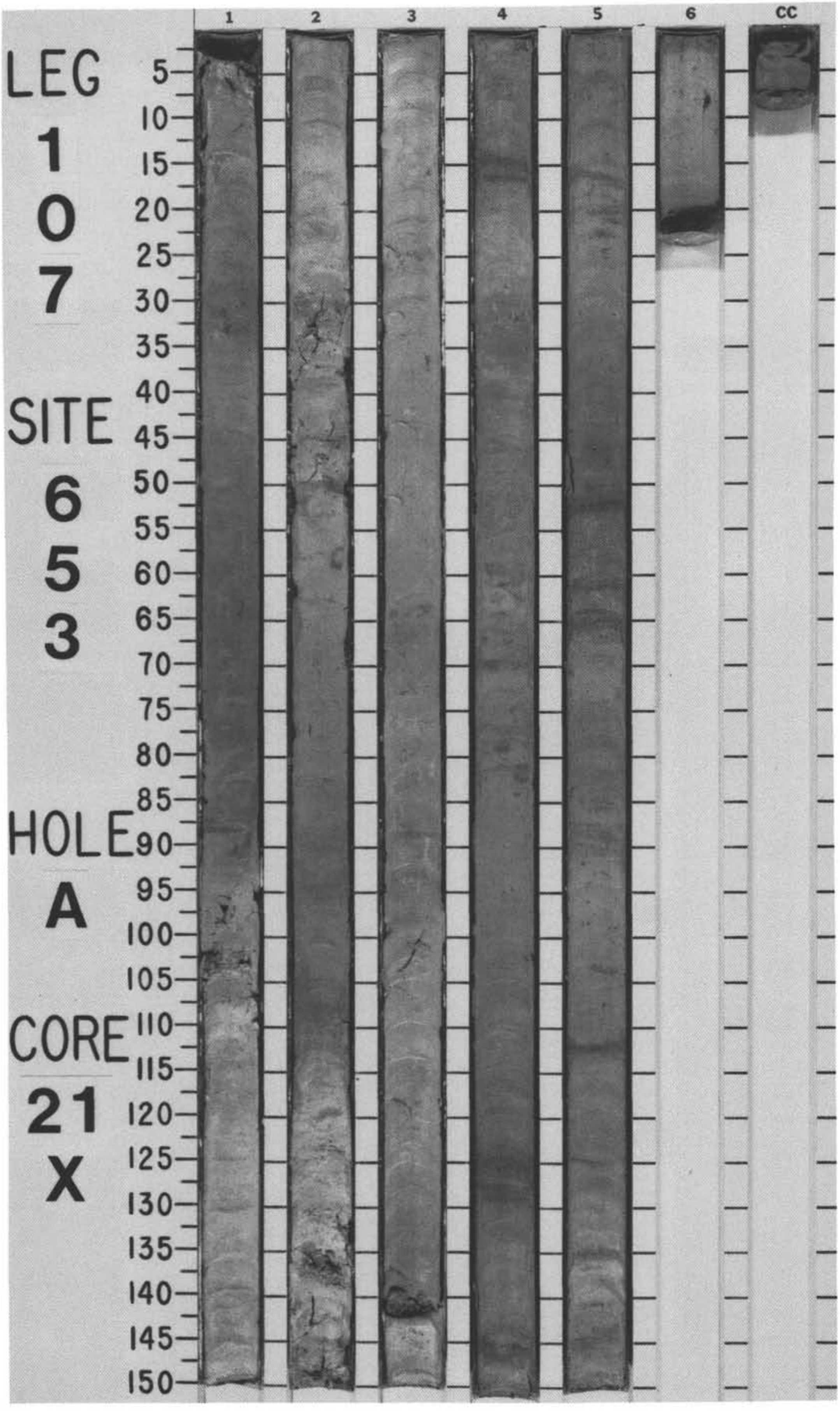
LEG
107
SITE
653
HOLE
A
CORE
21
X
1
2
3
4
5
6
CC
5
10
15
20
25
30
35
40
45
50
55
60
65
70
75
80
85
90
95
100
105
110
115
120
125
130
135
140
145
150

SITE 653 HOLE A CORE 22X CORED INTERVAL 3009.9-3019.4 mbsl; 192.9-202.4 mbsf

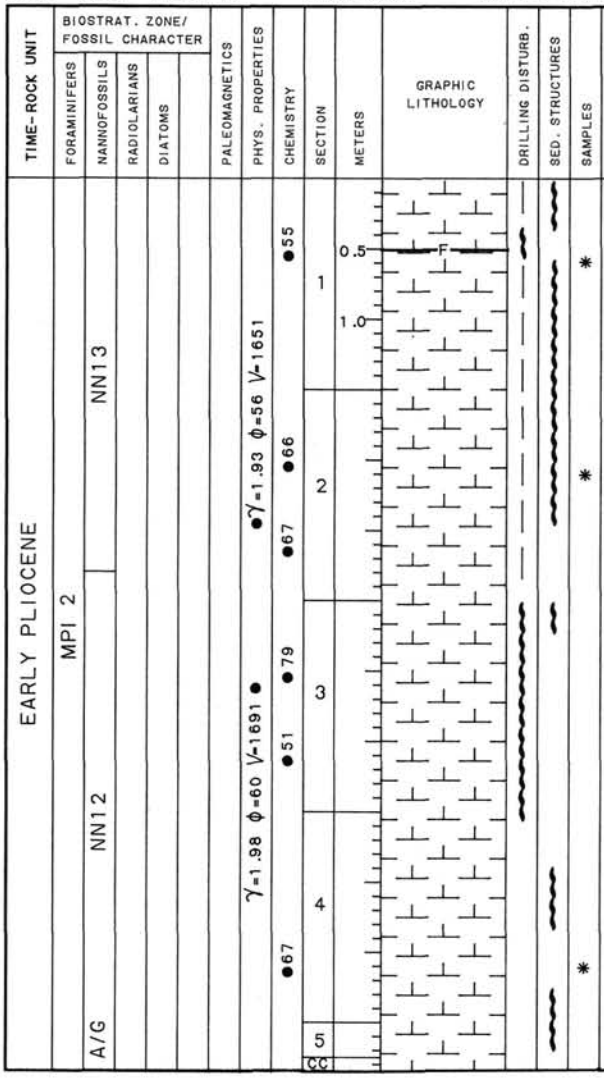

LITHOLOGIC DESCRIPTION

NANNOFOSSIL OOZE

Nannofossil ooze, light gray (2.5Y 7/2, 7/4, 7/6; 5Y 7/2), pale yellow (5Y 7/3), light olive-gray (5Y 6/2), white (5Y 8/2), and yellow (5Y 7/6). Burrowed in upper portion, and maybe throughout core. Drilling disturbances prevent better delineation. Most color changes are gradational. Core is texturally and compositionally homogeneous. Broken into pieces, thus layer contacts and continuity in core cannot be distinguished.

Minor lithology: foraminifer-bearing sandstone (5Y 6/2), Section 1, 49–53 cm.

SMEAR SLIDE SUMMARY (%):

	1, 54 M	2, 55 D	4, 103 D
TEXTURE:			
Sand	40	5	—
Silt	30	5	10
Clay	30	90	90
COMPOSITION:			
Quartz	—	Tr	—
Mica	—	—	3
Clay	25	30	45
Dolomite	—	—	2
Accessory minerals			
Analcime	—	Tr	Tr
Micrite	—	—	—
Foraminifers	40	10	5
Nannofossils	35	40	35

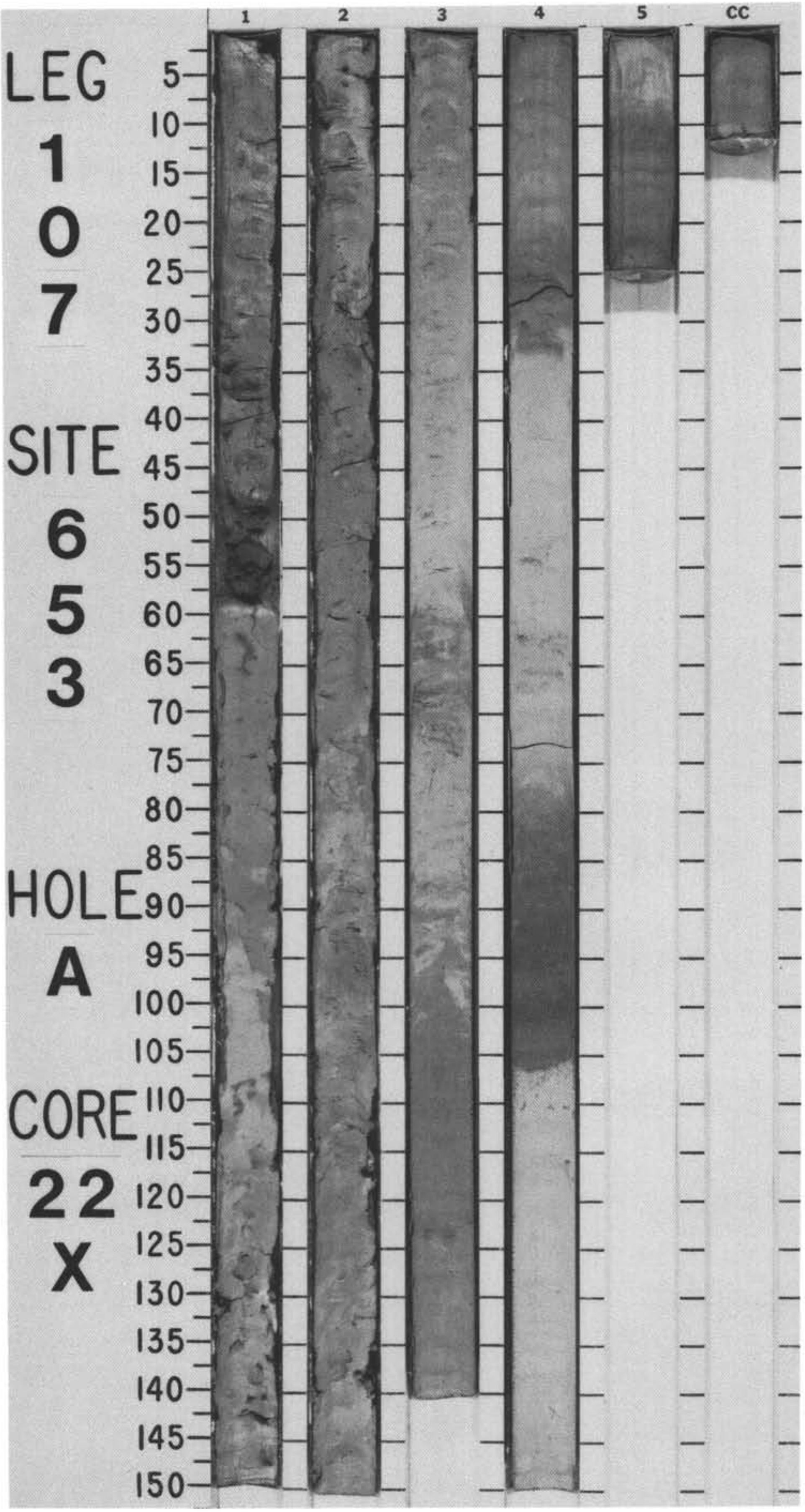
LEG
107
SITE
653
HOLE
A
CORE
22
X
1
2
3
4
5
CC
5
10
15
20
25
30
35
40
45
50
55
60
65
70
75
80
85
90
95
100
105
110
115
120
125
130
135
140
145
150

SITE 653 HOLE A CORE 23X CORED INTERVAL 3019.4-3028.9 mbsl; 202.4-211.9 mbsf

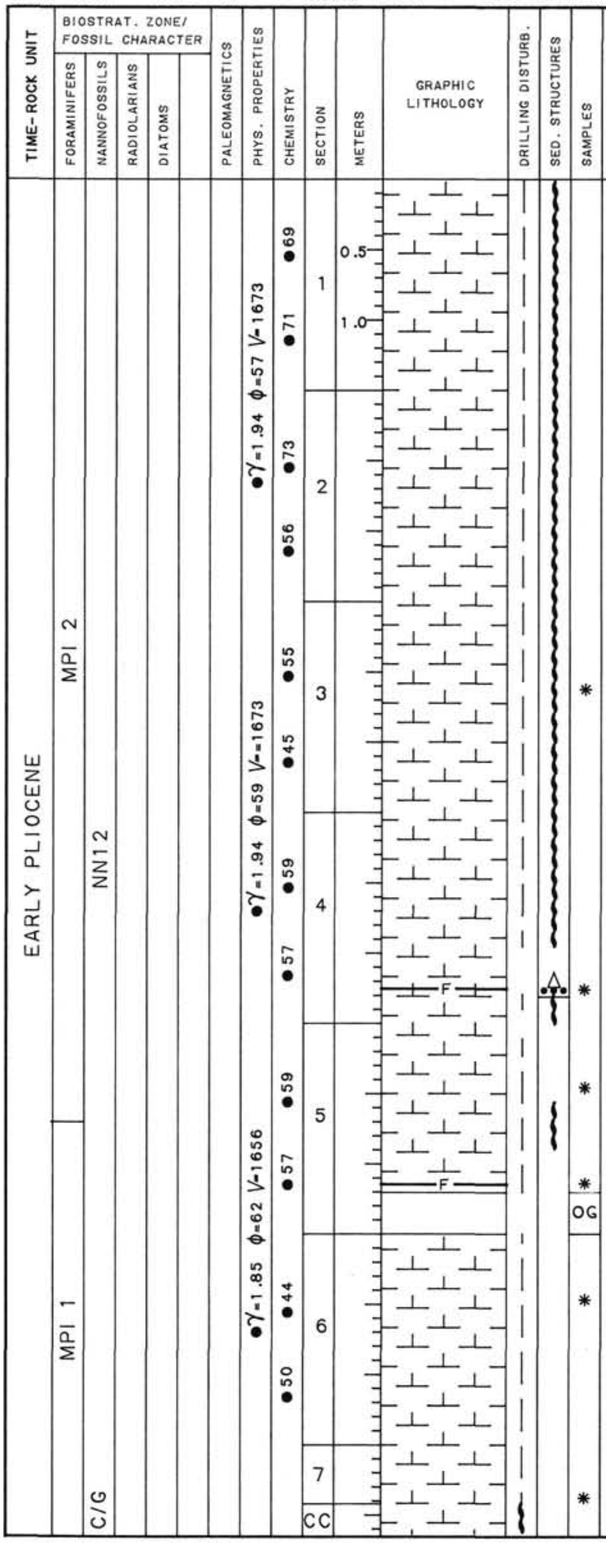

LITHOLOGIC DESCRIPTION

NANNOFOSSIL OOZE

Nannofossil ooze, light gray (5Y 7/1, 7/2), pale yellow (5Y 7/3), pale olive (5Y 6/3), light olive-gray (5YR 6/2, 7/6), and (2.5Y 4/4, 5/4, 5/6, 6/4, 6/6, 7/2, 7/4, 8/1, 8/4; 5Y 5/3, 7/6; 7.5Y 6/0; 10GY 7/2; 5YR 4/3; 7.5YR 6/6, 7/2, 7/4, 7/6; 10R 5/8); colors are transitional from very light grays and browns to darker browns and red-yellow-browns; much of variegated and mottled color patterns result from coring disturbances (soft biscuits).

Minor lithology: Silty foraminifer-nannofossil ooze, (2.5Y 7/2), Section 4, 122–129 cm, and Section 5, 117–120 cm. Normally graded layer in Section 4.

SMEAR SLIDE SUMMARY (%):

	3, 60 D	4, 129 D	5, 48 D	5, 118 M	6, 48 D	7, 34 D
TEXTURE:						
Sand	—	10	5	15	5	5
Silt	8	45	—	45	—	15
Clay	92	45	95	70	95	80
COMPOSITION:						
Quartz	—	—	1	Tr	1	—
Mica	Tr	2	—	—	—	—
Clay	35	36	10	20	—	35
Dolomite	—	2	—	Tr	1	Tr
Accessory minerals						
Analcime	Tr	Tr	—	Tr	—	Tr
Gypsum	—	—	1	—	1	2
Opaques	—	—	—	25	2	—
Micrite	13	—	—	—	—	5
Aragonite	—	Tr	—	—	—	—
Foraminifers	8	30	5	25	5	8
Nannofossils	42	30	83	30	80	50
Diatoms	—	—	—	—	5	—
Sponge spicules	—	—	Tr	—	—	—

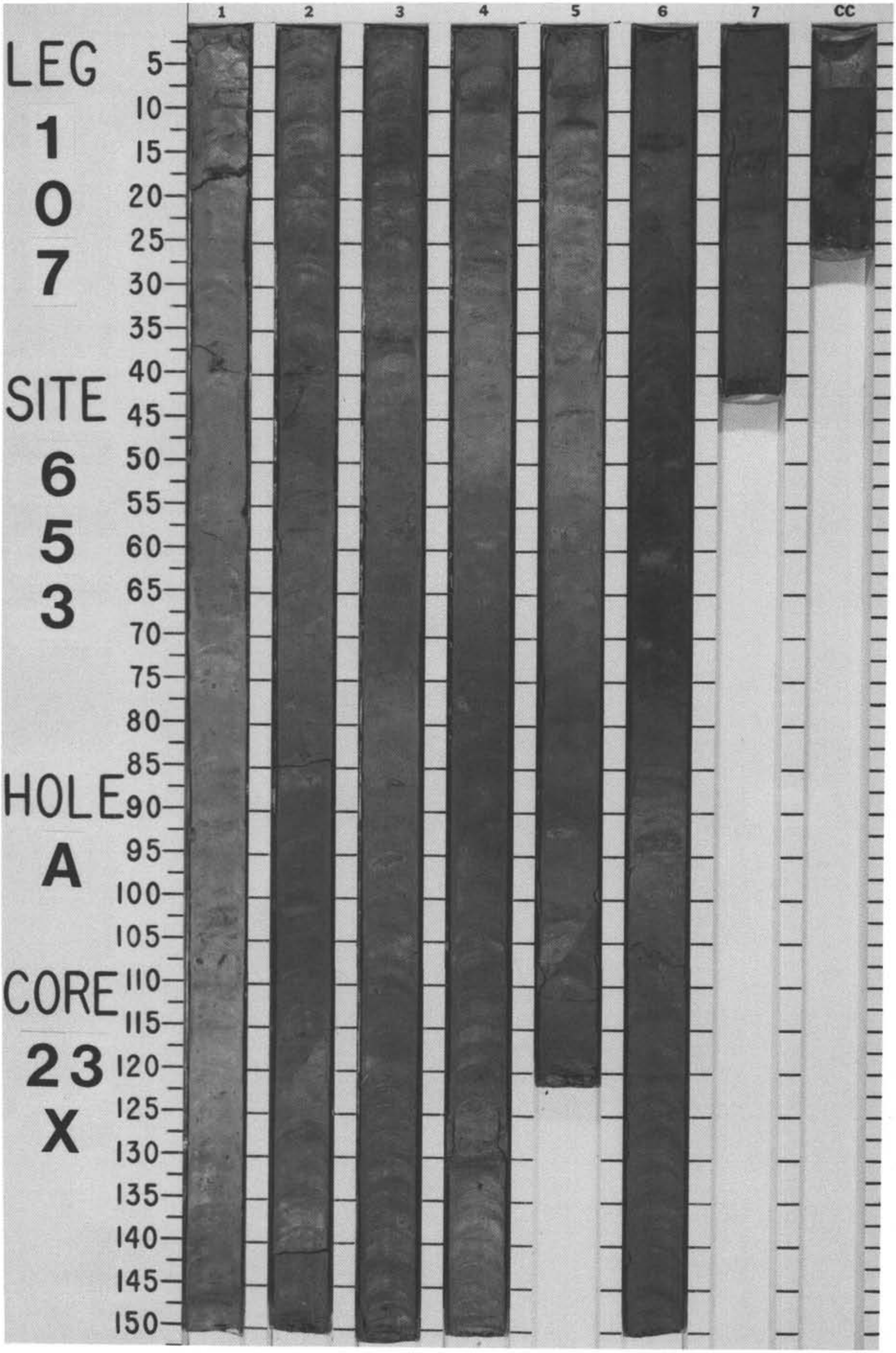
LEG
107
SITE
653
HOLE
A
CORE
23X
1
2
3
4
5
6
7
CC
5
10
15
20
25
30
35
40
45
50
55
60
65
70
75
80
85
90
95
100
105
110
115
120
125
130
135
140
145
150

SITE 653 HOLE A CORE 24X CORED INTERVAL 3028.9-3038.4 mbsl; 211.9-221.4 mbsf

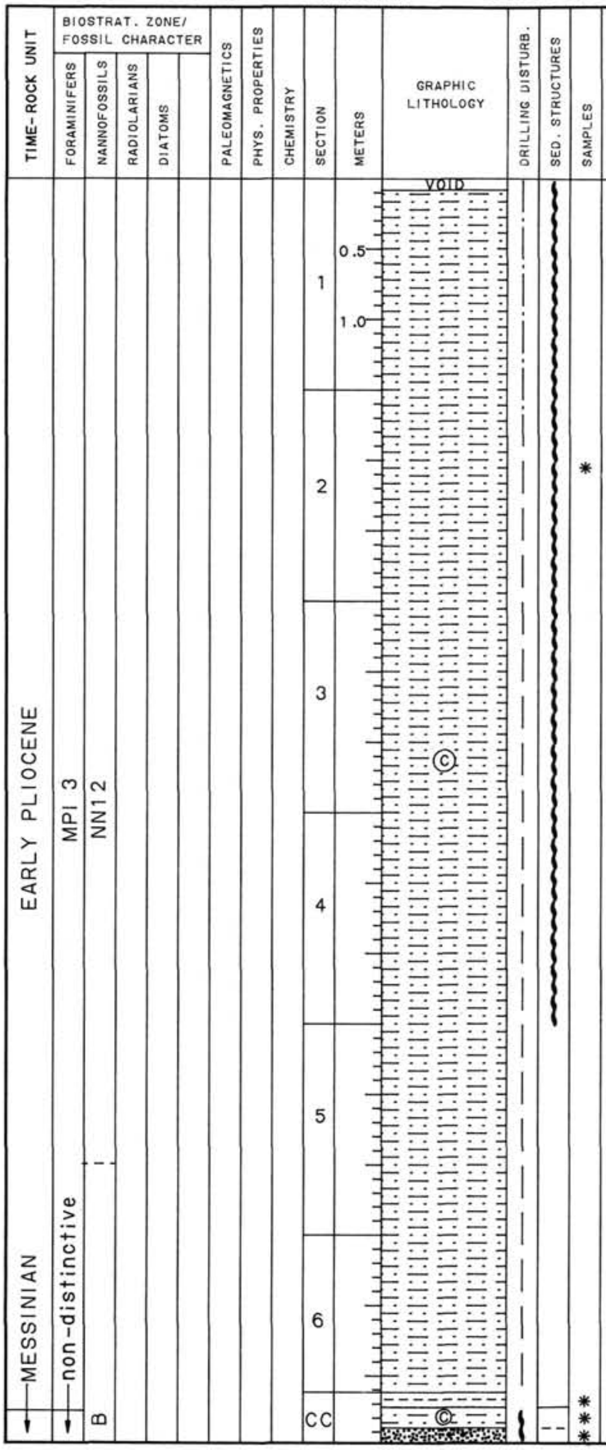

LITHOLOGIC DESCRIPTION

CALCAREOUS MUD

Calcareous mud, (5YR 5/6, 5YR 6/4, 2.5Y 6/4); (5Y 7/2, 2.5Y 4/0, 2.5YR 4/4, 5Y 5/2); (2.5YR 5/6, 7.5YR 4/4, 10YR 3/2). Multicolored and variegated, with few distinct contacts between colors. This probably represents biscuits formed because of drilling disturbance. Despite color differences, the sediment is texturally and compositionally homogeneous.

Minor lithologies:
a)Ferruginous clay, (10YR 2/2–2.5Y 4/2); color variations suggest at least six layers, disturbed by drilling; CC, 0–8 cm.
b)Biotite-bearing sand, (10YR 6/1); no structure or layering apparent in sand; CC, 25–34 cm.

SMEAR SLIDE SUMMARY (%):

	2, 54 D	CC, 3 M	CC, 18.5 D	CC, 31 M
TEXTURE:				
Sand	—	—	—	60
Silt	15	10	15	30
Clay	85	90	85	10
COMPOSITION:				
Quartz	1	1	1	2
Feldspar	—	5	2	1
Mica	1	—	1	22
Clay	67	64	61	34
Volcanic glass	—	—	—	12
Calcite	—	2	—	—
Dolomite	—	—	7	—
Accessory minerals				
Opaques	—	2	—	—
Analcime	4	—	3	—
Pyrite	—	—	3	5
Micrite	—	3	—	—
Zeolites	—	20	—	1
Foraminifers	4	—	2	—
Nannofossils	20	3	20	3
Spar cement	3	—	—	—
Detrital carbonate	—	—	—	20

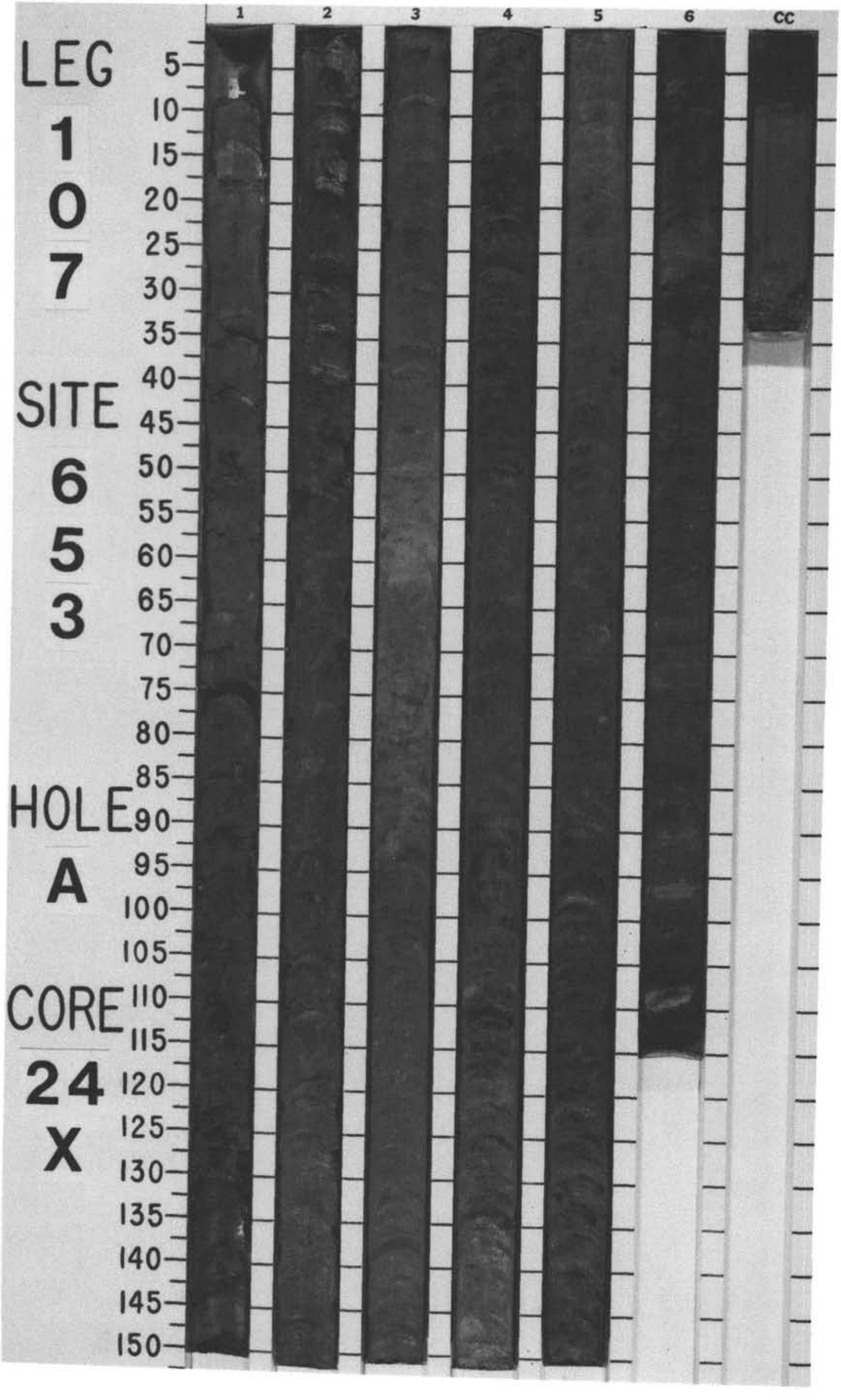
LEG
1
0
7
SITE
6
5
3
HOLE
A
CORE
24
X
1
2
3
4
5
6
CC
5
10
15
20
25
30
35
40
45
50
55
60
65
70
75
80
85
90
95
100
105
110
115
120
125
130
135
140
145
150

SITE 653 HOLE A CORE 25X CORED INTERVAL 3038.4-3048.0 mbsl; 221.4-231.0 mbsf

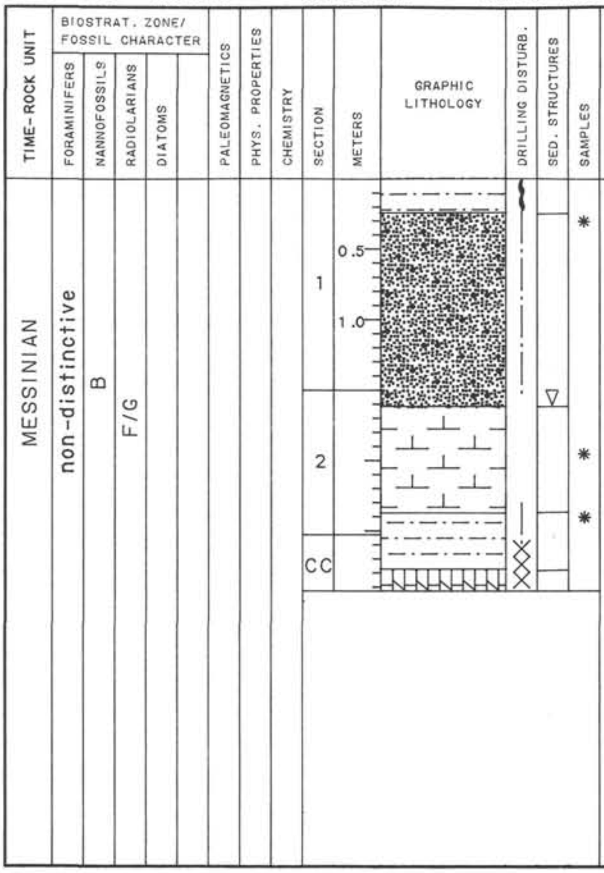

LITHOLOGIC DESCRIPTION

NANNOFOSSIL OOZE and SILTY SAND

Nannofossil ooze and silty sand, reddish brown (2.5YR 5/4), gray (5Y 5/1, 6/1), olive-gray (5Y 4/2), and olive (5Y 5/3); silty sand is homogeneous. Nannofossil ooze may be burrowed in lower 30 cm, or mottling could be the result of coring disturbances.

Minor lithologies:
- a) Sandy mud in Section 2, 86 cm, to CC, 27 cm, dusky red (10R 3/4).
- b) Gypsum in CC, 27 cm, to base of CC, white (2.5Y 8/2) to light brownish gray (2.5Y 6/2), broken into breccia by drilling.

SMEAR SLIDE SUMMARY (%):

	1, 30 D	2, 50 D	2, 90 D
TEXTURE:			
Sand	50	5	15
Silt	35	5	30
Clay	15	90	55
COMPOSITION:			
Quartz	20	1	10
Feldspar	5	1	2
Mica	5	—	—
Clay	15	50	56
Volcanic glass	10	2	5
Dolomite	5	2	2
Accessory minerals			
Gypsum	25	5	5
Zeolites(?)	—	Tr	—
Opaques	—	—	10
Iron oxides	—	—	10
Foraminifers	—	5	—
Nannofossils	15	34	—

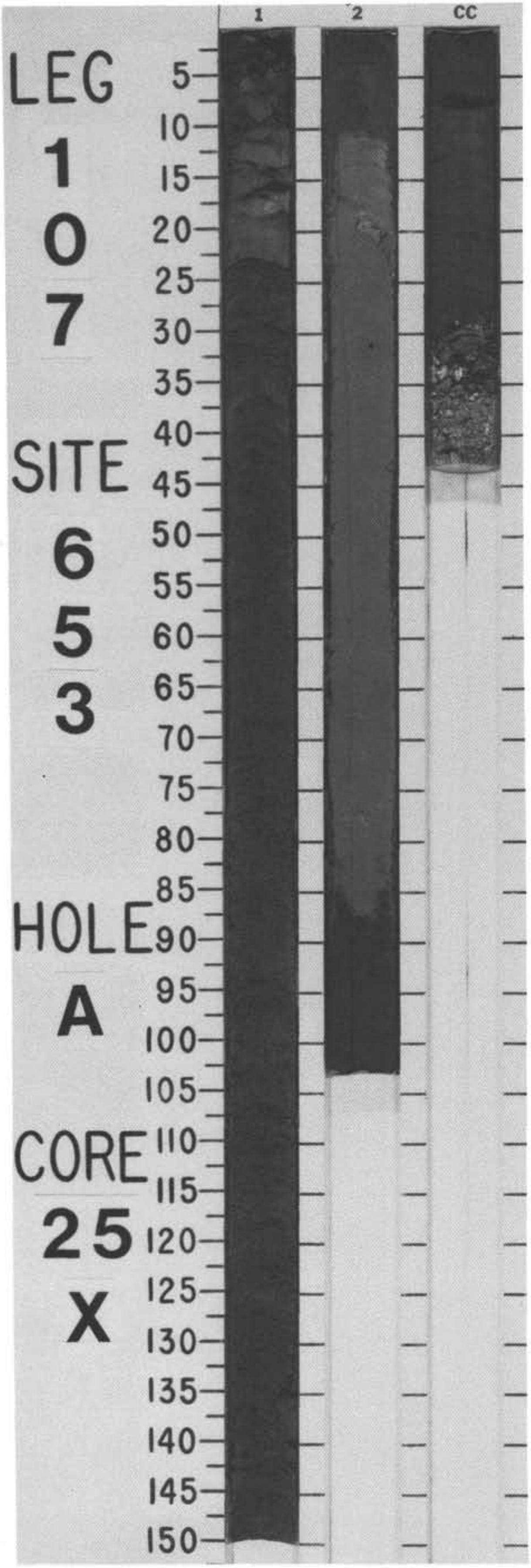
1
2
CC
LEG
107
SITE
653
HOLE
A
CORE
25
X
5
10
15
20
25
30
35
40
45
50
55
60
65
70
75
80
85
90
95
100
105
110
115
120
125
130
135
140
145
150

SITE 653 HOLE A CORE 26X CORED INTERVAL 3048.0-3057.7 mbsl; 231.0-240.7 mbsf

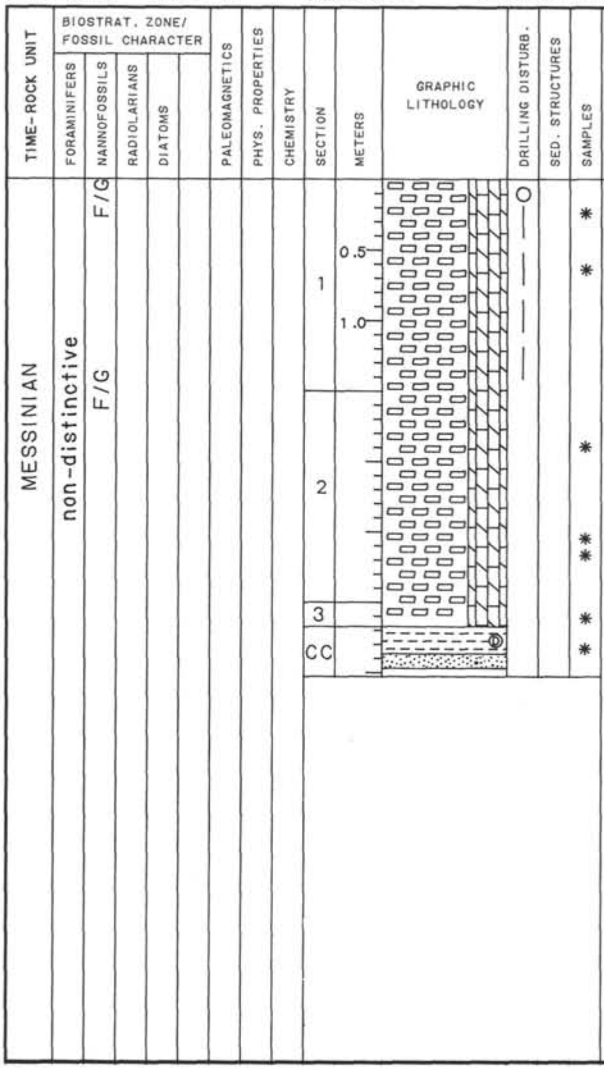

LITHOLOGIC DESCRIPTION

MARLY CALCAREOUS (DOLOMITIC) OOZE, CALCAREOUS NANNOFOSSIL MUD, and GYPSUM AND SILTSTONE

Major lithologies comprise alternations of marly calcareous (dolomitic) ooze, calcareous nannofossil mud and dolomitic clay, dark gray (5Y 4/1) and olive-gray (5Y 5/2); dark grayish brown (10YR 4/2) in CC. Finely laminated in Section 3, normally graded in few-mm intervals (enrichment of mica at the base). Foraminifers in patches of ooze.

Minor lithologies:
a) Gypsum, laminated to large crystals in compact layers or clusters to microcrystalline, white (5Y 8/1) to transparent.
b) Siltstone/sandstone in Section 2, 36–41 cm, dark gray (5Y 4/1), coarse silt to very fine-grained sand, well sorted, polymineralic composition (including mica).

SMEAR SLIDE SUMMARY (%):

	1, 25 M	1, 65 D	2, 40 M	2, 102 D	2, 119 M	3, 17 M	CC, 15 D
TEXTURE:							
Sand	5	2	40	3	65	5	2
Silt	20	5	20	25	25	25	20
Clay	75	93	40	72	10	70	78
COMPOSITION:							
Quartz	Tr	—	25	3	40	7	5
Feldspar	3	—	—	—	—	—	—
Mica	—	—	—	—	—	1	—
Clay	50	54	31	26	4	50	51
Volcanic glass	5	3	—	—	—	3	—
Calcite/dolomite	7	3	7	15	3	20	15
Accessory minerals	Tr	—	1	1	Tr	1	2
Gypsum	2	3	10	4	35	5	5
Pyrite	—	1	1	1	—	1	—
Micrite (dolomicrite?)	25	16	15	20	15	8	10
Aragonite needles	—	1	—	—	—	—	—
Foraminifers	1	—	—	—	—	—	—
Nannofossils	6	18	10	30	3	4	10
Radiolarians	1	Tr	Tr	—	—	—	Tr
Sponge spicules	—	1	Tr	—	—	—	—
Pollens	—	—	—	—	—	—	2

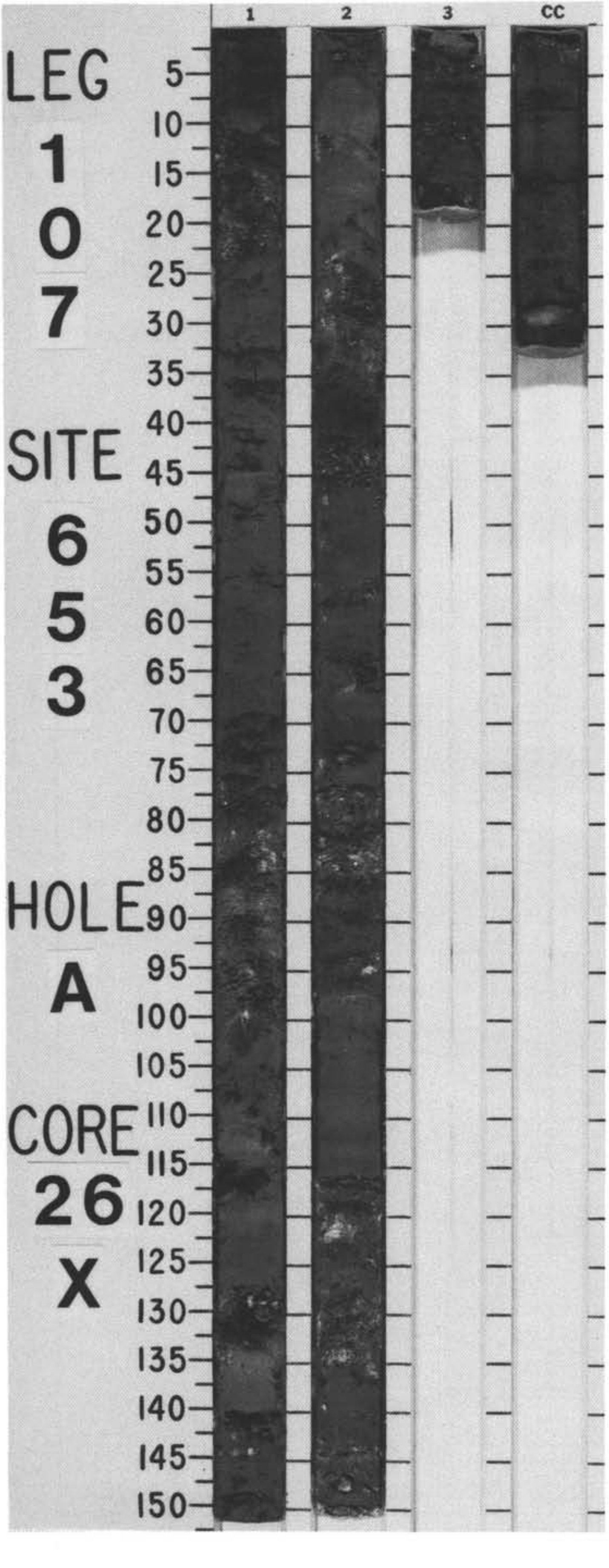
1
2
3
CC
LEG
107
SITE
653
HOLE
A
CORE
26
X
5
10
15
20
25
30
35
40
45
50
55
60
65
70
75
80
85
90
95
100
105
110
115
120
125
130
135
140
145
150

SITE 653 HOLE B CORE 1H CORED INTERVAL 2820.9-2827.0 mbsl; 0-6.1 mbsf

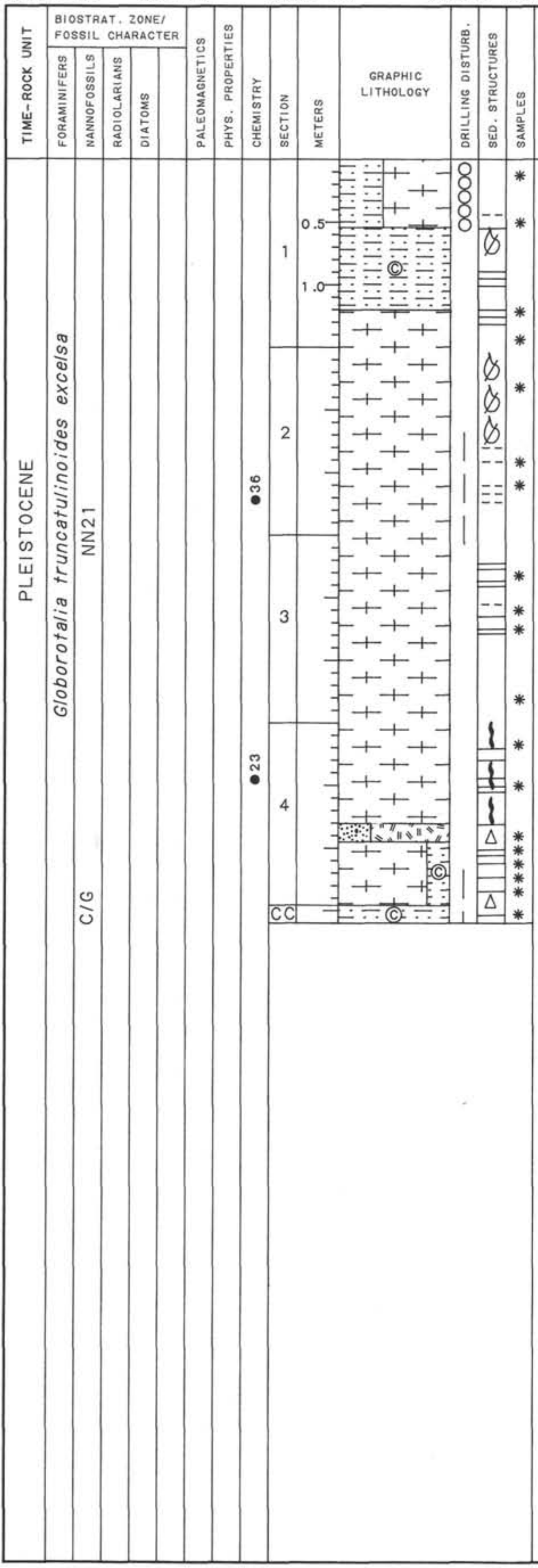

LITHOLOGIC DESCRIPTION

MARLY NANNOFOSSIL OOZE alternating with CALCAREOUS MUD

Marly nannofossil ooze alternating with calcareous mud. Alternations of variable thickness (generally decreasing downcore). Varicolored with olive, gray, brown, and yellow shades; both sharp and diffuse changes between various colors. Gritty in Section 2, upper part (possible detrital dolomite). Pteropod shell fragments in Section 7, 54–100 cm, and Section 2, downcore to 80 cm. Mollusk shell fragments in Section 2, 2–40 cm.

Minor lithologies:
a) Foraminiferal silty sand, Section 1, 49–54 cm.
b) Volcaniclastic mud, Section 1, around 120 cm, and Section 4, 80–94 cm, thin, faint gray to light yellowish brown (2.5Y 6/4) and light olive brown (2.5Y 54) laminae, normally graded.
c) Mud, Section 2, near the base, and Section 3, around 40 cm, thin, black and very dark gray to dark brown laminae (possible sapropel remnants).
d) Mn(?)-rich mud, Section 3, 27 cm, thin, dark bluish-gray laminae.
e) Mud, Section 3, 133 cm, and Section 4, 52 cm, faint greenish (possible diagenetic) laminae.

SMEAR SLIDE SUMMARY (%):

	1, 10 M	1, 52 M	1, 122 D	1, 144 M	2, 34 M	2, 91 M	2, 107 M
TEXTURE:							
Sand	10	65	18	—	—	—	15
Silt	40	20	22	10	15	15	40
Clay	50	15	60	90	85	85	45
COMPOSITION:							
Quartz	3	2	4	2	5	5	5
Feldspar	—	—	1	—	1	1	1
Mica	1	1	4	—	—	—	—
Clay	55	10	48	—	—	—	48
Volcanic glass	3	Tr	15	5	2	2	12
Calcite	—	—	4	—	—	—	6
Dolomite	—	—	—	5	10	5	3
Accessory minerals	2	1	2	—	2	2	—
Pyrite(?)	—	—	—	—	—	—	2
Micrite	—	—	4	—	—	—	4
Foraminifers	12	60	4	5	13	2	2
Nannofossils	18	25	12	81	66	82	12
Diatoms	2	—	—	1	1	1	1
Radiolarians	2	—	—	—	—	—	—
Sponge spicules	—	1	2	1	—	Tr	1
Silicoflagellates	1	—	—	—	—	—	1
Fish remains	1	—	—	—	—	—	Tr
Bioclasts	—	—	—	—	—	—	2

	3, 34 M	3, 63 M	3, 77 M	3, 132 M	4, 20 D	4, 52 M	4, 89 M
TEXTURE:							
Sand	—	—	25	15	—	—	50
Silt	10	10	40	60	5	40	20
Clay	90	90	35	25	95	60	30
COMPOSITION:							
Quartz	5	8	15	4	3	10	1
Feldspar	1	2	4	1	—	Tr	—
Mica	—	1	2	1	2	—	—
Clay	—	63	42	50	25	—	30
Volcanic glass	1	4	3	13	—	10	69
Calcite	—	—	—	22	—	—	—
Dolomite	10	—	2	2	Tr	Tr	Tr
Accessory minerals	2	2	4	2	—	Tr	—
Micrite	—	—	—	—	10	—	—
Pyroxene	—	—	—	—	Tr	—	—
Foraminifers	10	5	3	1	6	10	—
Nannofossils	69	12	15	3	50	69	—
Diatoms	1	—	—	—	—	—	—
Sponge spicules	1	3	2	1	—	1	—
Fish remains	—	Tr	—	—	—	—	—
Organics	—	—	3	—	—	—	—
Detrital carbs.	—	—	5	—	—	—	—
Pteropod-aragonite needles	—	—	—	—	4	—	—

	4, 105 M	4, 116 M	4, 124 M	4, 136 M	CC, 14 M
TEXTURE:					
Sand	5	60	15	—	10
Silt	5	30	30	10	30
Clay	90	10	55	90	60
COMPOSITION:					
Quartz	—	43	5	—	4
Feldspar	2	5	1	—	1
Mica	—	—	1	—	1
Clay	—	—	68	—	60
Volcanic glass	1	5	3	—	5
Calcite	—	10	4	—	4
Dolomite	5	5	Tr	2	1
Accessory minerals	—	2	2	—	1
Foraminifers	10	10	6	10	4
Nannofossils	80	20	9	88	18
Diatoms	1	—	—	—	—
Sponge spicules	1	—	1	—	1
Fish remains	—	—	—	—	Tr

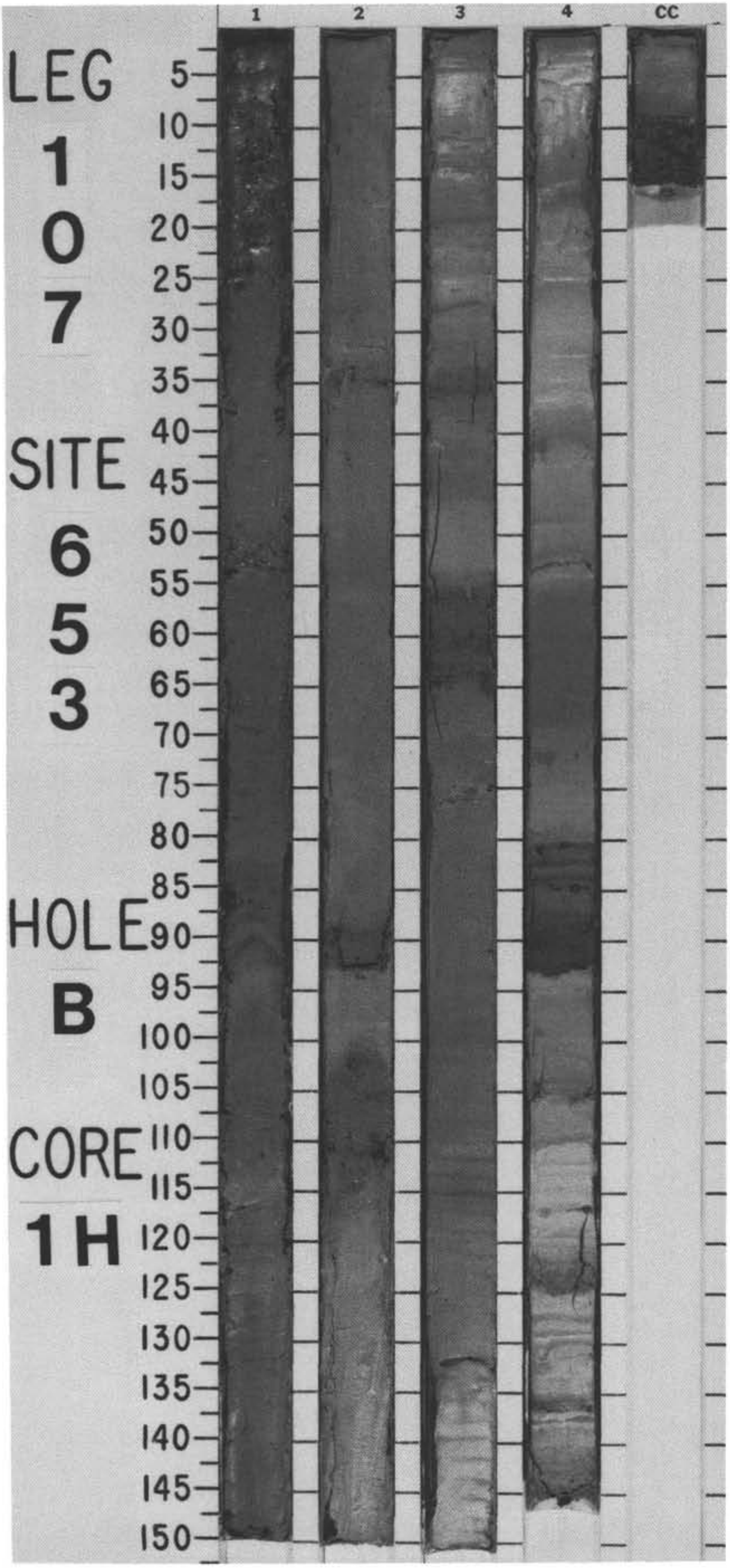
LEG
107
SITE
653
HOLE
B
CORE
1H
1
2
3
4
CC
5
10
15
20
25
30
35
40
45
50
55
60
65
70
75
80
85
90
95
100
105
110
115
120
125
130
135
140
145
150

SITE 653 HOLE B CORE 2H CORED INTERVAL 2827.0-2838.5 mbsl; 6.1-17.6 mbsf

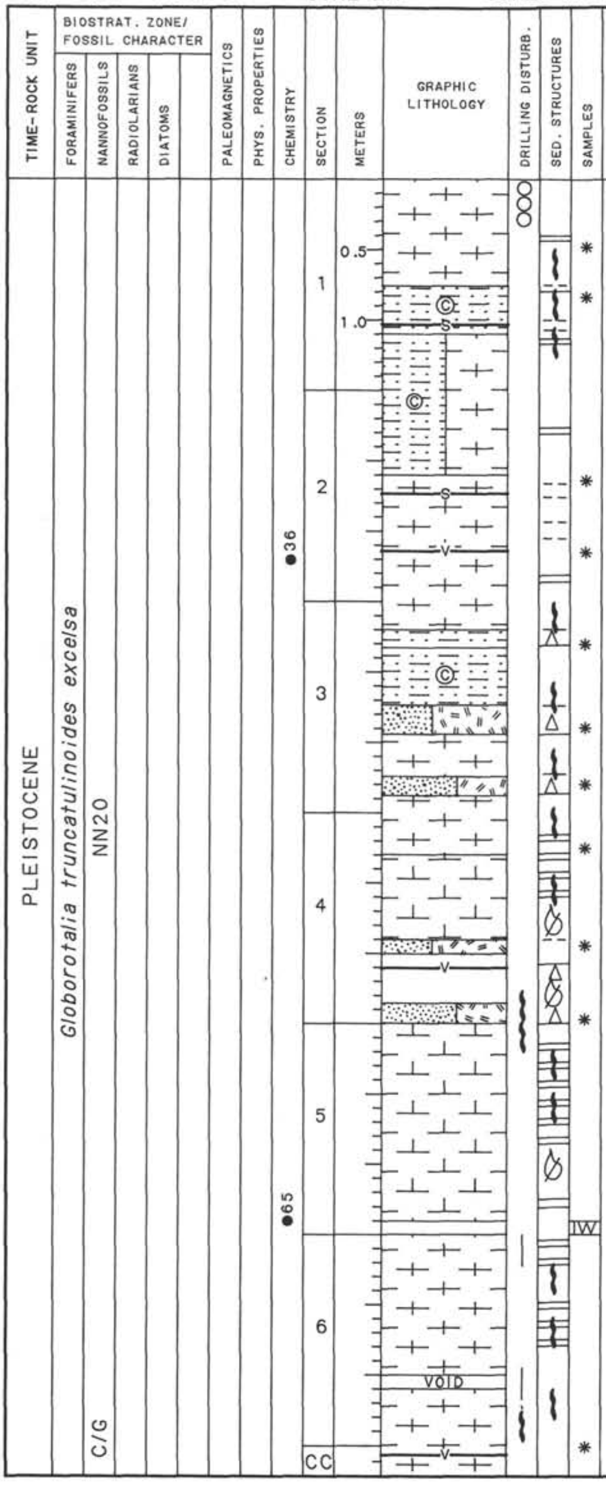

LITHOLOGIC DESCRIPTION

MARLY FORAMINIFER-NANNOFOSSIL OOZE with intercalations of MUD AND VOLCANIC GLASS-BEARING SANDY LAYERS

Marly nannofossil-foraminifer ooze; white (2.5Y N/8 or 5Y 8/1) to light olive brown (2.5Y 5/4) or olive (5Y 5/4), and light gray (10YR 7/2). Two thin indurated intervals in Section 4, 20–21 and 30–31 cm, greenish gray (5GY 5/2).

Minor lithologies:
- a)Calcareous mud, Section 1, 78–109 cm, alternating with marly nannofossil ooze from Section 1, 109 cm, to Section 2, 60 cm; very dark gray (5Y 3/1).
- b)Foraminifer-nannofossil ooze, Section 2, 96–105 cm; pale yellow (5Y 7/3).
- c)Volcanic ash layers, Section 2, 117–118 cm, Section 3, 76–91 and 126–136 cm, Section 4, 90–120, 109–111, and 136–150 cm, and CC, 3–5 cm; light olive-brown (2.5Y 5/4) and light olive-gray (5Y 6/1) to very dark gray (5Y 5/4), semi-indurated, thicker layers normally graded, layer in CC broken up and disturbed.
- d)Mn(?)-rich nannofossil mud, Section 1, 78 cm, Section 2, 68 cm, and Section 6, 13 cm, very dark gray (5Y 3/1).
- e)Sapropels, Section 1, 103–109 cm, and Section 2, 71–75 cm, olive (5Y 5/3) to dark olive-gray (5Y 3/2).

SMEAR SLIDE SUMMARY (%):

	1, 40 M	1, 78 M	2, 67.5 M	2, 117 M	3, 30 M	3, 86 M	3, 136 M
TEXTURE:							
Sand	5	5	10	30	5	15	40
Silt	20	15	30	40	15	70	40
Clay	75	80	60	30	80	15	20
COMPOSITION:							
Quartz	1	1	2	5	3	12	4
Feldspar	—	—	—	2	1	3	2
Mica	—	1	—	—	2	4	3
Clay	18	66	12	24	49	—	35
Volcanic glass	10	10	15	60	3	60	44
Calcite	—	—	4	—	—	2	3
Accessory minerals	—	2	—	2	—	—	2
Pyrite	2	—	—	—	—	—	—
Opaques	—	—	—	—	—	2	—
Micrite	—	1	—	3	2	—	2
Pyroxene	—	—	—	—	—	—	2
Foraminifers	—	5	15	3	12	15	1
Nannofossils	27	15	30	1	28	Tr	2
Sponge spicules	—	—	1	—	—	—	—
Silicoflagellates	—	—	1	—	—	—	—
Organics	40	—	20	—	—	—	—
Spar cement	2	—	—	—	—	—	—
Intraclasts	—	—	—	—	—	2	—

	4, 30 M	4, 101 M	4, 150 M	CC, 2 M
TEXTURE:				
Sand	—	20	40	20
Silt	—	30	20	20
Clay	—	50	40	60
COMPOSITION:				
Quartz	2	4	15	2
Feldspar	—	1	5	1
Mica	—	3	8	3
Clay	60	24	11	21
Volcanic glass	—	60	42	50
Calcite	4	—	4	2
Dolomite	—	1	—	1
Accessory minerals	1	3	3	—
Pyroxene	—	—	—	2
Micrite	—	1	—	1
Foraminifers	2	2	2	2
Nannofossils	31	1	10	14
Pteropod	—	—	—	1

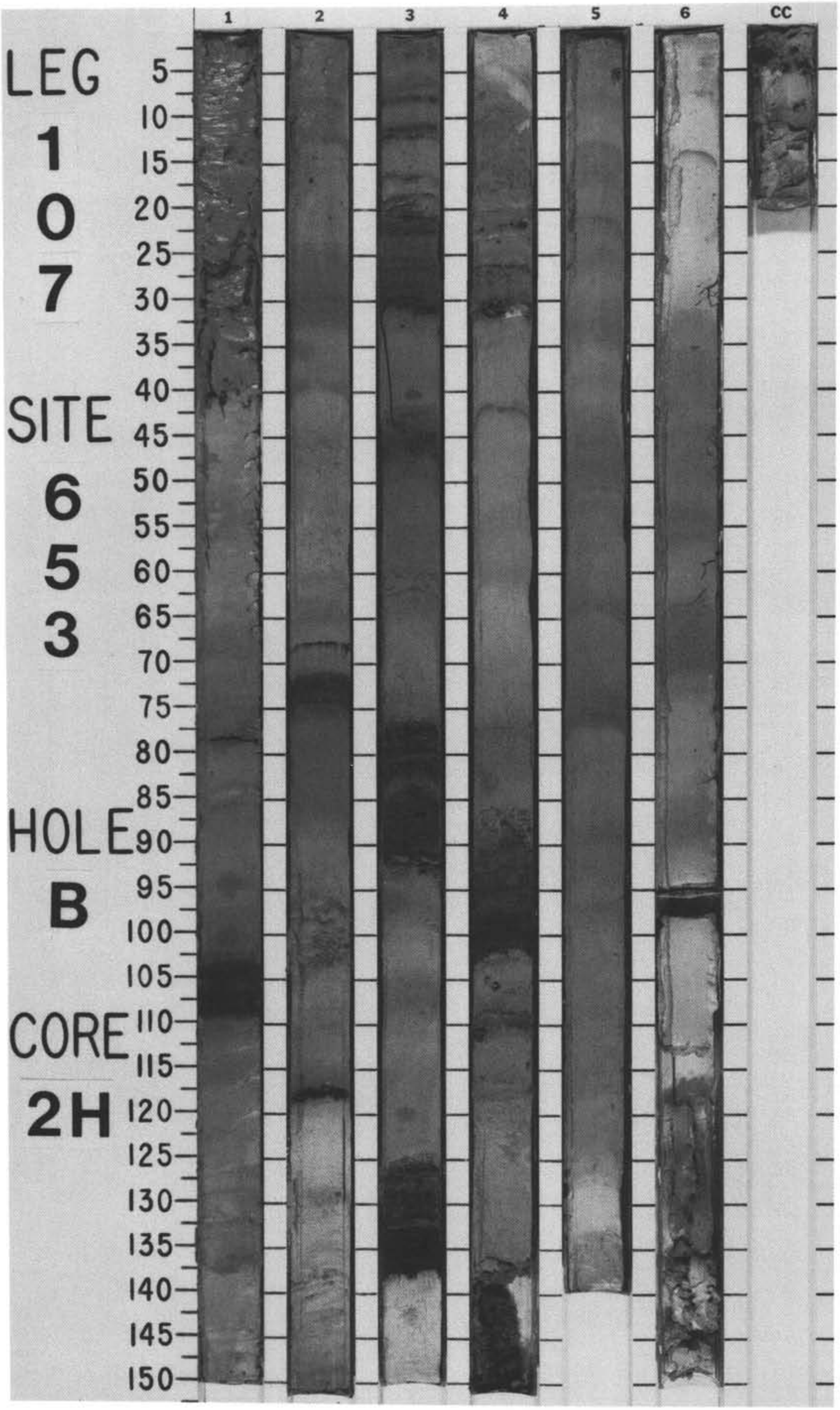
LEG
1
0
7
SITE
6
5
3
HOLE
B
CORE
2H
1
2
3
4
5
6
CC
5
10
15
20
25
30
35
40
45
50
55
60
65
70
75
80
85
90
95
100
105
110
115
120
125
130
135
140
145
150

SITE 653 HOLE B CORE 3H CORED INTERVAL 2838.5-2848.0 mbsl; 17.6-27.1 mbsf

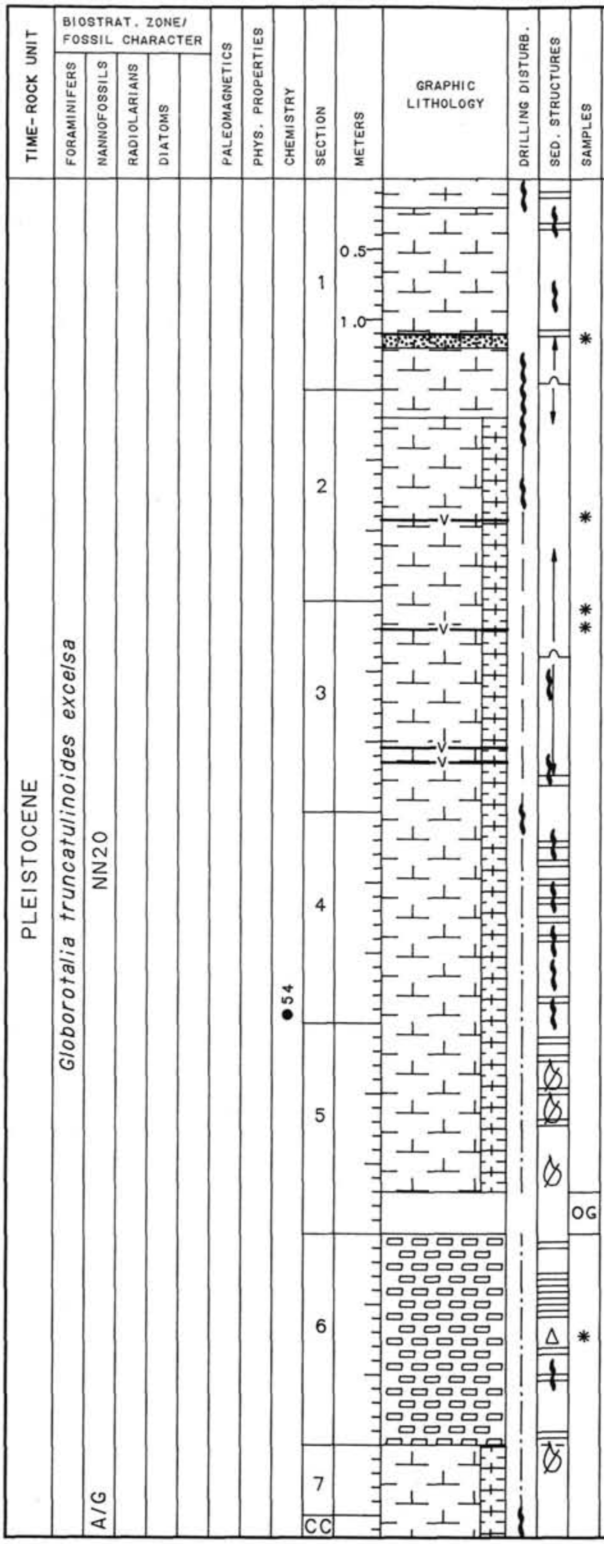

LITHOLOGIC DESCRIPTION

MARLY NANNOFOSSIL OOZE and intercalated SANDY/SILTY AND VOLCANIC GLASS-BEARING LAYERS

Marly nannofossil ooze, whte (2.5Y N8 or 5Y 8/2) to light yellowish brown (2.5Y 6/4) and pale olive (5Y 6/4). Pteropod shell fragments in Sections 5 and 7. In Section 1, 120 cm, to Section 2, 20 cm, mud-debris flow or slump containing balls of nannofossil ooze with different colors.

Minor lithologies:
a)Foraminifer-enriched, discrete layers; foraminifer sand in Section 1, 110–120 cm.
b)Mn(?)-rich volcanic glass-bearing black layer in Section 2, 91–92 cm.
c)Silt, Sections 4, 5, and 6; occurrence in numerous thin layers.
d)Sand, Section 6; occurrence in a thin layer, disrupted by coring disturbance. Similar layers in Section 3, 21, 102, and 115 cm, are probably repetitions due to slumping.

SMEAR SLIDE SUMMARY (%):

	1, 116	2, 90	3, 6	3, 22	3, 26	3, 102
	M	M	M	D	M	M
TEXTURE:						
Sand	5	50	5	10	80	10
Silt	25	30	15	50	15	30
Clay	70	20	80	40	5	60
COMPOSITION:						
Quartz	10	2	4	1	70	5
Feldspar	2	2	1	—	10	—
Mica	1	2	—	2	5	2
Clay	—	32	64	—	—	—
Volcanic glass	5	15	4	25	—	12
Calcite	—	2	2	—	1	—
Dolomite	5	—	—	2	—	2
Accessory minerals	—	—	—	5	1	3
Pyroxene	1	5	Tr	—	3	1
Opaques	—	32	—	—	—	—
Analcime	—	Tr	Tr	20	—	10
Foraminifers	15	2	5	10	4	12
Nannofossils	70	4	20	34	—	53
Diatoms	1	—	—	1	—	—
Bioclasts	—	2	—	—	2	—
Intraclasts	—	—	—	—	4	—

	6, 76	7, 12
	D	M
TEXTURE:		
Sand	5	10
Silt	15	40
Clay	80	50
COMPOSITION:		
Quartz	—	15
Mica	—	5
Clay	65	—
Volcanic glass	2	5
Dolomite	—	5
Cement	2	—
Accessory minerals		
Pyroxene	—	2
Opaques	—	10
Analcime	—	10
Foraminifers	5	5
Nannofossils	25	48
Sponge spicules	1	—

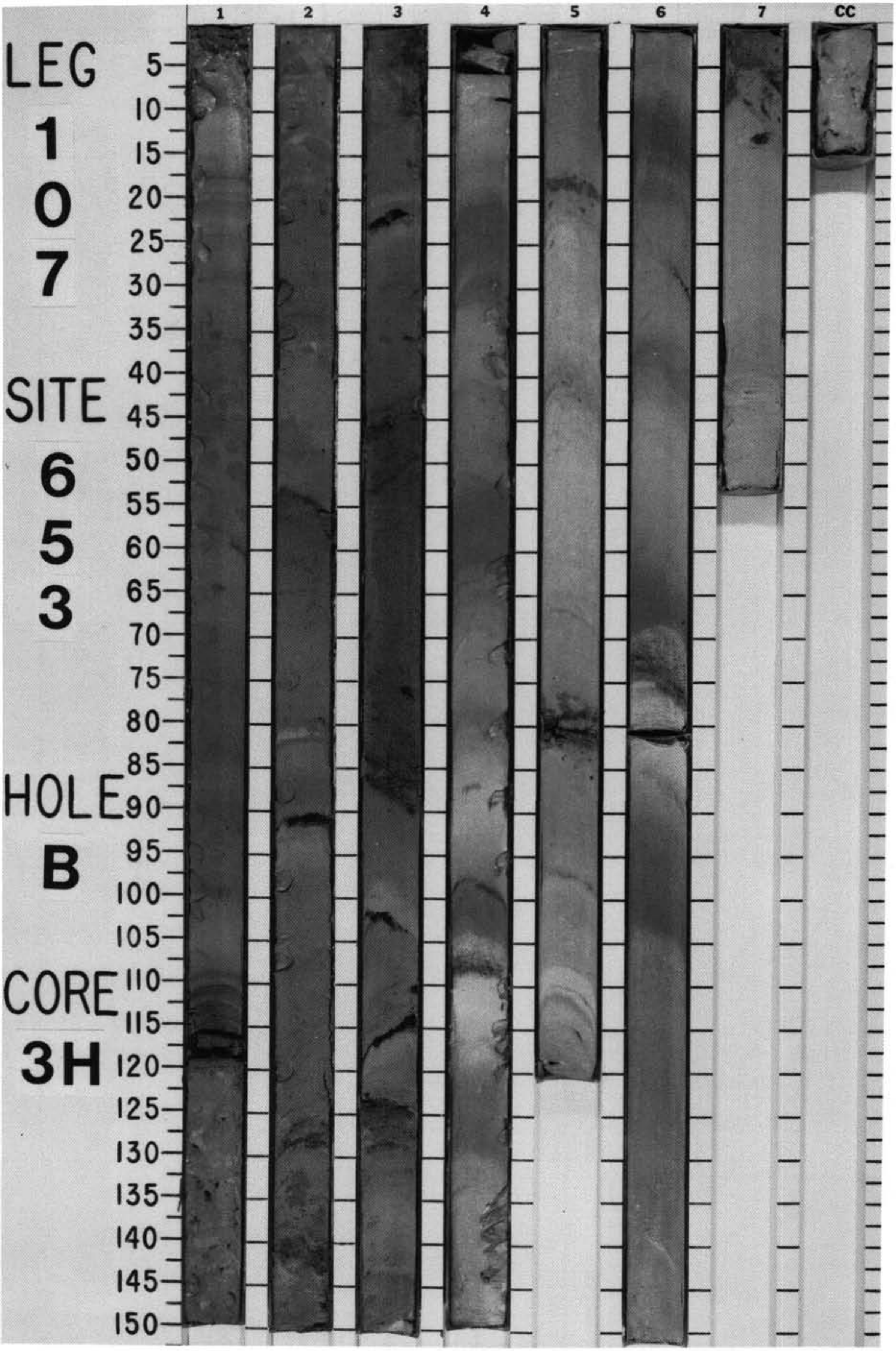
LEG
107
SITE
653
HOLE
B
CORE
3H
1
2
3
4
5
6
7
CC
5
10
15
20
25
30
35
40
45
50
55
60
65
70
75
80
85
90
95
100
105
110
115
120
125
130
135
140
145
150

SITE 653 HOLE B CORE 4H CORED INTERVAL 2848.0-2857.5 mbsl; 27.1-36.6 mbsf

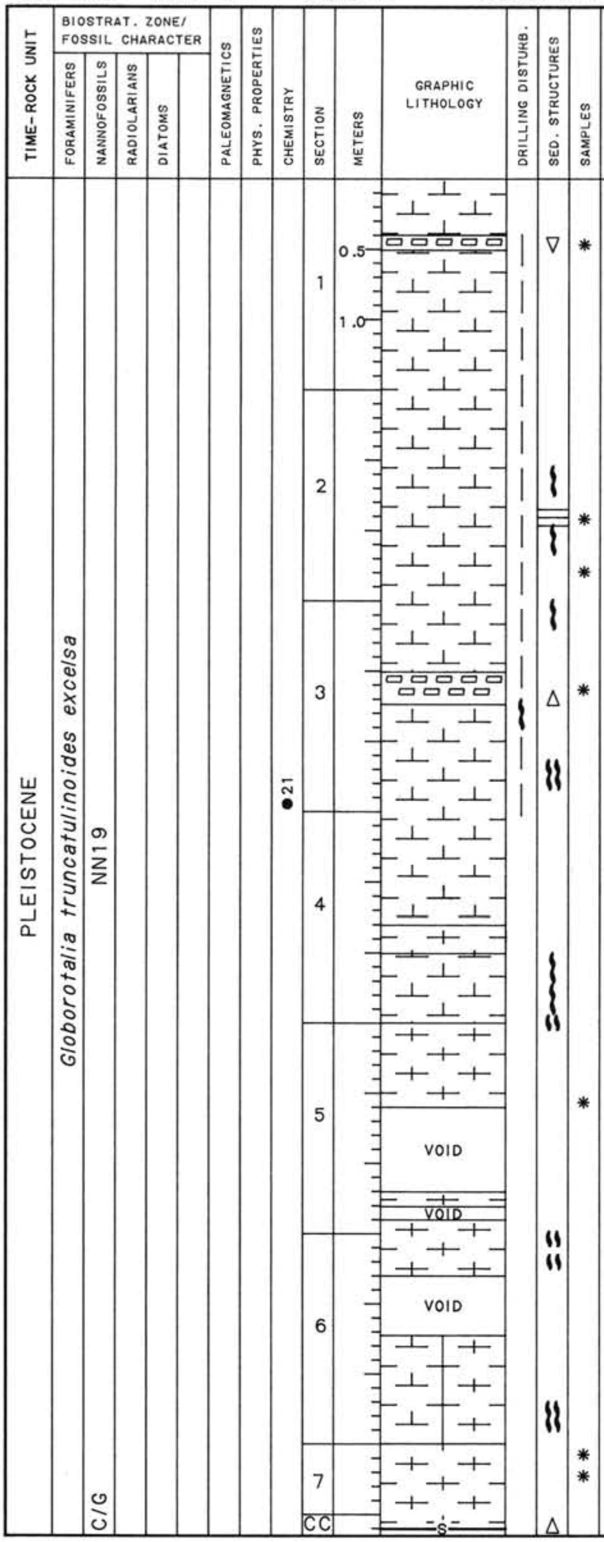

LITHOLOGIC DESCRIPTION

MARLY NANNOFOSSIL OOZE, with intercalations of CALCAREOUS OOZE and MINERAL-RICH LAYERS

Marly nannofossil ooze, varicolored in irregular laminae, including light gray, light olive-gray, gray, dark gray, pale olive, pinkish gray, white, and pale green intercalations of coarser grained intervals, some normally and reversely graded intervals. Numerous scattered biotic flakes.

Minor lithologies:

a)Gypsum- and quartz-sand-bearing calcareous ooze, Section 1, 40–50 cm, gray (5Y 5/1), reverse-graded, large mica flakes.

b)Mineral-rich(?) layers, Section 1, 135 and 144–145 cm, Section 2, 115 and 130 cm, and Section 4, 12 and 45 cm, black (5Y 2.5/1) and dark gray (5Y 4/1).

c)Sapropel, CC, 10–12 cm.

SMEAR SLIDE SUMMARY (%):

	1, 44 M	2, 98 D	2, 131 M	3, 68 M	5, 60 M	7, 6 M	7, 21 M
TEXTURE:							
Sand	40	15	60	30	20	10	50
Silt	25	15	20	20	20	20	20
Clay	35	70	20	50	60	70	30
COMPOSITION:							
Quartz	7	10	10	15	12	10	15
Feldspar	—	Tr	—	—	—	—	—
Mica	2	2	2	1	2	1	1
Clay	22	6	4	18	18	18	6
Volcanic glass	—	4	4	3	2	2	2
Calcite/dolomite	6	2	—	3	—	3	1
Accessory minerals	1	2	—	2	2	2	2
Gypsum	8	2	5	—	—	—	—
Opaques	4	—	—	—	—	—	—
Zeolites	2	Tr	2	Tr	2	1	1
Micrite	12	—	—	15	12	5	15
Dolomicrite	—	15	—	—	—	—	—
Opaques (Mn?)	—	—	40	—	—	—	—
Pyrite	—	1	—	—	—	—	—
Foraminifers	2	5	3	3	3	3	33
Nannofossils	34	50	30	40	45	55	20
Diatoms	—	Tr	Tr	—	—	Tr	Tr
Radiolarians	—	1	Tr	Tr	—	Tr	3
Sponge spicules	Tr	—	—	—	Tr	—	1
Silicoflagellates	—	—	—	—	—	—	Tr

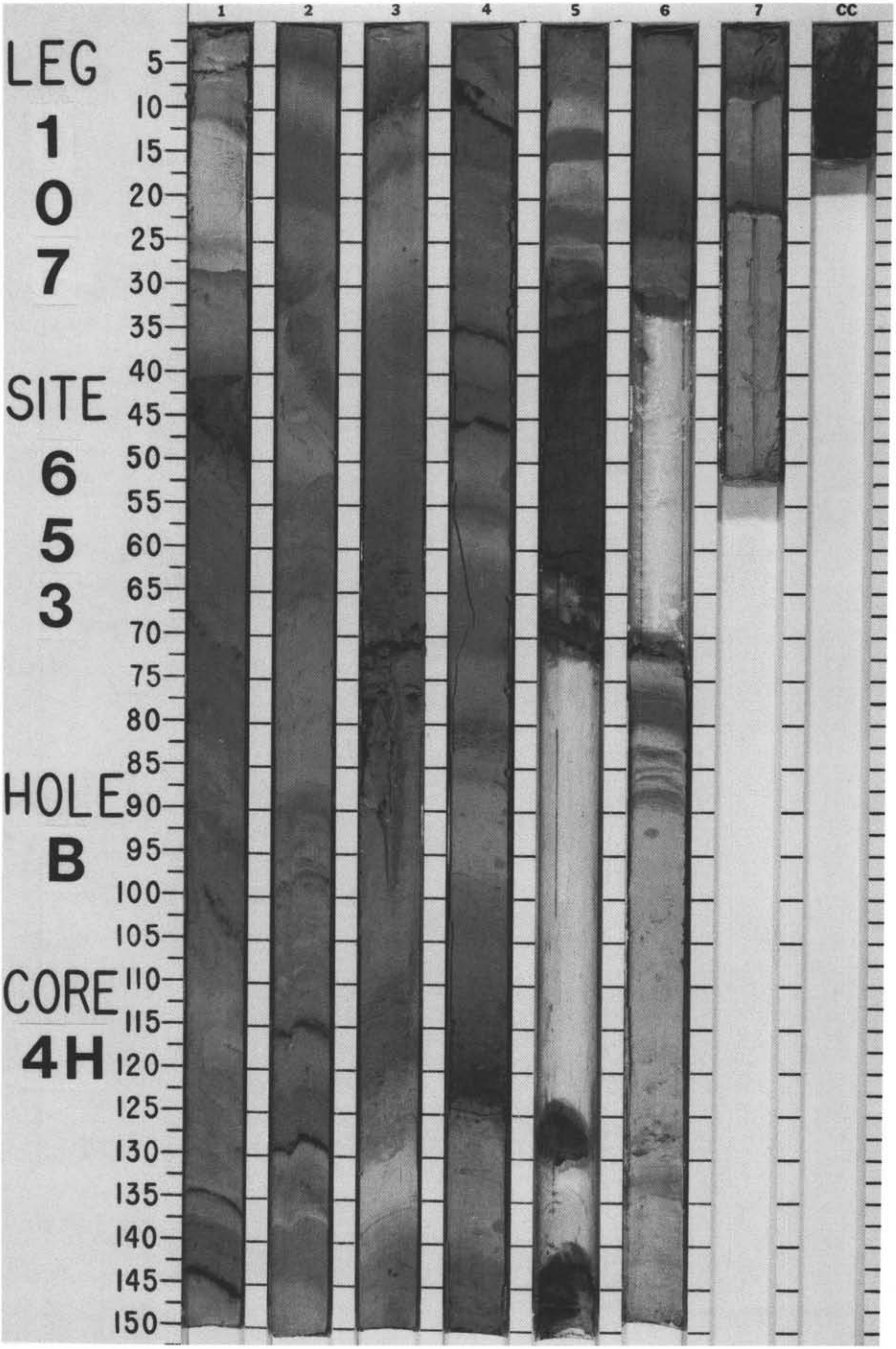
LEG
1
0
7
SITE
6
5
3
HOLE
B
CORE
4H
1
2
3
4
5
6
7
CC
5
10
15
20
25
30
35
40
45
50
55
60
65
70
75
80
85
90
95
100
105
110
115
120
125
130
135
140
145
150

SITE 653 HOLE B CORE 5H CORED INTERVAL 2857.5-2866.9 mbsl; 36.6-46.0 mbsf

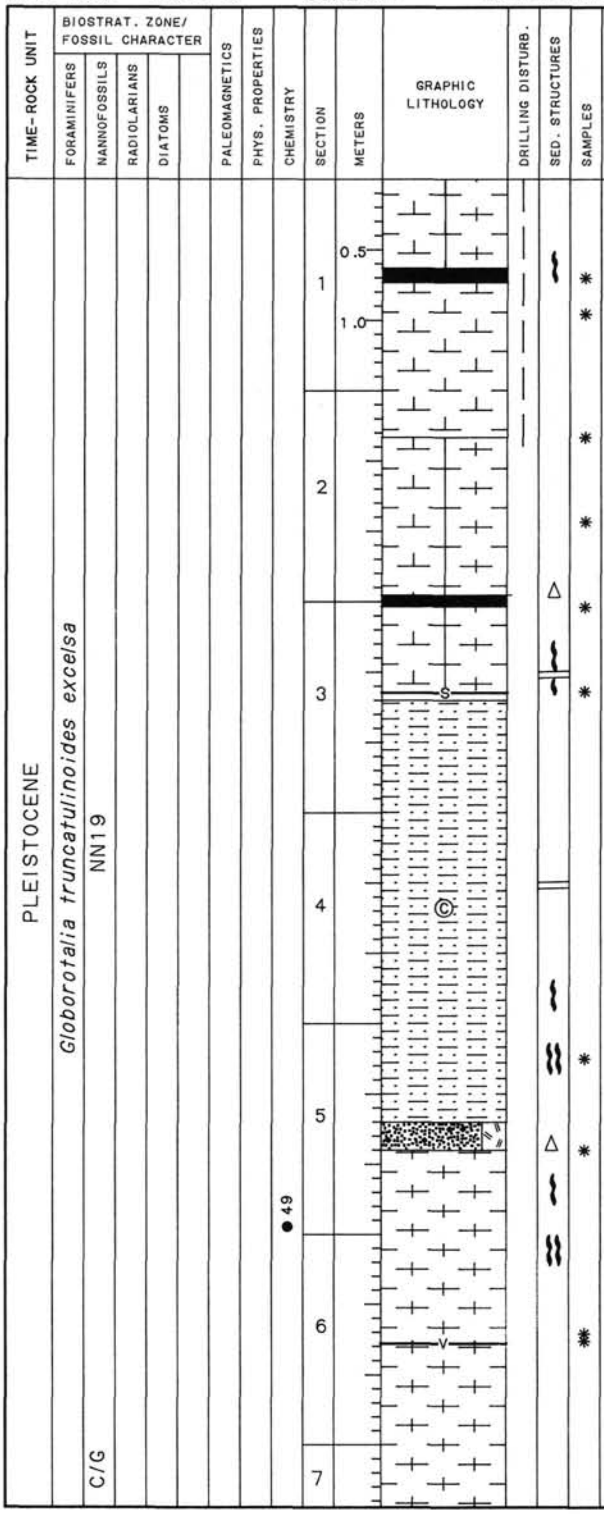

LITHOLOGIC DESCRIPTION

FORAMINIFER-NANNOFOSSIL OOZE, with intercalations of SANDY/SILTY LAYERS and SAPROPELS

Foraminifer-nannofossil ooze, varicolored in irregular streaks and halos, including white, light gray, light olive-gray, olive-gray, dark gray, pale olive, grayish brown, and dusky-green.

Minor lithologies:
a) Sapropels, Section 1, 65–75 cm, Section 2, 146–150 cm, and Section 3, 0–5 and 64–70 cm, dark grayish brown (2.5Y 4/2) to very dark grayish brown (2.5Y 3/2).
b) Mn(?)-rich layers, Section 2, 8 and 33 cm.
c) Sand-bearing nannofossil ooze/mud, Section 2, 95 cm, gray (5Y 5/1), reversely graded; Section 2, 140–146 cm, dark gray (2.5Y 4/1), normally graded.
d) Volcanic ash-bearing sandy silt, Section 5, 70–92 cm, light olive gray (5Y 6/2) to pale olive (5Y 6/3) toward base, normally graded, lithified at base; Section 6, 78–80 cm, light gray (10Y 7/1), normally graded(?), unlithified.

SMEAR SLIDE SUMMARY (%):

	1, 70 M	1, 100 M	2, 35 D	2, 94 M	3, 3 M	3, 67 M
TEXTURE:						
Sand	5	12	30	30	25	25
Silt	20	20	20	20	25	20
Clay	75	68	50	50	50	55
COMPOSITION:						
Quartz	6	10	5	20	10	10
Feldspar	1	—	—	—	—	1
Mica	1	Tr	1	1	1	1
Clay	6	13	25	15	17	40
Volcanic glass	2	3	3	4	3	5
Calcite/dolomite	2	3	5	5	10	10
Accessory minerals	2	—	3	2	3	2
Pyrite	1	—	—	—	—	1
Zeolites	1	3	20	1	—	—
Aragonite needles	Tr	—	—	—	1	—
Micrite	5	3	5	15	10	5
Opaques (amorph.)	—	—	—	—	—	1
Gypsum	—	—	2	—	—	2
Foraminifers	5	5	1	7	5	10
Nannofossils	64	60	30	25	35	10
Diatoms	—	—	—	—	1	—
Radiolarians	2	Tr	Tr	5	2	2
Sponge spicules	—	—	Tr	—	Tr	Tr
Silicoflagellates	1	—	—	—	2	—

	5, 28 M	5, 92 M	6, 77 M	6, 79 M
TEXTURE:				
Sand	35	35	35	25
Silt	20	25	25	20
Clay	45	40	40	55
COMPOSITION:				
Quartz	15	22	20	20
Feldspar	—	—	2	—
Mica	1	—	2	3
Clay	32	49	28	40
Volcanic glass	2	—	Tr	—
Calcite/dolomite	3	1	2	5
Accessory minerals	—	1	1	2
Pyrite	2	1	1	—
Gypsum	—	1	1	—
Opaques (amorph.)	—	—	1	1
Micrite	15	10	20	10
Foraminifers	15	5	20	4
Nannofossils	12	8	—	15
Radiolarians	3	2	2	Tr
Sponge spicules	—	Tr	—	—

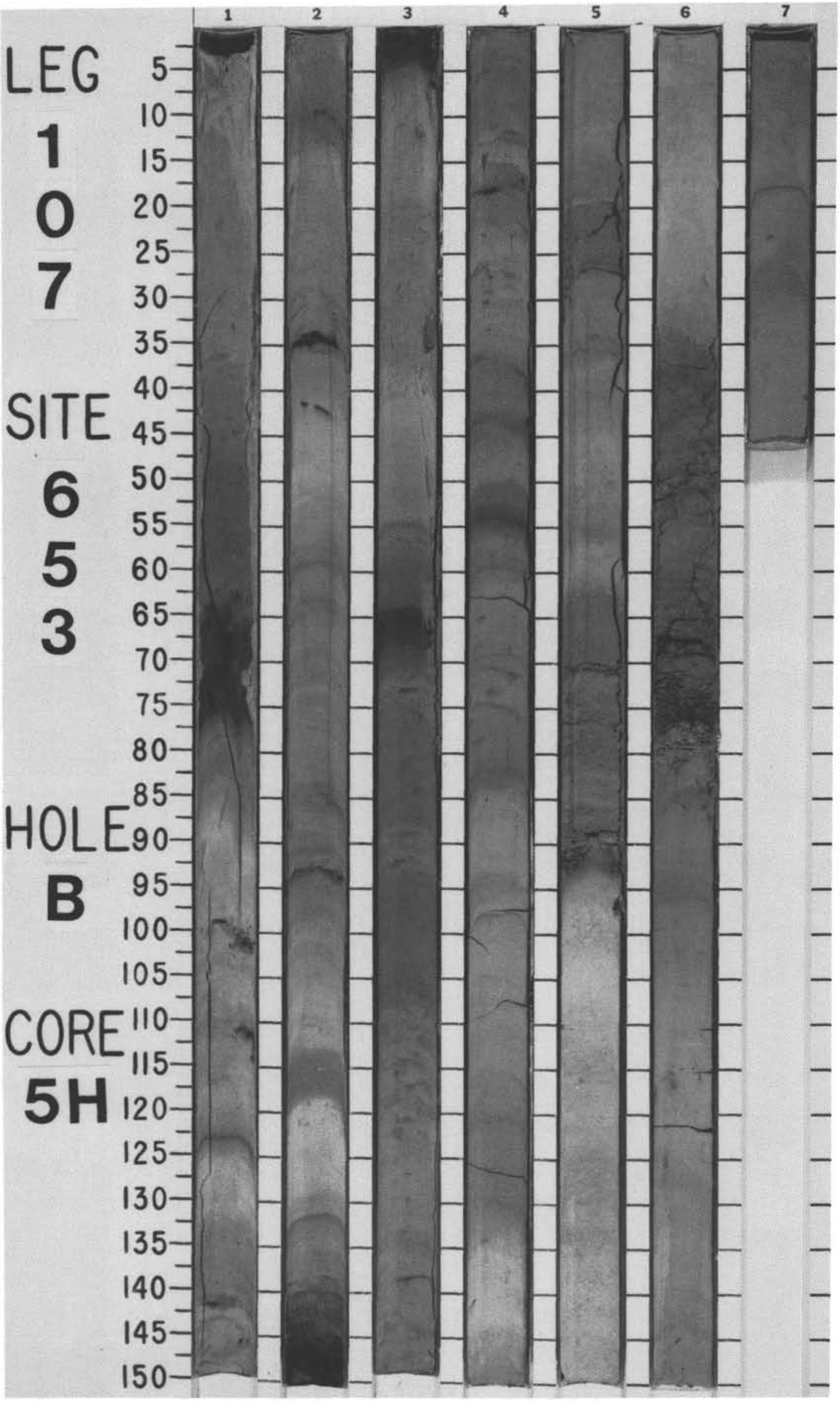
LEG
1
0
7
SITE
6
5
3
HOLE
B
CORE
5H
1
2
3
4
5
6
7
5
10
15
20
25
30
35
40
45
50
55
60
65
70
75
80
85
90
95
100
105
110
115
120
125
130
135
140
145
150

SITE 653 HOLE B CORE 6H CORED INTERVAL 2866.9-2876.3 mbsl; 46.0-55.4 mbsf

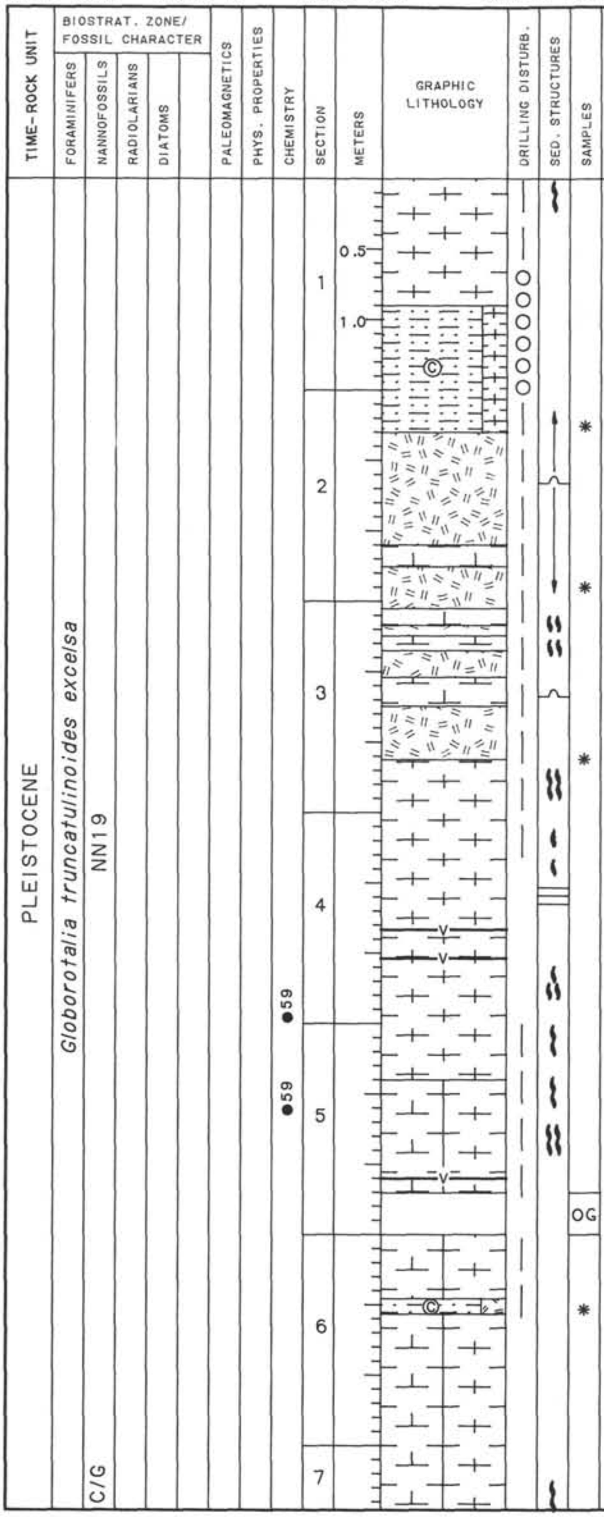

LITHOLOGIC DESCRIPTION

MARLY FORAMINIFER-NANNOFOSSIL OOZE with intercalated ASH LAYERS

Foraminifer-nannofossil ooze, varicolored, including white, light gray, light olive-gray, olive-gray, gray, light brownish gray, pale yellow, and pale green, some silty/sandy foraminifer-rich layers.

Minor lithology: volcaniclastic glass-rich layers with welded pumice at the base, Section 2, 30–110 cm; Section 2, 125 cm, to Section 3, 7 cm; Section 3, 18–25, 34–55, and 79–114 cm; Section 4, 86 and 103–111 cm; Section 5, 110 cm; and Section 6, 45–56 cm; light olive-gray (5Y 6/2) and gray (5Y 6/1). Section 2, 30–110 cm, is highly deformed.

SMEAR SLIDE SUMMARY (%):

	2, 26 M	2, 140 M	3, 113 M	6, 54 M
TEXTURE:				
Sand	5	35	30	5
Silt	15	20	20	20
Clay	80	45	50	75
COMPOSITION:				
Quartz	10	10	15	8
Mica	Tr	Tr	1	—
Clay	21	32	16	36
Volcanic glass	—	20	4	20
Calcite/dolomite	3	2	5	15
Accessory minerals	—	1	2	1
Zeolites	—	1	—	—
Gypsum	—	1	2	—
Micrite	40	5	15	5
Foraminifers	4	1	15	Tr
Nannofossils	20	25	25	15
Radiolarians	2	2	—	—

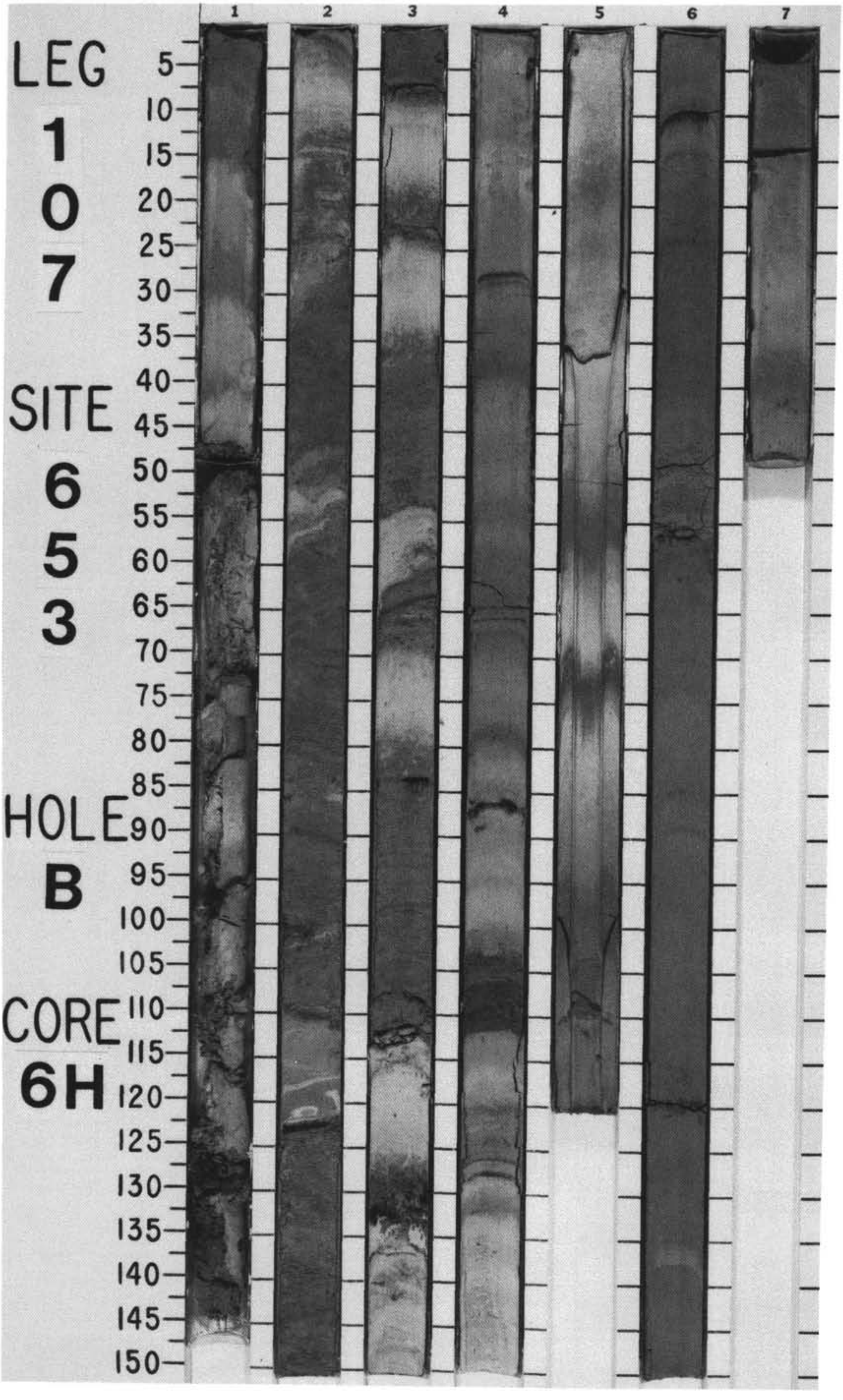
LEG
107
SITE
653
HOLE
B
CORE
6H
1
2
3
4
5
6
7
5
10
15
20
25
30
35
40
45
50
55
60
65
70
75
80
85
90
95
100
105
110
115
120
125
130
135
140
145
150

SITE 653 HOLE B CORE 7H CORED INTERVAL 2876.3-2885.8 mbsl; 55.4-64.9 mbsf

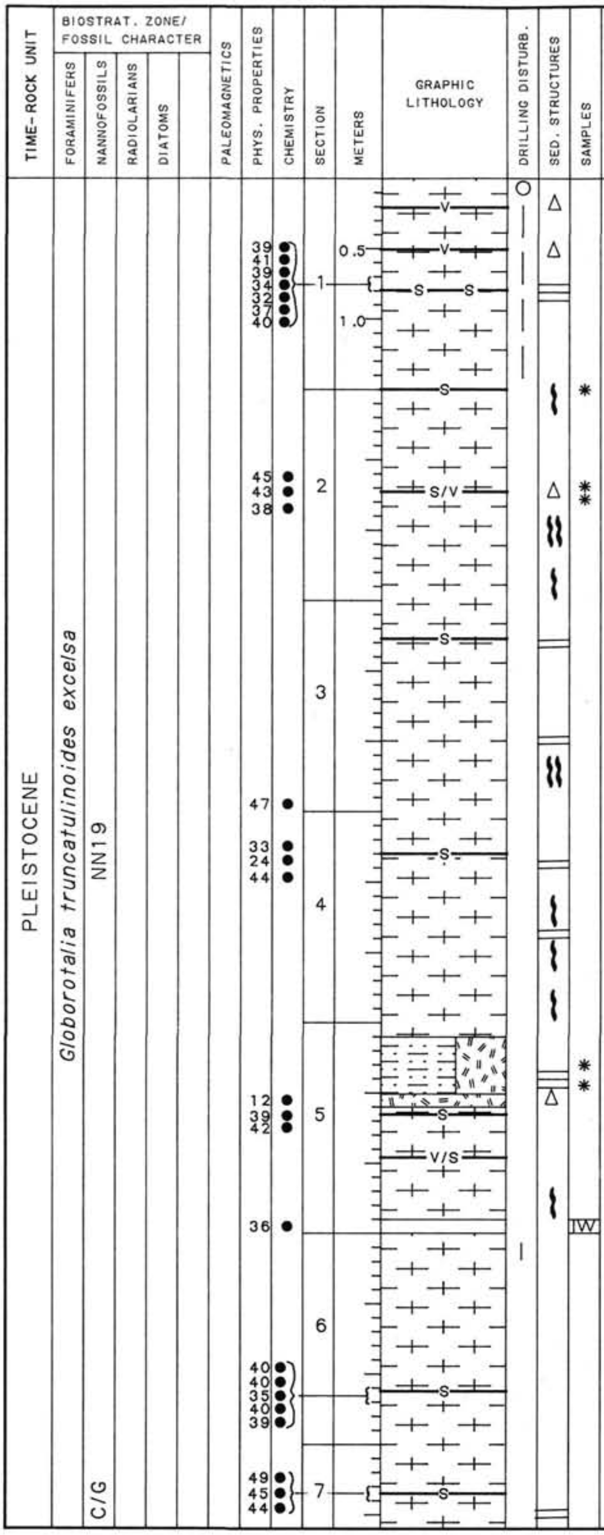

LITHOLOGIC DESCRIPTION

MARLY FORAMINIFER-NANNOFOSSIL OOZE, ASH LAYERS, and SAPROPELS

Marly foraminifer-nannofossil ooze, varicolored, including including white, light gray, dark gray, olive-gray, gray, dark gray, light brownish gray, grayish brown, pale yellow, and dusky yellow-green; foraminifera-enriched in clusters.

Minor lithologies:

a)Ash layers. Section 1, 17–20 cm: gray (5Y 6/1); Section 1, 51–55 cm: light olive-gray (5Y 6/2); Section 2, 76–80 cm: dark gray (5Y 4/1); Section 5, 50–60 cm: olive-gray (5Y 5/2); and Section 5, 90–96 cm: light brownish gray (2.5Y 6/2).

b)Sapropels. Section 1, 73–77 cm, Section 5, 60–70 cm, Section 6, 113–116 cm, and Section 7, 35–40 cm: dark olive-gray (5Y 3/2); Section 1, 148–150 cm, Section 2, 0–4 and 69–76 cm, Section 3, 26–32 cm: olive (5Y 4/3); Section 4, 26–32 cm: very dark grayish brown (2.5Y 3/2); and Section 5, 97–99 cm: very dark gray (5Y 3/1).

SMEAR SLIDE SUMMARY (%):

	1, 149 M	2, 73 M	2, 79 M	5, 33 M	5, 48 M
TEXTURE:					
Sand	35	5	25	50	10
Silt	10	15	20	25	20
Clay	55	80	55	25	70
COMPOSITION:					
Quartz	5	4	20	20	5
Feldspar	—	—	—	1	—
Mica	1	1	—	3	Tr
Clay	10	40	49	13	50
Volcanic glass	4	3	—	50	2
Calcite/dolomite	5	5	8	3	15
Accessory minerals	1	1	2	1	1
Opaques, amorphous Mn(?)	30	—	—	—	—
Pyrite	—	2	2	1	—
Micrite	15	10	10	5	10
Gypsum	—	—	1	1	—
Foraminifers	7	4	—	2	2
Nannofossils	20	20	5	—	15
Diatoms	—	1	—	—	—
Radiolarians	2	4	—	—	Tr
Sponge spicules	—	Tr	—	—	—
Silicoflagellates	—	1	—	—	—
Organic matter	—	3	3	—	—
Pollens	—	1	—	—	—

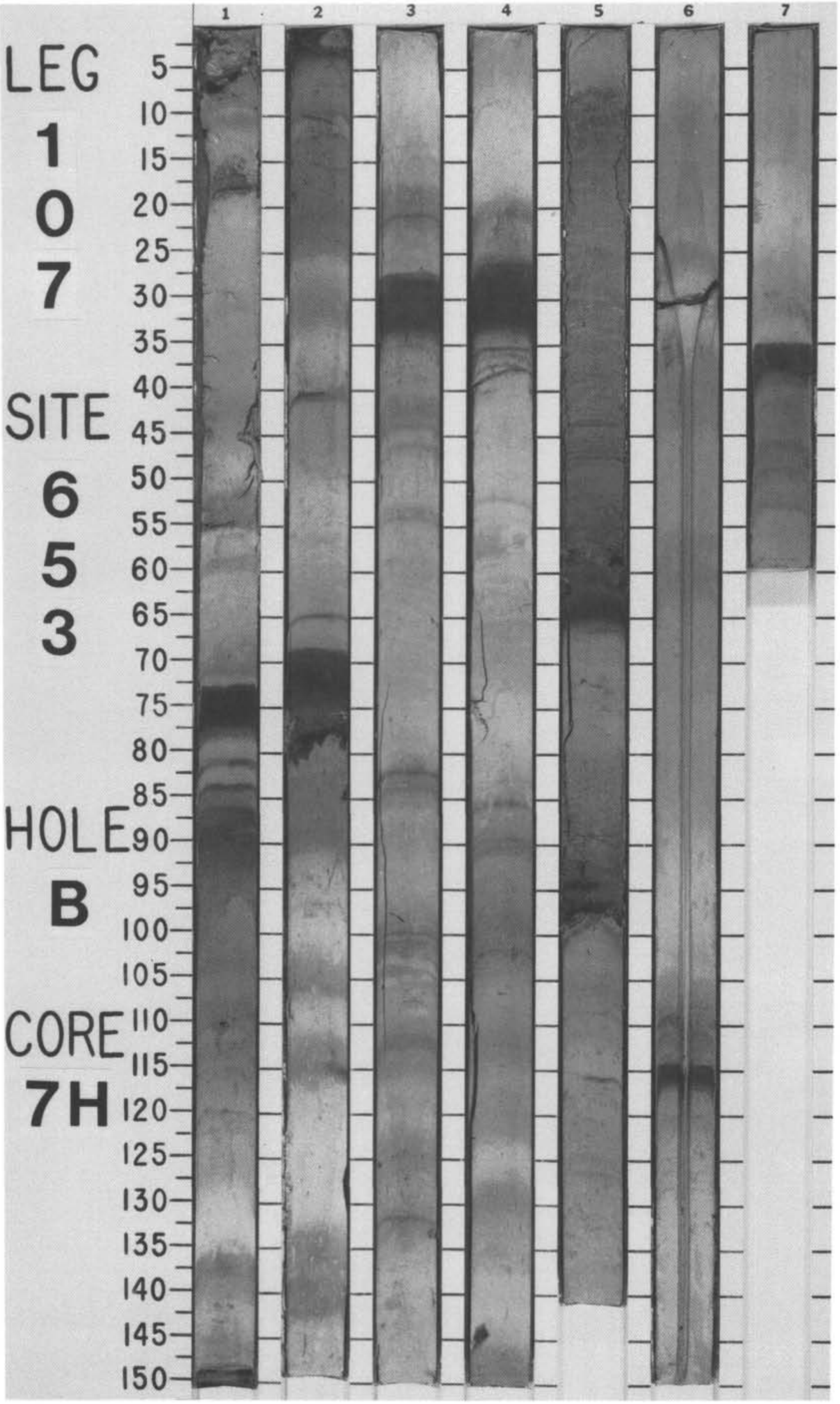
LEG
1
0
7
SITE
6
5
3
HOLE
B
CORE
7H
1
2
3
4
5
6
7
5
10
15
20
25
30
35
40
45
50
55
60
65
70
75
80
85
90
95
100
105
110
115
120
125
130
135
140
145
150

SITE 653 HOLE B CORE 8H CORED INTERVAL 2885.8-2895.3 mbsl; 64.9-74.4 mbsf

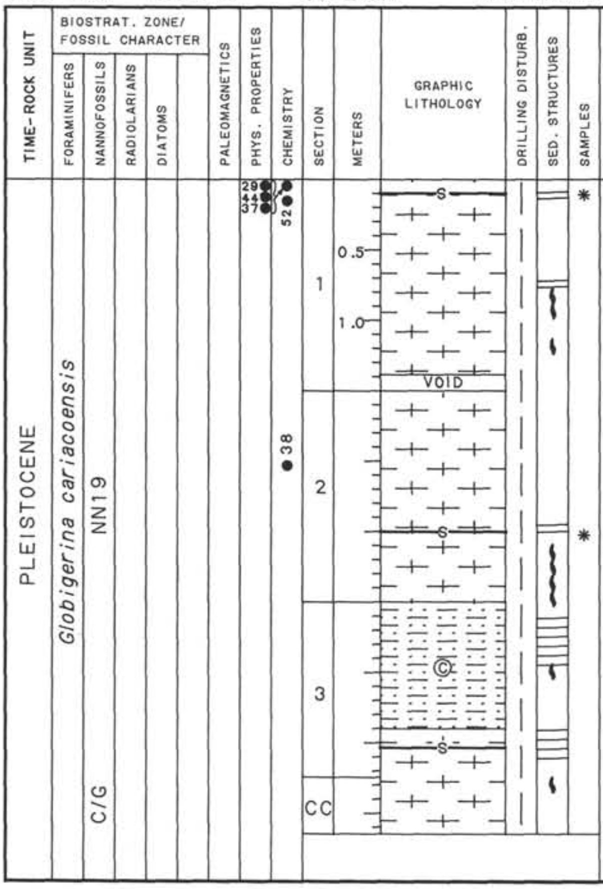

LITHOLOGIC DESCRIPTION

FORAMINIFER-NANNOFOSSIL OOZE with intercalated SAPROPELS

Foraminifer-nannofossil ooze, varicolored, including light gray, olive-gray, gray, dark gray, brownish gray, grayish brown, and pale green; some levels enriched in foraminifers.

Minor lithology: Sapropels, Section 1, 7–14 cm, and Section 3, 99–107 cm, dark olive-gray (5Y 3/2); Section 2, 103–105 cm, dark grayish brown (2.5Y 4/2).

SMEAR SLIDE SUMMARY (%):

	1, 12 M	2, 102 M
TEXTURE:		
Sand	25	30
Silt	15	15
Clay	60	55
COMPOSITION:		
Quartz	2	6
Mica	Tr	—
Clay	15	8
Volcanic glass	—	2
Calcite/dolomite	5	5
Accessory minerals	1	1
Pyrite (hydrotroilite)	2	2
Foraminifers	12	20
Nannofossils	50	45
Diatoms	—	Tr
Radiolarians	6	5
Sponge spicules	Tr	1
Plant debris	1	—
Organic matter	6	5

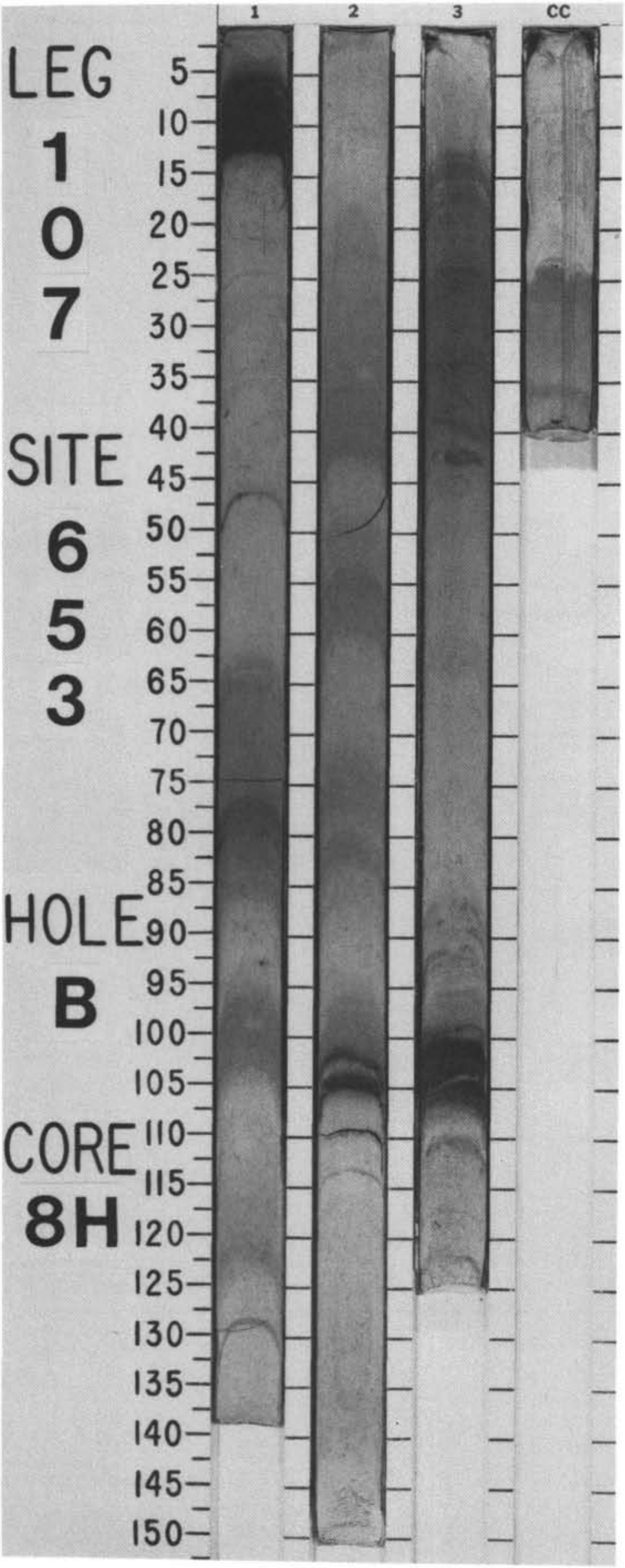
LEG
1
0
7
SITE
6
5
3
HOLE
B
CORE
8H
1
2
3
CC
5
10
15
20
25
30
35
40
45
50
55
60
65
70
75
80
85
90
95
100
105
110
115
120
125
130
135
140
145
150

SITE 653 HOLE B CORE 9X CORED INTERVAL 2895.3-2904.9 mbsl; 74.4-84.0 mbsf

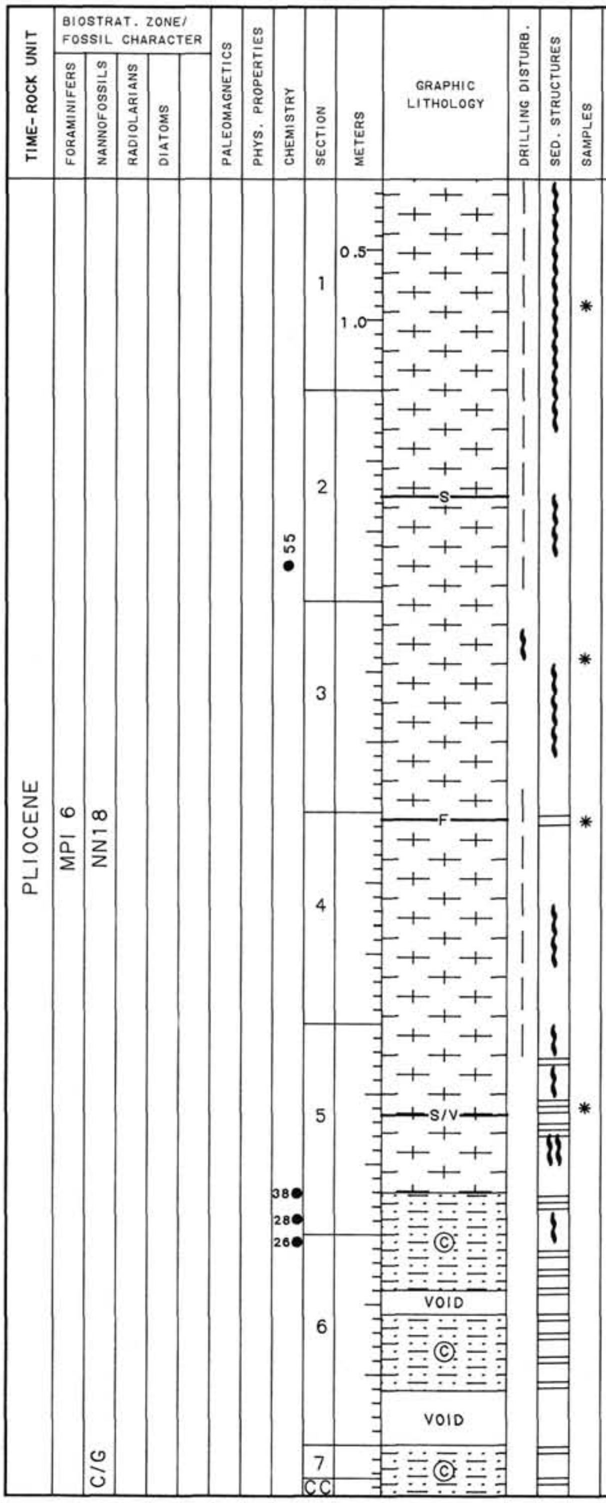

LITHOLOGIC DESCRIPTION

MARLY FORAMINIFER-NANNOFOSSIL OOZE

Marly foraminifer-nannofossil ooze, white (2.5Y 8/2) to olive-yellow (2.5Y 6/6) and pale yellow (5Y 7/3) to dark olive-gray (5Y3/2).

Minor lithologies:
- a)Sapropel layers, Section 2, 70–77 cm.
- b)Foraminifer sand, Section 4, 2–8 cm, white (2.5Y N8/).
- c)Volcanic ash, Section 5, 60–69 cm, dark olive-gray, (5Y 3/2). (Intercalation of an ash layer at 64 cm.)

SMEAR SLIDE SUMMARY (%):

	1, 90 D	3, 38 M	4, 3 M	5, 65 M
TEXTURE:				
Sand	—	—	70	15
Silt	10	15	20	50
Clay	90	85	10	35
COMPOSITION:				
Quartz	2	—	4	18
Feldspar	—	—	1	8
Mica	—	Tr	1	6
Clay	30	—	28	20
Volcanic glass	1	1	4	40
Calcite	1	—	—	—
Dolomite	—	5	—	—
Accessory minerals	1	2	2	—
Zeolites	Tr	1	—	—
Gypsum	—	—	3	—
Siderite(?)	—	2	—	—
Pyroxene	—	—	—	1
Opaques	—	—	—	2
Foraminifers	15	15	40	—
Nannofossils	50	66	20	3
Diatoms	—	5	—	2

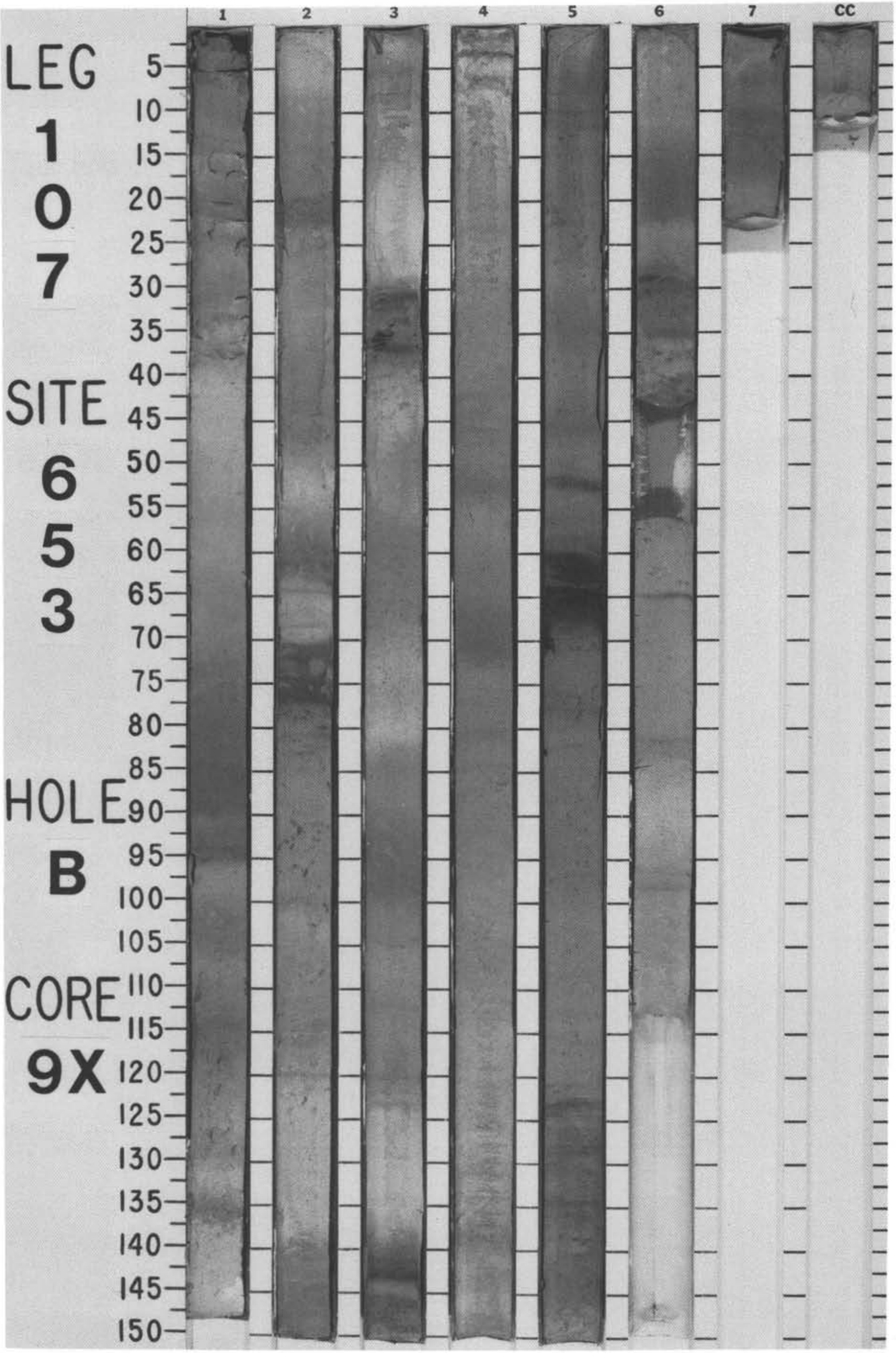
LEG
107
SITE
653
HOLE
B
CORE
9X
1
2
3
4
5
6
7
CC
5
10
15
20
25
30
35
40
45
50
55
60
65
70
75
80
85
90
95
100
105
110
115
120
125
130
135
140
145
150

SITE 653 HOLE B CORE 10X CORED INTERVAL 2904.9-2914.3 mbsl; 84.0-93.4 mbsf

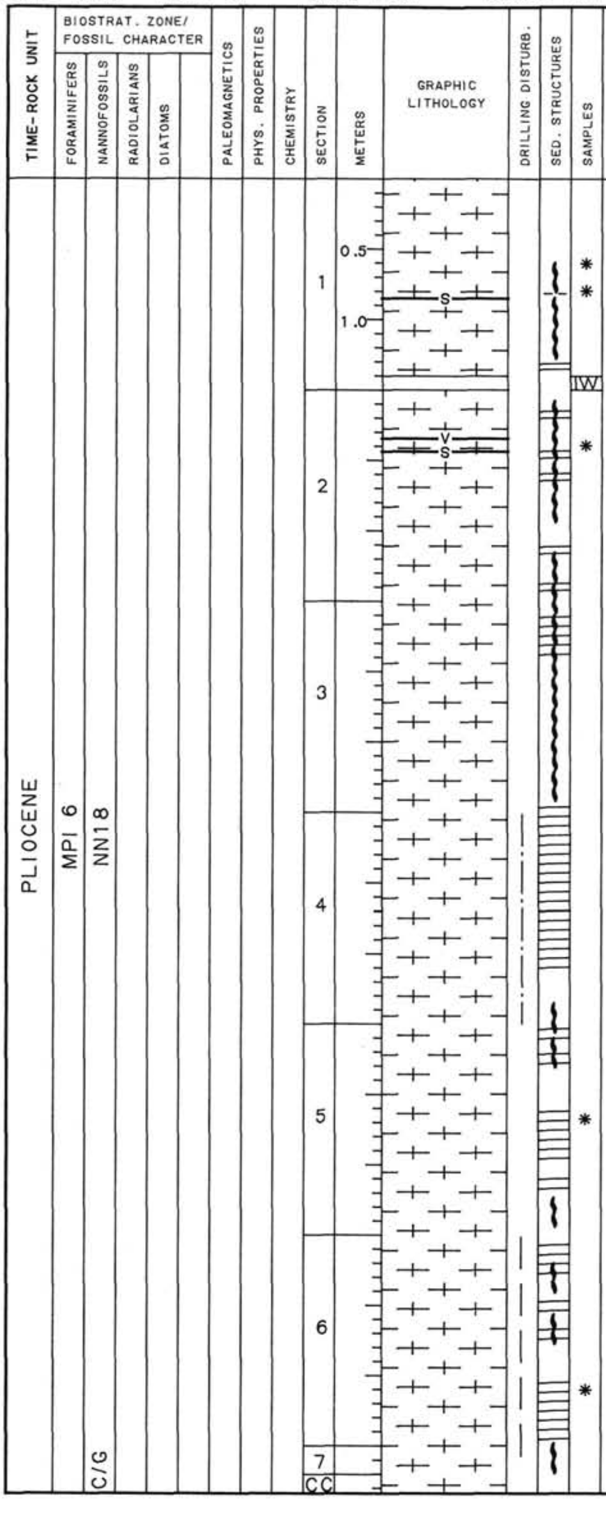

LITHOLOGIC DESCRIPTION

FORAMINIFER-NANNOFOSSIL OOZE

Foraminifer-nannofossil ooze, light gray (2.5Y 7/2) to grayish brown (2.5Y 5/2), white (5Y 8/1) to olive (5Y 5/4) and dark gray (5Y 41); color changes are gradational and diffuse; burrowing throughout which is particularly observed due to dark gray halos around four areas within burrows accentuated by iron sulfides. Numerous diagenetic laminae.

Minor lithologies:
a)Sapropel-layers, Section 1, 85–87 cm, and Section 2, 42- -46 cm, very dark gray (5Y 3/1).
b)volcanic ash, Section 2, 38–40 cm, black (5Y 2.5/1), slightly burrowed.

SMEAR SLIDE SUMMARY (%):

	1, 60 D	1, 84 M	2, 40 M	5, 70 D	6, 116 M
TEXTURE:					
Sand	5	—	5	2	60
Silt	15	5	70	22	10
Clay	80	95	25	76	30
COMPOSITION:					
Quartz	2	5	6	1	8
Feldspar	—	—	3	3	2
Mica	—	—	2	1	1
Clay	47	—	24	33	8
Volcanic glass	—	2	55	Tr	Tr
Calcite	1	—	—	—	—
Dolomite	1	8	1	—	—
Accessory minerals	1	—	—	—	Tr
Opaques	—	8	—	—	—
Gypsum	—	3	—	—	—
Pyrite spheres	—	8	—	—	—
Pyrite	—	—	3	—	—
Analcime	—	—	4	—	—
Micrite	—	—	—	—	1
Foraminifers	8	—	—	3	50
Nannofossils	38	65	Tr	55	30
Flagellates	—	1	—	3	—
Fish remains	—	—	—	1	—
Bioclasts	2	—	—	—	—

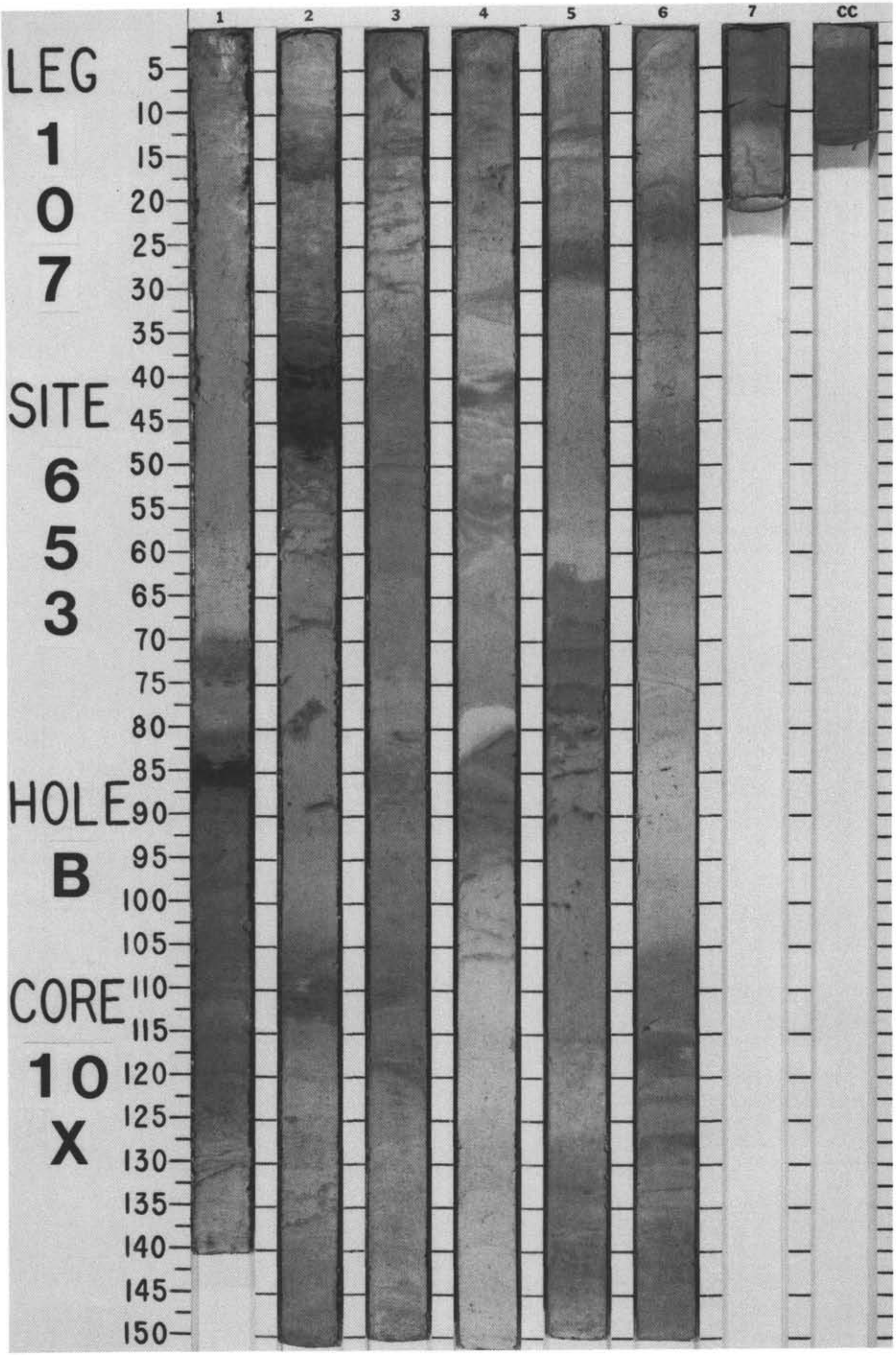
LEG
107
SITE
653
HOLE
B
CORE
10
X
1
2
3
4
5
6
7
CC
5
10
15
20
25
30
35
40
45
50
55
60
65
70
75
80
85
90
95
100
105
110
115
120
125
130
135
140
145
150

SITE 653 HOLE B CORE 11X CORED INTERVAL 2914.3-2923.5 mbsl; 93.4-102.6 mbsf

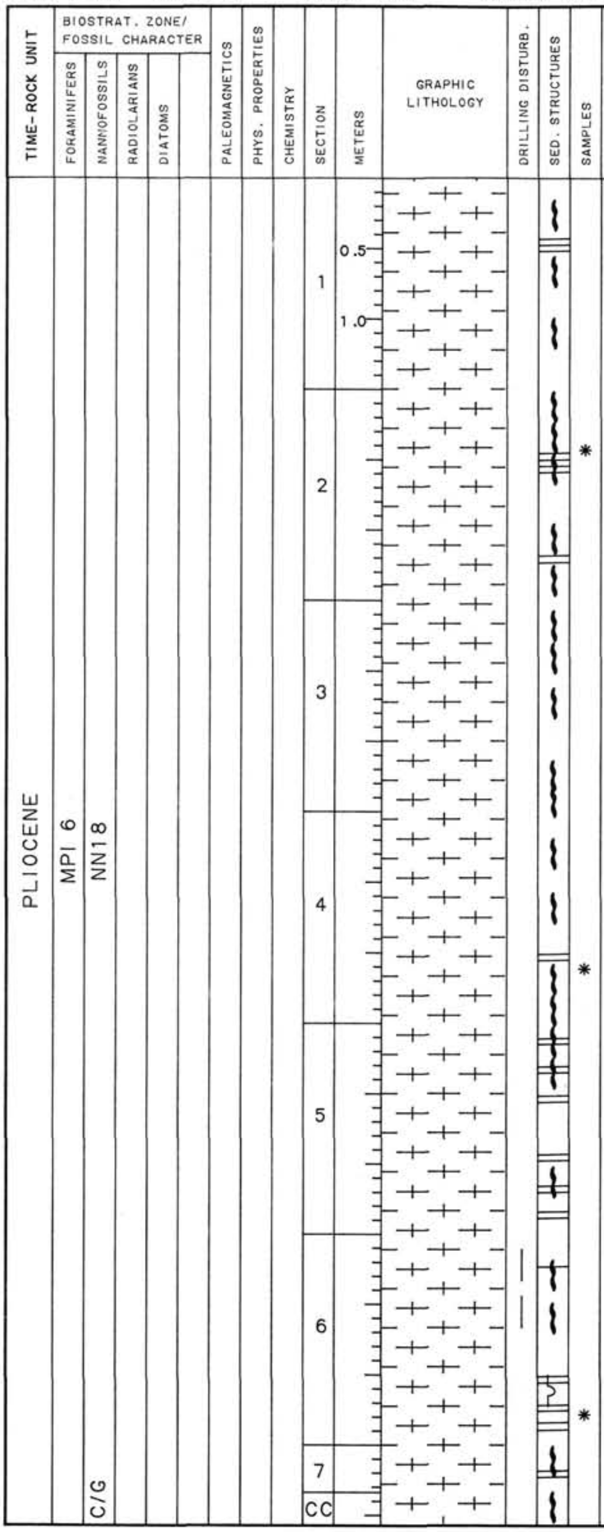

LITHOLOGIC DESCRIPTION

MARLY FORAMINIFER-NANNOFOSSIL OOZE

Marly foraminifer-nannofossil ooze, light gray (2.5Y 7/2 or 5Y 7/1) to light olive-brown (2.5Y 56) and olive-gray (5Y 52). Color changes gradational with diffuse contacts. Burrowed throughout with a particularly big vertical burrow in Section 4. All burrows enhanced by a halo or edge of dark (iron sulfide) sediment. Numerous diagenetic laminae.

SMEAR SLIDE SUMMARY (%):

	2, 47 D	4, 106 M	6, 126 M
TEXTURE:			
Sand	15	10	—
Silt	10	5	10
Clay	75	85	90
COMPOSITION:			
Quartz	1	1	2
Mica	Tr	1	—
Clay	31	31	—
Volcanic glass	Tr	Tr	—
Calcite	—	—	3
Dolomite	2	2	2
Accessory minerals	1	1	2
Gypsum	—	—	5
Zeolites	—	—	1
Foraminifers	5	10	10
Nannofossils	60	50	70
Diatoms	—	4	5

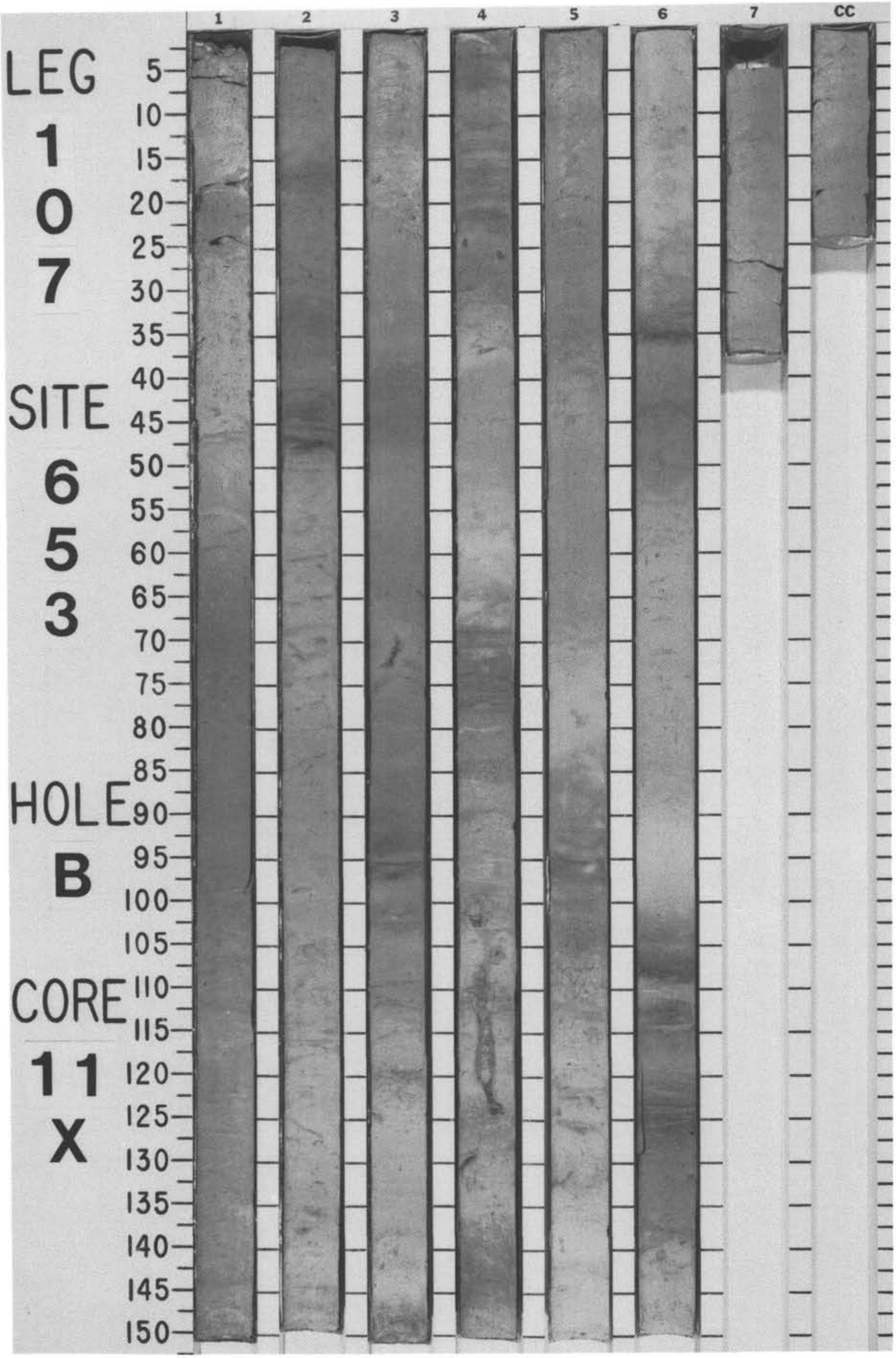
LEG
107
SITE
653
HOLE
B
CORE
11
X
1
2
3
4
5
6
7
CC
5
10
15
20
25
30
35
40
45
50
55
60
65
70
75
80
85
90
95
100
105
110
115
120
125
130
135
140
145
150

SITE 653 HOLE B CORE 12X CORED INTERVAL 2923.5-2933.0 mbsl; 102.6-112.1 mbsf

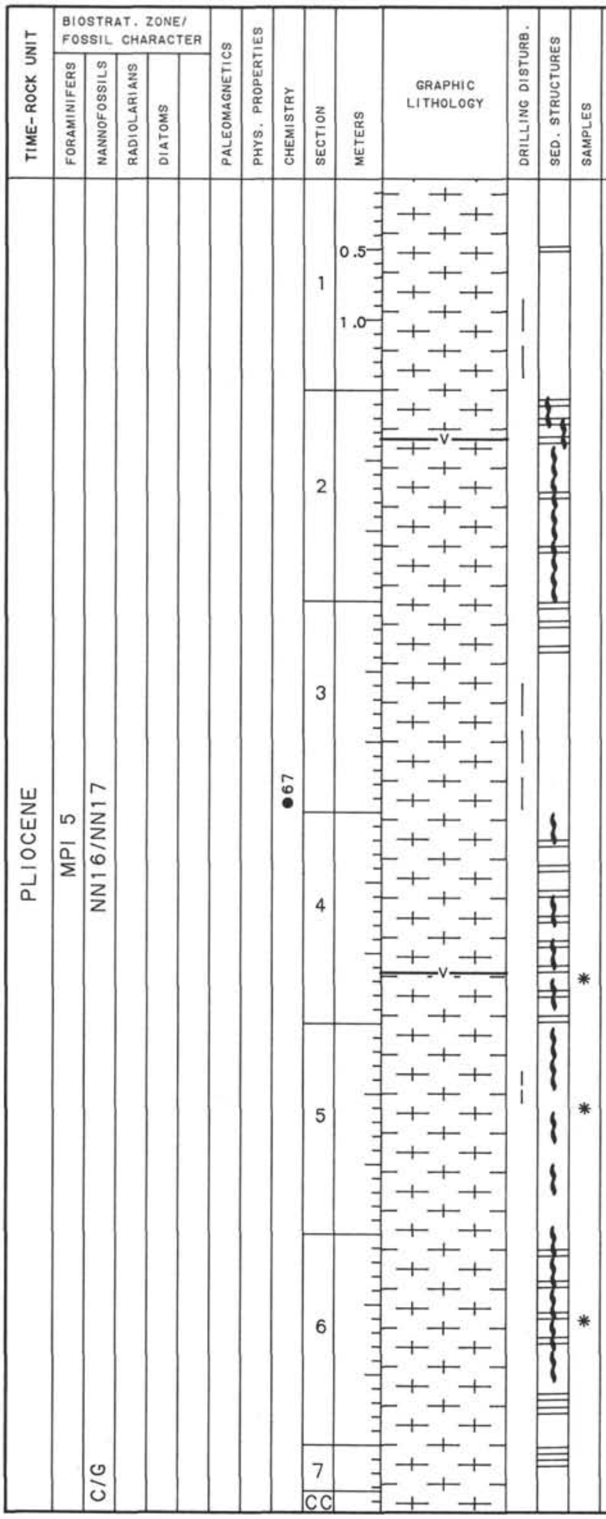

LITHOLOGIC DESCRIPTION

FORAMINIFER-NANNOFOSSIL OOZE

Foraminifer-nannofossil ooze, white (2.5Y N8/ or 5Y 8/2) and pinkish white (5YR 8/2) to olive-yellow (2.5YR 6/6), brownish yellow (10YR 66), and olive-gray (5Y 52). Foraminifer tests often filled with pyritic framboids. Numerous diagenetic laminae.

Minor lithology: Probable ash layers in Section 2, 33–35 cm, and Section 4, 113 cm.

SMEAR SLIDE SUMMARY (%):

	4, 113 M	5, 62 D	6, 62 D
TEXTURE:			
Silt	15	10	20
Clay	85	90	80
COMPOSITION:			
Quartz	10	10	8
Feldspar	—	—	1
Volcanic glass	10	3	5
Dolomite	2	2	2
Accessory minerals	—	—	2
Gypsum	2	Tr	2
Zircon	Tr	Tr	—
Pyroxene	—	1	—
Foraminifers	10	10	10
Nannofossils	64	72	68
Diatoms	2	2	2

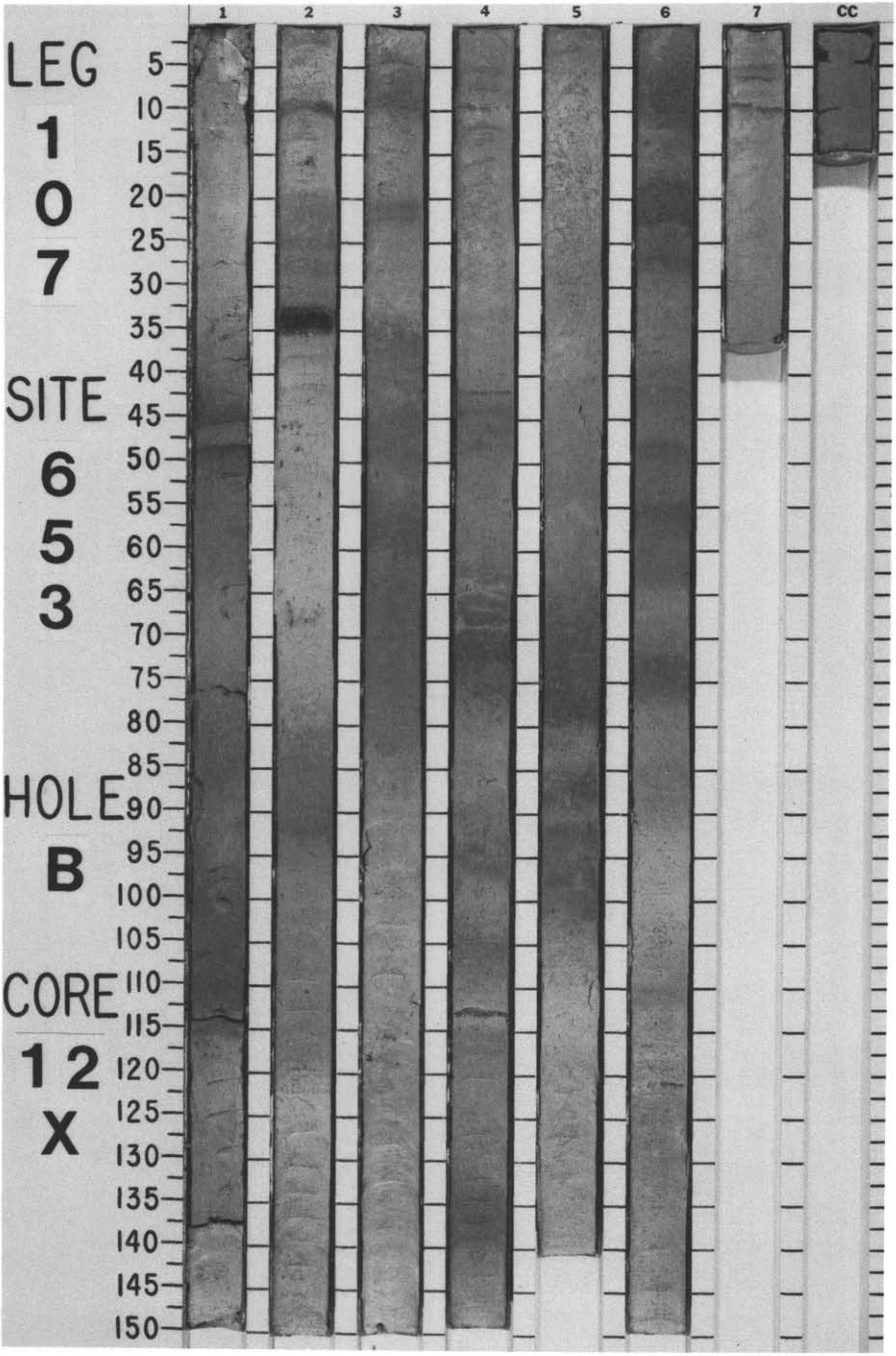
LEG
107
SITE
653
HOLE
B
CORE
12X
1
2
3
4
5
6
7
CC
5
10
15
20
25
30
35
40
45
50
55
60
65
70
75
80
85
90
95
100
105
110
115
120
125
130
135
140
145
150

SITE 688 HOLE B CORE 13X CORED INTERVAL 2933.0-2942.5 mbsl; 112.1-121.6 mbsf

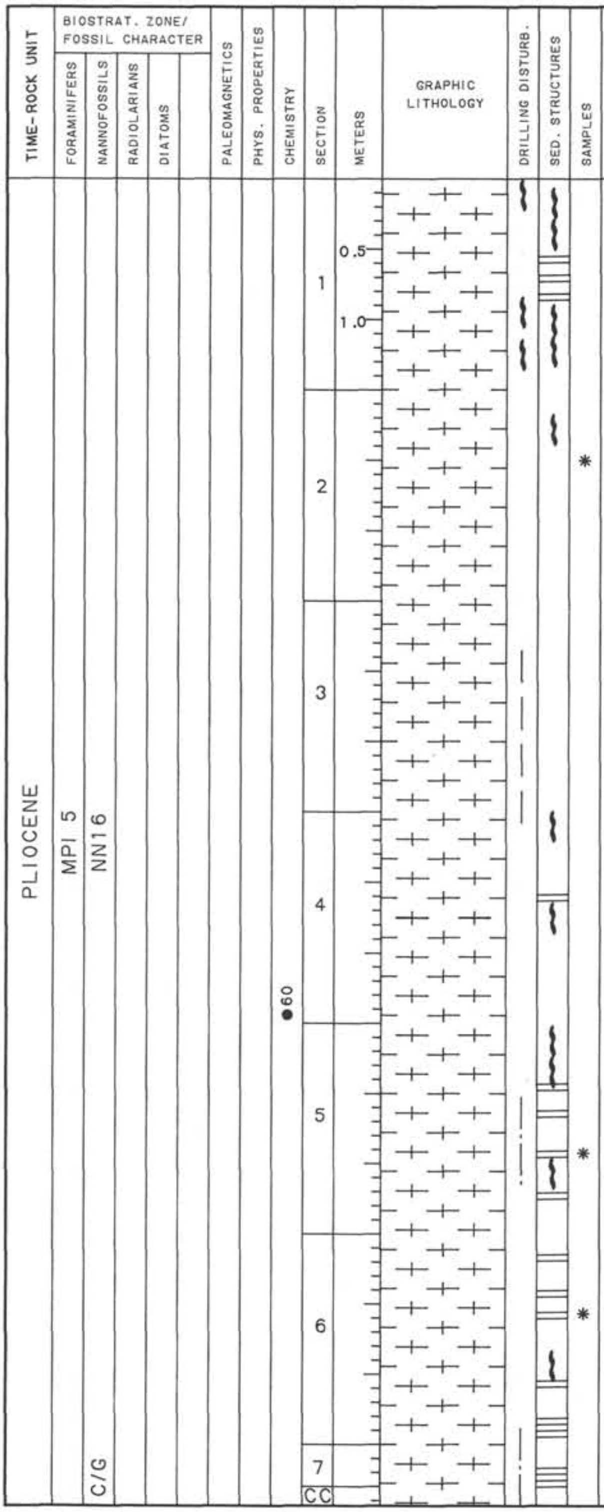

LITHOLOGIC DESCRIPTION

NANNOFOSSIL and FORAMINIFER-NANNOFOSSIL OOZE

Nannofossil and foraminifer-nannofossil ooze, white (2.5Y N8/ or 5Y 8/1) and light gray (10YR 7/1, 2.5Y 7/2, 5Y 7/2) to brownish yellow (10YR 6/8) and yellow (2.5Y 7/6). Homogenous in texture and composition; color changes are gradational over indistinct boundaries. Some diagenetic laminae.

SMEAR SLIDE SUMMARY (%):

	2, 60 D	5, 93 M	6, 59 M
TEXTURE:			
Sand	10	—	—
Silt	20	25	20
Clay	80	75	80
COMPOSITION:			
Quartz	1	1	1
Feldspar	4	4	2
Mica	1	Tr	—
Clay	14	12	31
Volcanic glass	Tr	Tr	—
Calcite	—	2	—
Dolomite	—	1	1
Accessory minerals	1	1	—
Opaques	—	——	11
Foraminifers	10	10	3
Nannofossils	70	70	50
Bioclasts	—	—	1

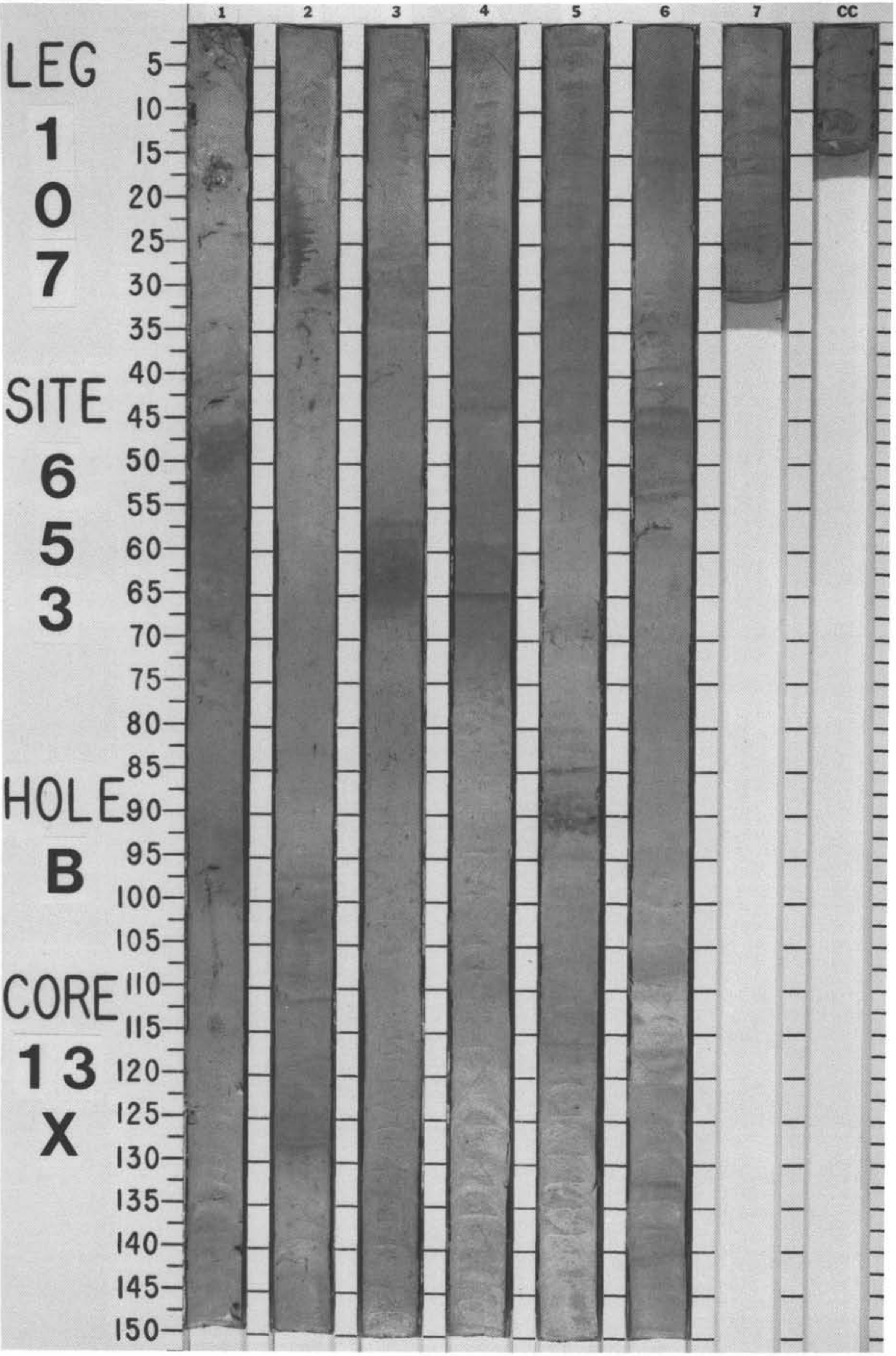
LEG
107
SITE
653
HOLE
B
CORE
13
X
1
2
3
4
5
6
7
CC
5
10
15
20
25
30
35
40
45
50
55
60
65
70
75
80
85
90
95
100
105
110
115
120
125
130
135
140
145
150

SITE 653 HOLE B CORE 14X CORED INTERVAL 2942.5-2951.9 mbsl; 121.6-131.0 mbsf

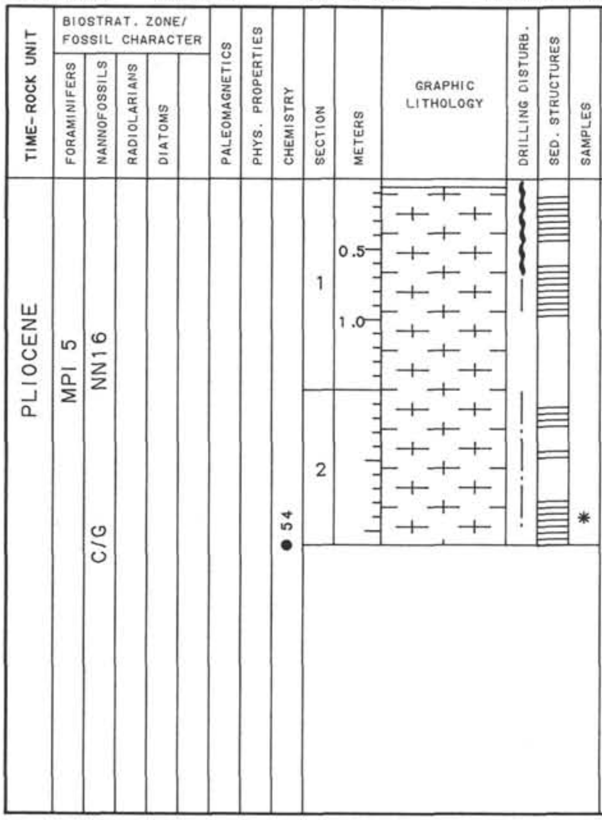

LITHOLOGIC DESCRIPTION

FORAMINIFER-NANNOFOSSIL OOZE

Foraminifer-nannofossil ooze, white (5Y 8/1) to light olive-gray (5Y 6/2) and pale olive (5Y 6/4). Color changes are gradational; homogenous texture and composition.

SMEAR SLIDE SUMMARY (%):

	2, 87 D
TEXTURE:	
Silt	20
Clay	80
COMPOSITION:	
Quartz	1
Volcanic glass	4
Dolomite	4
Accessory minerals	1
Zircon	Tr
Foraminifers	9
Nannofossils	71
Diatoms	5
Flagellates	5

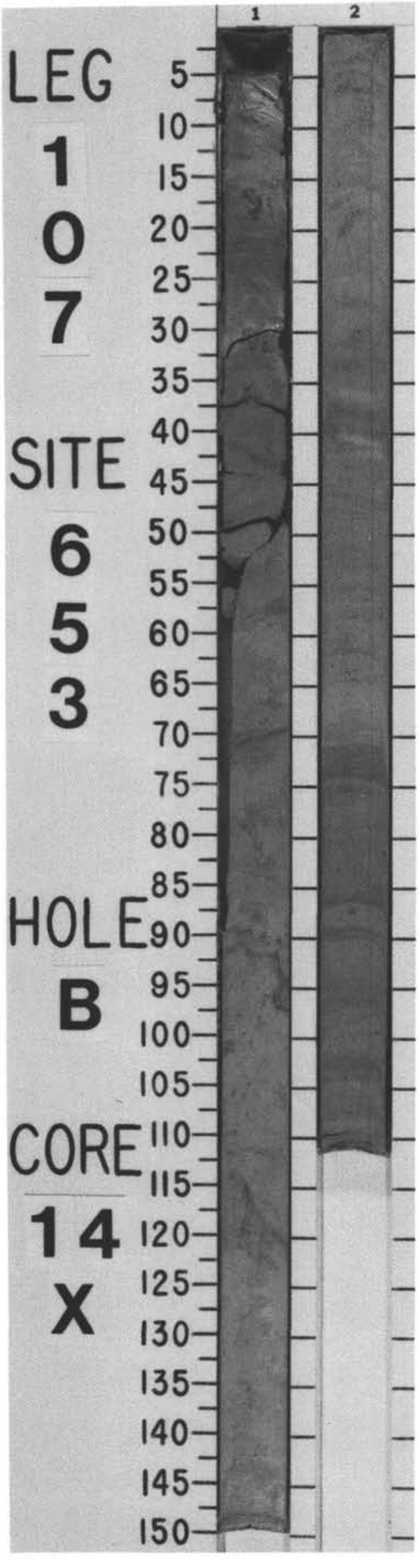
LEG
1
0
7
SITE
6
5
3
HOLE
B
CORE
14
X
1
2
5
10
15
20
25
30
35
40
45
50
55
60
65
70
75
80
85
90
95
100
105
110
115
120
125
130
135
140
145
150

SITE 653 HOLE B CORE 15X CORED INTERVAL 2951.9-2961.4 mbsl; 131.0-140.5 mbsf

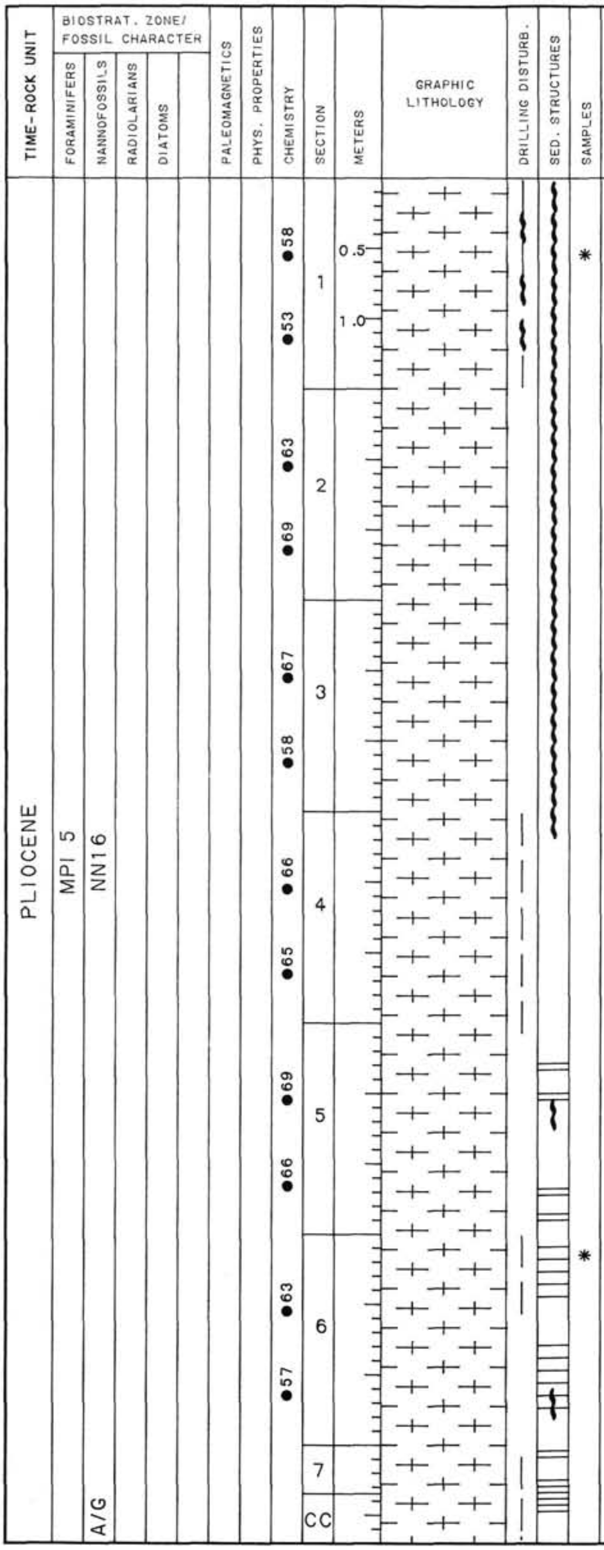

LITHOLOGIC DESCRIPTION

NANNOFOSSIL OOZE and FORAMINIFER-NANNOFOSSIL OOZE

Nannofossil ooze and foraminifer-nannofossil ooze, white (2.5Y 8/2) to light gray (2.5Y 7/2) and yellow (2.5Y 7/6). Color changes are indistinct and gradational. Texturally and compositionally homogeneous.

SMEAR SLIDE SUMMARY (%):

	1, 60 D	6, 13 M
TEXTURE:		
Silt	10	15
Clay	90	85
COMPOSITION:		
Quartz	2	6
Clay	20	—
Volcanic glass	Tr	3
Dolomite	—	3
Accessory minerals		
Gypsum	—	2
Foraminifers	—	15
Nannofossils	75	68
Diatoms	3	—
Sponge spicules	—	1
Flagellates	—	2

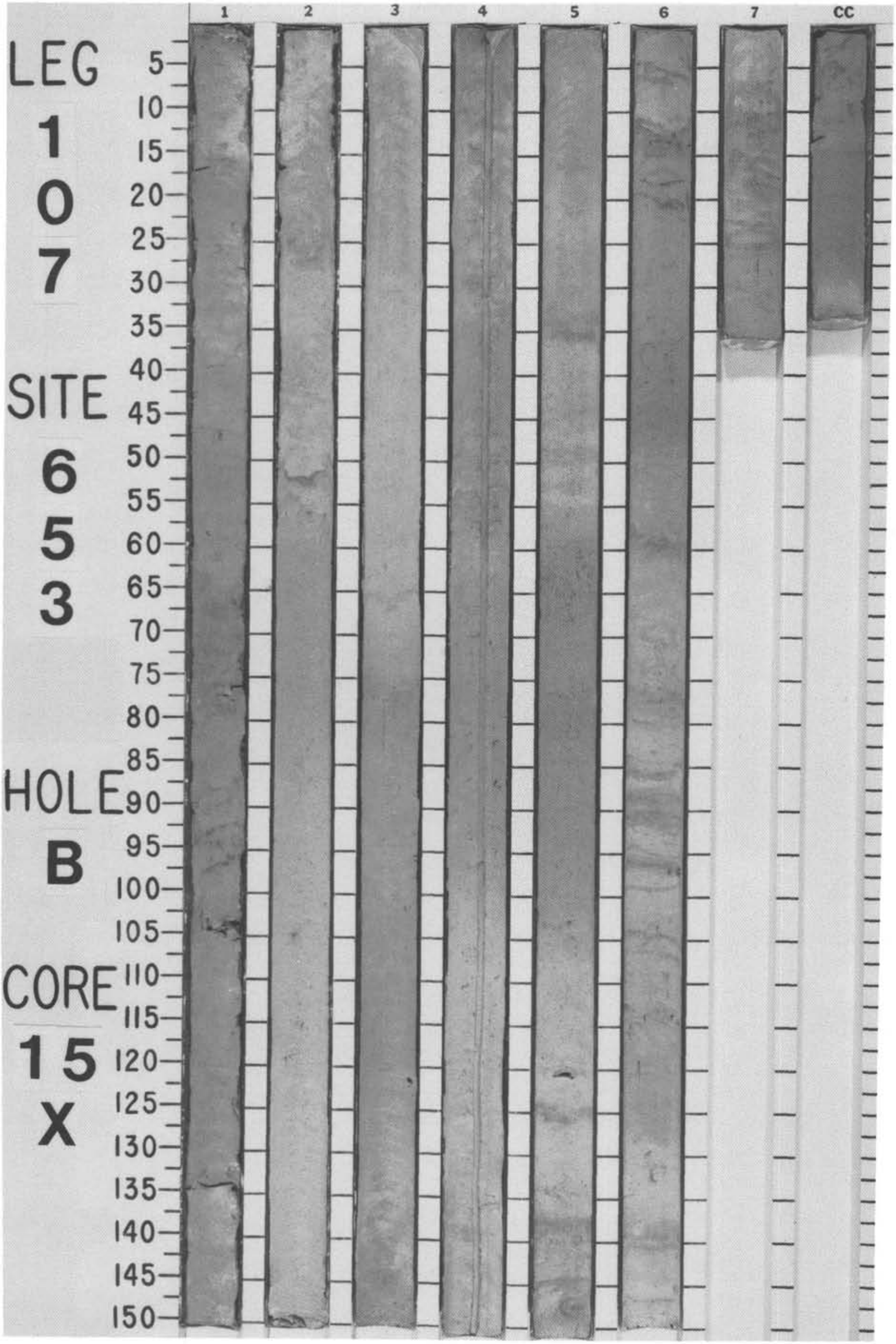
LEG
107
SITE
653
HOLE
B
CORE
15X
1
2
3
4
5
6
7
CC
5
10
15
20
25
30
35
40
45
50
55
60
65
70
75
80
85
90
95
100
105
110
115
120
125
130
135
140
145
150

SITE 653 HOLE B CORE 16X CORED INTERVAL 2961.4-2970.9 mbsl; 140.5-150.0 mbsf

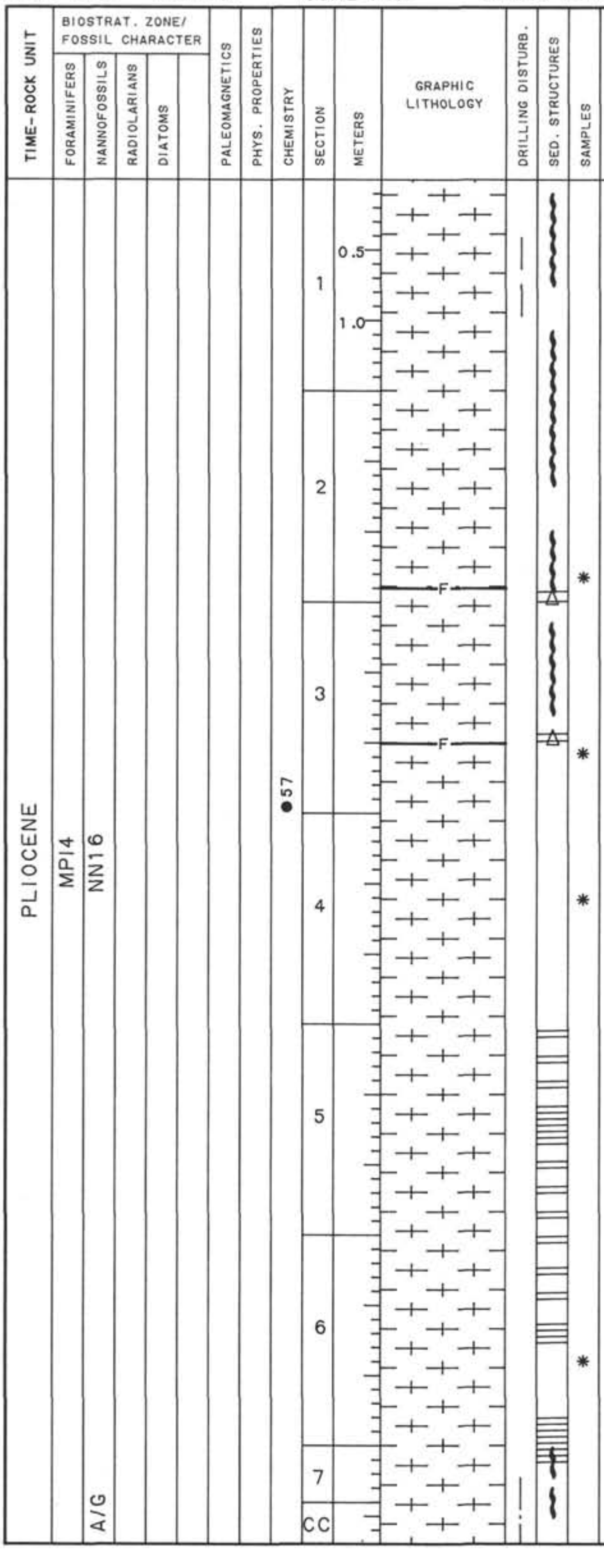

LITHOLOGIC DESCRIPTION

NANNOFOSSIL OOZE and FORAMINIFER-NANNOFOSSIL OOZE

Nannofossil ooze and foraminifer-nannofossil ooze, light grayish green (5GY 7/2) to greenish gray (5GY 6/1), and white (2.5Y N8/ or 5Y 8/1) to yellow (2.5Y 7/6) and light olive-gray (5Y 6/2). Color changes are indistinct and gradual. Core is texturally and compositionally homogeneous with exception of graded foraminifer sands. Common diagenetic laminae.

Minor lithology: Foraminifer sand, Section 2, 139–144 cm, and Section 3, 99–101 cm, white (2.5Y N8/), Lower foraminifer sand is indurated.

SMEAR SLIDE SUMMARY (%):

	2, 143 M	3, 101 M	4, 60 D	6, 90 D
TEXTURE:				
Sand	70	70	—	—
Silt	5	25	15	10
Clay	20	5	85	90
COMPOSITION:				
Quartz	1	2	2	2
Feldspar	—	4	—	—
Mica	—	—	Tr	—
Clay	8	4	15	—
Volcanic glass	—	—	—	3
Calcite	—	2	—	—
Dolomite	—	—	—	3
Accessory minerals	1	—	—	—
Zeolites	Tr	—	Tr	—
Gypsum	—	—	—	1
Micrite	—	—	1	—
Foraminifers	60	50	11	10
Nannofossils	30	35	70	77
Sponge spicules	—	1	—	1
Flagellates	—	—	1	3
Spar cement	—	2	—	—

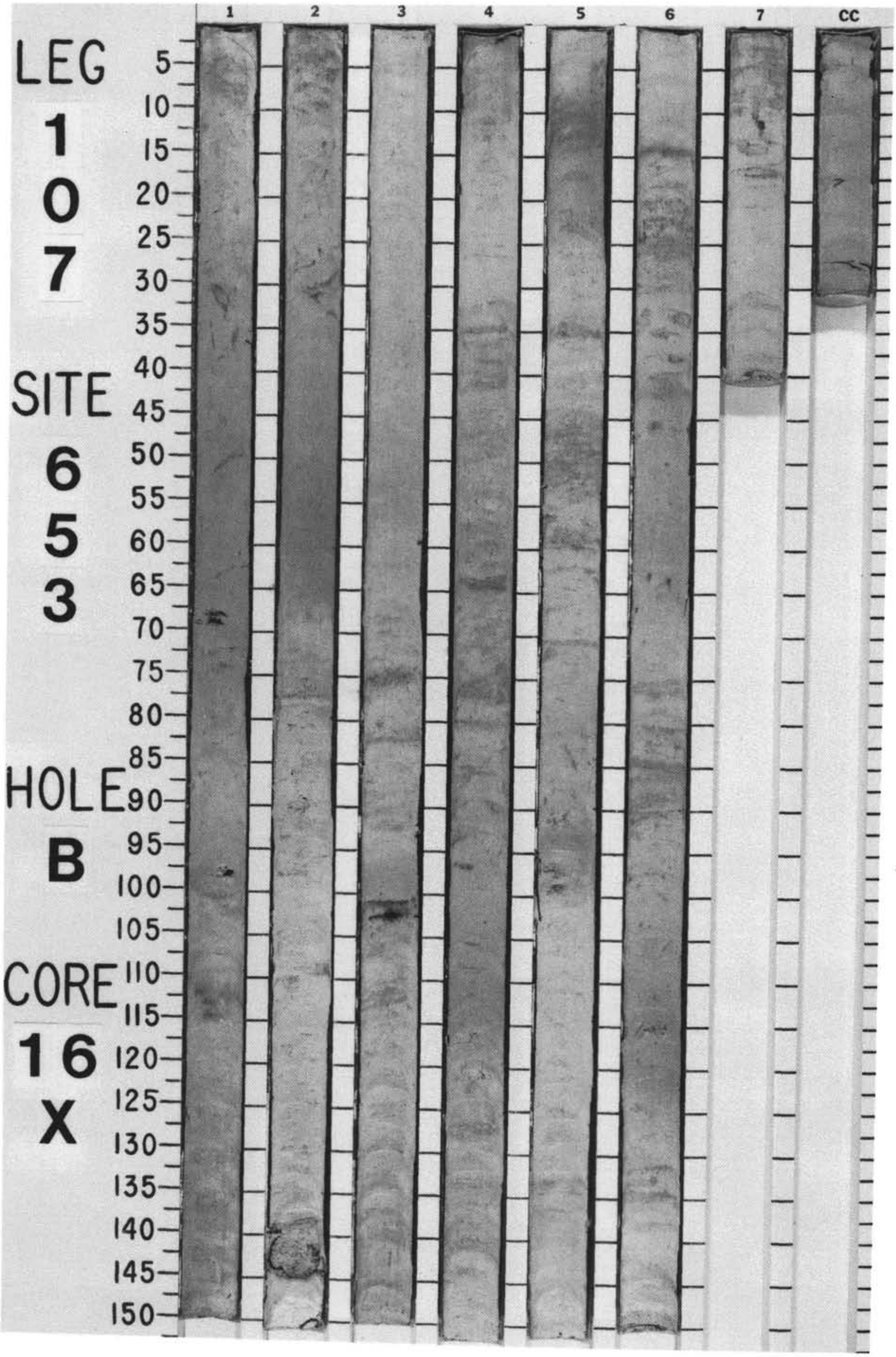
LEG
107
SITE
653
HOLE
B
CORE
16X
1
2
3
4
5
6
7
CC
5
10
15
20
25
30
35
40
45
50
55
60
65
70
75
80
85
90
95
100
105
110
115
120
125
130
135
140
145
150

SITE 653 HOLE B CORE 17X CORED INTERVAL 2970.9-2980.5 mbsl; 150.0-159.6 mbsf

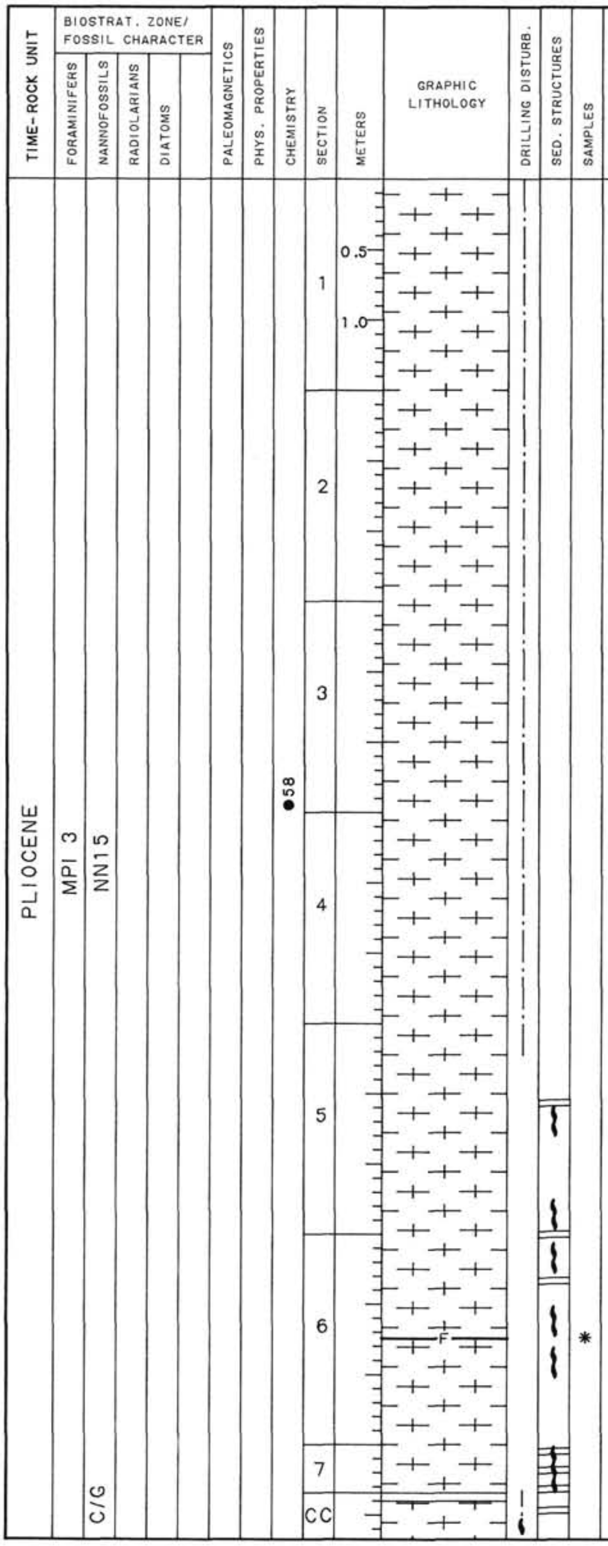

LITHOLOGIC DESCRIPTION

FORAMINIFER-NANNOFOSSIL OOZE

Foraminifer-nannofossil ooze, white (5Y 8/1) to light gray (5Y 7/1) and and pale yellow (5Y 7/3), colors gradational.

Minor lithology: foraminifer-sand, Section 6, 75 cm, light olive-gray (5Y 6/1).

SMEAR SLIDE SUMMARY (%):

	6, 75 M
TEXTURE:	
Sand	50
Silt	20
Clay	30
COMPOSITION:	
Quartz	2
Dolomite	2
Accessory minerals	
Gypsum	1
Foraminifers	50
Nannofossils	45

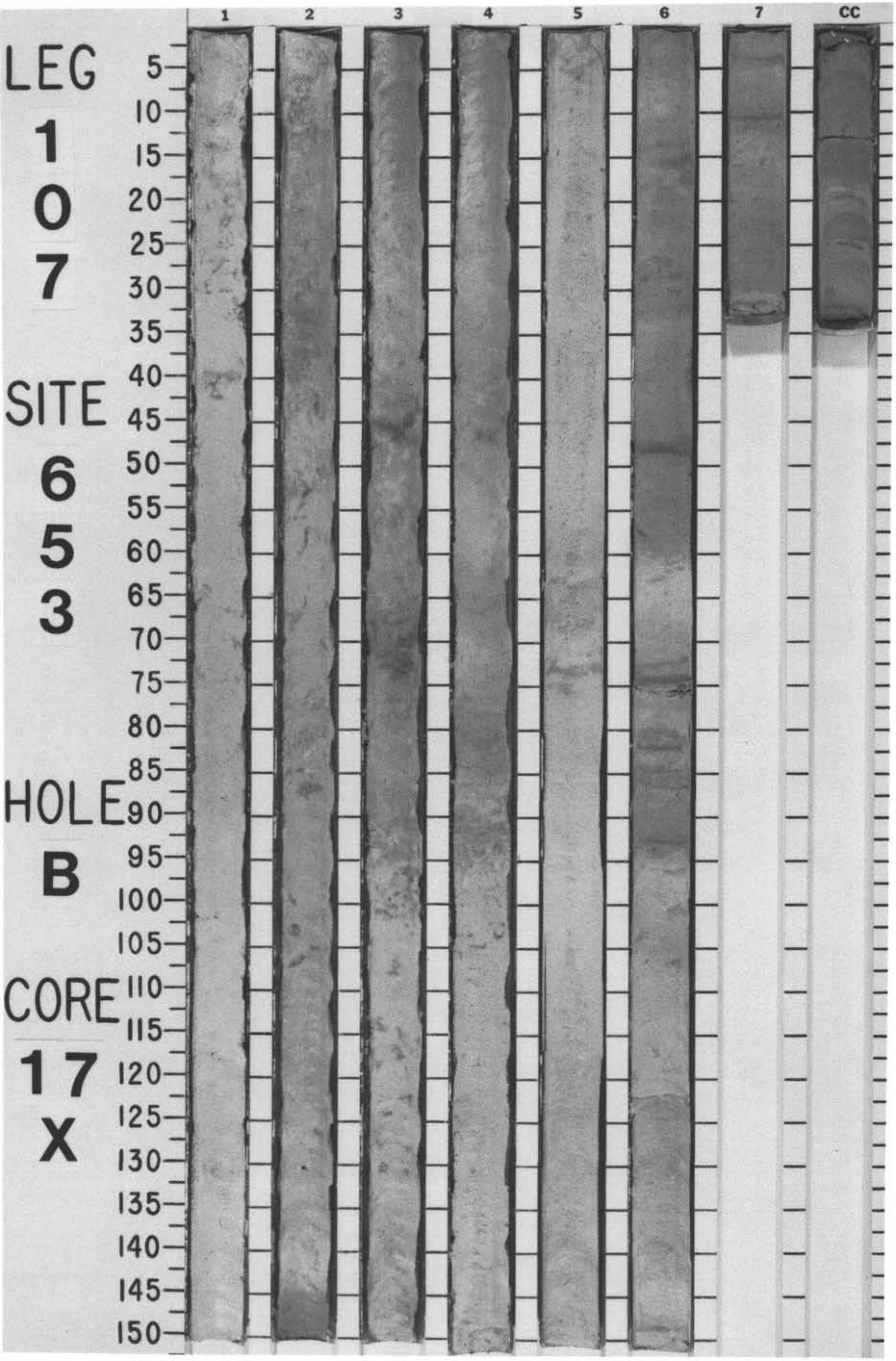
LEG
107
SITE
653
HOLE
B
CORE
17
X
1
2
3
4
5
6
7
CC
5
10
15
20
25
30
35
40
45
50
55
60
65
70
75
80
85
90
95
100
105
110
115
120
125
130
135
140
145
150

SITE 653 HOLE B CORE 18X CORED INTERVAL 2980.5-2989.4 mbsl; 159.6-168.5 mbsf

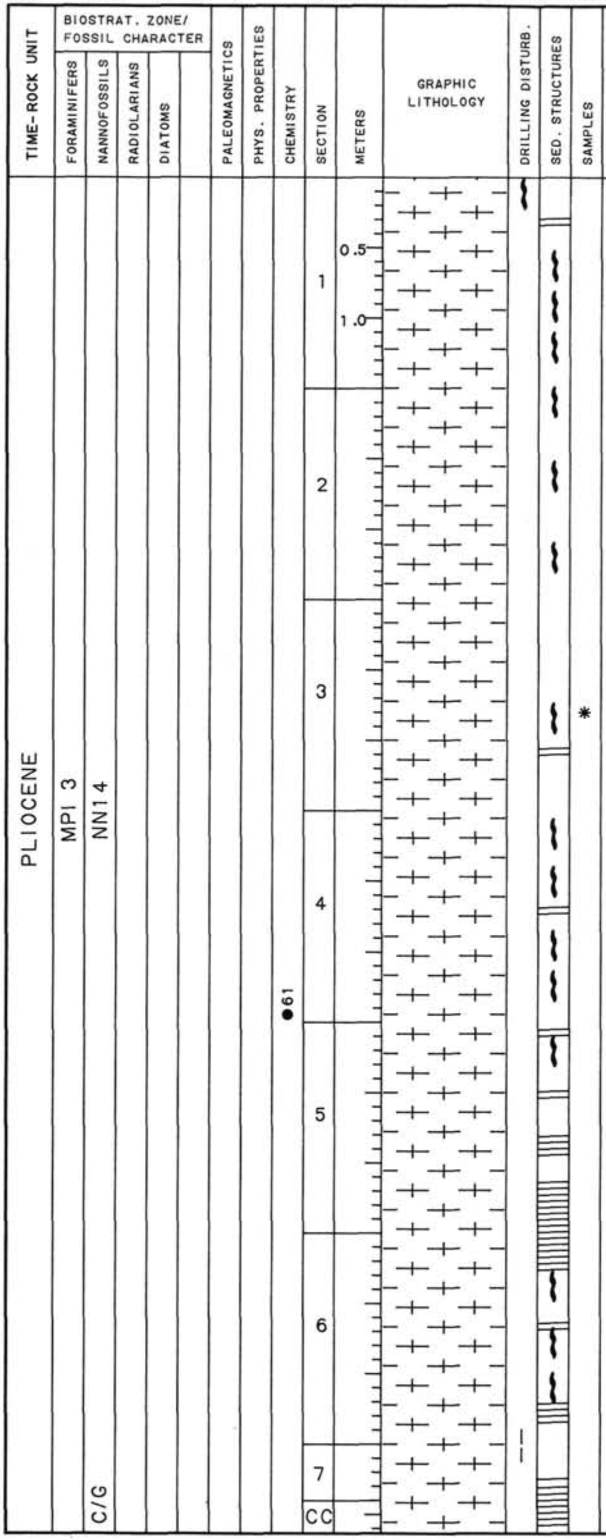

LITHOLOGIC DESCRIPTION

FORAMINIFER-NANNOFOSSIL OOZE

Foraminifer-nannofossil ooze, very pale brown (10YR 7/4) and light gray (2.5Y 7/2 or 5Y 7/2) to light yellowish brown (2.5Y 6/4), pale yellow (5Y 8/4) and pale olive (5Y 6/4), colors gradational. Few large burrows (up to 3-cm diameter), often oval, with diagenetic halos of dark (iron sulfide) sediment. Sediment fill in burrows is enriched in foraminifers. Few diagenetic laminae.

SMEAR SLIDE SUMMARY (%):

	3, 80 D
TEXTURE:	
Silt	5
Clay	95
COMPOSITION:	
Quartz	Tr
Mica	Tr
Clay	15
Accessory minerals	
Gypsum	Tr
Micrite	20
Foraminifers	5
Nannofossils	60
Flagellates	Tr

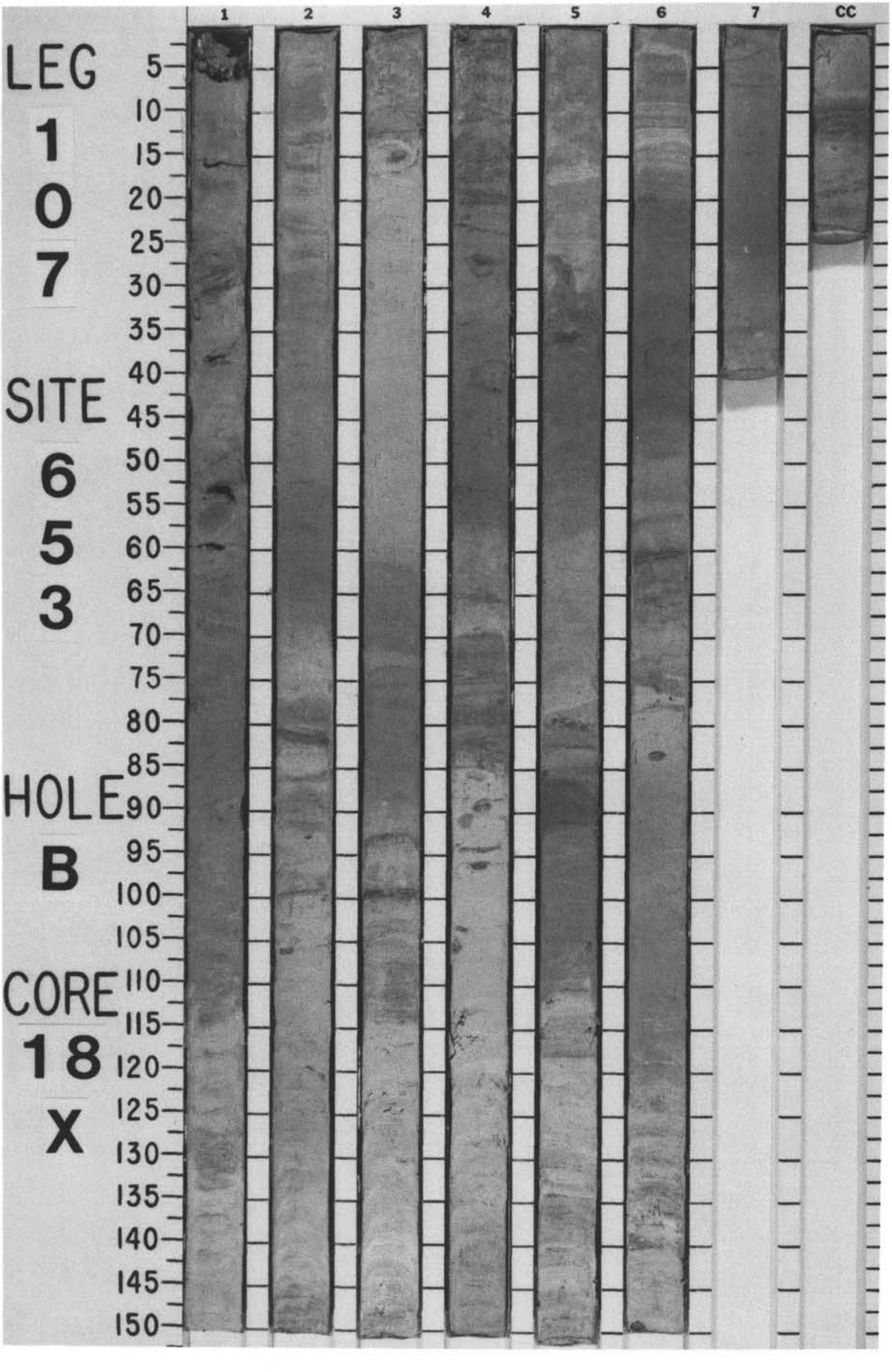
LEG
1
0
7
SITE
6
5
3
HOLE
B
CORE
1
8
X
1
2
3
4
5
6
7
CC
5
10
15
20
25
30
35
40
45
50
55
60
65
70
75
80
85
90
95
100
105
110
115
120
125
130
135
140
145
150

SITE 653 HOLE B CORE 19X CORED INTERVAL 2989.4-2998.9 mbsl; 168.5-178.0 mbsf

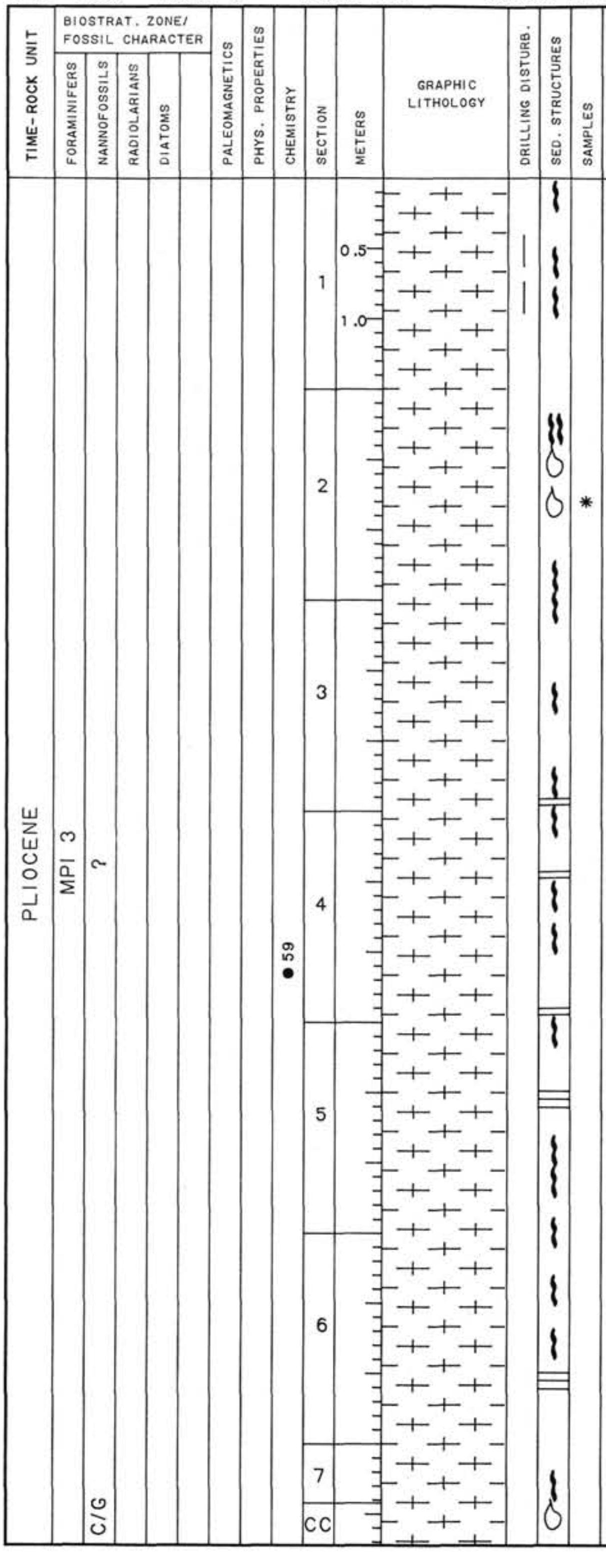

LITHOLOGIC DESCRIPTION

FORAMINIFER-NANNOFOSSIL OOZE

Foraminifer-nannofossil ooze, varicolored, including white, light gray, gray, light olive-gray, light yellowish brown, and pale yellow. Some foraminifer-rich layers.

SMEAR SLIDE SUMMARY (%):

	2, 82 M
TEXTURE:	
Sand	35
Silt	15
Clay	50
COMPOSITION:	
Quartz	3
Mica	1
Clay	10
Accessory minerals	1
Foraminifers	35
Nannofossils	45
Radiolarians	5

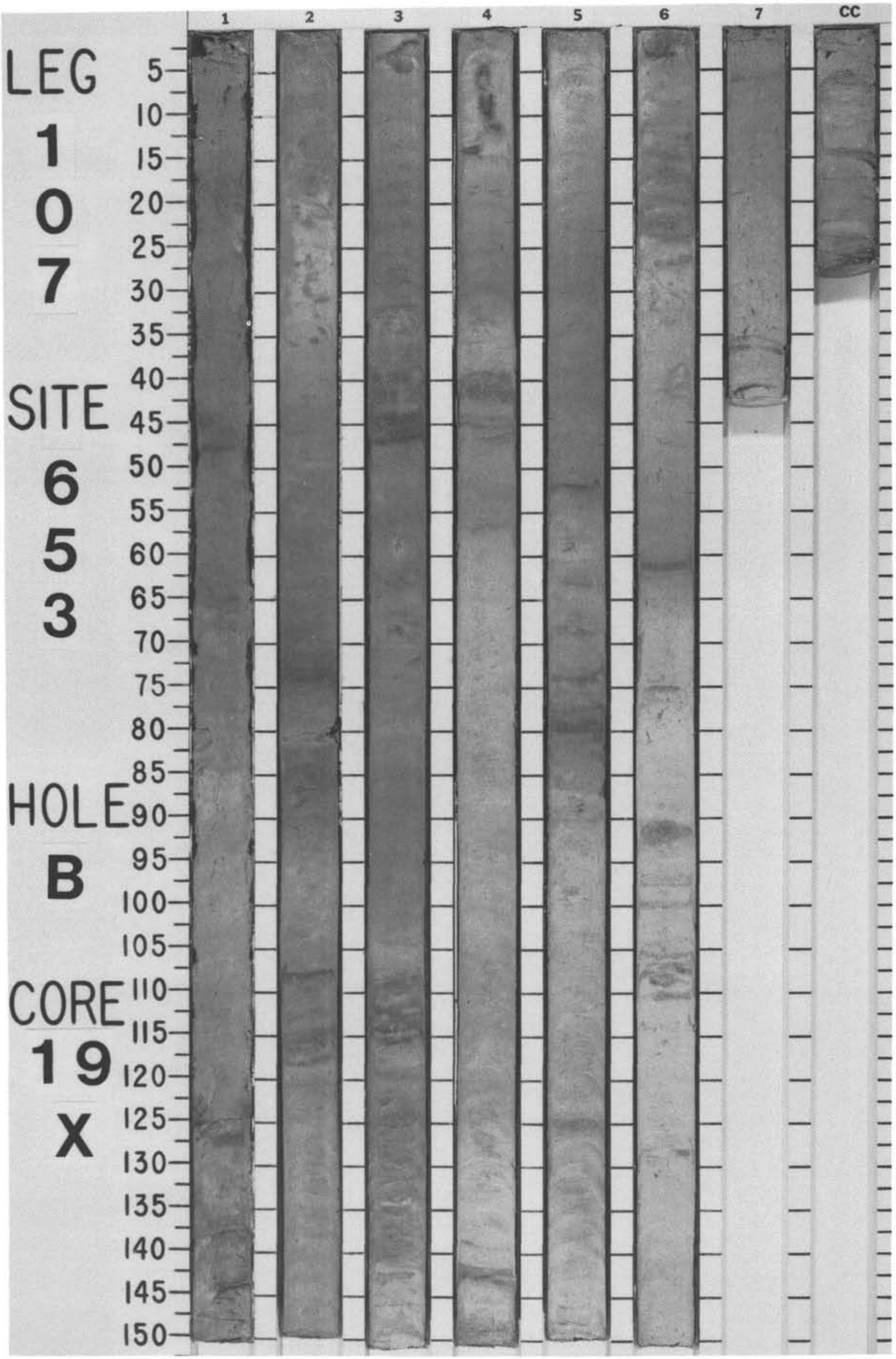
LEG
1
0
7
SITE
6
5
3
HOLE
B
CORE
19
X
1
2
3
4
5
6
7
CC
5
10
15
20
25
30
35
40
45
50
55
60
65
70
75
80
85
90
95
100
105
110
115
120
125
130
135
140
145
150

SITE 653 HOLE B CORE 20X CORED INTERVAL 2998.9-3008.4 mbsl; 178.0-187.0 mbsf

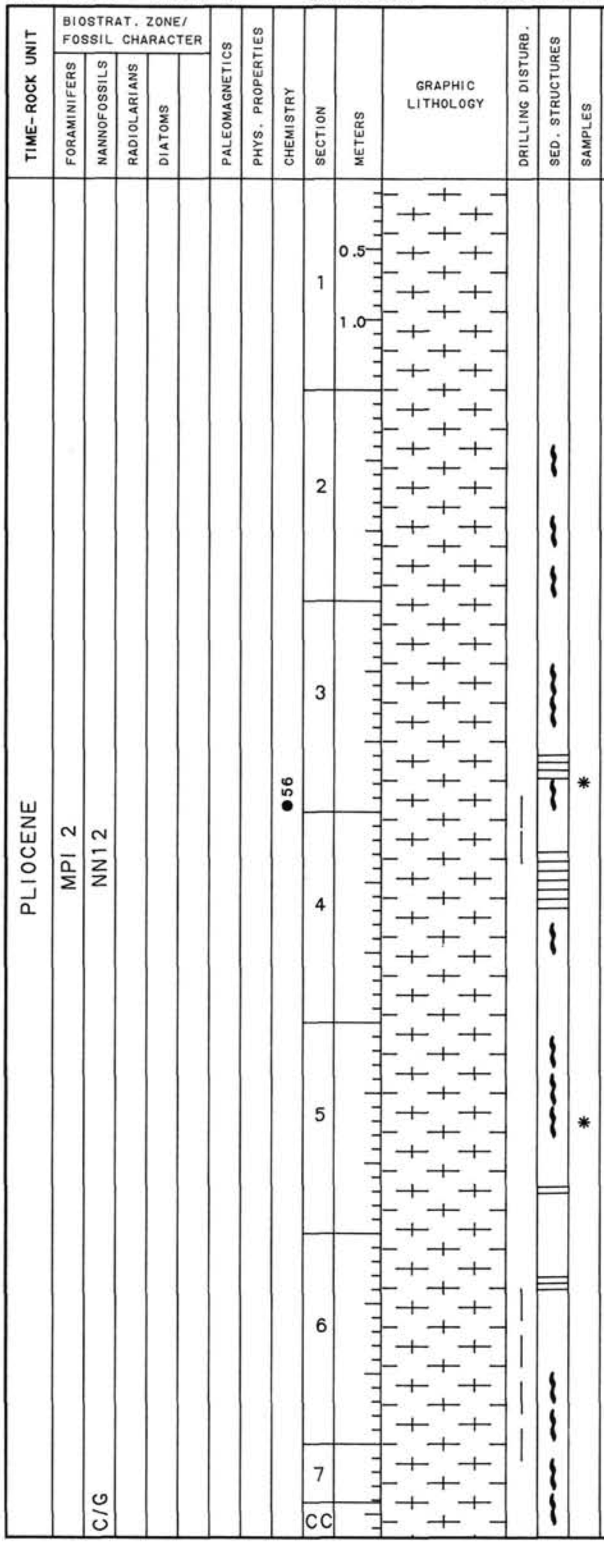

LITHOLOGIC DESCRIPTION

FORAMINIFER-NANNOFOSSIL OOZE

Foraminifer-nannofossil ooze, light gray (2.5Y 7/2 or 5Y 7/1), to yellow (2.5Y 7/6), light yellowish brown (2.5Y 6/4), dark gray (5Y 4/1) and pale yellowish green (10GY 7/2).

SMEAR SLIDE SUMMARY (%):

	3, 119 M	5, 69 M
TEXTURE:		
Sand	25	35
Silt	20	15
Clay	55	50
COMPOSITION:		
Quartz	5	5
Mica	Tr	—
Clay	9	2
Volcanic glass	1	1
Calcite/dolomite	—	3
Accessory minerals	—	1
Glauconite	1	—
Pyrite	1	—
Micrite	10	10
Foraminifers	25	35
Nannofossils	45	40
Radiolarians	3	3

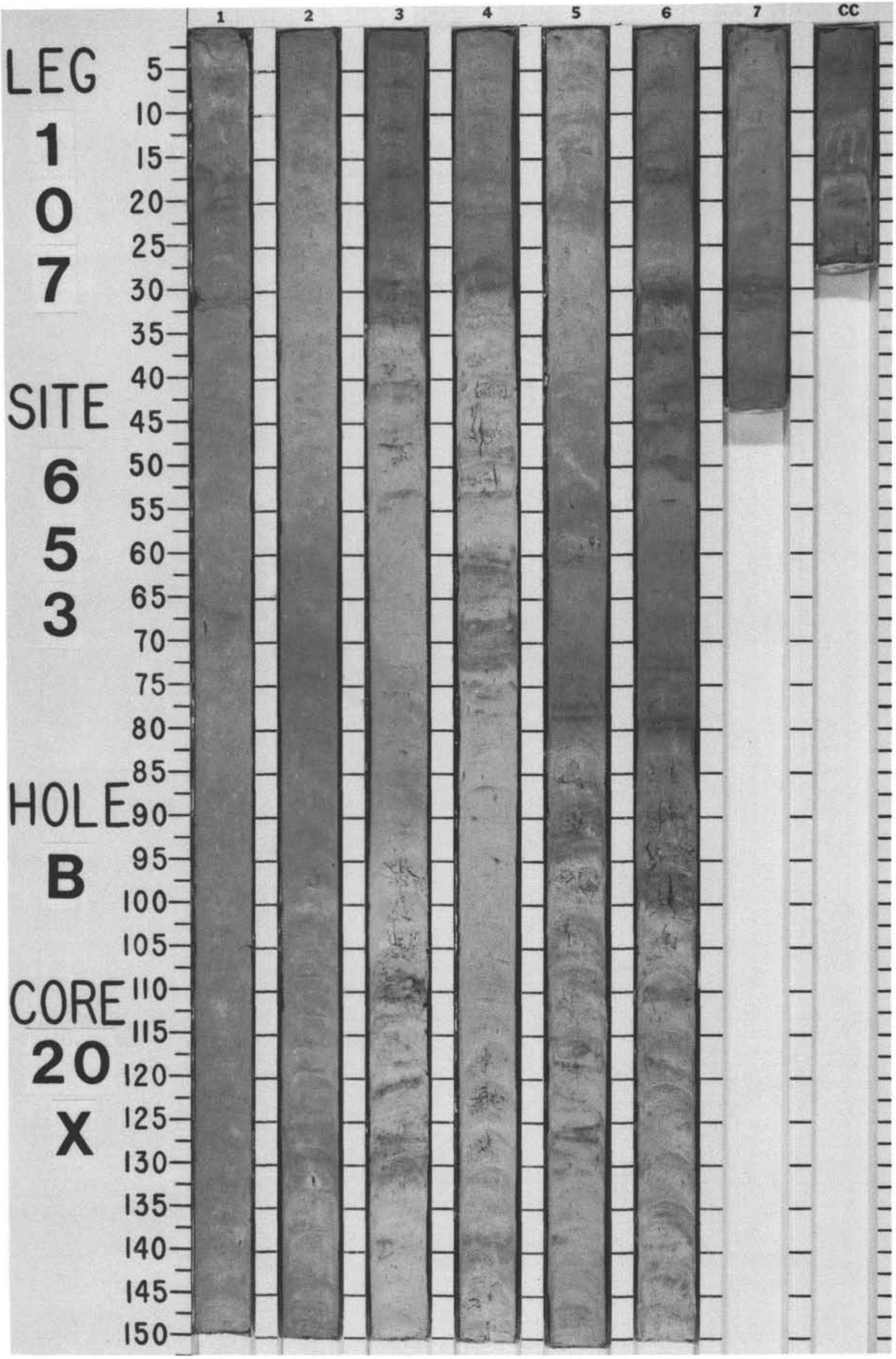
LEG
107
SITE
653
HOLE
B
CORE
20
X
1
2
3
4
5
6
7
CC
5
10
15
20
25
30
35
40
45
50
55
60
65
70
75
80
85
90
95
100
105
110
115
120
125
130
135
140
145
150

SITE 653 HOLE B CORE 21X CORED INTERVAL 3008.4-3018.1 mbsl; 187.0-197.2 mbsf

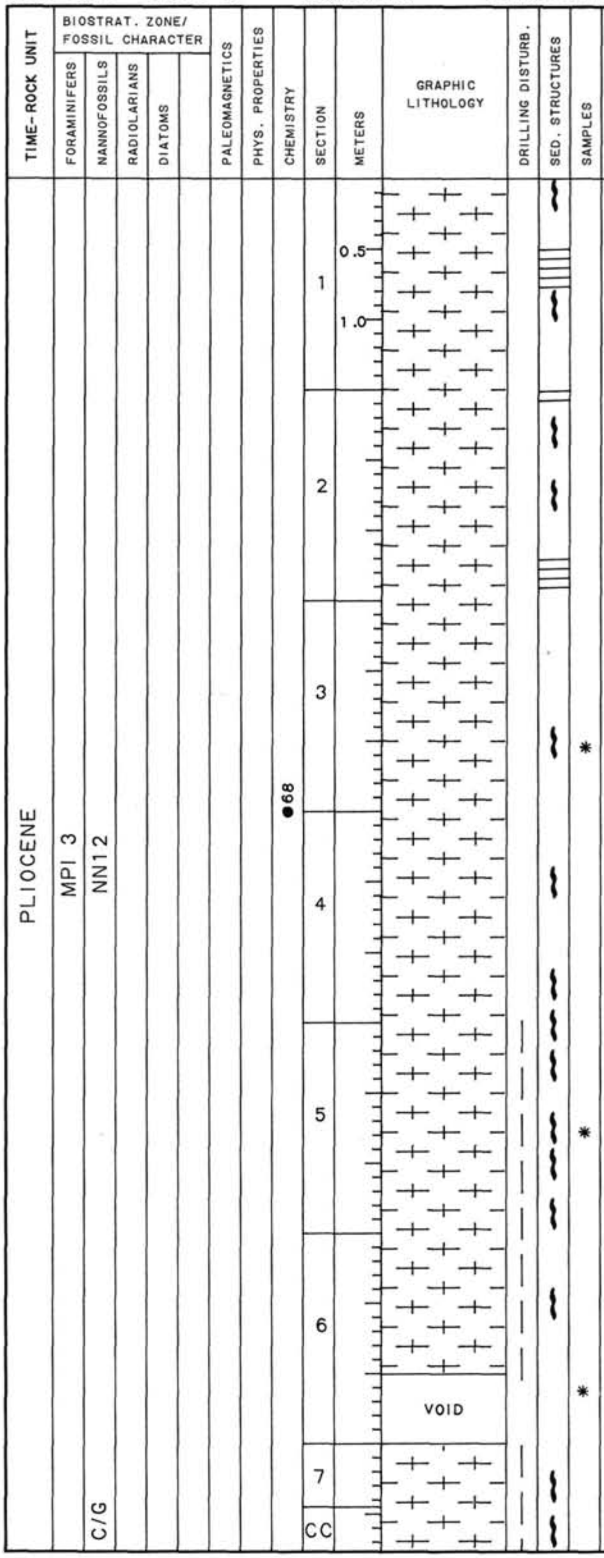

LITHOLOGIC DESCRIPTION

FORAMINIFER-NANNOFOSSIL OOZE

Foraminifer-nannofossil ooze, light yellowish brown (2.5Y 6/4) and white (5Y 8/1) to pale yellow (5Y 7/3), pale olive (5Y 6/3), gray (5Y 5/1), pale green (10G 6/2) and grayish green (10GY 5/2).

SMEAR SLIDE SUMMARY (%):

	3, 103 D	5, 77 M	6, 115 D
TEXTURE:			
Sand	20	3	25
Silt	10	25	10
Clay	70	72	65
COMPOSITION:			
Quartz	2	2	3
Mica	Tr	Tr	Tr
Clay	11	16	9
Volcanic glass	Tr	1	2
Calcite/dolomite	2	5	5
Accessory minerals	1	1	1
Opaques (hydrotroilites?) organic matter(?)	2	—	—
Pyrite	—	1	1
Micrite	—	10	—
Gypsum(?)	—	—	1
Foraminifers	20	3	25
Nannofossils	60	60	50
Radiolarians	2	—	3
Silicoflagellates	—	1	—

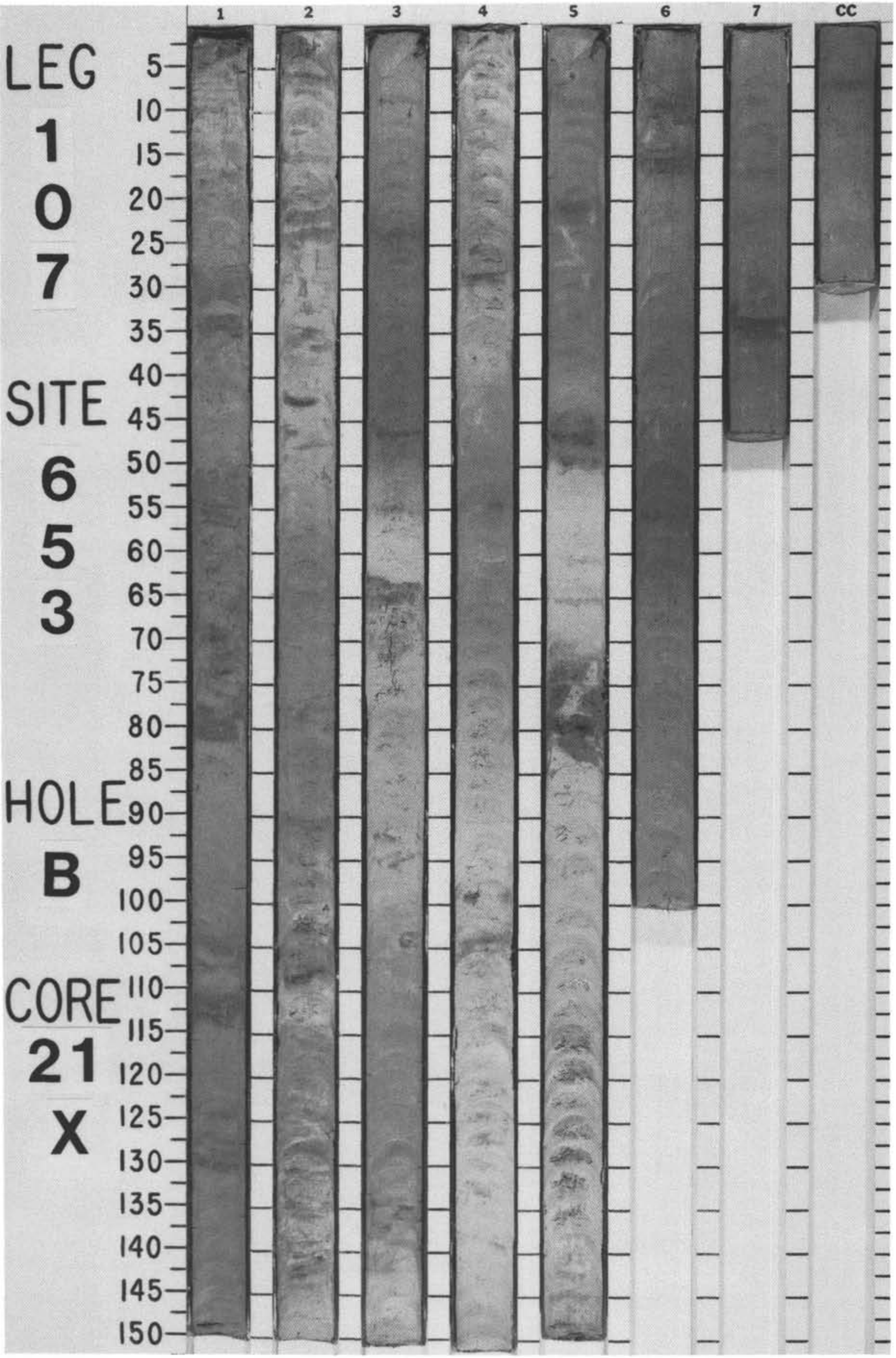
LEG
1
0
7
SITE
6
5
3
HOLE
B
CORE
21
X
1
2
3
4
5
6
7
CC
5
10
15
20
25
30
35
40
45
50
55
60
65
70
75
80
85
90
95
100
105
110
115
120
125
130
135
140
145
150

SITE 653 HOLE B CORE 22X CORED INTERVAL 3018.1-3027.6 mbsl; 197.2-206.7 mbsf

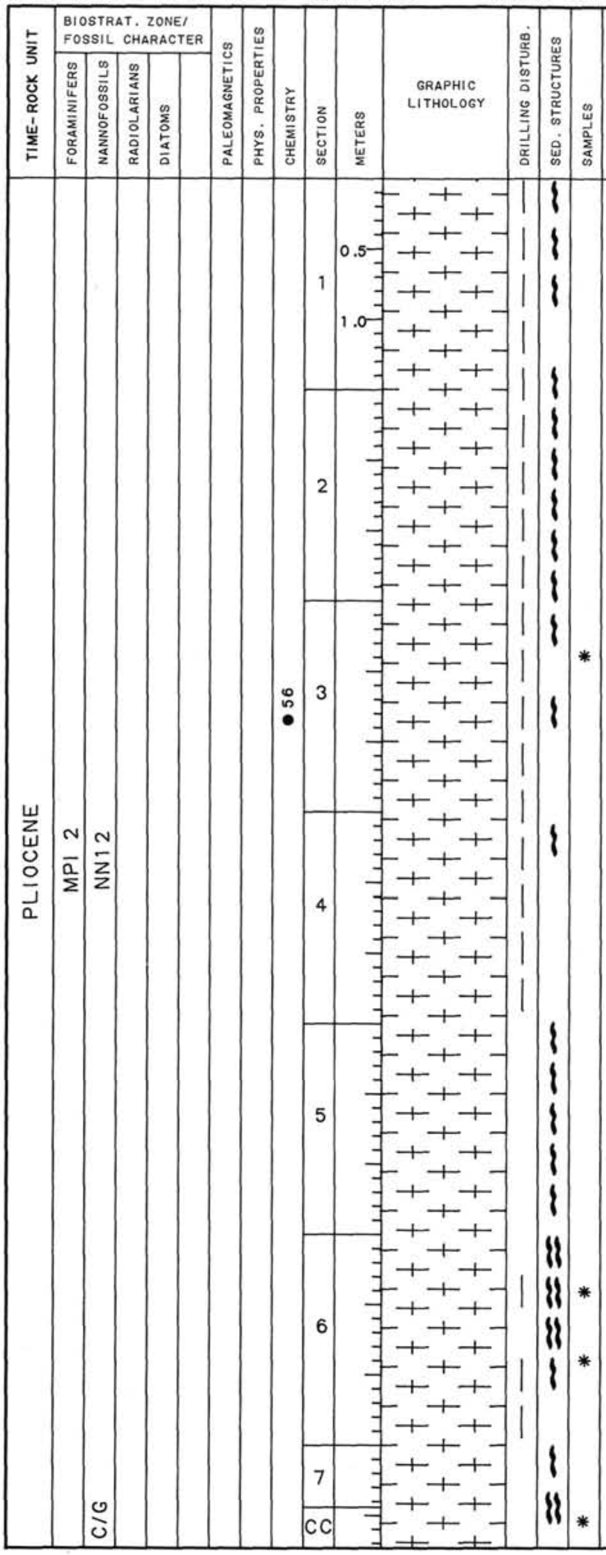

LITHOLOGIC DESCRIPTION

FORAMINIFER-NANNOFOSSIL OOZE

Foraminifer-nannofossil ooze, light brownish gray (2.5Y 6/2) and light gray (5Y 7/1) to olive-yellow (2.5Y 6/6), olive-brown (2.5Y 4/4), pale yellow (5Y 7/3), and olive-gray (5Y 4/2). One indurated layer in Section 3, 46–49 cm.

SMEAR SLIDE SUMMARY (%):

	3, 47 M	6, 41 D	6, 94 D	CC, 10 M
TEXTURE:				
Sand	25	3	15	5
Silt	10	10	10	10
Clay	65	87	75	85
COMPOSITION:				
Quartz	5	1	3	2
Mica	—	—	10	Tr
Clay	5	11	—	6
Volcanic glass	—	3	Tr	Tr
Calcite/dolomite	2	3	2	5
Accessory minerals	1	—	1	1
Opaques	2	—	—	—
Gypsum	—	2	1	—
Pyrite	—	—	2	1
Micrite	—	4	8	—
Foraminifers	25	4	8	5
Nannofossils	60	70	65	80
Diatoms	—	—	Tr	—
Radiolarians	Tr	1	Tr	—
Sponge spicules	Tr	1	Tr	—
Silicoflagellates	Tr	Tr	—	—

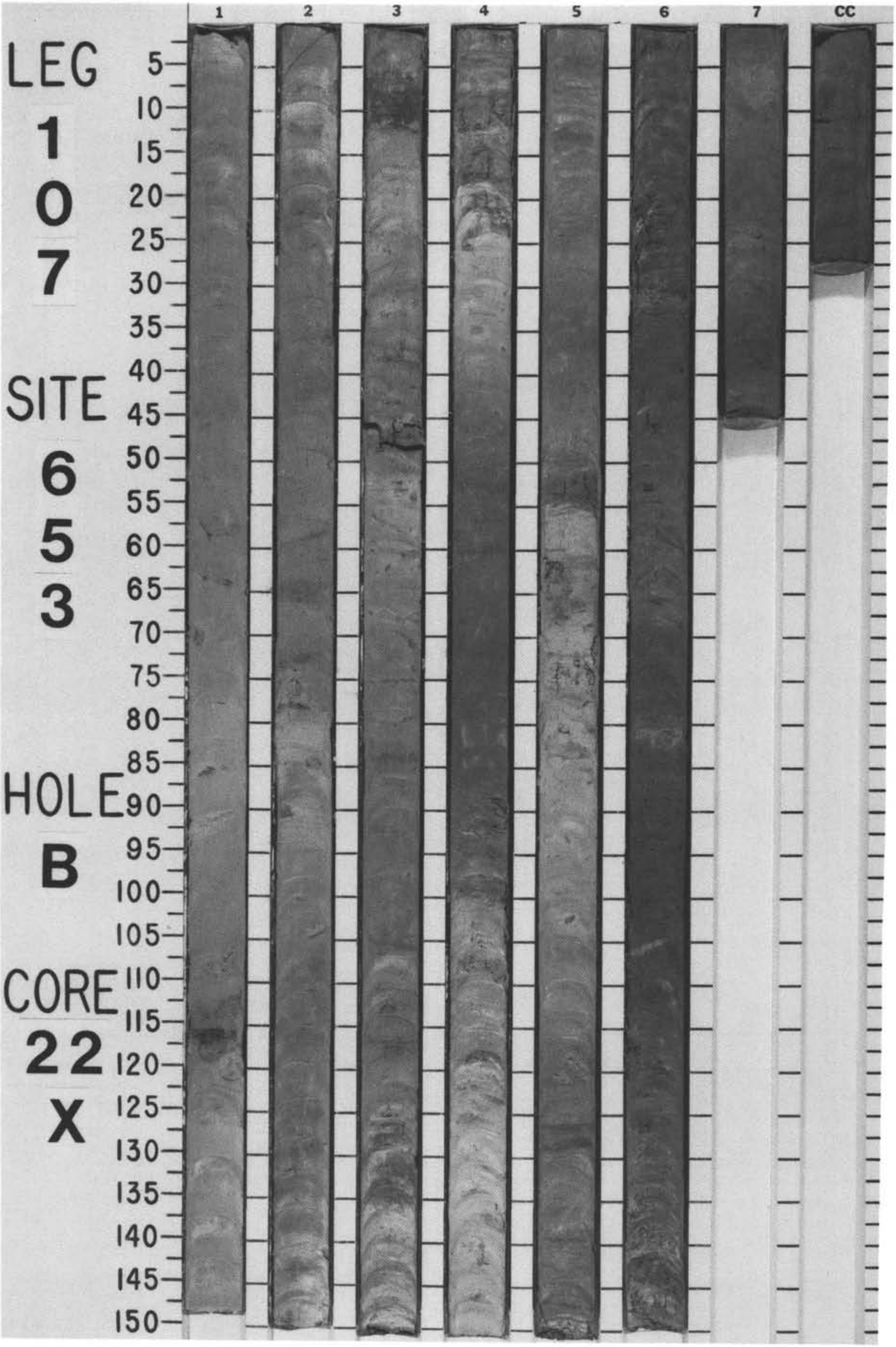
LEG
107
SITE
653
HOLE
B
CORE
22
X
1
2
3
4
5
6
7
CC
5
10
15
20
25
30
35
40
45
50
55
60
65
70
75
80
85
90
95
100
105
110
115
120
125
130
135
140
145
150

SITE 653 HOLE B CORE 23X CORED INTERVAL 3027.6-3037.0 mbsl; 206.7-216.1 mbsf

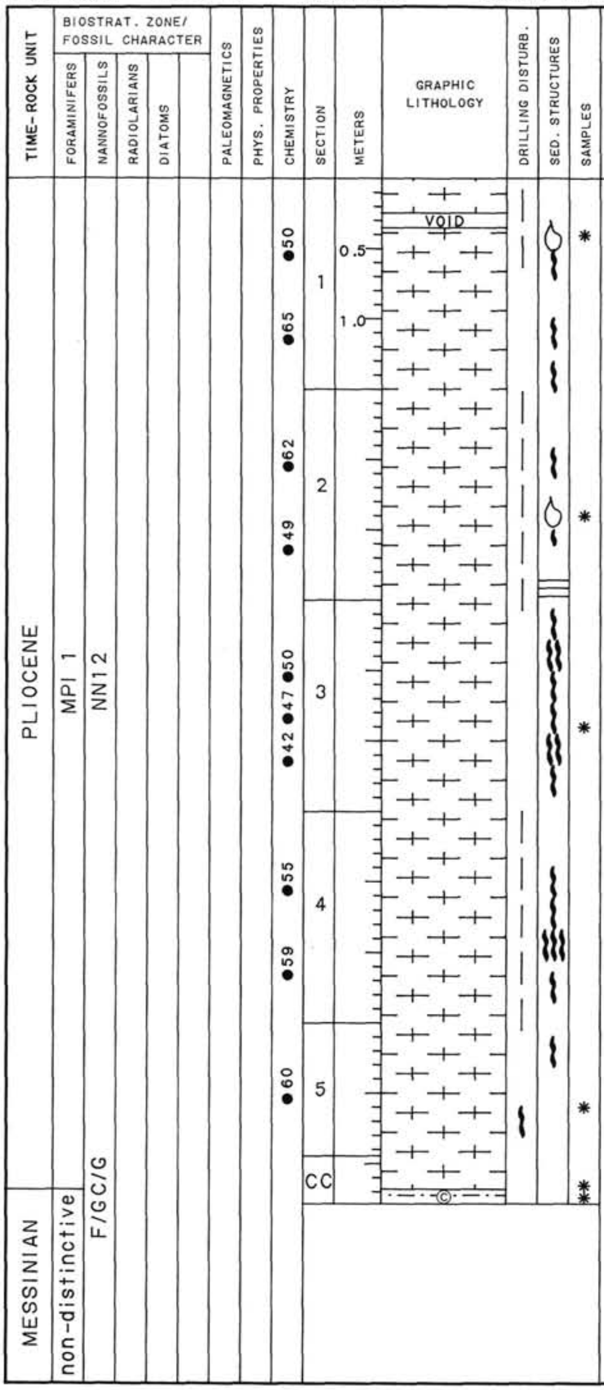

LITHOLOGIC DESCRIPTION

FORAMINIFER-NANNOFOSSIL OOZE

Foraminifer-nannofossil ooze, varicolored, including white, light gray, pale olive, light olive-brown, reddish brown, brownish yellow, red, and black. Reddish brownish colors dominant downsection; some coarser-grained intercalations (foraminifer-rich layers); drilling breccia in Section 5, 55–75 cm.

Minor lithologies: Quartz- and foraminifer-bearing calcareous sandy mud, CC, 23–30 cm, dark gray (5Y 4/1).

SMEAR SLIDE SUMMARY (%):

	1, 42 M	2, 90 M	3, 94 D	5, 58 M	CC, 21 D	CC, 28 D
TEXTURE:						
Sand	30	70	10	3	25	30
Silt	15	10	5	10	20	20
Clay	55	20	85	87	55	50
COMPOSITION:						
Quartz	10	10	8	2	1	15
Feldspar	—	—	—	—	—	Tr
Mica	—	Tr	1	1	1	2
Clay	2	2	—	7	—	19
Volcanic glass	—	Tr	—	Tr	1	1
Calcite/dolomite	5	3	1	2	2	8
Accessory minerals	1	1	1	1	1	2
Opaques	1	—	—	—	—	—
Gypsum	2	—	—	—	—	2
Limonite(?)	—	—	4	3	—	—
Micrite	—	10	—	2	4	15
Pyrite	—	—	—	—	—	1
Foraminifers	30	60	10	2	20	10
Nannofossils	45	10	75	80	70	25
Radiolarians	4	2	—	Tr	—	Tr
Sponge spicules	—	1	—	—	—	—
Silicoflagellates	—	1	—	—	—	—
Plant debris(?)	—	—	—	Tr	—	—

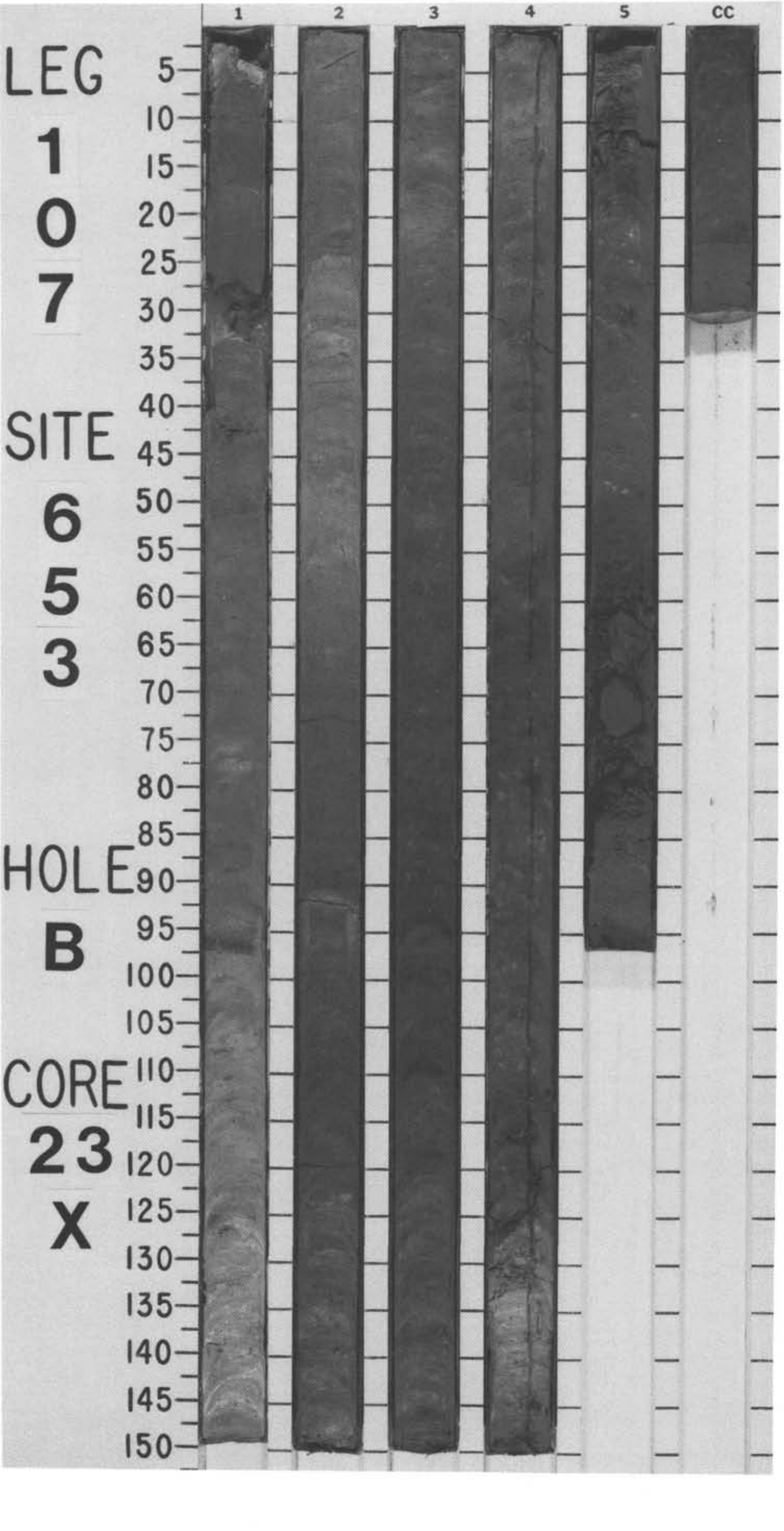
LEG
107
SITE
653
HOLE
B
CORE
23
X
1
2
3
4
5
CC
5
10
15
20
25
30
35
40
45
50
55
60
65
70
75
80
85
90
95
100
105
110
115
120
125
130
135
140
145
150

SITE 653 HOLE B CORE 24X CORED INTERVAL 3037.0-3046.6 mbsl; 216.1-225.7 mbsf

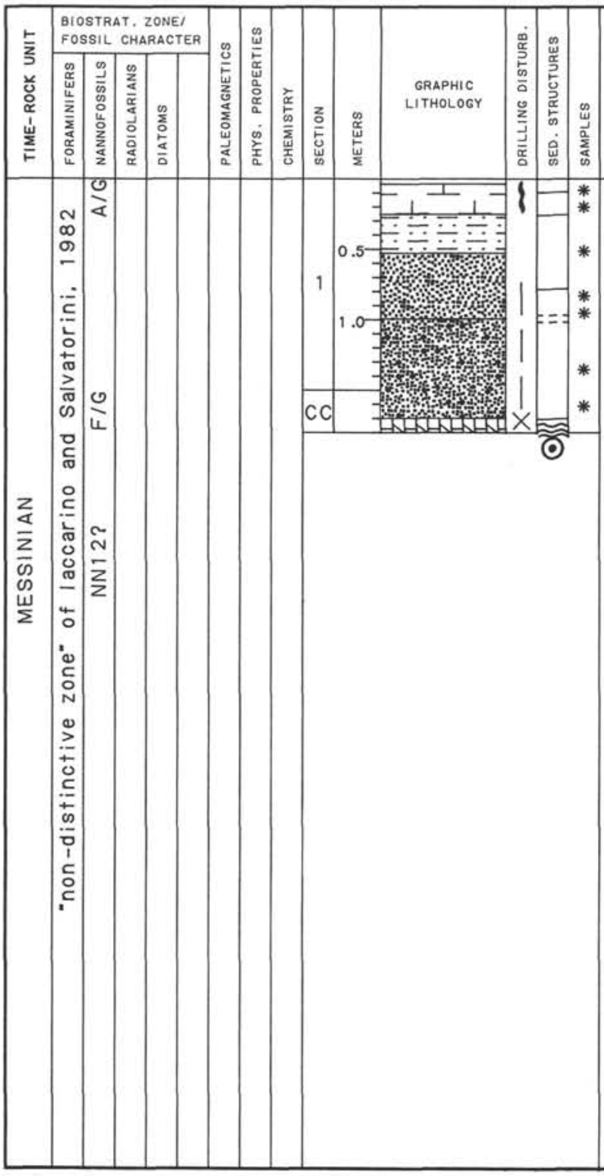

LITHOLOGIC DESCRIPTION

NANNOFOSSIL OOZE, MUD, GYPSIFEROUS SAND, and GYPSUM

Nannofossil ooze, light gray (2.5Y 7/2), Section 1, 5–8 cm. Marly nannofossil ooze, reddish yellow and red (7.5Y 6/6, 10R 5/8), Section 1, 8–23 cm; entire layer a series of drilling biscuits.

Mud, grayish brown (2.5Y 5/2), Section 1, 23–53 cm; streaks of underlying gypsiferous sand throughout seem to have been injected between biscuits by drilling.

Gypsiferous sand, grayish brown (2.5Y 5/2), Section 1, 53–98 cm; slight suggestion of normal grading in upper 20 cm and vague parallel laminations may be drilling disturbance. Upper contacts of layers in Section 1, 8–98 cm, disrupted by drilling, but appear to have had sharp, well-defined boundaries. Sandy mud, grayish brown (2.5Y 5/2), Section 1, 98–99 cm; thin clay layer within sand unit may have been injected during drilling. Gypsiferous silty sand, light olive-brown (2.5Y 5/4), Section 1, 99–145 cm, and CC, 0–20 cm; vague parallel lamination may be drilling disturbance.

Gypsum, base of CC; nodules and coarser laminae are pale yellow (5Y 8/3) and white (5Y 8/2); matrix and finer laminae are pale olive (5Y 6/4) and pale yellow (5Y 8/3). Rounded piece (7 × 5 cm). Wavy laminations with nodules within coarser laminae have chicken-wire texture.

SMEAR SLIDE SUMMARY (%):

	1, 5 D	1, 10 D	1, 50 D	1, 90 D	1, 98 D	1, 134 D	CC D
TEXTURE:							
Sand	5	5	10	70	30	60	60
Silt	10	20	40	25	40	30	30
Clay	85	75	50	5	30	10	10
COMPOSITION:							
Quartz	2	3	10	15	15	20	20
Feldspar	—	—	2	3	—	1	—
Mica	—	—	—	5	5	2	15
Clay	20	20	30	—	15	10	—
Volcanic glass	2	2	5	5	5	15	10
Calcite	—	10	—	10	—	—	—
Dolomite	5	10	5	10	15	15	10
Accessory minerals	4	—	10	10	5	6	10
Gypsum	5	10	13	40	20	30	30
Pyroxene	—	—	—	—	—	1	—
Opaques	—	10	—	—	—	—	—
Analcime	—	—	Tr	—	—	—	—
Foraminifers	5	—	25	2	—	—	—
Nannofossils	50	33	25	—	20	—	5
Sponge spicules	2	—	—	—	—	—	—
Flagellates	5	2	—	—	—	—	—

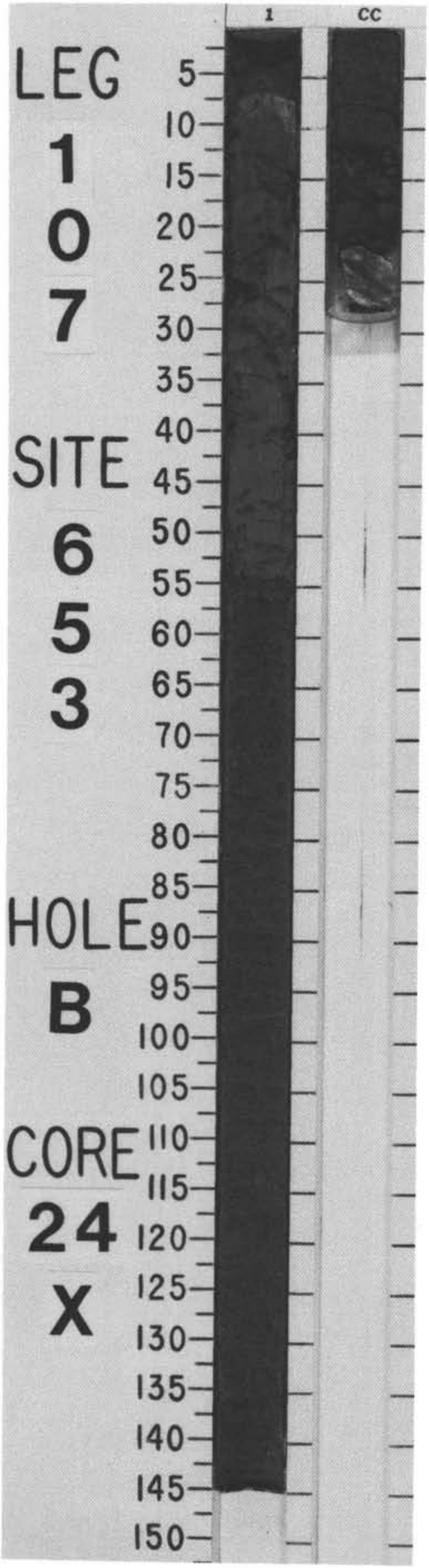
LEG
107
SITE
653
HOLE
B
CORE
24
X
1
CC
5
10
15
20
25
30
35
40
45
50
55
60
65
70
75
80
85
90
95
100
105
110
115
120
125
130
135
140
145
150

SITE 653 HOLE B CORE 25X CORED INTERVAL 3046.6-3056.2 mbsl; 225.7-235.3 mbsf

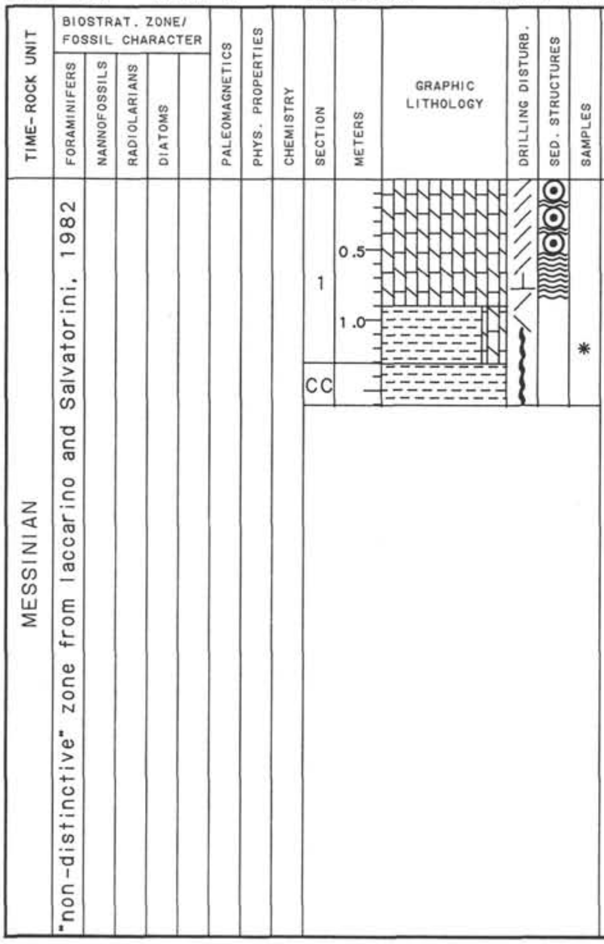

LITHOLOGIC DESCRIPTION

GYPSUM and GYPSIFEROUS CLAY

Nodular gypsum, olive-gray (5Y 5/2), light gray (nodules) (5Y 7/2), olive (5Y 5/4), and dusky yellow (matrix) (5Y 6/4), Section 1, 0–46 cm. Nodules with chicken-wire texture where not recrystallized to selenitic gypsum or anhydrite; matrix between nodules has wavy laminations.

Laminated gypsum, olive-gray (5Y 4/2, 5/2), gray (5Y 5/1), white (5Y 8/2), Section 1, 46–87 and 95–99 cm. Wavy laminations, "partings", laminae 1–4-mm thick; small normal faults with millimeters of throw.

Gypsiferous clay, very dark gray (5Y 3/1), olive-gray (5Y 5/2), olive (5Y 5/3), light gray (5Y 7/1), pale yellow (5Y 7/3), olive yellow (2.5Y 6/6), and white (2.5Y 8/1), Section 1, 99–132 cm, and CC.

Minor lithology:

a) Siltstone, carbonate-cemented, Section 1, 87–95 cm; occurs as a broken fragment rounded during drilling, thus bedding relationship to surrounding gypsum and gypsiferous clay cannot be determined.

b) Black shale, Section 1, lower 4 cm. Fissility natural or due to coring compaction?

c) Broken large selenitic gypsum crystals, as large as 5 × 15 mm, often as lenses within a clay matrix, lower CC. Layer of broken gypsum crystals with little clay, lower 5 cm of CC.

SMEAR SLIDE SUMMARY (%):

	1, 124 D
TEXTURE:	
Sand	10
Silt	10
Clay	80
COMPOSITION:	
Quartz	2
Clay	50
Volcanic glass	3
Dolomite	10
Accessory minerals	5
Gypsum	25
Spheroid	5

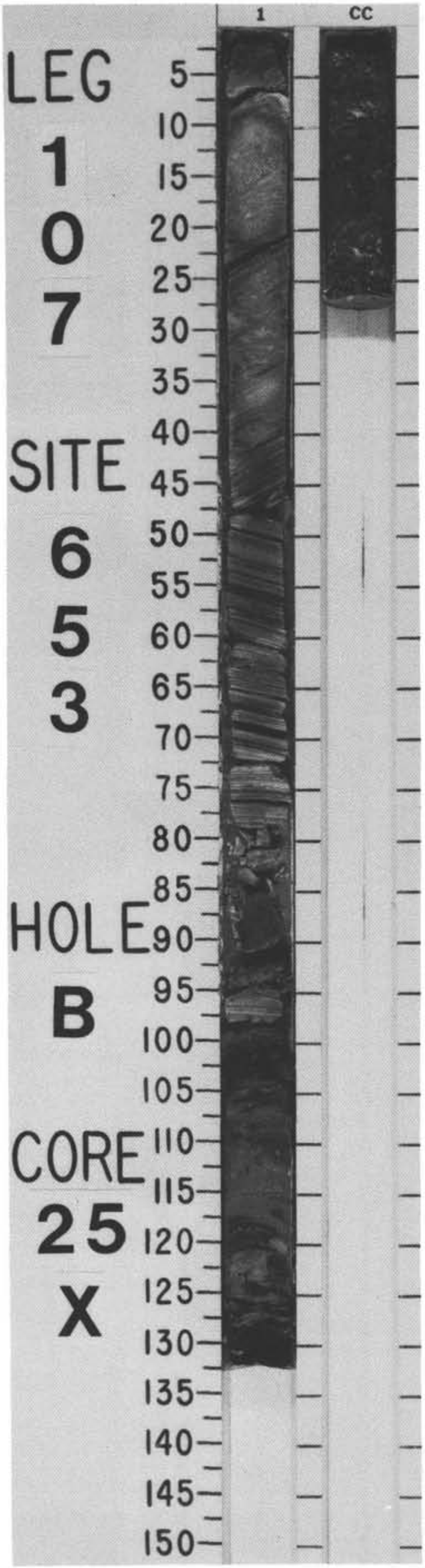
LEG
1
0
7
SITE
6
5
3
HOLE
B
CORE
25
X
1
CC
5
10
15
20
25
30
35
40
45
50
55
60
65
70
75
80
85
90
95
100
105
110
115
120
125
130
135
140
145
150

SITE 653 HOLE B CORE 26X CORED INTERVAL 3056.2-3065.8 mbsl; 235.3-244.9 mbsf

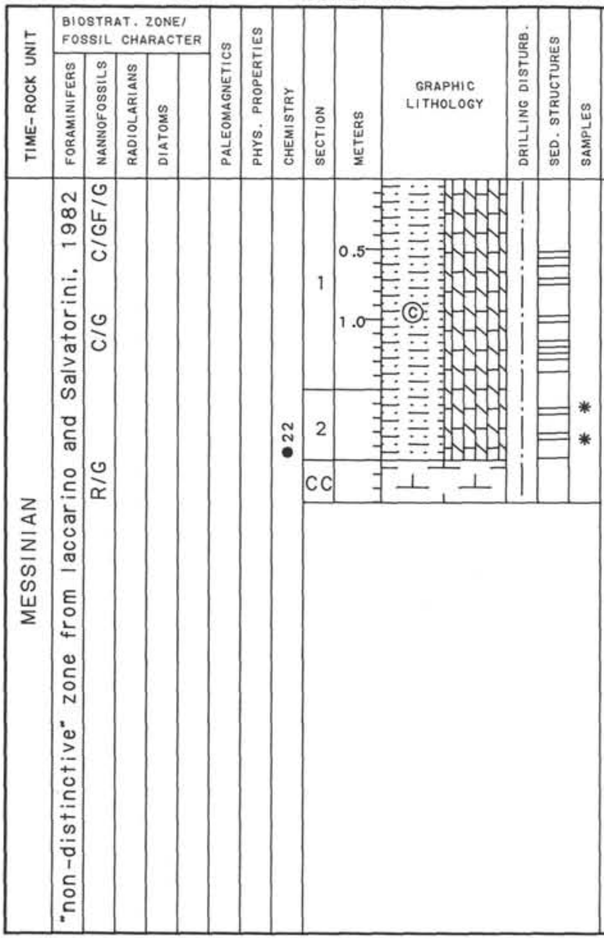

LITHOLOGIC DESCRIPTION

CALCAREOUS GYPSIFEROUS MUD with NANNOPLANKTON, alternating with SELENITE GYPSUM

Calcareous gypsiferous mud with nannoplankton, dark gray (5Y 4/1), gray (5Y 5/1, 6/1), olive (5Y 5/3), light olive-gray (5Y 6/2), and pale olive (5Y 6/3); alternating with selenite gypsum, olive-gray (5Y 5/2) and light olive-gray (5Y 6/2). Crystals broken along split surface of core by cutting.

SMEAR SLIDE SUMMARY (%):

	2, 14 D	2, 33
TEXTURE:		
Silt	30	5
Clay	70	95
COMPOSITION:		
Quartz	5	5
Clay	30	30
Dolomite	10	10
Accessory minerals	8	13
Gypsum	15	40
Nannofossils	30	2
Diatoms	2	–

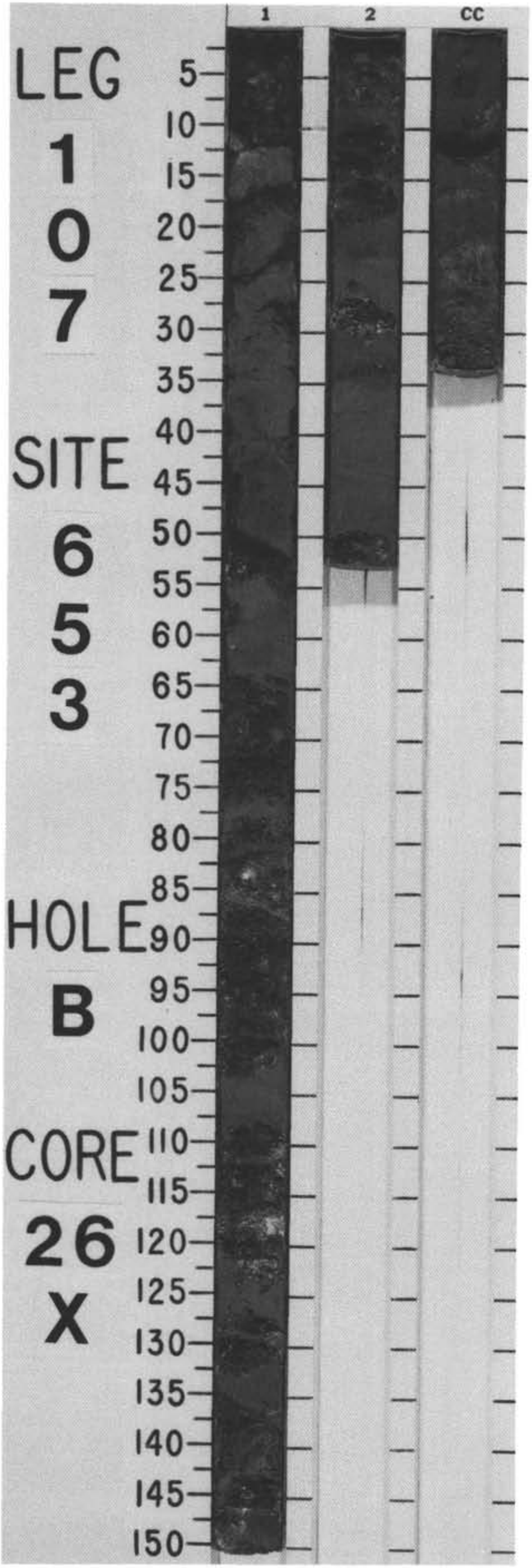
LEG 107
SITE 653
HOLE B
CORE 26 X
1
2
CC
5
10
15
20
25
30
35
40
45
50
55
60
65
70
75
80
85
90
95
100
105
110
115
120
125
130
135
140
145
150

SITE 653 HOLE B CORE 27X CORED INTERVAL 3065.8-3075.5 mbsl; 2449.9-254.6 mbsf

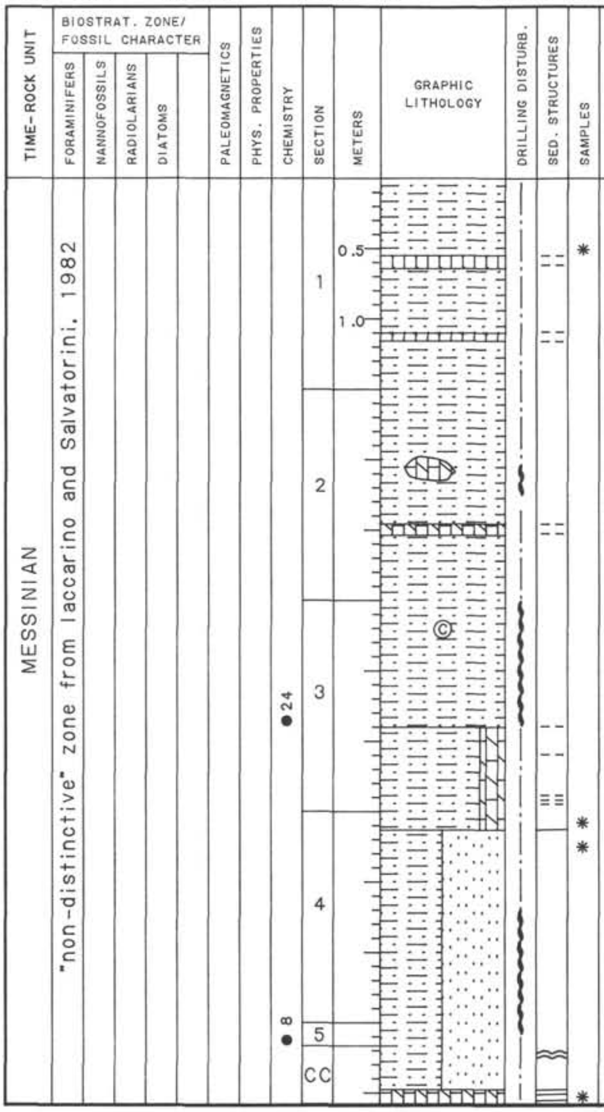

LITHOLOGIC DESCRIPTION

MUD and SILT

Mud, light olive-brown (2.5Y 5/6), light yellowish brown (2.5Y 6/4), olive-yellow (2.5Y 6.6), light gray (2.5Y 7/2), olive (5Y 5/3), and reddish yellow (2.5YR 6/6), Sections 1, 2, 3, and Section 4, 0–13 cm. Includes numerous selenite gypsum crystals. Intervals of intensive coring deformation, obvious by vertical and convolute streaking and displaced selenite layers.

Silt alternating with mud, colored by contents of limonite and hematite, reddish yellow (7.5YR 6/6, 6/8, 7/6, 7/8), olive-yellow (2.5Y 6/8), red (10R 4/6, 4/8), and gray (10YR 6/1, 5YR 6/1), Section 4, 13–150 cm, Section 5, and CC. Silt and mud alternate with both distinct and indistinct boundaries, presumably the result of coring disturbance; chips of black shale and selenite gypsum mixed in throughout.

Minor lithology:

a)Broken crystals of selenite gypsum, scattered in zones within unit, presumably broken by drilling and core-splitting; colors are those of host mud which stained crystals. Remnants also within core portion with intense coring disturbance, Section 3, 0–90 cm.

b)Gypsum, white, gray, and black, CC, 9–10 and 36–40 cm; occurs in silt-sized particles in 1-mm-thick laminae and alternates with red mud laminae (described above).

c)Broken gypsum at the very base of the core, overlain by 3 cm of laminations of white and black gypsum, red and yellow (hematite- and limonite-rich) layers, and layers rich in sulfur.

SMEAR SLIDE SUMMARY (%):

	1,50	4,18	4,26	CC,35
TEXTURE:				
Sand	—	—	—	70
Silt	15	100	20	—
Clay	85	—	80	30
COMPOSITION:				
Quartz	—	—	5	—
Clay	60	—	—	—
Dolomite	7	—	5	—
Accessory minerals	—	—	—	10
Opaques, limonite	—	100	—	—
Gypsum	2	—	10	90
Opaques, hematite	—	—	80	—
Analcime	3	—	—	—
Foraminifers	3	—	—	—
Nannofossils	20	—	—	—
Intraclasts	5	—	—	—

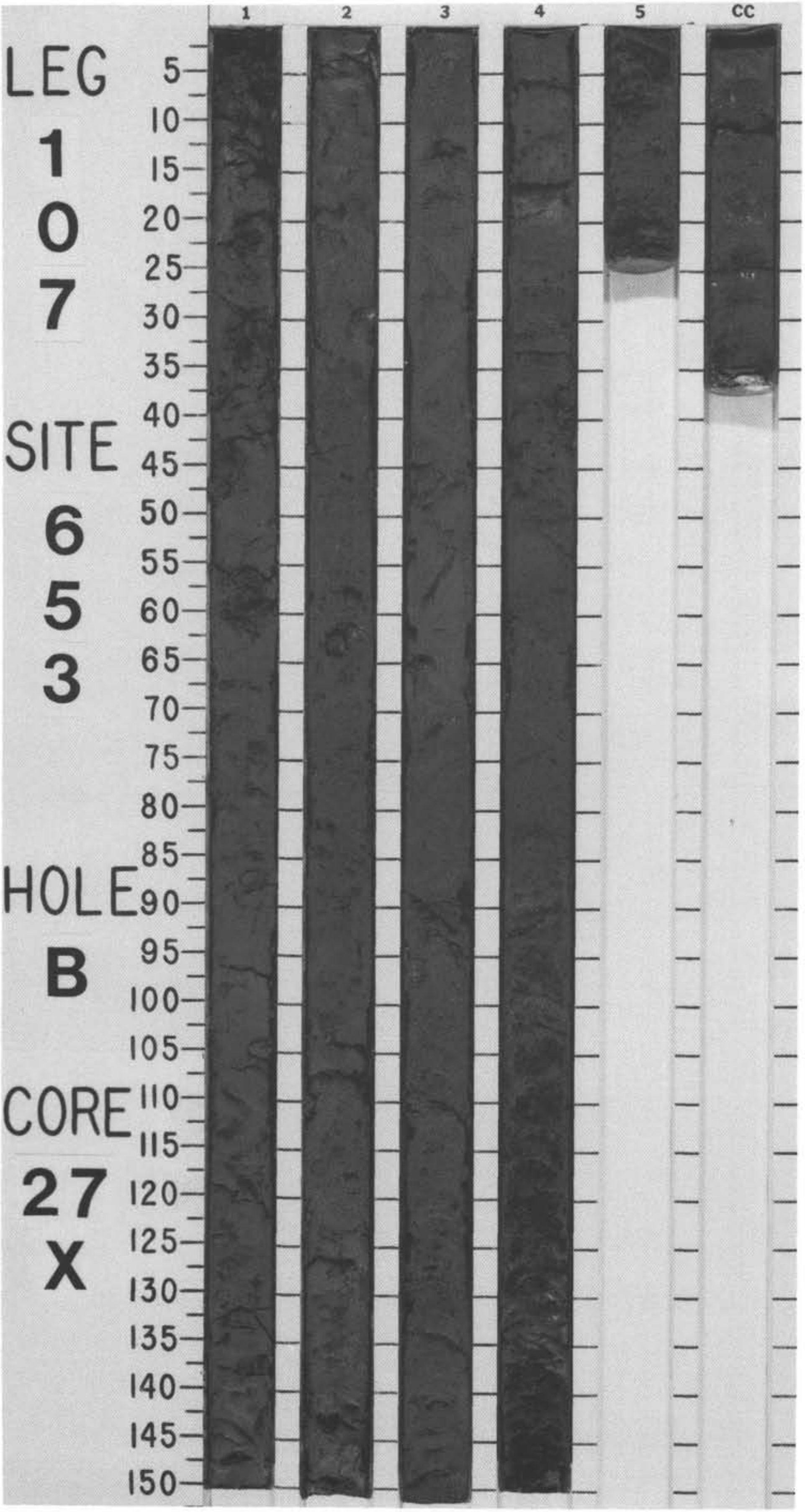

LEG
107
SITE
653
HOLE
B
CORE
27
X
1
2
3
4
5
CC
5
10
15
20
25
30
35
40
45
50
55
60
65
70
75
80
85
90
95
100
105
110
115
120
125
130
135
140
145
150

SITE 653 HOLE B CORE 28X CORED INTERVAL 3075.5-3083.2 mbsl; 254.6-264.3 mbsf

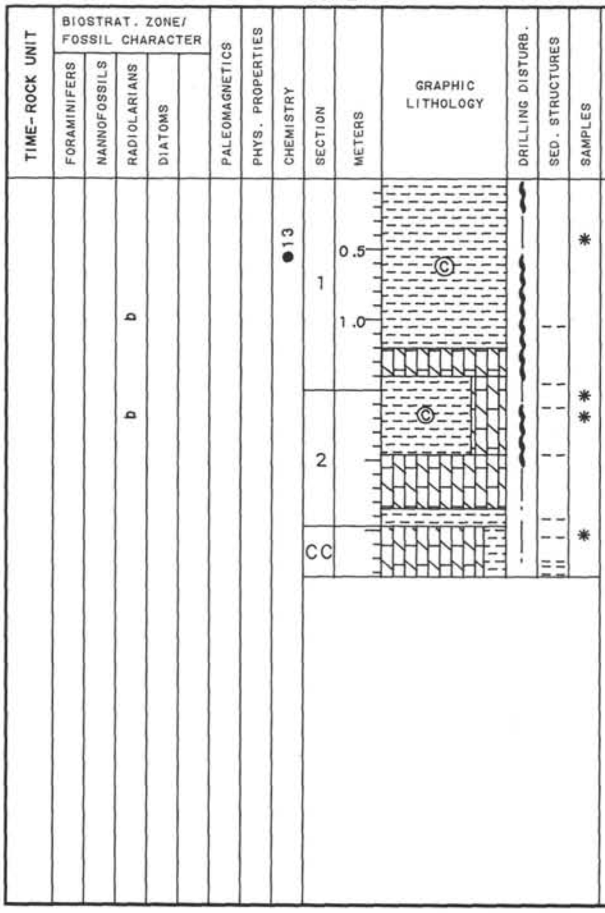

LITHOLOGIC DESCRIPTION

CLAY

Clay, olive-gray (5Y 5/2–7/8), olive-yellow (2.5Y 5/4–7/8), and gray (2.5Y 7/1–N8/, 2.5Y 6/6–6/1). These three color groups occur with other minor olive-gray, yellow, and light gray colors. The light gray is full of selenite gypsum crystals, with tiny crystals present in minor amounts within the olive-gray and yellow clay. Contacts between various clay intervals appear sharp but have been disturbed by drilling.

Minor lithology:
a)Shale and mud, black (2.5Y N4/), Section 1, 0–25 and 46–150 cm, and Section 2, 0–9 cm. Upper occurrence appears to be displaced pieces within a void; other occurrences contain scattered selenite gypsum crystals; upper and lower contacts disturbed by drilling.
b)Gypsum, white, CC, 30–35 cm. Occurs as tiny powdery material, often in larger lithified clumps.

SMEAR SLIDE SUMMARY (%):

	1, 43 D	2, 5 D	2, 23 D	CC, 4 D
TEXTURE:				
Silt	10	50	—	—
Clay	90	50	100	100
COMPOSITION:				
Quartz	10	10	—	—
Feldspar	—	—	—	Tr
Clay	30	30	30	30
Dolomite	20	20	Tr	30
Accessory minerals	10	—	—	10
Gypsum	10	15	15	15
Anhydrite	20	15	15	15
Opaques	—	10	—	—
Limonite	—	—	40	—

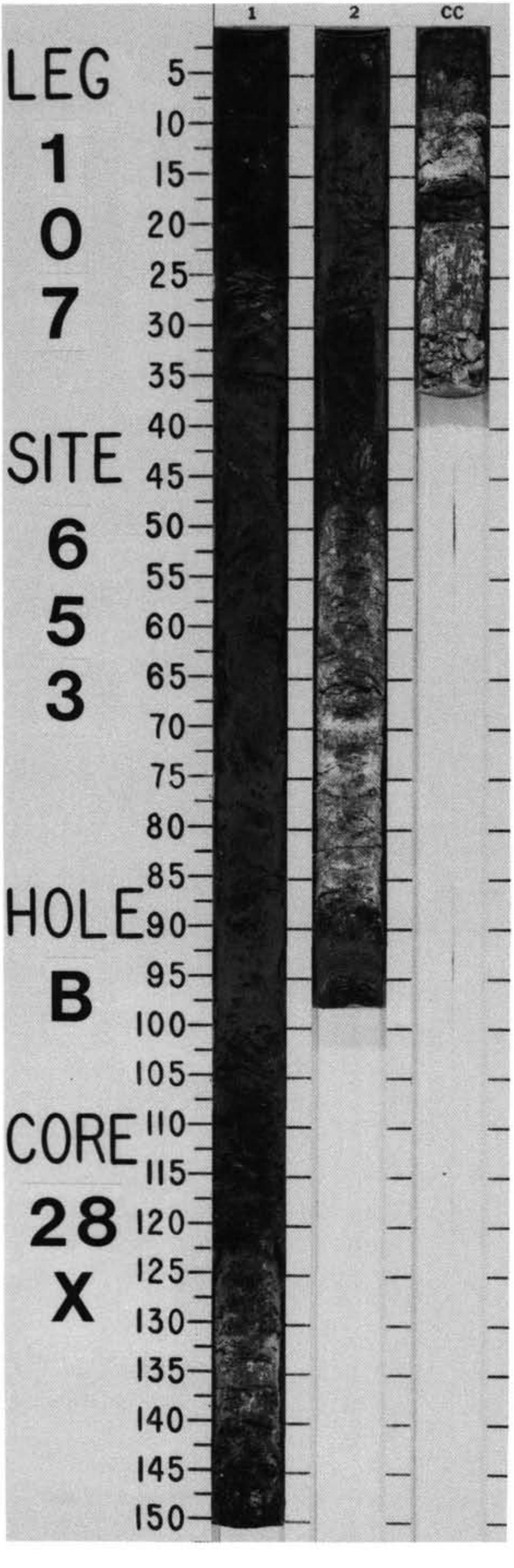
LEG
1
0
7
SITE
6
5
3
HOLE
B
CORE
28
X
1
2
CC
5
10
15
20
25
30
35
40
45
50
55
60
65
70
75
80
85
90
95
100
105
110
115
120
125
130
135
140
145
150